Stability and Optimal Control Approach of Mathematical Models of COVID-19 in Thailand

JIRAPORN LAMWONG

A THESIS SUBMITTED IN PARTIAL FULFILLMENT OF THE REQUIREMENT FOR THE DEGREE OF DOCTOR OF PHILOSOPHY IN APPLIED MATHEMATICS
DEPARTMENT OF MATHEMATICS SCHOOL OF SCIENCE
KING MONGKUT'S INSTITUTE OF TECHNOLOGY LADKRABANG
2025
KMITL-2025-SC-D-001-005

Thesis Title	Stability and Optimal Control Approach of Mathematical Models of COVID-19 in Thailand
Student Name	Miss Jiraporn Lamwong
Student ID	65056018
Degree	Doctor of Philosophy (Applied Mathematics)
Department	Mathematics
Year	2025
Thesis Advisor	Assoc. Prof. Dr. Puntani Pongsumpun

Abstract

COVID-19, caused by the virus SARS-CoV-2, was first identified in Wuhan, China, in December 2019. The disease quickly spread globally, significantly impacting public health and livelihoods. This work focuses on developing and designing mathematical models to understand the dynamics of the COVID-19 outbreak. Three models were created: Model 1: Focuses on vaccination, patient quarantine, and hospitalization. Model 2: Separates vaccinated and unvaccinated groups, considering asymptomatic individuals, symptomatic individuals, and hospitalization. An optimal control model was incorporated to manage the spread. Model 3: Considers symptomatic individuals and patient quarantine, with an optimal control function applied. Each model was analyzed to assess stability, response characteristics, and equilibrium conditions. The basic reproduction number, which indicates potential spread, was calculated using the next-generation matrix method. Numerical data were used to examine the outbreak's behavior, and sensitivity analysis was conducted to determine which factors most impacted the spread. Model fitting was performed to align parameters with real outbreak data from Thailand. The results aim to provide practical guidelines for controlling the spread of COVID-19 and supporting public health measures.

Keywords: COVID-19, global stability, Lyapunov function, optimal control, standard dynamical modeling

Acknowledgments

To complete the thesis on Mathematical Models of COVID-19 In Thailand: Stability and Optimal Control Approach, the author is very grateful to Assoc. Prof. Dr.Puntani Pongsumpun, the thesis advisor guided and provided basic knowledge, and concepts, as well as giving advice and being a consultant in solving obstacles for conducting the research.

The author would like to thank the Chairman of the Program Committee, curriculum lecturers, and outside experts consisting of Asst. Prof. Dr. Klot Patanarapeelert, Asst. Prof. Dr.Sukrawan Mavecha, Asst. Prof. Dr.Thawatchai Khumprapussorn and Asst. Prof. Dr.Puttha Sakkaplangkul, who considered the topic and examined the thesis kindly advised until the thesis was completed. Special thanks are given to Prof. Dr.I-Ming Tang and Asst. Prof. Dr. Napasool Wongvanich for providing assistance and support for my research.

The author would like to thank the School of Science, King Mongkut's Institute of Technology Ladkrabang for funding the thesis.

In addition, I would like to thank my friends in the Department of Mathematics for the knowledge, suggestions, and assistance given to me in this study.

Finally, I would like to thank my parents and my family for their continued support and encouragement until I graduate. The benefits of this thesis are given to all benefactors.

Miss Jiraporn Lamwong

Table of Contents

List of Tables

List of Figures

Figure **Page**

Chapter 1
Introduction

1.1 Research Motivation

By the end of December 2019, the coronavirus outbreak was detected [1-4], causing damage to people's health, properties, and livelihood, including the economy [5]. People needed to adjust their way of life and work to survive the outbreak. It was considered a global threat since the virus spread rapidly. Many countries could not cope with the situation, contributing to a crisis in the public health system. COVID-19 caused millions of people to lose their lives. COVID-19 is the virus that is causing the illness [6]. It belongs to the Coronaviridae virus family and is a single-stranded RNA virus that causes respiratory diseases [7-15]. A new strain of coronavirus known as 2019 is responsible for respiratory illnesses. By touching or coming into close contact with an infected person, one can disseminate the virus from one person to another [15-18]. People can become infected by touching surfaces of things that contain COVID-19 before touching their mouth, nose, or eyes. It can also spread through respiratory droplets produced by breathing, coughing, or sneezing [19,20]. The incubation period following viral exposure lasts between two and fourteen days [1,11,21-25] from the date of exposure. Next, COVID-19 illness symptoms in cases of inadequate immunity in the body range from high fever, sore and dry throat, and muscular and joint discomfort to severe symptoms that can damage the respiratory system [16,17,24-29].

The World Health Organization (WHO) released a report on the COVID-19 pandemic that states that 773,819,856 confirmed cases were discovered worldwide between January 5, 2020, and December 31, 2023. As shown in Figure 1.1, the global distribution of COVID-19 cases highlights the concentration in specific regions. The region with the highest number of confirmed cases was Europe as 278,442,668 cases were detected, followed by the Western Pacific with 207,953,190 confirmed cases, Americas with 193,211,105 confirmed cases, South-East Asia with 61,234,065 confirmed cases, Eastern Mediterranean with 23,409,122 confirmed cases, and Africa with 9,568,942 confirmed cases. As for the situation of the spread at a national level, the United States of America, with 103,436,829 confirmed cases, China, with 99,322,727 confirmed cases, and India, with 45,013,172 confirmed cases, were the top three

countries with the most confirmed cases. As shown in Figure 1.2, The number of confirmed deaths from COVID-19 across the world is 7,010,568 deaths, the region with the highest number of confirmed deaths was the Americas with 2,992,191 deaths, followed by Europe with 2,263,749 deaths, Southeast Asia with 808,217 deaths, Western Pacific with 419,056 deaths, the Eastern Mediterranean with 351,865 deaths, and Africa with 175,477 deaths. The United States of America (1,161,235 deaths), Brazil (702,116 deaths), and India (533,361 deaths) were the top three nations with the most confirmed deaths. Respectively [30,31]. As for the COVID-19 outbreak in Thailand, there were 4,762,375 confirmed cases and 34,517 confirmed deaths [32,33]. Though the outbreak situation has unfolded, every country has monitored the situation continuously as the spread of the virus appears to have subsided.

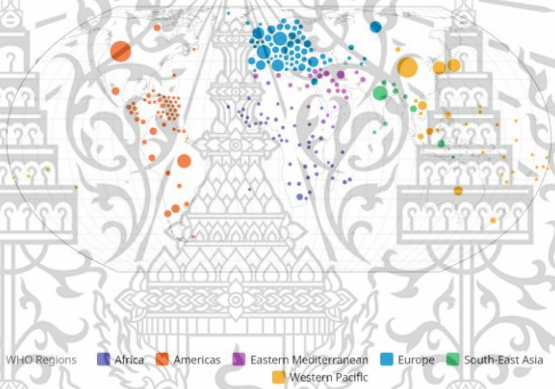

Figure 1.1 Total number of COVID-19 cases reported to WHO as of December 31, 2023, cumulatively [30].

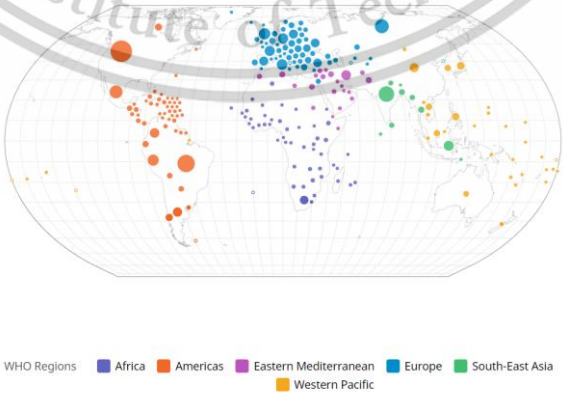

Figure 1.2 Total number of COVID-19 deaths reported to WHO as of December 31, 2023, cumulatively [30].

Vaccination is considered an important measure for controlling and reducing the spread of COVID-19 [10, 20, 34-39]. There was a huge demand for vaccines to keep pace with the ongoing spread situation. Many companies rushed to develop vaccines to meet the needs of the governments and people. Several vaccine manufacturers were approved by the World Health Organization (WHO) and those vaccines have been used widely. The currently approved COVID-19 vaccines were Pfizer, Johnson and Johnson, AstraZeneca, Covishied, Moderna COVID-19 vaccine, SINOPHARM, SINOVAC, etc. [38]. Each vaccine brand is suitable for different uses. As shown in Figure 1.3, As to the global report on COVID-19 immunization on November 26, 2023, 67% of the global population had received all recommended vaccinations, and Figure 1.4 shows that 32% had received at least one booster dose. According to Thailand's immunization statistics, 46% of people had at least one booster shot and 78% of people had obtained all recommended vaccinations [41, 42]. Vaccination, on the other hand, is one strategy that works to stop COVID-19 from spreading. Numerous methods, including social separation, mask-wearing, quarantine, etc., are helping to contain the problem.

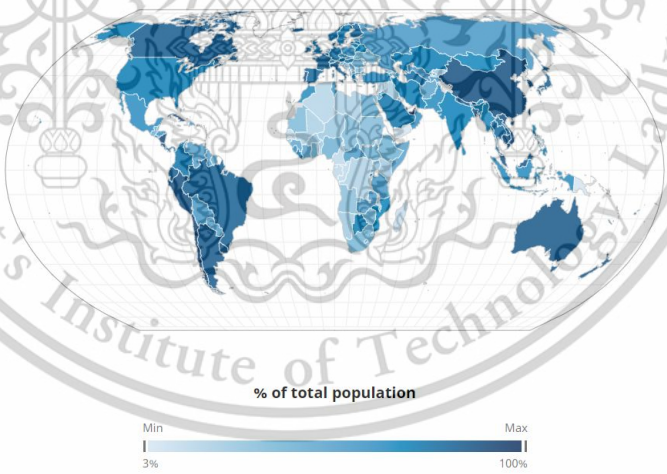

Figure 1.3 Percentage of people worldwide who received the full primary series of the COVID-19 vaccine, on November 26, 2023 [41].

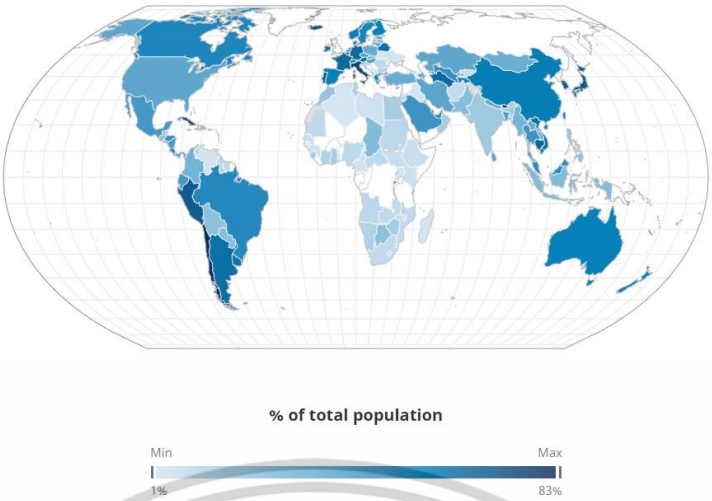

Figure 1.4 World, November 26, 2023, percentage of people who received at least one booster dose of the COVID-19 vaccination [41].

To manage COVID-19, a mathematical model was used to analyze the situation and formulate policies to reduce the spread of the disease. Several researchers proposed different models of the spread of COVID-19 to study the dynamics of COVID-19 outbreak. To monitor the infection from tourists, Lamwong et al. [43] developed a mathematical SEIQR model for MERS-CoV by taking into account two groups of the population: the group from Thailand and the group of South Korean tourists visiting Thailand. A basic model of MERS-CoV reported in the Arabian Peninsula, Europe, North America, Southeast Asia, the Middle East, and the United States of America was examined by Gardner Rey et al. [44]. Unlike SARS, which spreads from person to person, MERS did not spread through person-to-person contact. A mathematical model was developed to explain the gap using epidemiological data. The MERS transmission occurred at a transit center, where hosts were together. It involved delving into the mechanism and source of viral persistence in the human population. Based on an SEIR model, Mwalili et al. [45] developed a COVID-19 model. Pathogens in the environment and social separation were taken into account. The study found that while social distance may have an impact on the dissemination, infected individuals should be quarantined to stop the infection from spreading. A SEIR model was presented by Yohanres et al. [46] to explain the COVID-19 pandemic. To lower the number of infected patients, save money on vaccinations, and lower medical expenditures, the best course of action was taken. The study's conclusions demonstrated that vaccination-based control may stop the spread by demonstrating that immunization

could lower the number of infectious and risk groups. A mathematical model was created by Enahoro et al. [47] to examine the dynamics of COVID-19 spread and control in Nigeria. To evaluate the effects both nationally and locally, the model examined and established parameters using COVID-19 data released by the Nigeria Center for Disease Control (NCDC). According to the numerical model, COVID-19 in Nigeria was successfully contained by implementing a moderate social distancing policy nationwide. A dynamic mathematical model that managed the COVID-19 and cholera outbreaks in Yemen was presented by Hezam et al. [48]. Four control functions were applied: social separation, lockout, test count, and water-dispersible granules containing choline chloride.

From what is mentioned above, it can be seen that understanding the risks to people's health, properties, and livelihoods from infection is critical for improving public health outcomes. Therefore, this research focuses on analyzing and mitigating these risks by gathering information on the dynamics of COVID-19 spread in Thailand. The researcher developed a series of mathematical models to evaluate the impact of vaccination, isolation, and preventive strategies on disease transmission. These models aim to provide insights into the spread of the disease and identify effective control measures. To quantify risk in this study, the basic reproduction number (R_0) was calculated to assess the potential of disease spread under different scenarios, while sensitivity analysis was conducted to determine the most influential parameters affecting transmission rates. The models measured risk by evaluating the probability of infection among susceptible individuals, the effectiveness of vaccination in reducing susceptibility, and the role of isolation in breaking transmission chains. Key results demonstrated that an increase in vaccination rates led to a significant reduction in R_0, indicating a lower risk of widespread infection. Additionally, isolation strategies for symptomatic individuals were found to be highly effective in containing outbreaks. The insights gained from these analyses provide a detailed understanding of risk factors associated with COVID-19 transmission and help in formulating optimized intervention strategies to mitigate these risks. Furthermore, the findings can serve as primary data for crafting prevention policies, reducing the number of cases, and offering statistical support to the Department of Disease Control, Ministry of Public Health, for managing future outbreaks effectively.

1.2 Objectives of the study

This research aims to develop and analyze mathematical models for understanding and controlling the spread of COVID-19 in Thailand. The specific objectives are as follows:

1) To analyze the dynamics of COVID-19 transmission in Thailand by identifying critical factors influencing the spread, including vaccination, quarantine, hospitalization, and asymptomatic carriers.

2) Develop and evaluate three mathematical models that incorporate different intervention strategies:

Model 1: Examines the impact of vaccination, patient quarantine, and hospitalization on disease transmission.

Model 2: Differentiates between vaccinated and unvaccinated populations, considering asymptomatic and symptomatic cases, and incorporates an optimal control function for managing the spread.

Model 3: Focuses on symptomatic transmission and quarantine strategies, applying optimal control measures to mitigate the outbreak.

3) Calculate and analyze key epidemiological parameters, including the basic reproduction number, stability conditions, and sensitivity analysis, to determine the most influential factors affecting the spread of COVID-19.

4) To implement an optimal control framework based on Pontryagin's Maximum Principle to identify effective intervention strategies for minimizing infection rates while balancing public health and economic considerations.

5) To validate the proposed models using real-world data from Thailand, collected during the period from January 1, 2022, to April 10, 2022, ensuring practical applicability and providing quantitative insights for public health policy recommendations.

6) To provide recommendations for controlling future outbreaks based on numerical simulations and model findings, offering guidelines for public health organizations such as the Department of Disease Control, Ministry of Public Health, Thailand.

1.3 Scopes of the study

The scope of this work on modeling the spread of COVID-19 includes the following aspects:

1) Data was obtained from weekly reports by the Department of Disease Control, Ministry of Public Health, covering the number of COVID-19 cases from 2019 to 2023. This data was used to study the behavior of COVID-19 transmission.

2) The number of cases was analyzed to develop a standard dynamic model of COVID-19 spread in the form of a non-linear equation. The population size for each group was considered constant.

3) The standard dynamic model was used to analyze the model's behavior, describing the characteristics of solutions and identifying conditions for the stability of each equilibrium point.

4) Pontryagin's Maximum Principle was applied to explore optimal control conditions, providing guidelines for managing the spread of COVID-19 effectively.

1.4 Process of the study

The study process of the mathematical model for COVID-19 is as follows:

1) Study and collect statistical data on the spread of COVID-19 from the reports by the Department of Disease Control, Ministry of Public Health, on the number of patients from 2019–2023. This data serves as the foundation for designing a mathematical model.

2) Study definitions, theories of epidemiology, and relevant literature to understand the key factors influencing the dynamics of COVID-19 and identify the gaps in existing research.

3) Formulate research questions and hypotheses to guide the study. The primary research questions include:

3.1) What are the critical factors influencing the spread of COVID-19 in Thailand?

3.2) How effective are vaccination, quarantine, and isolation strategies in controlling the spread of COVID-19? The hypothesis is that optimal control strategies, including vaccination and isolation measures, can significantly reduce the basic reproduction number and mitigate the spread of COVID-19.

4) Design a mathematical model for COVID-19 based on the collected data and guided by the research questions and hypotheses. The model incorporates critical parameters such as vaccination, quarantine, and hospitalization.

5) Analyze the mathematical model to identify factors affecting the spread of COVID-19 and evaluate the stability and effectiveness of the proposed interventions.

6) Develop the model to reflect current and evolving outbreak situations, ensuring its applicability to real-world scenarios.

7) Summarize study results and propose guidelines for future research and the development of advanced models for controlling similar outbreaks.

1.5 Benefits of the study

The benefits of the study on the mathematical model for COVID-19 are as follows:

1) The mathematical model for the spread of COVID-19 provides a detailed description of the disease's dynamic spread, offering valuable insights into its transmission patterns.

2) This study enhances the understanding of COVID-19 spread through both uncontrolled and optimal control models, enabling a comprehensive analysis of various intervention strategies.

3) This study introduces and evaluates innovative approaches to reduce the spread of COVID-19, particularly through optimal control strategies that integrate vaccination, quarantine, and isolation measures.

4) This study serves as a research guideline for those interested in optimal control strategies for COVID-19 and provides a framework for developing advanced mathematical models applicable to other infectious diseases.

Chapter 2

Theory and Literature Reviews

In this part, the origin of COVID-19 is described to understand the dynamic of the epidemic, the cause of the disease, the transmission of COVID-19, symptoms, COVID-19 vaccines, COVID-19 spread situation in Thailand, recall, definitions, theories, and the review of relevant literature to discuss the model of the spread of COVID-19 of this study.

2.1 Background of COVID-19 disease

The novel coronavirus disease 2019 (COVID-19) is caused by coronavirus. It was first discovered in December 2019 in Wuhan City, China [1,49-51]. After that, it was found that the virus spread over a wide range of every region in the world. According to reports of the epidemic, it was found that it spread from one person to another person by breathing through droplets [16,17]. Droplets are generated and released into the air when an infected person coughs or sneezes [20,52]. The incubation period takes from 2 to 14 days [1,11,21-25]. The most common symptoms of COVID-19 include muscle pain, body stiffness, sore throat, dry throat, high fever, and severe symptoms that can damage the respiratory system [16,17,24-29]. Currently, COVID-19 vaccines are available, which can control and gradually reduce the number of COVID-19 patients.

2.1.1 Cause of the disease

The novel coronavirus 2019 disease or COVID-19 is caused by a new strain of virus called severe acute respiratory syndrome coronavirus 2 or SARS-Cov-2. It is a single-stranded RNA virus that belongs to the Family Coronaviridae [6-15,53], the same family causing respiratory diseases ranging from common cold to very severe diseases [26,54]. SARS-CoV-2 virus is a pathogenic virus that must live in tissue cells or be covered with mucus-like phlegm. It cannot live independently. Besides, it is a virus whose outer envelope is made from a layer of lipids, which can be broken down when it comes in with detergent or soap. There are currently 7 types of coronaviruses that cause diseases in humans:

Type 1-4: Common cold.

Type 5: SARS caused by a new strain of virus in 2002-2003.

Type 6: MERS caused by a new strain of virus in 2014.

Type 7: COVID-19 is caused by a new strain of virus, which has never been detected before in humans, causing respiratory illness in humans and the virus can be transmitted from person to person. They will be able to catch the virus in the air released from infected persons when they cough, sneeze, speak, or when they get exposed to the virus or respiratory tract secretions [55].

2.1.2 The spread of the disease

The spread of COVID-19 started on 1 December 2019 when a patient with pneumonia of unknown cause was found in Wuhan city, China. Later, it was officially reported on 3 January 2020 that the pneumonia found in Wuhan was caused by the 2019 novel coronavirus [17, 47,56-59]. The epidemic took around 12 weeks, from the first confirmed case in China (1 December 2019) until the virus spread to six of the world's seven continents. Next, the virus spread rapidly throughout all continents of the world. In Thailand, the first wave of the COVID-19 outbreak was assumed to start in January 2020. The source of the epidemic was likely to come from animals, as the vector of the disease to humans and the spread of the epidemic from person to person. The spread from one person to another person is through a variety of ways; breathing through droplets produced by infected persons when they cough or sneeze. Infectious droplets get into the mouth or nose of persons nearby or get into the lungs, or it is possible that persons can be infected with COVID-19 by getting exposed to surfaces or objects contaminated with COVID-19 and touching their nose, eyes, and face [30,32, 60,61].

2.1.3 Signs and symptoms of the disease

The incubation period of COVID-19 is 2-14 days [11,21-25]. That is the reason why those getting exposed to the virus are required to isolate from other people or to quarantine for 14 days, from the first day of being exposed to the virus. According to the report on the cases outside Wuhan, it was found that 97.5% of patients had an incubation period of less than 11.5 days and the median was 5.1 days. In addition, there were several factors affecting the COVID-19 incubation period and individual incubation period of COVID-19, i.e. the amount of virus in an infected person. A large

amount of the virus in an infected person results in a shorter incubation period while a small amount of the virus in an infected person results in a longer incubation period, or even replication speed of the virus, the health of an infected person, routes of transmission, and the immune response to the infection of an infected person, which affect the virus elimination and the incubation period. As shown in Figure 2.1, the common signs and symptoms of persons getting infected with COVID-19 are similar to influenza, dry cough, sneezing, sore throat, runny nose, fever, respiratory symptoms, shortness of breath, and difficulty breathing. In severe cases of COVID-19, complications may occur, such as pneumonia, kidney failure, or death [16,17,24-29].

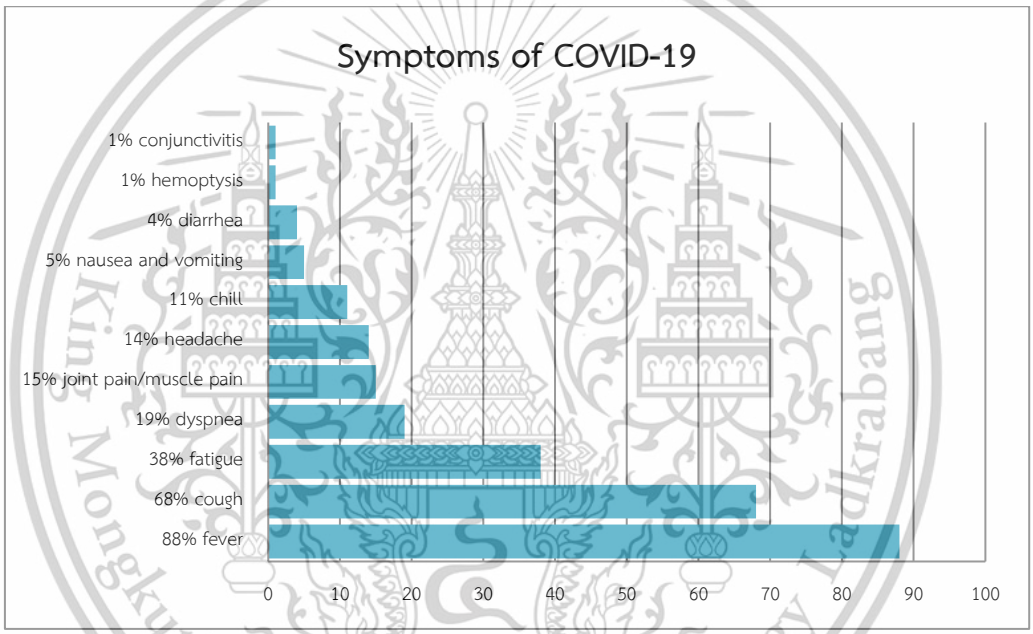

Figure 2.1 Signs and symptoms of COVID-19 infection.

2.2 Vaccines preventing the disease

The development of effective vaccines to prevent and inhibit the spread of COVID-19 took place worldwide. Controlling the spread of the virus through vaccination stimulates the formation of immunity to the SARS-CoV-2 virus. When a person receives a vaccine, it promotes the development of active immunity, helping reduce the risk of infection and lessening the severity of the disease. Many companies accelerated vaccine development to meet global demand, leading to the successful approval and distribution of various vaccines in many countries.

In Thailand, the Ministry of Public Health allocated several COVID-19 vaccines for public use:

- AstraZeneca: Administered to individuals aged 18 years and above, with 2 doses spaced 10-12 weeks apart.
- CoronaVac (Sinovac): An inactivated vaccine for individuals aged 18-59 years, with 2 doses spaced 2-4 weeks apart.
- Pfizer: An RNA-based vaccine for individuals aged 12 years and above, with 2 doses spaced 3 weeks apart [62,63].

As shown in Figures 2.2 and 2.3, as of November 26, 2023, 78% of Thailand's population received the complete primary series of a COVID-19 vaccine, and 46% received at least one booster dose, demonstrating substantial vaccine coverage and booster uptake across the country.

Preparation for Receiving COVID-19 Vaccines:

It is recommended to get plenty of sleep before vaccination and to avoid alcoholic drinks. After receiving the vaccine, mild side effects such as pain, swelling, and redness at the injection site may occur. Most symptoms are not severe, but in some cases, severe allergic reactions may happen. Therefore, it is necessary to observe symptoms for 30 minutes in a medical facility or vaccination site following the injection. Individuals with a history of COVID-19 infection may still be susceptible to reinfection. Therefore, those who have recovered from COVID-19 are advised to get vaccinated, waiting at least 3 months after their initial infection [40].

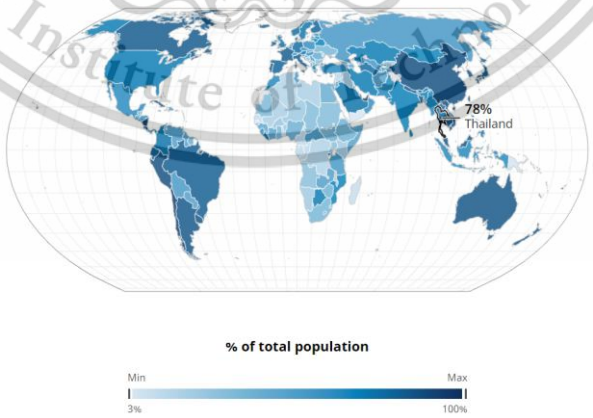

Figure 2.2 On November 26, 2023, in Thailand, the documented proportion of the entire population completing the primary round of COVID-19 vaccinations is noted in the data [42].

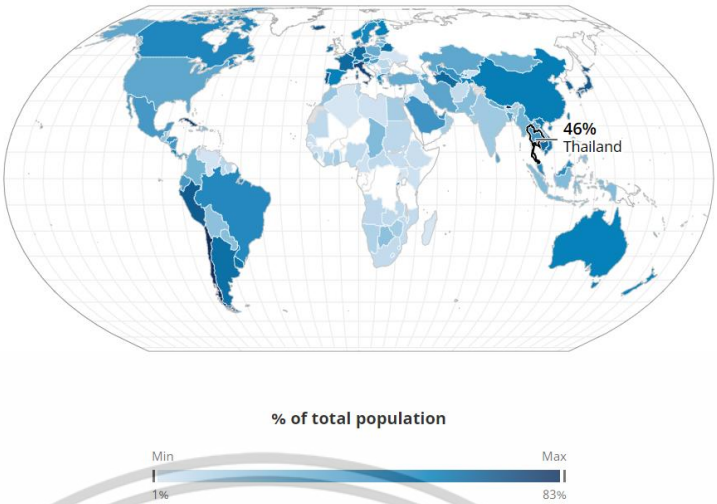

Figure 2.3 depicts the percentage of individuals within Thailand's population who had been administered at least one booster dose of a COVID-19 vaccine as of November 26, 2023 [42].

2.3 COVID-19 in Thailand

The COVID-19 pandemic in Thailand was first identified in January 2020, when the initial case was detected through screening procedures implemented at entry and exit checkpoints. The infected person was a Chinese tourist who entered Thailand on 12 January 2020. Later, on 31 January 2020, Thailand reported its first confirmed case of local transmission in a taxi driver who had never traveled abroad. After that, the pandemic in Thailand continued, with the virus spreading widely across all regions. According to reports on COVID-19 transmission periods, there have been a total of 5 waves:

- First Wave (January – November 2020): Related to a large cluster outbreak in crowded areas like a boxing stadium and gambling venues.
- Second Wave (December 2020 – March 2021): The major source of the spread was a shrimp market in Samut Sakhon province.
- Third Wave (April – June 2021): Originated in Bangkok's Thonglor nightlife venues.
- Fourth Wave (July – December 2021)
- Fifth Wave (January 2022 to present): The largest spread to date.

As shown in Figures 2.4 and 2.5, from the beginning of the pandemic until 31 December 2023, Thailand reported a total of 4,762,375 confirmed cases and 34,517 deaths [30,31].

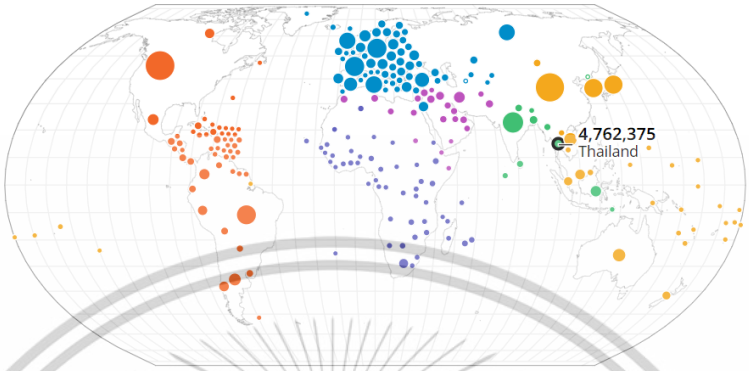

Figure 2.4 Total cumulative COVID-19 cases reported to the WHO in Thailand as of December 31, 2023 [32].

Figure 2.5 Presents the cumulative number of COVID-19 fatalities reported to the WHO in Thailand as of December 31, 2023 [33].

2.4 Basic theorem and definition background

Definition 2.1 (Equilibrium point [17]) The point $X^* \in \mathbb{R}^n$ is **the equilibrium point** of

$$\frac{dX}{dt} = f(t, X) \tag{2.1}$$

if $f(t, X^*) = 0$ for all t.

From Prathumwan et al. [17] is the model for COVID-19 and the equation can be described as follows:

$$\begin{cases} \dfrac{dS}{dt} = \Lambda - a_1 SL - a_2 SI - \mu S \\ \dfrac{dL}{dt} = a_1 SL + a_2 SI - a_3 L - a_4 L - \mu L \\ \dfrac{dI}{dt} = a_3 L - k\alpha I - k\beta I - k(1-\alpha-\beta)I - \varepsilon I - \mu I \\ \dfrac{dQ}{dt} = a_4 L + k\beta I - a_5 Q - a_6 Q - \mu Q \\ \dfrac{dH}{dt} = k\alpha I + a_6 Q - a_7 H - \mu H \\ \dfrac{dR}{dt} = k(1-\alpha-\beta)I + a_5 Q + a_7 H - \mu R \end{cases} \tag{2.2}$$

when $N(t) = S(t) + L(t) + I(t) + Q(t) + H(t) + R(t)$.

The equilibrium point of equation (2.2) can be found by taking the right equation of equation (2.2) equal to zero, two equilibrium points are obtained:

I. The disease-free equilibrium point, $E^0 = \left(\frac{\Lambda}{\mu}, 0, 0, 0, 0, 0\right)$.

II. The endemic equilibrium point, $E^* = \left(S^*, L^*, I^*, Q^*, H^*, R^*\right)$,

where $S^* = \dfrac{AB}{a_1 B + a_2 a_3}$,

$L^* = \dfrac{\Lambda}{A} - \dfrac{\mu B}{a_1 B + a_2 a_3}$,

$I^* = \dfrac{a_3 L^*}{B}$,

$Q^* = \dfrac{a4L^* + k\beta I^*}{a_5 + a_6 + \mu}$,

$H^* = \dfrac{k\alpha I^* + a_6 Q^*}{a_7 + \mu}$,

$R^* = \dfrac{k(1-\alpha-\beta) + a_5 Q^* + a_7 H^*}{\mu}$,

with and $B = k + \mu + \varepsilon$.

Definition 2.2 (The basic reproductive number [64]). The basic reproductive number is the average number of secondary infections that one infected individual that shall take place during the period of infection, provided that when the population is at risk (R_0 can be calculated using the next-generation matrix method).

Definition 2.3 (Next-generation matrix method [64]) When X is the vector of a new infection, such as carrier, infectious, exposed, etc. When Y is the vector transmission of infection from one group to another group. Therefore,

$$\frac{dX}{dt} = \bar{F}(X,Y) - \bar{V}(X,Y).$$

$\bar{F}(X,Y)$: The rate that infected persons in Y shall cause a new infection in X.

$\bar{V}(X,Y)$: Vector transmission of infection from one group to another group.

Vector-valued functions $\bar{F}(X,Y)$ and $\bar{V}(X,Y)$ of X and Y are determined to be

$$F=\left(\frac{\partial \bar{F}}{\partial X}\right),\ V=\left(\frac{\partial \bar{V}}{\partial X}\right),$$

At the disease-free equilibrium, FV^{-1} is called the next-generation matrix method to derive the basic reproductive number (R_0) given by the distinctive radius shown by $\rho(FV^{-1})$. The distinctive radius of FV^{-1} is the most distinctive characteristic value of FV^{-1}. Therefore, the basic reproductive number (R_0) is the most distinctive characteristic value of FV^{-1}.

From Prathumwan et al. [17], based on the equation (2.2) Expressions L, I and Q are considered to make Matrix F and Matrix V.

$$f=\begin{bmatrix} a_1SL+a_2SI \\ 0 \\ a_4L+k\beta I \end{bmatrix}, v=\begin{bmatrix} (a_3+a_4+\mu)L \\ -a_3L+(k+\mu+\varepsilon)I \\ (a_5+a_6+\mu)Q \end{bmatrix}$$

Therefore, it is obtained that the Jacobian matrices of f and v at the disease-free equilibrium $E^0=\left(\frac{\Lambda}{\mu},0,0,0,0,0\right)$ F and V :

$$F=\begin{bmatrix} \frac{\partial(a_1SL+a_2SI)}{\partial L} & \frac{\partial(a_1SL+a_2SI)}{\partial I} & \frac{\partial(a_1SL+a_2SI)}{\partial Q} \\ \frac{\partial(0)}{\partial L} & \frac{\partial(0)}{\partial I} & \frac{\partial(0)}{\partial Q} \\ \frac{\partial(a_4L+k\beta I)}{\partial L} & \frac{\partial(a_4L+k\beta I)}{\partial I} & \frac{\partial(a_4L+k\beta I)}{\partial Q} \end{bmatrix}=\begin{bmatrix} a_1S & a_2S & 0 \\ 0 & 0 & 0 \\ a_4 & k\beta & 0 \end{bmatrix},$$

$$V=\begin{bmatrix} \frac{\partial(a_3+a_4+\mu)L}{\partial L} & \frac{\partial(a_3+a_4+\mu)L}{\partial I} & \frac{\partial(a_3+a_4+\mu)L}{\partial Q} \\ \frac{\partial(-a_3L+(k+\mu+\varepsilon)I)}{\partial L} & \frac{\partial(-a_3L+(k+\mu+\varepsilon)I)}{\partial I} & \frac{\partial(-a_3L+(k+\mu+\varepsilon)I)}{\partial Q} \\ \frac{\partial(a_5+a_6+\mu)Q}{\partial L} & \frac{\partial(a_5+a_6+\mu)Q}{\partial I} & \frac{\partial(a_5+a_6+\mu)Q}{\partial Q} \end{bmatrix}$$

$$=\begin{bmatrix} a_3+a_4+\mu & 0 & 0 \\ -a_3 & k+\mu+\varepsilon & 0 \\ 0 & 0 & a_5+a_6+\mu \end{bmatrix},$$

and

$$V^{-1}=\begin{bmatrix} \frac{1}{a_3+a_4+\mu} & 0 & 0 \\ \frac{a_3}{(a_3+a_4+\mu)(k+\mu+\varepsilon)} & \frac{1}{k+\mu+\varepsilon} & 0 \\ 0 & 0 & \frac{1}{a_5+a_6+\mu} \end{bmatrix}.$$

Then $$FV^{-1} = \begin{bmatrix} \frac{a_1 S}{A} & \frac{a_2 a_3 S}{AB} & 0 \\ 0 & 0 & 0 \\ \frac{a_4}{A} & \frac{k\beta a_3}{AB} & 0 \end{bmatrix},$$

where $A = a_3 + a_4 + \mu$ and $B = k + \mu + \varepsilon$.

Therefore

$$R_0 = \frac{(a_1 B + a_2 a_3)S}{AB}.$$

Theorem 2.1 (Lyapunov [65,66]) when x^* is the equilibrium point of the system, when $\dot{x} = f(x)$ is the continuous function and the continuous real-valued function V in a neighborhood with an equilibrium point $x^* \in \Omega$ that shall become Lyapunov function when

1. $V(x^*) = 0$,
2. $V(x) > 0$ if $x \neq x^*$,
3. $\dot{V}(x^*) < 0$ in $\Omega - x^*$.

If $\dot{V}(x^*) < 0$ in $\Omega - x^*$. Therefore, x^* has globally asymptotically stable.

Theorem 2.2 (Lasalle's [65,66]) Let f be a locally Lipschiptz function defined over a domain $D \subset \mathbb{R}^n$ and $\Omega \subset D$ be a compact set that is positively invariant with respect to $\dot{x} = f(x)$. Let $V(x)$ be a C^1 function defined over C^1 such that $\dot{V}(x^*) < 0$ in Ω. Let E be a set all points in Ω where $V(x^*) = 0$ and M be the largest invariant set in E Then every solution stating in Ω approaches M as $t \to \infty$, means that $d(x(t, x_0), M)_{t \to \infty} \to 0$, for all $x_0 \in \Omega$.

Proof. Suppose $p \in \Omega$ and consider the curve $t \to x(t, p)$. Since V is continuous it is bounded from below from on the compact set Ω. Since Ω is invariant by hypothesis,

$$\text{for all } t \geq 0, \quad x(t, p) \in \Omega.$$

Moreover, using that Ω is compact, and hence bounded, the positive limit set L^+ is non-empty. Since Ω is closed,

$$L^+ \subseteq \Omega.$$

Using the Lemma above,

$$\text{for all } q \in L^+, \quad V'(q) = 0$$

and therefore,

$$L^+ \subseteq \{y : V'(y) = 0\} = E \subseteq M.$$

Since the positive limit sets are invariant,

$$L^+ \subseteq M.$$

Since

$$L^+ \subseteq M,$$

it follows that

$$q \in M.$$

Thus, the solution curve starts at an arbitrary $p \in \Omega$ approaches M as $t \to \infty$.

Definition 2.4 (Basic Optimal control problem in Lagrange formulation [52,67,68]) An optimal control problem is in the form

$$J[x(t),u(t)] = \max_u \int_{t_0}^{t_f} f(t,x(t),u(t))dt.$$

Subject to

$$\begin{aligned} x'(t) &= g(t,x(t),u(t)), \\ x(t_0) &= x_0. \end{aligned} \tag{2.3}$$

$x(t_f)$ could be free, which means that the value of $x(t_f)$ is unrestricted, or could be fixed, i.e, $x(t_f) = x_f$.

Definition 2.5 (Hamiltonian [52,67,68]) Let the previous optimal control problem be considered in (2.3). The function

$$H(t,x(t),u(t),\lambda(t)) = f(t,x(t),u(t)) + \lambda(t)g(t,x(t),u(t))$$

is called the Hamiltonian function and λ is the adjoint variable.

Definition 2.6 (Pontryagin's Maximum Principle [52,68-70]). If $u^*(t)$ and $x^*(t)$ are optimal for problem (2.3), then there exists a piecewise differentiable adjoint variable $\lambda(t)$ such that

$$H(t,x^*(t),u(t),\lambda(t)) \le H(t,x^*(t),u^*(t),\lambda(t))$$

for all controls u at each time t, where H is the Hamiltonian previously defined and

$$\begin{aligned} \lambda'(t) &= -\frac{\partial H(t,x^*(t),u^*(t),\lambda(t))}{\partial x}, \\ \lambda(t_f) &= 0. \end{aligned}$$

We have already show with this adjoint and Hamiltonian, $H_u = 0$ at $u^*(t)$. Namely, the Hamiltonian has a critical point, in the u variable, at $u^*(t)$.

Theorem 2.3 [52,67,68,70] Suppose that $f(t,x,u)$ and $g(t,x,u)$ are both continuously differentiable functions in their three arguments and concave in u. Suppose u^* is an

optimal control for problem equation (2.3), with associated state x^*, and λ a piecewise differentiable function with $\lambda(t) \geq 0$ for all t. Suppose for all $t_0 \leq t \leq t_1$

$$H_u(t, x^*(t), u^*(t), \lambda(t)) = 0.$$

Then for all controls u and each $t_0 \leq t \leq t_1$, we have

$$H(t, x^*(t), u(t), \lambda(t)) \leq H(t, x^*(t), u^*(t), \lambda(t)).$$

2.5 Mathematical modeling studies

The mathematical model is essential for analyzing disease spread and control. A review of literature relevant to the research objectives was conducted in this section. Some of them are shown in the following part.

In 2020, Carcione et al. [71] used a SEIR model to calculate the number of infected populations and the number of populations that died of COVID-19 to analyze the epidemic situation in Lombardy, Italy, as follows:

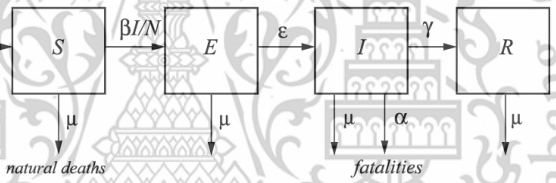

Figure 2.6 A typical SEIR model.

Based on the mathematical model as shown in Figure 2.6, a differential equation to describe the relationship can be written as follows:

$$\begin{cases} \frac{dS}{dt} = \Lambda - \mu S - \beta S \frac{I}{N}, \\ \frac{dE}{dt} = \beta S \frac{I}{N} - (\mu + \varepsilon)E, \\ \frac{dI}{dt} = \varepsilon E - (\gamma + \mu + \alpha)I, \\ \frac{dR}{dt} = \gamma I - \mu R. \end{cases} \tag{2.4}$$

Where $N = S + E + I + R.$ (2.5)

Table 2.1 Shows the variable and parameter values of the model.

Parameters/Variables	Definition
S	The number of susceptible populations.
E	The number of exposed populations.

I	The number of infected populations.
R	The number of recovered populations.
N	The total number of populations.
Λ	The number of initial populations.
β	The infection rate.
ε	The incubation rate.
γ	The recovery rate.
μ	The natural mortality rate.
α	The mortality rate from COVID-19.

According to the study, there was uncertainty in the parameter values which may be caused by the variation of the quarantine, social distancing, incubation period, mortality rate, etc. Thus, analysis and modification were made to the parameter values and the initial condition values to obtain a model suitable for the actual data of the deaths caused by COVID-19. The data used in the analysis and comparison this time were from the actual data of the deaths caused by the disease reported in Lombardy, Italy until 5 May 2020.

In 2021, Bhadauria et al. [72] formulated a mathematical model and analyzed a SEIQR model as shown in Figure 2.7 by considering the delay in conversion of the exposed population to the infected population. According to the study, the findings highlight that increasing delays can reduce infection rates by allowing stronger immune responses but may cause oscillatory behavior in infected populations. An increase in the delays enabled patients to be in the asymptomatic stage for a long time, recovery shall replace infection. If that person has sufficient immunity, the size of the infected population shall decrease. However, it can be seen that the size of the infected population indicates that the asymptomatic stage affected an increased number of the infected population and the number of recovered populations. As a result, the number of infected populations fluctuates over time.

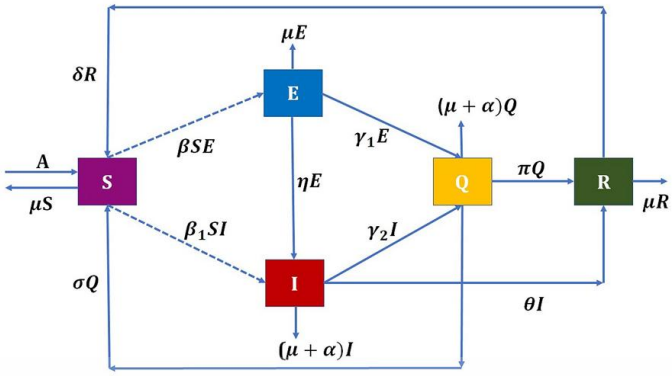

Figure 2.7 A typical SEIQR model.

The equation system can be described as follows:

$$\begin{cases} \dfrac{dS}{dt} = A - \beta SE - \beta_1 SI - \mu S + \delta R + \sigma Q, \\ \dfrac{dE}{dt} = \beta SE - (\mu + \eta + \gamma_1)E, \\ \dfrac{dI}{dt} = \beta_1 SI + \eta E - (\mu + \alpha + \gamma_2 + \theta)I, \\ \dfrac{dQ}{dt} = \gamma_1 E + \gamma_2 I - (\mu + \pi + \sigma + \alpha)Q, \\ \dfrac{dR}{dt} = \theta I + \pi Q - (\mu + \delta)R. \end{cases} \tag{2.6}$$

Where $N = S + E + I + Q + R.$ (2.7)

Table 2.2 Shows the variables and parameter values of the SEIQR model.

Parameters/Variables	Definition
S	The number of susceptible populations.
E	The number of exposed populations.
I	The number of infected populations.
Q	The number of quarantined populations.
R	The number of recovered populations.
A	The number of initial populations.
β	Infection rate from the exposed population.
β_1	Infection rate.
η	Incubation rate.
γ_1	Moving rate from the group of exposed population to the group of quarantined population.

γ_2	Moving rate from the group of infected population to the group of quarantined population.
π	The recovery rate of the quarantined group.
θ	The recovery rate of the infected group.
δ	Moving rate from the recovered group to the susceptible group.
σ	Moving rate from the quarantined group to the susceptible group.
μ	Natural mortality rate.
α	Mortality rate from COVID-19.

Yang and Wang [27] formulate a mathematical model to study the spread of COVID-19 in Hamilton County in the state of Tennessee, United States of America to examine the dynamic of the spread, the routes of transmission from person to person, and from environment to humans. Different transmission rates were used to study the characteristics of the spread at different times. Moreover, data fitting was used to ensure the model was suitable for the data of the spread in Hamilton County. As shown in Figure 2.8, a schematic representation of the model illustrates the components and transmission routes of COVID-19 in the studied population.

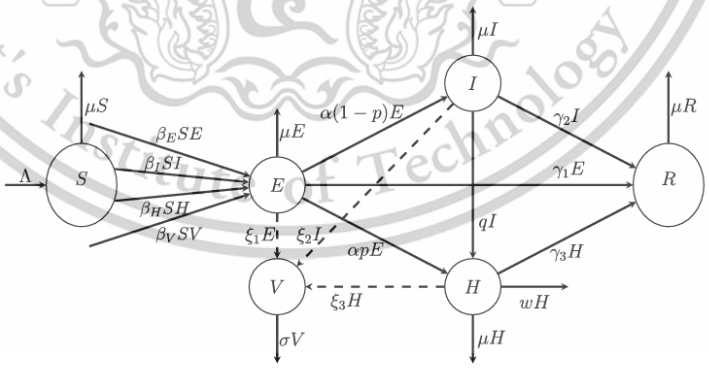

Figure 2.8 A schematic representation of the model (2.8).

According to the above diagram of the model, a differential equation system can be written as follows:

$$\begin{cases} \frac{dS}{dt} = \Lambda - \beta_E SE - \beta_I SI - \beta_H SH - \beta_V SV - \mu S, \\ \frac{dE}{dt} = \beta_E SE + \beta_I SI + \beta_H SH + \beta_V SV - (\alpha + \gamma_1 + \mu)E, \\ \frac{dI}{dt} = \alpha(1-p)E - (q + \gamma_2 + \mu)I, \\ \frac{dH}{dt} = \alpha pE - qI - (\omega + \gamma_3 + \mu)H, \\ \frac{dR}{dt} = \gamma_1 E + \gamma_2 I + \gamma_3 H - \mu R, \\ \frac{dV}{dt} = \xi_1 E + \xi_2 I + \xi_3 H - \sigma V. \end{cases} \quad (2.8)$$

Table 2.3 Shows definitions of variables and parameters of the model (2.8).

Parameters/Variables	Definition
S	The number of susceptible populations.
E	The number of exposed populations.
I	The number of infected populations.
H	The number of hospitalized populations.
R	The number of recovered populations.
V	The concentration of the coronavirus in the environment.
Λ	Inflow rate of population.
β_E	Transmission rate between exposed groups and susceptible groups.
β_I	Transmission rate between infected people and susceptible groups.
β_H	Transmission rate between hospitalized people and susceptible groups.
β_V	Transmission rate between environmental groups to humans.
α	Incubation rate.
p	The ratio of people exposed to COVID-19 to severely ill and being hospitalized after incubation period.
q	The ratio of infected people and being hospitalized.
ω	The mortality rate from COVID-19.
ξ_1	Transmission rate of the coronavirus to the environment from groups of exposed people.

ξ_2	Transmission rate of the coronavirus to the environment from groups of infected people.
ξ_3	Transmission rate of the coronavirus to the environment from groups of hospitalized people.
γ_1	The recovery rate of groups of exposed people.
γ_2	The recovery rate of groups of infected people.
γ_3	The recovery rate of groups of hospitalized people.
μ	The natural mortality rate.
σ	Virus removal rate from the environment.

As for the case study in Hamilton County, it was found that the environment plays an important role in disease transmission. It was also found that many limitations were not considered by the model like the impact on the gate of the population, since age is considered one of the risk factors of disease severity, affecting the mortality rate in different age groups, including age-dependent parameters, i.e. transmission rate, the hospitalization rate, and incubation period of the virus. Thus, these factors should be considered in future research.

In 2022, Khan and Atangana [3] studied the dynamic of COVID-19, Omicron variant spread by making a mathematical model to understand new variables of the spread in conjunction with the use of actual data of the spread from South Africa from 1 November 2021 to 23 January 2022. In addition, consideration was made to the infection from the Omicron variant, symptomatic infection, and asymptomatic infection from a numerical model to see the outcomes and parameters affecting the spread. It was found that people were able to reduce the infection rate by social distancing, wearing masks, hand washing, and social gathering. Figure 2.9 illustrates the transmission diagram of the model, highlighting key components and transmission routes related to the Omicron variant.

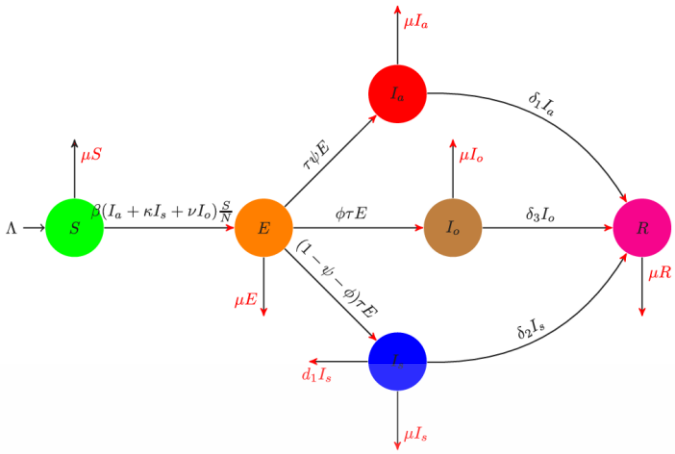

Figure 2.9 Transmission diagram of the model (2.9).

From the diagram, an equation can be written as follows:

$$\begin{cases} \frac{dS(t)}{dt} = \Lambda - \frac{\beta(I_a+\kappa I_s+\nu I_o)S}{N} - \mu S, \\ \frac{dE(t)}{dt} = \frac{\beta(I_a+\kappa I_s+\nu I_o)S}{N} - (\tau+\mu)E, \\ \frac{dI_a(t)}{dt} = \tau\psi E - (\delta_1+\mu)I_a, \\ \frac{dI_s(t)}{dt} = (1-\psi-\phi)\tau E - (\delta_2+\mu+d_1)I_s, \\ \frac{dI_o(t)}{dt} = \phi\tau E - (\delta_3+\mu)I_o, \\ \frac{dR(t)}{dt} = \delta_1 I_a + \delta_2 I_s + \delta_3 I_o - \mu R. \end{cases} \quad (2.9)$$

Table 2.4 Describes the definition of the model (2.9).

Parameters/Variables	Definition
S	Susceptible population.
E	Exposed population.
I_a	Asymptomatic population.
I_s	Symptomatic population.
I_o	Population infected with COVID-19 Omicron variant.
R	Recovered population.
Λ	Birth rate.
β	Contact rate.
κ	Infection rate of symptomatic population.

ν	Infection rate of population infected with COVID-1 9 Omicron variant.
τ	Incubation rate.
ψ	The rate of flow to asymptomatic population.
ϕ	The rate of flow to population infected with COVID-19 Omicron variant.
δ_1	Recovery rate of asymptomatic population.
δ_2	Recovery rate of symptomatic population.
δ_3	Recovery rate of population infected with COVID-1 9 Omicron variant.
d_1	Mortality rate of asymptomatic population.
μ	Natural mortality rate.
N	Total population.

The review of the literature is relevant to the optimal control model.

In 2021 Hussain et al. [73] designed a SEIQR mathematical model to cope with the epidemic situation. Data were collected from infected people in Pakistan to analyze and predict the outcomes obtained from the model analysis. In addition, the sensitivity was analyzed to study parameters affecting the epidemic for extending to find a strategy for controlling the epidemic accordingly. A basic model obtained is as follows:

$$\begin{cases} \frac{dS}{dt} = \Lambda - \beta SI - \mu S, \\ \frac{dE}{dt} = \beta SI - \alpha_1 E - \mu E, \\ \frac{dI}{dt} = \alpha_1 E - (\mu + \gamma + \eta) I, \\ \frac{dQ}{dt} = -\phi Q - \mu Q + \gamma(1-\delta) I, \\ \frac{dR}{dt} = \phi Q + \delta\gamma I - \mu R. \end{cases} \tag{2.10}$$

Table 2.5 Description of variables and parameters of the model (2.10).

Parameters/Variables	Definition
S	Susceptible population.
E	Exposed population.

I	Infected population.
Q	Quarantined population.
R	Recovered population.
Λ	The birth rate of the susceptible population
β	Transmission rate.
α_1	Incubation rate.
γ	The recovery rate of the infected population.
η	Mortality rate from the disease.
ϕ	Quarantine rate of infected population.
δ	The resting part of infected individuals who are quarantined.
μ	Natural mortality rate.

The sensitivity index analysis made known an optimal control strategy for the spread of the disease to win against COVID-19. Next, the model (2.10) was expanded by designing an optimal control model to control a spread situation that may occur in the future as seen from the equation below:

$$\begin{cases} \frac{dS}{dt} = \Lambda - \beta(1-u_1)SI - \mu S, \\ \frac{dE}{dt} = \beta(1-u_1)SI - \alpha_1 E - \mu E - r_1 u_2 E, \\ \frac{dI}{dt} = \alpha_1 E - (\mu + \gamma + \eta)I, \\ \frac{dQ}{dt} = -\phi Q - \mu Q + \gamma(1-\delta)I + r_1 u_2 E, \\ \frac{dR}{dt} = \phi Q + \delta\gamma I - \mu R. \end{cases} \tag{2.11}$$

The design of the control strategy was implemented using a preventive measure through social distancing and mask-wearing. It was determined to be $u_1(t)$ to reduce transmission to people and $u_2(t)$, namely, a rapid measure for isolation and quarantine of infected people to inhibit the spread of COVID-19 as soon as possible. The optimal control function was sought by determining the objective function J to reduce the number of infected people and to reduce the cost of disease control. The objective functions obtained are as follows:

$$J(u_1, u_2) = \int_0^T \left(M_1 E + M_2 I + M_3 Q + D_1 u_1^2 + D_2 u_2^2 \right) dt. \tag{2.12}$$

When M_1, M_2, M_3, D_1, D_2 are the positive weights. Based on the optimal control function through social distancing, and mask-wearing, including isolation and quarantine of infected people, according to the numerical result analysis, it was found that if the control strategy was used, the number of patients would be decreased. However, to control the situation, additional strategies may be determined or groups of hospitalized people should be added, in case there will be disease intervention in the future.

Shen et al. [5] considered a COVID-19 model in a new way by designing a model by considering the vaccinated population and studying the detailed results of a vaccine model while the optimal control was considered to reduce the spread of the virus and control the infection. Four different measures were used to control the results suitable for the actual information of the spread. A differential equation system obtained is as follows:

$$\begin{cases} \frac{dS(t)}{dt} = \Pi + \omega V - \frac{(\beta_1 A + \beta_2 I)}{N} S - (\nu + \mu) S, \\ \frac{dV(t)}{dt} = \nu S - (1-\theta)\frac{(\beta_1 A + \beta_2 I)}{N} V - (\omega + \mu) V, \\ \frac{dE(t)}{dt} = \frac{(\beta_1 A + \beta_2 I)}{N} S + (1-\theta)\frac{(\beta_1 A + \beta_2 I)}{N} V - (\delta + \mu) E, \\ \frac{dA(t)}{dt} = \rho\delta E - (\gamma_1 + \mu) A, \\ \frac{dI(t)}{dt} = (1-\rho)\delta E - (\gamma_2 + \mu + d) I, \\ \frac{dR(t)}{dt} = \gamma_1 A + \gamma_2 I - \mu R. \end{cases} \tag{2.13}$$

Table 2.6 Description of variables and parameters of the model.

Parameters/Variables	Definition
S	Susceptible population.
V	Population receiving COVID-19 vaccination.
E	Exposed population.
A	Asymptomatic population.
I	Infected population.
R	Recovered population.
Π	Birth rate.
β_1	Infection rate of the asymptomatic population.

β_2	Infection rate of the symptomatic population.
ν	Vaccination rate.
ω	Vaccine waning rate.
δ	Incubation rate.
ρ	Proportion rate.
γ_1	Recovery rate of asymptomatic population.
γ_2	Recovery rate of symptomatic population.
μ	Natural mortality rate.
d	Mortality rate from COVID-19.

From the equation system (2.13), the research team used the theory of optimal control to design different controls to find a guideline to reduce the number of infected people and reduce the spread of the virus in communities. Control variables were determined as follows: The first control variable u_1 is to control by prevention/isolation to reduce the contact between healthy persons and infected persons. The second control variable u_2 is to control by vaccination since vaccination can reduce the risk of infection. The third control variable u_3 is rapid screening for infected persons, and the last control variable u_4 is to control infected persons without screening. From what was mentioned above, the control problem can be written as follows:

$$\begin{cases} \dfrac{dS(t)}{dt} = \Pi + \omega V - \dfrac{(\beta_1 A + \beta_2 I)}{N} S(1-u_1) - (\nu u_2 + \mu)S, \\ \dfrac{dV(t)}{dt} = \nu u_2 S - (1-\theta)\dfrac{(\beta_1 A + \beta_2 I)}{N} V - (\omega + \mu)V, \\ \dfrac{dE(t)}{dt} = \dfrac{(\beta_1 A + \beta_2 I)}{N} S + (1-\theta)\dfrac{(\beta_1 A + \beta_2 I)}{N} V - ((1-u_3)\delta + \mu)E, \\ \dfrac{dA(t)}{dt} = \rho\delta u_3 E - (\gamma_1 + \mu + b_1 u_4)A, \\ \dfrac{dI(t)}{dt} = (1-\rho)\delta u_3 E - (\gamma_2 + \mu + d + b_2 u_4)I, \\ \dfrac{dR(t)}{dt} = \gamma_1 A + \gamma_2 I - \mu R. \end{cases} \tag{2.14}$$

Objective function is determined as follow:

$$J(u_1, u_2, u_3, u_4) = \int_0^{T_f} \left(B_1 E + B_2 A + B_3 I + \frac{1}{2}\left[B_4 {u_1}^2 + B_5 {u_2}^2 + B_6 {u_3}^2 + B_7 {u_4}^2 \right] \right) dt. \tag{2.15}$$

When B_j for $j = 1,\ldots,7$ describing the weight or the balancing constants, and T_f is the final time. The results based on using all 4 control measures, considered from the

numerical analysis, revealed that the control was able to reduce the number of infected persons and the recovery rate of patients increased efficiently. However, the control measures utilizing social distancing, mask-wearing, washing hands using alcohol gel regularly, and vaccination should be performed continuously to reduce future spread sustainably.

In 2022 Khan et al. [10] surveyed the dynamic of the COVID-19 pandemic and the effects of COVID-19 vaccines. A model was made and a vaccination class was introduced. The sensitivity index was analyzed to observe the behavior of parameters towards the spread of the disease. A numerical simulation was given to describe effects in various situations of vaccine efficacy and control measures. From what was mentioned above, the vaccination model obtained is as follows:

$$\begin{cases} \dfrac{dS}{dt} = \Theta - \beta(I+\kappa E)\dfrac{S}{N} - (\psi_v + \mu)S + \eta_v V + \theta R, \\ \dfrac{dE}{dt} = \beta(I+\kappa E)\dfrac{S}{N} - (\mu+\gamma)E, \\ \dfrac{dI}{dt} = \gamma E - (\mu+\mu_0+\omega)I, \\ \dfrac{dV}{dt} = \psi_v S - (\mu+\eta_v)V, \\ \dfrac{dR}{dt} = \omega I - (\mu+\theta)R. \end{cases} \tag{2.16}$$

Table 2.7 Definition of variables and parameters of the model (2.16).

Parameters/Variables	Definition
S	Susceptible population.
E	Exposed population.
I	Infected population.
V	Vaccinated population.
R	Recovered population.
Θ	Initial population.
β	The effective contact rate.
κ	The relative transmissibility rate.
ψ_v	Vaccination rate.
η_v	Vaccine waning rate.
θ	Loss of immunity to the disease.
γ	Rate of infection development with symptoms.

ω	The recovery rate of the infected population.
μ_0	Mortality rate from the disease.
μ	Natural mortality rate.
N	Total population.

The model was restructured by using the optimal control model according to the following controls: $u_1(t)$ is the control for isolation, $u_2(t)$ is the control for vaccine efficacy, and $u_3(t)$ is the control for efficacy of treatments. The control model obtained is as follows:

$$\begin{cases} \frac{dS}{dt} = \Theta - \beta(I+\kappa E)\frac{S}{N}(1-u_1(t)) - (u_2(t)+\mu)S + \eta_v V + \theta R, \\ \frac{dE}{dt} = \beta(I+\kappa E)\frac{S}{N}(1-u_1(t)) - (\mu+\gamma)E, \\ \frac{dI}{dt} = \gamma E - (\mu+\mu_0+u_3(t))I, \\ \frac{dV}{dt} = u_2(t)S - (\mu+\eta_v)V, \\ \frac{dR}{dt} = u_3(t)I - (\mu+\theta)R. \end{cases} \tag{2.17}$$

Under a non-negative condition to reduce the spread of COVID-19, the objective function obtained is as follows:

$$J(u_1,u_2,u_3) = \int_0^{T_f} \left(A_1E + A_2V + A_3I + \frac{1}{2}\left(A_4{u_1}^2 + A_5{u_2}^2 + A_6{u_3}^2 \right) \right) dt. \tag{2.18}$$

In this study, the research team designed 3 control strategies as shown below:

Strategy 1: Controlling for one variable

To control only one variable, 3 cases of the control are required:

Case 1 – the control for isolation only, which will increase the efficiency of exposure to the virus.

$$(u_1 \neq 0, u_2 = 0, u_3 = 0)$$

Case 2 – the control for vaccine efficacy only.

$$(u_1 = 0, u_2 \neq 0, u_3 = 0)$$

Case 3 – the control for treatment efficacy only.

$$(u_1 = 0, u_2 = 0, u_3 \neq 0)$$

Strategy 2: Controlling for dual variables

To control dual variables, 3 cases of the control are required.

Case 1 – the control for isolation and the control for vaccine efficacy.

$(u_1 \neq 0, u_2 \neq 0, u_3 = 0)$

Case 2 – the control for isolation and the control for treatment efficacy.

$(u_1 \neq 0, u_2 = 0, u_3 \neq 0)$

Case 3 – the control for vaccine efficacy and the control for treatment efficacy.

$(u_1 = 0, u_2 \neq 0, u_3 \neq 0)$

Strategy 3: Controlling for all variables simultaneously $(u_1 \neq 0, u_2 \neq 0, u_3 \neq 0)$

According to the situation simulation by controlling different strategies, it can be concluded that controlling for all variables simultaneously in Strategy 3 is more appropriate than controlling Strategy 1 and 2, which will be able to reduce infection in communities and prevent future incidents to a minimum.

According to the review of literature relevant to the research, a mathematical model for COVID-19 was designed and developed from the model [12,53,71,72,74-79] and the optimal control model [23,46,73,80-83]. The pattern of COVID-19 spread was determined by introducing a vaccination class, symptomatic infection, and asymptomatic infection, quarantine for infected persons, and hospitalization. First, a model and a differential equation system were made to describe the model. Next, an equilibrium point of the system and basic reproductive number were analyzed and the stability of the equilibrium point obtained was examined. Lyapunov function was used in the examination. A numerical analysis of the model was performed to examine the behavior of the disease spread. The control, control problem, and objective function were specified, and control strategies were designed to find a guideline for reducing the number of infected persons.

Chapter 3

Research Methodology

3.1 Statistical Data

Coronavirus disease or COVID-19 is caused by a new strain of virus called severe acute respiratory syndrome coronavirus 2 or SARS-CoV-2 [7, 8-15]. The COVID-19 pandemic in Thailand began in January 2020, after which it spread widely and rapidly in every region of the country and has been ongoing since then. The World Health Organization (WHO) reported the situation of the pandemic in Thailand from 5 January 2020 to 31 December 2023. 4,762,375 confirmed cases accounting for 6,823 cases per 100,000 populations and confirmed 34,571 deaths accounting for 49 cases per 100,000 populations [30, 31]. As shown in Figures 3.1 and 3.2, the weekly number of infected people and deaths reported to WHO illustrates the fluctuations in case and death counts over time, capturing significant peaks and declines in the spread and severity of the pandemic in Thailand.

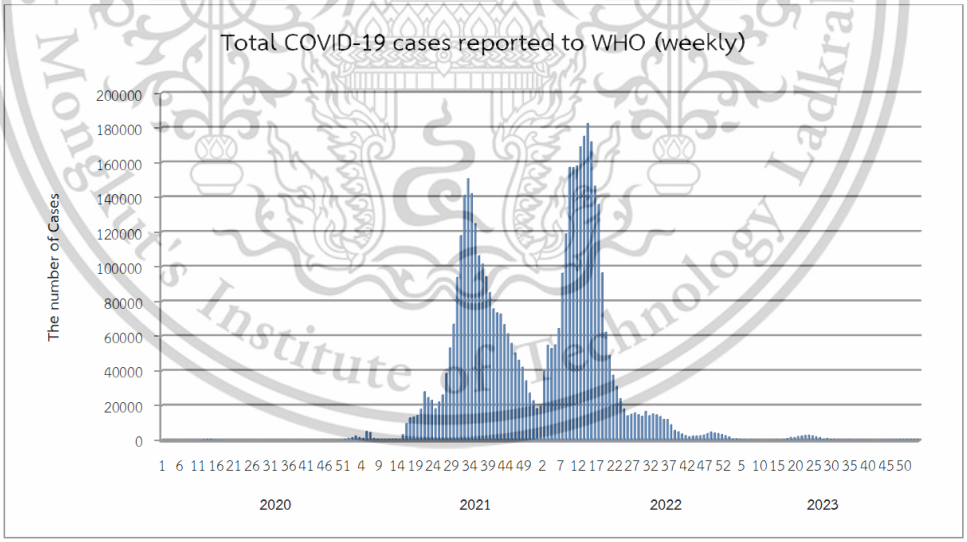

Figure 3.1 Weekly number of infected people [30].

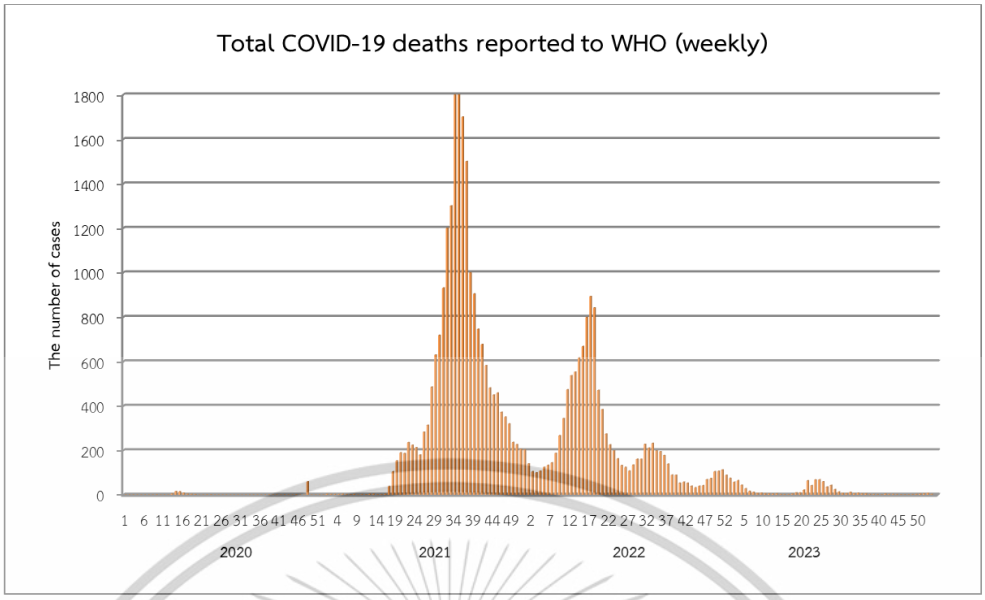

Figure 3.2 Weekly number of deaths [31].

3.2 Mathematical model for COVID-19

Three mathematical models were designed and developed in this research to study spreading behavior in each phase of the pandemic to be a guideline for controlling the pandemic accordingly. Three models were presented as follows:

3.2.1 Mathematical model 1 for COVID-19 considered vaccination, quarantine, and hospitalization.

Mathematical model 1, the population was divided into 7 groups, i.e. the susceptible group, the vaccinated group, the quarantine group, the hospitalization group, and the recovery group. The relationship can be described as follows: The susceptible group shifted to the exposed group and to the vaccinated group (since some people were vaccinated to prevent COVID-19). Similarly, the vaccinated group had a chance to get infected with COVID-19 due to low immunity. When they get COVID-19, they can shift to the exposed group. The incubation period for COVID-19 is 2-14 days. If people lack immunity in the body, they can get COVID-19 and shift to the infected group. After getting infected, some people need to quarantine, and some people need to be hospitalized. After undergoing quarantine and treatment until COVID-19 is no longer in the body, they will enter the recovery phase. From what was mentioned earlier, a diagram can show the relationship as follows:

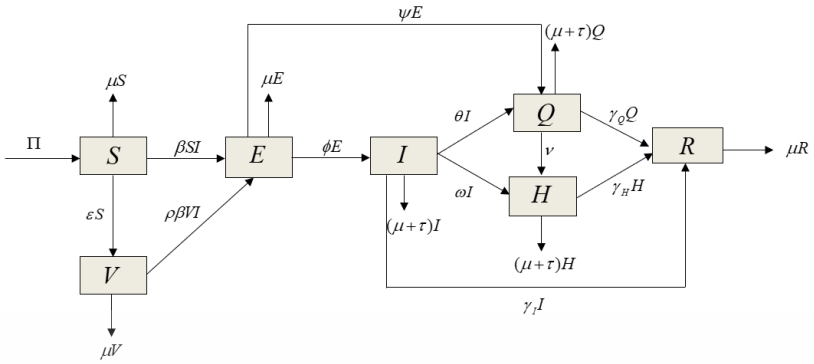

Figure 3.3 Shows the relationship concept for the COVID-19 mathematical model 1.

Notice: According to the model, inward-pointing arrows have positive values and outward-pointing arrows have negative values.

Figure 3.3 shows the basic concept which can be written a mathematical equation as follows:

$$\frac{dS(t)}{dt} = \Pi - \beta S(t)I(t) - (\varepsilon + \mu)S(t), \tag{3.1}$$

$$\frac{dV(t)}{dt} = \varepsilon S(t) - \rho\beta V(t)I(t) - \mu V(t), \tag{3.2}$$

$$\frac{dE(t)}{dt} = \beta S(t)I(t) + \rho\beta V(t)I(t) - (\phi + \psi + \mu)E(t), \tag{3.3}$$

$$\frac{dI(t)}{dt} = \phi E(t) - (\theta + \omega + \gamma_I + \mu + \tau)I(t), \tag{3.4}$$

$$\frac{dQ(t)}{dt} = \theta I(t) + \psi E(t) - (\nu + \gamma_Q + \mu + \tau)Q(t), \tag{3.5}$$

$$\frac{dH(t)}{dt} = \omega I(t) + \nu Q(t) - (\gamma_H + \mu + \tau)H(t), \tag{3.6}$$

$$\frac{dR(t)}{dt} = \gamma_I I(t) + \gamma_Q Q(t) + \gamma_H H(t) - \mu R(t). \tag{3.7}$$

Where $N(t) = S(t) + V(t) + E(t) + I(t) + Q(t) + H(t) + R(t).$ (3.8)

Table 3.1 Symbols representing the message of the model 1.

Symbols	Descriptive
S	The susceptible population.
V	The vaccinated population.
E	The exposed population.
I	The infected population.

Q	The quarantine population.
H	The hospitalized population.
R	The recovered population.
Π	The number of the initial population.
β	Infection rate.
ε	Vaccination rate.
ρ	Protective efficacy of vaccines.
ϕ	Incubation rate.
ψ	The transition rate from the exposed group to the quarantine group.
θ	The transition rate from the infected group to the quarantine group.
ω	The transition rate from the infected group to the hospitalized group.
ν	The transition rate from the quarantine group to the hospitalized group.
γ_I	The recovery rate from the infected population.
γ_Q	The recovery rate from the quarantine group.
γ_H	The recovery rate from the hospitalized group.
μ	The natural mortality rate.
τ	The mortality rate from COVID-19.
N	The number of the entire population.

3.2.2 Mathematical model 2 for COVID-19 by separating the vaccinated population with the consideration of symptomatic, asymptomatic, and hospitalized.

Mathematical model 2, the population was divided into 2 groups, i.e. the unvaccinated population and the vaccinated population, to study the differences between the 2 groups of the population. The unvaccinated population was divided into sub-groups as follows: the susceptible group, the exposed group, the asymptomatic group, and the symptomatic group. In the same way, the vaccinated population was divided into sub-groups as follows: the susceptible group, the exposed group, the asymptomatic group, and the symptomatic group. Both groups entered the hospitalized group and the recovered group. The relationship of the spread of the

model can be described as follows: In the group of unvaccinated population, people are at risk of getting infected with COVID-19. After being exposed to the virus, the virus takes time to incubate in the body. That means people get into the incubation period and the infectious period. Getting infected will depend on the body's immunity. In some cases, there may be no symptoms, but in other cases, symptoms are visible. In those who are asymptomatic, after getting better, they will enter the recovered state while those who are symptomatic, need to be hospitalized. After undergoing treatment, they will enter the recovered state similarly. The vaccinated group has the same infection characteristics, which can be seen in Figure 3.4.

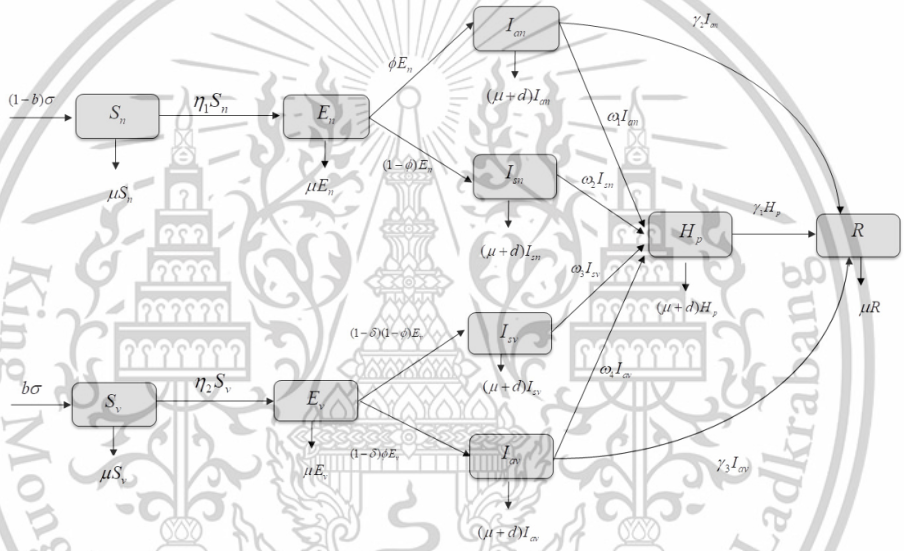

Figure 3.4 Shows the concept of the relationship of Mathematical Model 2 for COVID-19.

Notice: According to the model, inward-pointing arrows have positive values and outward-pointing arrows have negative values.

The risk of a group of the unvaccinated population being exposed to COVID-19 with the rate of infection rate of the group of the unvaccinated population λ_1 was defined as.

$$\eta_1 = \beta_{an} I_{an} + \beta_{sn} I_{sn}. \tag{3.9}$$

Similarly, the infection rate of the group of vaccinated population λ_2 was defined as

$$\eta_2 = \beta_{av} I_{av} + \beta_{sv} I_{sv}. \tag{3.10}$$

Assumption: In Model 2, we assume that the transmission of COVID-19 occurs exclusively within each population group. That is:

1. The vaccinated population transmits the infection only within the vaccinated group. This means that individuals who have received the vaccine can spread the virus only to others within the vaccinated population.
2. The unvaccinated population transmits the infection only within the unvaccinated group. This implies that individuals who have not received the vaccine do not infect vaccinated individuals and vice versa.

This assumption reflects a scenario where interactions between vaccinated and unvaccinated groups are limited in a way that prevents cross-group transmission, potentially due to behavioral factors, immunity barriers, or intervention strategies.

Figure 3.4 shows the basic concept which can be written a mathematical equation as follows:

$$\frac{dS_n}{dt} = (1-b)\sigma - \eta_1 S_n - \mu S_n, \tag{3.11}$$

$$\frac{dE_n}{dt} = \eta_1 S_n - \phi E_n - (1-\phi)E_n - \mu E_n, \tag{3.12}$$

$$\frac{dI_{an}}{dt} = \phi E_n - (\omega_1 + \gamma_2 + \mu + d)I_{an}, \tag{3.13}$$

$$\frac{dI_{sn}}{dt} = (1-\phi)E_n - (\omega_2 + \mu + d)I_{sn}, \tag{3.14}$$

$$\frac{dS_v}{dt} = b\sigma - \eta_2 S_v - \mu S_v, \tag{3.15}$$

$$\frac{dE_v}{dt} = \eta_2 S_v - (1-\delta)\phi E_v - (1-\delta)(1-\phi)E_v - \mu E_v, \tag{3.16}$$

$$\frac{dI_{av}}{dt} = (1-\delta)\phi E_v - (\omega_4 + \gamma_3 + \mu + d)I_{av}, \tag{3.17}$$

$$\frac{dI_{sn}}{dt} = (1-\delta)(1-\phi)E_v - (\omega_3 + \mu + d)I_{sv}, \tag{3.18}$$

$$\frac{dH_p}{dt} = \omega_1 I_{an} + \omega_2 I_{sn} + \omega_3 I_{sv} + \omega_4 I_{av} - (\gamma_1 + \mu + d)H_p, \tag{3.19}$$

$$\frac{dR}{dt} = \gamma_1 H_p + \gamma_2 I_{an} + \gamma I_{av} - \mu R. \tag{3.20}$$

where $N_h = S_n + E_n + I_{an} + I_{sn} + S_v + E_v + I_{av} + I_{sv} + H_p + R.$ (3.21)

Table 3.2 Symbols representing the message of the model 2.

Symbols	Descriptive
S_n	The number of unvaccinated and susceptible populations.
E_n	The number of unvaccinated and exposed populations.
I_{an}	The number of unvaccinated and asymptomatic populations.

I_{sn}	The number of unvaccinated and symptomatic populations.
S_v	The number of vaccinated and susceptible populations.
E_v	The number of vaccinated and exposed populations.
I_{av}	The number of vaccinated and asymptomatic populations.
I_{sv}	The number of vaccinated and symptomatic populations.
H_p	The number of hospitalized populations.
R	The number of recovered populations.
b	The efficacy of vaccination.
σ	The birth rate of the population.
β_{an}	The infection rate of the unvaccinated and asymptomatic population.
β_{sn}	The infection rate of the unvaccinated and symptomatic population.
β_{av}	The infection rate of the vaccinated and asymptomatic population.
β_{sv}	The infection rate of the vaccinated and symptomatic population.
ϕ	COVID-19 incubation period.
δ	Efficacy and effectiveness of COVID-19 vaccination.
ω_1	The hospitalization rate of unvaccinated and asymptomatic population.
ω_2	The hospitalization rate of the unvaccinated and symptomatic population.
ω_3	The hospitalization rate of the vaccinated and symptomatic population.
ω_4	The hospitalization rate of the vaccinated and asymptomatic population.
γ_1	The recovery rate from hospitalization.
γ_2	The recovery rate of the unvaccinated and asymptomatic population.
γ_3	The recovery rate of the vaccinated and asymptomatic population.
μ	The natural mortality rate.
d	COVID-19 mortality rate.
N_h	The number of the entire population.

3.2.3 Mathematical model 3 for COVID-19 by considering the separation of the symptomatic population, asymptomatic population, and the quarantine population.

In mathematical model 3, we divided the population into 6 sub-groups, i.e. the susceptible group, the exposed group, the symptomatic group, the asymptomatic group, the quarantine group, and the recovered group. The relationship of the model can be described as follows: When the susceptible group gets COVID-19, the virus will incubate in the body for 2-14 days. After that, they get infected. In some cases, they are symptomatic and others are asymptomatic, depending on individual immunity. Symptomatic persons whose symptoms are observed need to undergo quarantine to reduce the transmission to other people. After the quarantine, if the test shows no infection, they enter the recovered state. The relationship can be described as seen in Figure 3.5.

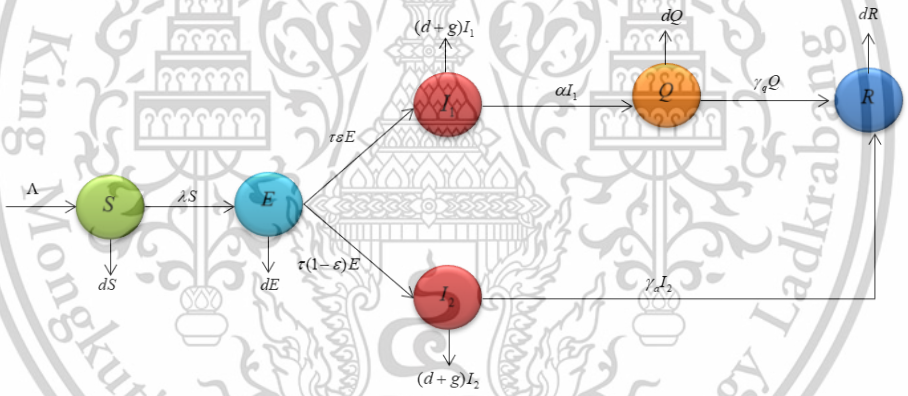

Figure 3.5 Shows the concept of the relationship of Mathematical Model 3 for COVID-19.

Notice: According to the model, inward-pointing arrows have positive values and outward-pointing arrows have negative values.

The susceptible population was determined to get COVID-19 infection from the group of symptomatic population (I_1) and the group of asymptomatic population (I_2). The intensity of the infection is

$$\lambda(t) = \beta_s I_1(t) + \beta_a I_2(t). \tag{3.22}$$

Figure 3.5 shows the basic concept which can be written a differential equation as follows:

$$\frac{dS(t)}{dt} = \Lambda - \lambda S(t) - dS(t), \quad (3.23)$$

$$\frac{dE(t)}{dt} = \lambda S(t) - (\tau\varepsilon + \tau(1-\varepsilon) + d)E(t), \quad (3.24)$$

$$\frac{dtI_1(t)}{dt} = \tau\varepsilon E(t) - (\alpha + g + d)I_1(t), \quad (3.25)$$

$$\frac{dI_2(t)}{dt} = \tau(1-\varepsilon)E(t) - (\gamma_a + g + d)I_2(t), \quad (3.26)$$

$$\frac{dQ(t)}{dt} = \alpha I_1(t) - (\gamma_q + d)Q(t), \quad (3.27)$$

$$\frac{dR(t)}{dt} = \gamma_a I_2(t) + \gamma_q Q(t) - dR(t), \quad (3.28)$$

and $N = S + E + I_1 + I_2 + Q + R$. (3.29)

Table 3.3 Symbols representing the message of the model 3.

Symbols	Descriptive
S	The number of susceptible populations.
E	The number of exposed populations.
I_1	The number of the symptomatic, infected population.
I_2	The number of the asymptomatic, infected population.
Q	The number of quarantine population.
R	The number of recovered populations.
Λ	Initial number in the population.
β_s	The infection rate of the symptomatic, infected population.
β_a	The infection rate of the asymptomatic, infected population.
a	Incubation rate.
τ	The rate of progression from the exposed compartment to the infectious compartment.
ε	The fraction of exposed individuals who show clinical symptoms after the incubation period.
α	The quarantine rate of the symptomatic, infected population.
γ_q	The recovery rate after quarantine.
γ_a	The recovery rate of the asymptomatic, infected population.
g	COVID-19 mortality rate.
d	The natural mortality rate.
N	The number of the entire population.

Chapter 4

Main Results and Discussion

4.1 Mathematical Model Analysis of Model 1

From the mathematical model for COVID-19, by extending the components to include vaccination, quarantine, and hospitalization, as considered in Model 1, the following equations are derived:

$$\frac{dS(t)}{dt} = \Pi - \beta S(t)I(t) - (\varepsilon + \mu)S(t), \tag{4.1}$$

$$\frac{dV(t)}{dt} = \varepsilon S(t) - \rho\beta V(t)I(t) - \mu V(t), \tag{4.2}$$

$$\frac{dE(t)}{dt} = \beta S(t)I(t) + \rho\beta V(t)I(t) - (\phi + \psi + \mu)E(t), \tag{4.3}$$

$$\frac{dI(t)}{dt} = \phi E(t) - (\theta + \omega + \gamma_I + \mu + \tau)I(t), \tag{4.4}$$

$$\frac{dQ(t)}{dt} = \theta I(t) + \psi E(t) - (\nu + \gamma_Q + \mu + \tau)Q(t), \tag{4.5}$$

$$\frac{dH(t)}{dt} = \omega I(t) + \nu Q(t) - (\gamma_H + \mu + \tau)H(t), \tag{4.6}$$

$$\frac{dR(t)}{dt} = \gamma_I I(t) + \gamma_Q Q(t) + \gamma_H H(t) - \mu R(t). \tag{4.7}$$

Where $N(t) = S(t) + V(t) + E(t) + I(t) + Q(t) + H(t) + R(t).$ (4.8)

Lemma 4.1 [84-86] The feasible region Γ defined by

$$\Gamma = \left\{ (S,V,E,I,Q,H,R) \in \mathbb{R}_+^7 : N \le \frac{\Pi}{\mu} \right\}$$

with initial conditions $S(0) > 0, V(0) > 0, E(0) > 0, I(0) > 0, Q(0) > 0, H(0) > 0, R(0) > 0$ is positively invariant for system (4.1) - (4.7).

Proof. Considering the population group, when $N(t) = S(t) + V(t) + E(t) + I(t) + Q(t) + H(t) + R(t),$ we obtain the following:

$$\frac{dN(t)}{dt} = \frac{dS(t)}{dt} + \frac{dV(t)}{dt} + \frac{dE(t)}{dt} + \frac{dI(t)}{dt} + \frac{dQ(t)}{dt} + \frac{dH(t)}{dt} + \frac{dR(t)}{dt}$$

$$\frac{dN(t)}{dt} = \Pi - \mu N - \tau(I + Q + H)$$

$$\frac{dN(t)}{dt} \le \Pi - \mu N$$

It can be observed that $\frac{dN(t)}{dt} \le \Pi - \mu N$, and therefore $N(t) \le N(0)e^{-\mu t} + \frac{\Pi}{\mu}[1 - e^{-\mu t}]$ when $t \to \infty, e^{-\mu t} \to 0$. This implies that $N \le \frac{\Pi}{\mu}$ with respect to the condition $N(0) \le \frac{\Pi}{\mu}$.

Consequently, we define Γ as positively invariant, meaning that every solution of the system of equations (4.1) - (4.7) remains within the set Γ. Thus, the boundary of all solutions in Γ will be contained within $\mathbb{R}^7_+$. □

4.1.1 Equilibrium Points and Basic Reproduction Number of Model 1

Equilibrium Points

To determine the equilibrium points of the system in Model 1, we set the right-hand side of equations (4.1) through (4.7) equal to zero. This approach yields the following system of equations:

$$\Pi - \beta S(t)I(t) - (\varepsilon + \mu)S(t) = 0 \tag{4.9}$$

$$\varepsilon S(t) - \rho\beta V(t)I(t) - \mu V(t) = 0 \tag{4.10}$$

$$\beta S(t)I(t) + \rho\beta V(t)I(t) - (\phi + \psi + \mu)E(t) = 0 \tag{4.11}$$

$$\phi E(t) - (\theta + \omega + \gamma_I + \mu + \tau)I(t) = 0 \tag{4.12}$$

$$\theta I(t) + \psi E(t) - (\nu + \gamma_Q + \mu + \tau)Q(t) = 0 \tag{4.13}$$

$$\omega I(t) + \nu Q(t) - (\gamma_H + \mu + \tau)H(t) = 0 \tag{4.14}$$

$$\gamma_I I(t) + \gamma_Q Q(t) + \gamma_H H(t) - \mu R(t) = 0 \tag{4.15}$$

From the calculation of the equilibrium points, two equilibrium points are identified as follows:

I. The first equilibrium point is the disease-free equilibrium point.

$$K_0^* = (S_0^*, V_0^*, E_0^*, I_0^*, Q_0^*, H_0^*, R_0^*) = \left(\frac{\Pi}{\varepsilon + \mu}, \frac{\varepsilon\Pi}{\mu(\varepsilon + \mu)}, 0, 0, 0, 0, 0\right). \tag{4.16}$$

II. The second equilibrium point is the endemic equilibrium point.

$$K_1^* = (S_1^*, V_1^*, E_1^*, I_1^*, Q_1^*, H_1^*, R_1^*), \tag{4.17}$$

where

$$S_1^* = \frac{\Pi}{\beta I^* + \varepsilon + \mu},$$

$$V_1^* = \frac{\varepsilon\Pi}{(\beta I^* + \varepsilon + \mu)(\rho\beta I^* + \mu)},$$

$$E_1^* = \frac{\Pi\beta I^*(\mu + (\beta I^* + \varepsilon)\rho)}{(\beta I^* + \varepsilon + \mu)(\rho\beta I^* + \mu)(\phi + \psi + \mu)},$$

$$I_1^* = \frac{\phi E^*}{\theta + \omega + \gamma_I + \mu + \tau},$$

$$Q_1^* = \frac{\theta I^* + \psi E^*}{\nu + \gamma_Q + \mu + \tau},$$

$$H_1^* = \frac{\nu Q^* + \omega I^*}{\gamma_H + \mu + \tau},$$

$$R_1^* = \frac{\gamma_I I^* + \gamma_Q Q^* + \gamma_H H^*}{\mu}.$$

The basic reproduction number

The basic reproduction number, R_0, represents the average number of secondary infections generated by one infected individual in a fully susceptible population. As R_0 indicates the transmission potential of a disease, it is a crucial parameter in epidemiological analysis. In this subsection, we utilize the next-generation matrix method [87,88] to calculate the basic reproduction number. The key expressions involved in this calculation are related to the compartments $E(t), I(t), Q(t)$, and $H(t)$. These compartments represent different stages of the disease within the population, and the corresponding vector for these compartments is given as follows:

$$F = \begin{bmatrix} \beta SI + \rho\beta VI \\ 0 \\ 0 \\ 0 \end{bmatrix}, \quad V = \begin{bmatrix} (\phi+\psi+\mu)E \\ -\phi E + (\theta+\omega+\gamma_I+\mu+\tau)I \\ -\theta I - \psi E + (\nu+\gamma_Q+\mu+\tau)Q \\ -\omega I - \nu Q + (\gamma_H+\mu+\tau)H \end{bmatrix}.$$

Let F represent the matrix of new infections and V represent the matrix of transitions of infected individuals between compartments. Using the disease-free equilibrium point (4.16), the Jacobian matrices F and V are obtained as follows

$$F = \begin{bmatrix} 0 & \beta S + \rho\beta V & 0 & 0 \\ 0 & 0 & 0 & 0 \\ 0 & 0 & 0 & 0 \\ 0 & 0 & 0 & 0 \end{bmatrix}, V = \begin{bmatrix} (\phi+\psi+\mu) & 0 & 0 & 0 \\ -\phi & (\theta+\omega+\gamma_I+\mu+\tau) & 0 & 0 \\ -\psi & -\theta & (\nu+\gamma_Q+\mu+\tau) & 0 \\ 0 & -\omega & -\nu & (\gamma_H+\mu+\tau) \end{bmatrix}.$$

The basic reproduction number (R_0) is calculated from the spectral radius of $\rho(FV^{-1})$, which is determined by considering the largest positive eigenvalue. The calculation proceeds as follows

$$R_0 = \rho(FV^{-1}) = \frac{\Pi\beta\phi(\mu+\varepsilon\rho)}{\mu(\varepsilon+\mu)(\phi+\psi+\mu)(\theta+\omega+\gamma_I+\mu+\tau)}. \tag{4.18}$$

4.1.2 Stability Analysis of Model 1

We have examined the stability of Model 1 at both the disease-free equilibrium and the endemic equilibrium using the Lyapunov function. This examination is demonstrated in the following theorem.

Theorem 4.1 Let K_0^* be the Disease-Free Equilibrium (DFE) of a compartmental epidemiological model described by a system of ordinary differential equations (ODEs). Assume all parameters are positive, and all state variables (e.g., susceptible, exposed,

infected) remain nonnegative within the positively invariant set Γ. If $R_0 < 1$, then K_0^* is globally asymptotically stable in Γ.

Proof. Since the evidence involves considering the Lyapunov function, it is defined as follows:

$$X(t) = X(E(t), I(t)) = a_1 E + a_2 I.$$

It can be observed that $X(t) > 0$ for all $(E(t), I(t))^T \in \Gamma$ and it follows that

$$X(E_0^*, I_0^*) = a_1(0) + a_2(0) = 0,$$

where a_1, and a_2 be positive constants. The derivative of the function $X(t)$ can be obtained, and by substituting the corresponding expressions from the system of equations (4.1) - (4.7), we derive the following

$$\begin{aligned} X'(t) &= a_1 E' + a_2 I' \\ &= a_1(\beta SI + \rho\beta VI - (\phi + \psi + \mu)E) + a_2(\phi E - (\theta + \omega + \gamma_I + \mu + \tau)I). \end{aligned}$$

Rearranging the equation and substituting the disease-free equilibrium point $K_0^* = (S_0^*, V_0^*, E_0^*, I_0^*, Q_0^*, H_0^*, R_0^*) = \left(\frac{\Pi}{\varepsilon + \mu}, \frac{\varepsilon\Pi}{\mu(\varepsilon + \mu)}, 0, 0, 0, 0, 0\right)$, we obtain the following:

$$\begin{aligned} X'(t) &= \left(a_2\phi - a_1(\phi + \psi + \mu)\right)E + \left(a_1(\beta S + \rho\beta V) - a_2(\theta + \omega + \gamma_I + \mu + \tau)\right)I \\ &= \left(a_2\phi - a_1(\phi + \psi + \mu)\right)E + \left(a_1(\beta\frac{\Pi}{\varepsilon + \mu} + \rho\beta\frac{\varepsilon\Pi}{\mu(\varepsilon + \mu)}) - a_2(\theta + \omega + \gamma_I + \mu + \tau)\right)I. \end{aligned}$$

Let $a_1 = \theta + \omega + \gamma_I + \mu + \tau$, and $a_2 = \frac{\beta\mu\Pi + \rho\beta\varepsilon\Pi}{\mu(\varepsilon + \mu)}$, upon incorporating this value into the equation, the resulting expression is:

$$\begin{aligned} X'(t) &= \left(\left(\frac{\beta\mu\Pi + \rho\beta\varepsilon\Pi}{\mu(\varepsilon + \mu)}\right)\phi - (\theta + \omega + \gamma_I + \mu + \tau)(\phi + \psi + \mu)\right)E \\ &= (\theta + \omega + \gamma_I + \mu + \tau)(\phi + \psi + \mu)\left(\frac{(\mu + \rho\varepsilon)\beta\Pi\phi}{\mu(\varepsilon + \mu)(\theta + \omega + \gamma_I + \mu + \tau)(\phi + \psi + \mu)} - 1\right)E \\ X'(t) &= (\theta + \omega + \gamma_I + \mu + \tau)(\phi + \psi + \mu)\left(R_0 - 1\right)E \end{aligned} \tag{4.19}$$

Thus, $X'(t) < 0$ for all states t, if $R_0 < 1$, and $X'(t) = 0$ only when $E = 0$ at the disease-free equilibrium, then K_0^* is globally asymptotically stable in the region Γ. □

Theorem 4.2 Let K_1^* be the endemic equilibrium of epidemiological model (with positive parameters) in the positively invariant set Γ. Suppose the basic reproduction number $R_0 > 1$. Then K_1^* is globally asymptotically stable in Γ.

Proof. Define the Lyapunov function as follows [89]:

$$\begin{aligned} Y(t) &= (S - S_1^* - S_1^* \ln\frac{S}{S_1^*}) + (V - V_1^* - V_1^* \ln\frac{V}{V_1^*}) + (E - E^* - E^* \ln\frac{E}{E^*}) + (I - I^* - I^* \ln\frac{I}{I^*}) \\ &\quad + (Q - Q^* - Q^* \ln\frac{Q}{Q^*}) + (H - H^* - H^* \ln\frac{H}{H^*}) + (R - R^* - R^* \ln\frac{R}{R^*}) \end{aligned}$$

One can note that $Y(t)$ holds true for every $(S(t),V(t),E(t),I(t),Q(t),H(t),R(t))^T \in \Gamma$, leading to the conclusion that

$$\begin{aligned}Y(S_1^*,V_1^*,E_1^*,I_1^*,Q_1^*,H_1^*,R_1^*) &= (S_1^* - S_1^* - S_1^* \ln\frac{S_1^*}{S_1^*}) + (V_1^* - V_1^* - V_1^* \ln\frac{V_1^*}{V_1^*}) + (E^* - E^* - E^* \ln\frac{E^*}{E^*}) \\ &+ (I^* - I^* - I^* \ln\frac{I^*}{I^*}) + (Q^* - Q^* - Q^* \ln\frac{Q^*}{Q^*}) + (H^* - H^* - H^* \ln\frac{H^*}{H^*}) \\ &+ (R^* - R^* - R^* \ln\frac{R^*}{R^*}) \\ &= 0.\end{aligned}$$

Consider finding the derivative of the function $Y(t)$, which yields

$$Y'(t) = S'\left(1-\frac{S_1^*}{S}\right) + V'\left(1-\frac{V_1^*}{V}\right) + E'\left(1-\frac{E^*}{E}\right) + I'\left(1-\frac{I^*}{I}\right) + Q'\left(1-\frac{Q^*}{Q}\right) + H'\left(1-\frac{H^*}{H}\right) + R'\left(1-\frac{R^*}{R}\right)$$

Substituting the equations from (4.1) - (4.7), we obtain

$$\begin{aligned}Y'(t) &= \{\Pi - \beta SI - (\varepsilon+\mu)S\}\left(1-\frac{S_1^*}{S}\right) + \{\varepsilon S - \rho\beta VI - \mu V\}\left(1-\frac{V_1^*}{V}\right) + \{\beta SI + \rho\beta VI - (\phi+\psi+\mu)E\}\left(1-\frac{E^*}{E}\right) \\ &+ \{\phi E - (\theta+\omega+\gamma_I+\mu+\tau)I\}\left(1-\frac{I^*}{I}\right) + \{\theta I + \psi E - (\nu+\gamma_Q+\mu+\tau)Q\}\left(1-\frac{Q^*}{Q}\right) \\ &+ \{\omega I + \nu Q - (\gamma_H+\mu+\tau)H\}\left(1-\frac{H^*}{H}\right) + \{\gamma_1 I + \gamma_Q Q + \gamma_H H - \mu R\}\left(1-\frac{R^*}{R}\right)\end{aligned}$$

Putting $S = S - S_1^*, V = V - V_1^*, E = E - E_1^*, I = I - I_1^*, Q = Q - Q_1^*, H = H - H_1^*$ and $R = R - R_1^*$ is obtained

$$\begin{aligned}Y'(t) &= \left\{\Pi - \beta I\left(S - S_1^*\right) - (\varepsilon+\mu)\left(S - S_1^*\right)\right\}\left(\frac{S-S_1^*}{S}\right) + \left\{\varepsilon S - \rho\beta I\left(V - V_1^*\right) - \mu\left(V - V_1^*\right)\right\}\left(\frac{V-V_1^*}{V}\right) \\ &+ \left\{\beta SI + \rho\beta VI - (\phi+\psi+\mu)\left(E - E_1^*\right)\right\}\left(\frac{E-E_1^*}{E}\right) + \left\{\phi E - (\theta+\omega+\gamma_I+\mu+\tau)\left(I - I_1^*\right)\right\}\left(\frac{I-I_1^*}{I}\right) \\ &+ \left\{\theta I + \psi E - (\nu+\gamma_Q+\mu+\tau)\left(Q - Q_1^*\right)\right\}\left(\frac{Q-Q_1^*}{Q}\right) + \left\{\omega I + \nu Q - (\gamma_H+\mu+\tau)\left(H - H_1^*\right)\right\}\left(\frac{H-H_1^*}{H}\right) \\ &+ \left\{\gamma_I I + \gamma_Q Q + \gamma_H H - \mu\left(R - R_1^*\right)\right\}\left(\frac{R-R_1^*}{R}\right) \\ &= \Pi - \Pi\left(\frac{S_1^*}{S}\right) - \beta I\frac{\left(S-S_1^*\right)^2}{S} - (\varepsilon+\mu)\frac{\left(S-S_1^*\right)^2}{S} + \varepsilon S - \varepsilon S\left(\frac{V_1^*}{V}\right) - \rho\beta I\frac{\left(V-V_1^*\right)^2}{V} - \mu\frac{\left(V-V_1^*\right)^2}{V} \\ &+ \beta SI - \beta SI\left(\frac{E_1^*}{E}\right) + \rho\beta VI - \rho\beta VI\left(\frac{E_1^*}{E}\right) - (\phi+\psi+\mu)\frac{\left(E-E_1^*\right)^2}{E} + \phi E - \phi E\left(\frac{I_1^*}{I}\right) - (\theta+\omega+\gamma_I+\mu+\tau)\frac{\left(I-I_1^*\right)^2}{I} \\ &+ \theta I - \theta I\left(\frac{Q_1^*}{Q}\right) + \psi E - \psi E\left(\frac{Q_1^*}{Q}\right) - (\nu+\gamma_Q+\mu+\tau)\frac{\left(Q-Q_1^*\right)^2}{Q} + \omega I - \omega I\left(\frac{H_1^*}{H}\right) + \nu Q - \nu Q\left(\frac{H_1^*}{H}\right) \\ &- (\gamma_H+\mu+\tau)\frac{\left(H-H_1^*\right)^2}{H} + \gamma_I I - \gamma_I I\left(\frac{R_1^*}{R}\right) + \gamma_Q Q - \gamma_Q Q\left(\frac{R_1^*}{R}\right) + \gamma_Q Q - \gamma_Q Q\left(\frac{R_1^*}{R}\right) - \mu\frac{\left(R-R_1^*\right)^2}{R}.\end{aligned}$$

To facilitate the analysis, the equation can be rearranged as follows

$$Y'(t) = A - B,$$

where

$$A = \Pi + \varepsilon S + \beta SI + \rho\beta VI + \phi E + \theta I + \psi E + \omega I + \nu Q + \gamma_I I + \gamma_Q Q + \gamma_Q Q,$$

$$B = \Pi\left(\frac{S_1^*}{S}\right) + \beta I\frac{\left(S - S_1^*\right)^2}{S} + (\varepsilon + \mu)\frac{\left(S - S_1^*\right)^2}{S} + \varepsilon S\left(\frac{V_1^*}{V}\right) + \rho\beta I\frac{\left(V - V_1^*\right)^2}{V} + \mu\frac{\left(V - V_1^*\right)^2}{V}$$
$$+ \beta SI\left(\frac{E_1^*}{E}\right) + \rho\beta VI\left(\frac{E_1^*}{E}\right) + (\phi + \psi + \mu)\frac{\left(E - E_1^*\right)^2}{E} + \phi E\left(\frac{I_1^*}{I}\right) + (\theta + \omega + \gamma_I + \mu + \tau)\frac{\left(I - I_1^*\right)^2}{I}$$
$$+ \theta I\left(\frac{Q_1^*}{Q}\right) + \psi E\left(\frac{Q_1^*}{Q}\right) + (\nu + \gamma_Q + \mu + \tau)\frac{\left(Q - Q_1^*\right)^2}{Q} + \omega I\left(\frac{H_1^*}{H}\right) + \nu Q\left(\frac{H_1^*}{H}\right) + (\gamma_H + \mu + \tau)\frac{\left(H - H_1^*\right)^2}{H}$$
$$+ \gamma_I I\left(\frac{R_1^*}{R}\right) + \gamma_Q Q\left(\frac{R_1^*}{R}\right) + \gamma_Q Q\left(\frac{R_1^*}{R}\right) + \mu\frac{\left(R - R_1^*\right)^2}{R}.$$

It can be seen that, $Y'(t) < 0$, when $A < B$ for $R_0 > 1$ and $Y'(t) = 0$ when $S = S_1^*, V = V_1^*, E = E_1^*, I = I_1^*, Q = Q_1^*, H = H_1^*$ and $R = R_1^*$. Since all parameters have positive values, it is compliant with LaSalle's invariance principle. The endemic equilibrium point K_1^* is global asymptotically stable in its feasible region, if $A < B$. □

4.1.3 Numerical Analysis Results of Model 1

The numerical analysis of Model 1 focused on simulating the dynamics of COVID-19 transmission while accounting for critical control measures, including vaccination, quarantine, and hospitalization. The model parameters, derived through rigorous fitting techniques and informed by observed disease trends, demographic data, and a comprehensive literature review (refer to Tables 4.1 and 4.2), were utilized to evaluate the system's behavior under varied conditions.

Table 4.1 Parameter Values for the Numerical Analysis of Model 1 at the Disease-Free Equilibrium.

Parameters	Disease-free	Units	Source
Π	1	person	Assume
β	0.000009	Per person · days^{-1}	Estimated
ε	0.4	day^{-1}	Estimated
ρ	0.5	N/A	Estimated
ϕ	1/6	day^{-1}	Estimated
ψ	0.08	day^{-1}	Estimated
θ	0.02	day^{-1}	Estimated

ω	0.005	day^{-1}	[90]
ν	0.03	day^{-1}	Estimated
γ_I	0.001	day^{-1}	[91]
γ_Q	0.03	day^{-1}	[91]
γ_H	1/14	day^{-1}	[90]
μ	0.000036529	day^{-1}	[89]
τ	0.00286	day^{-1}	[92]

Table 4.2 Parameter Values for the Numerical Analysis of Model 1 at the Endemic Equilibrium.

Parameters	Endemic	Units	Source
Π	560	person	Fitted
β	0.000009	Per person $\cdot$ $days^{-1}$	Fitted
ε	0.4	day^{-1}	Fitted
ρ	0.5	N/A	Fitted
ϕ	1/6	day^{-1}	Fitted
ψ	0.08	day^{-1}	Fitted
θ	0.02	day^{-1}	Fitted
ω	0.005	day^{-1}	[90]
ν	0.03	day^{-1}	Fitted
γ_I	0.001	day^{-1}	[91]
γ_Q	0.03	day^{-1}	[91]
γ_H	1/14	day^{-1}	[90]
μ	0.000036529	day^{-1}	[89]
τ	0.00286	day^{-1}	[92]

4.1.3.1 Model Fitting of Model 1

To ensure the accuracy of parameter values in representing the real-world epidemic situation in Thailand, model fitting was conducted utilizing the fminunc algorithm in MATLAB. This approach was applied to epidemic data collected from Thailand from January 1, 2022, to April 10, 2022 [93]. The fitting process aimed to minimize discrepancies between the model's output and the observed daily infection

data, achieving a coefficient of determination R^2 =0.9544, which indicates a high level of agreement between the model predictions and actual observations. The parameters derived from this fitting process are summarized in Table 4.2. These parameters serve as the foundation for accurately capturing the dynamics of COVID-19 transmission within the model. Additional parameters not obtained directly through fitting were supplemented by observations of the disease's behavior and insights drawn from an extensive literature review.

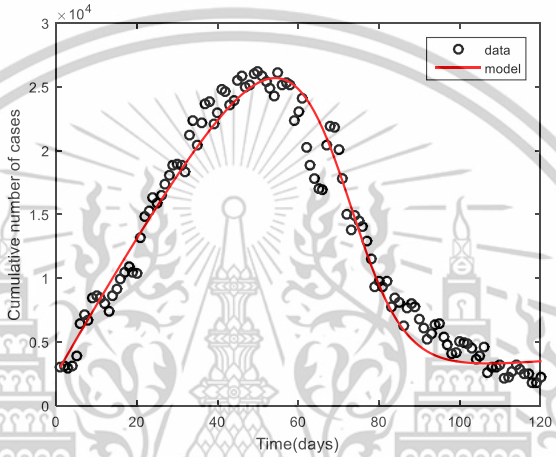

Figure 4.1 Model Fitting with Daily Epidemic Data in Thailand from January 1 to April 10, 2022 [93].

The results of the fitting are visually represented in Figure 4.1, where the black circles denote the daily reported infection cases in Thailand, providing a clear view of the real-world data. In comparison, the solid red line illustrates the model's numerical analysis based on equations (4.1) to (4.17). This alignment demonstrates the robustness of the fitted parameters and their ability to replicate the epidemic trends, thereby validating the model's applicability to the observed scenario.

4.1.3.2 Numerical Analysis Results of Model 1

Numerical Analysis of the Disease-Free Equilibrium

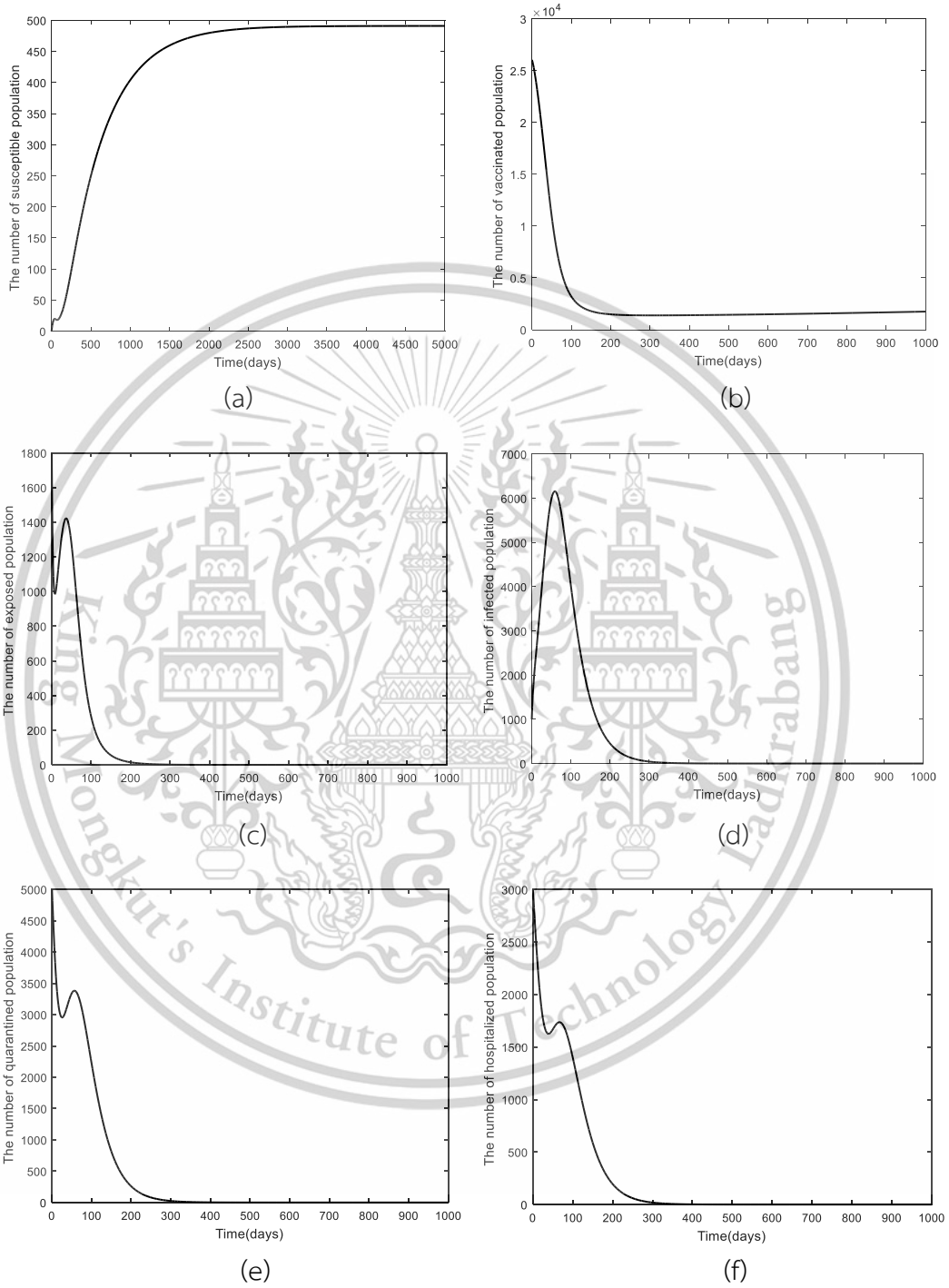

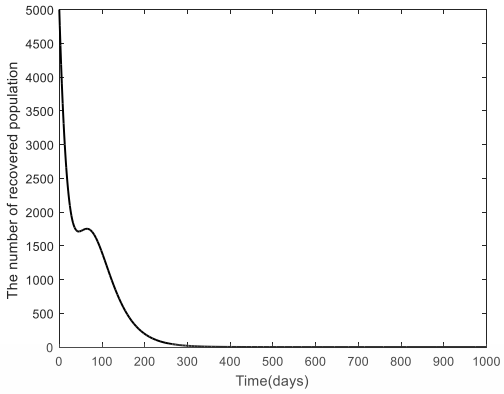

(g)

Figure 4.2 Solutions of equations (4.1) - (4.7): Graph showing the relationship between time and $S_0^*, V_0^*, E_0^*, I_0^*, Q_0^*, H_0^*, R_0^*$ for $R_0 = 0.500007$.

Numerical Analysis of the Endemic Equilibrium

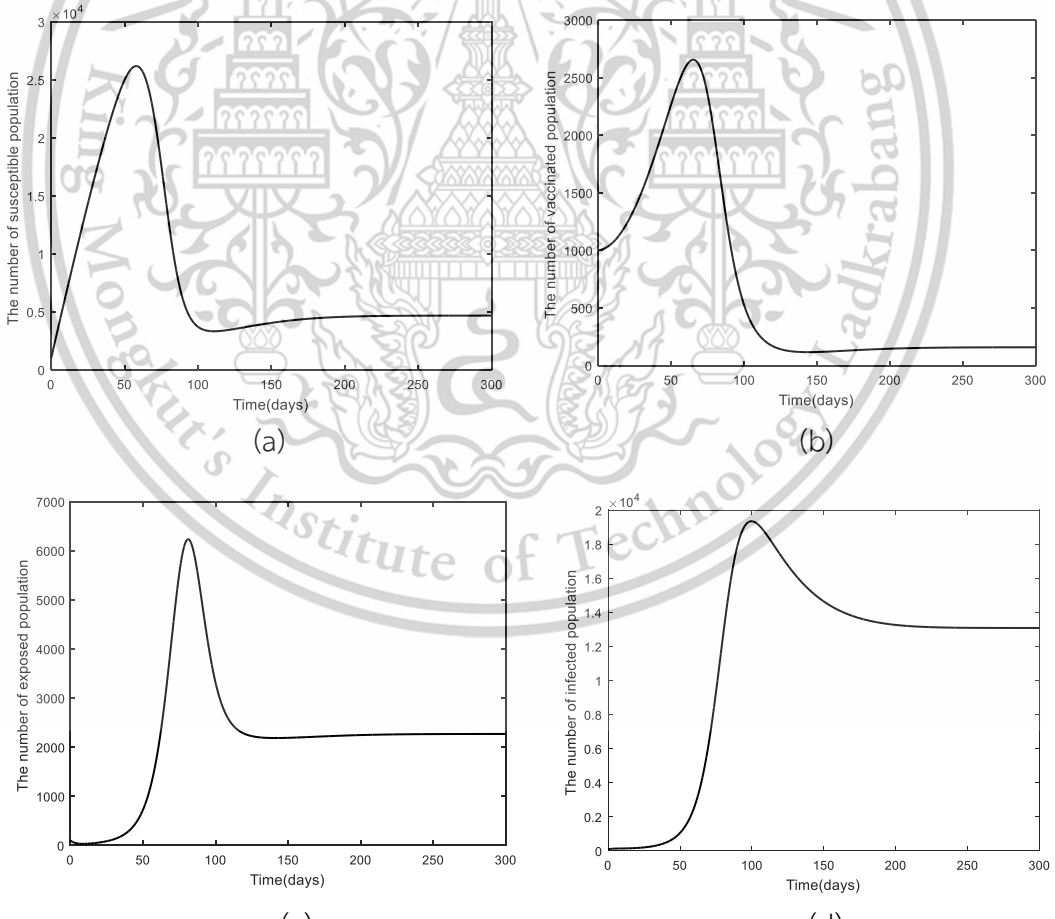

(a) (b)

(c) (d)

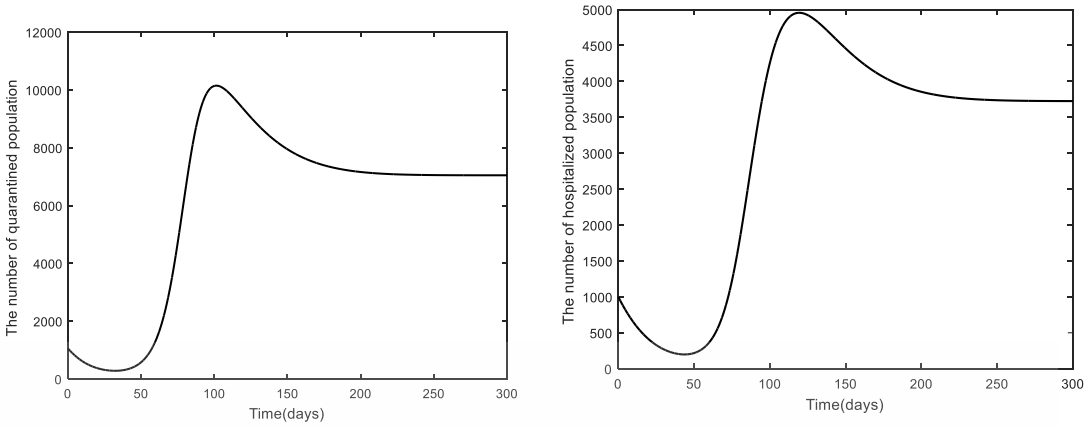

(e) (f)

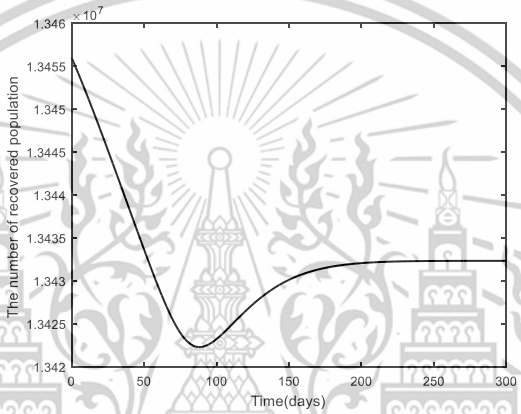

(g)

Figure 4.3 Solutions of the system of equations (4.1) -(4.7): Graph showing the relationship between time and $S_1^*, V_1^*, E_1^*, I_1^*, Q_1^*, H_1^*, R_1^*$ for $R_0 = 1.64177$.

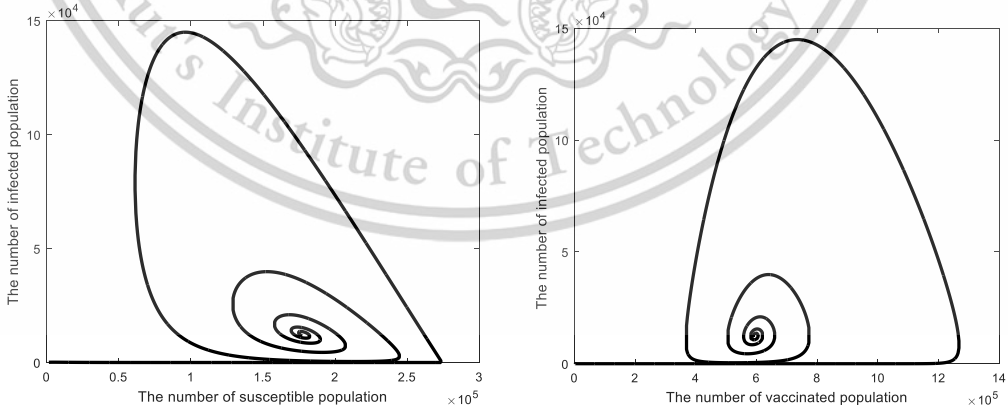

(a) (S_1^*, I_1^*). (b) (V_1^*, I_1^*).

Figure 4.4 Solutions of the system of equations (4.1) -(4.7): Graph showing the relationship between (S_1^*, I_1^*) and (V_1^*, I_1^*) for $R_0 = 1.64177$.

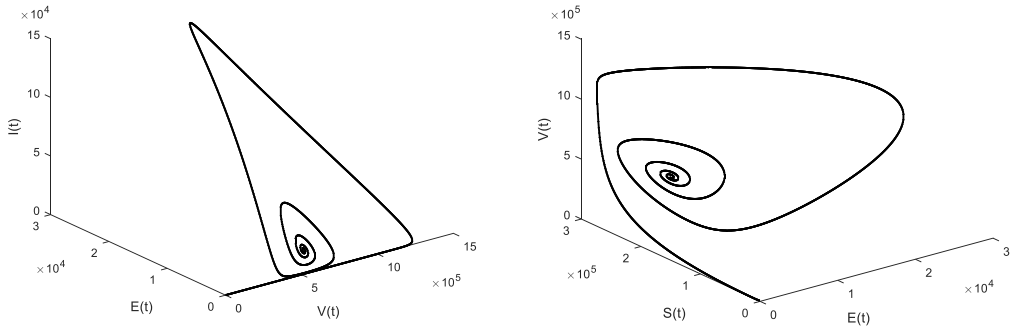

(a) (V_1^*, E_1^*, I_1^*). (b) (E_1^*, S_1^*, V_1^*).

Figure 4.5 Solutions of the system of equations (4.1) -(4.7): Graph showing the relationship between (V_1^*, E_1^*, I_1^*) and (E_1^*, S_1^*, V_1^*) for $R_0 = 1.64177$.

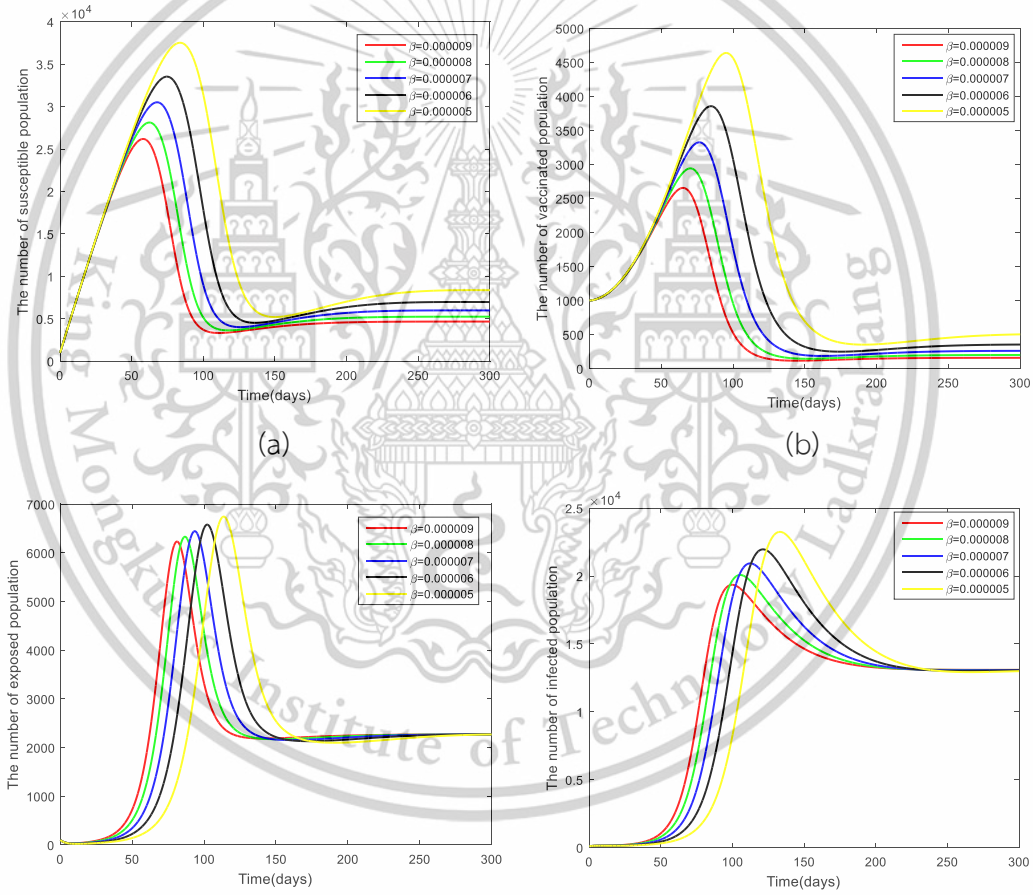

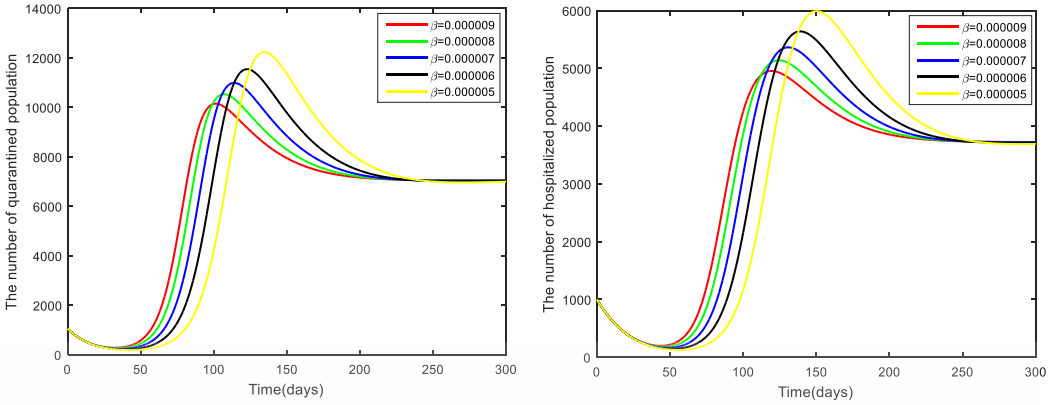

(e) (f)

Figure 4.6 Solutions of the system of equations (4.1) -(4.7): Graph comparing the infection rate (β) for $R_0 > 1$.

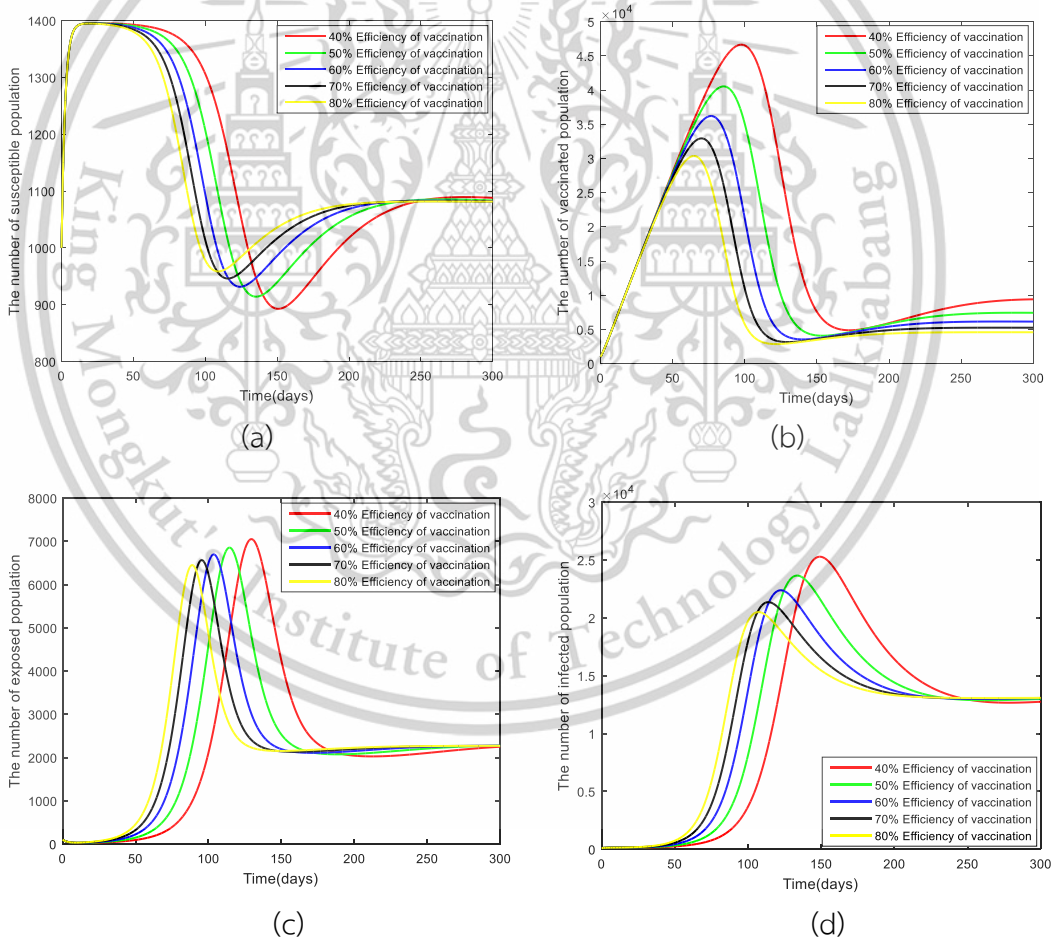

(a) (b)

(c) (d)

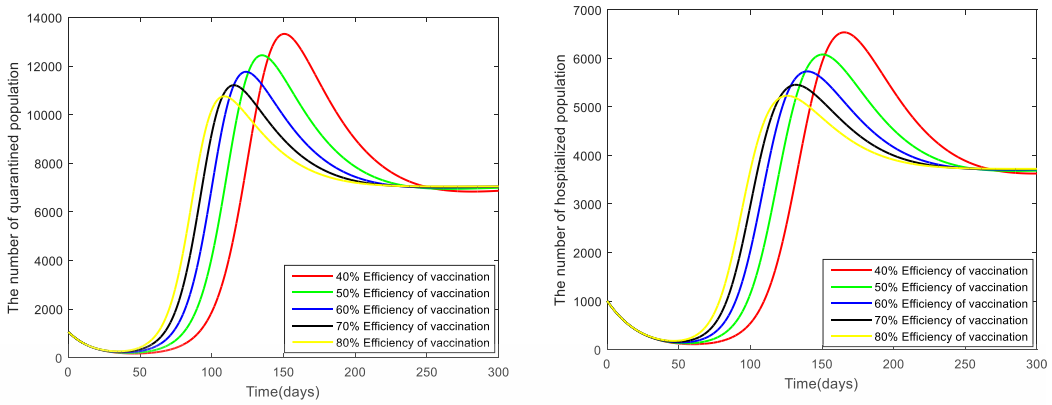

(e) (f)

Figure 4.7 Solutions of the system of equations (4.1) -(4.7): Graph comparing the vaccination prevention efficacy (ρ) for $R_0 > 1$.

We present the numerical results of the model (4.1) – (4.7) by analyzing the disease-free equilibrium and endemic equilibrium, displaying 2D and 3D phase plane graphs at the endemic state. We also compare the infection rate and vaccination efficacy to support the theoretical results. The numerical results from Figures 4.2-4.7 can be discussed comprehensively and coherently, divided into three sections as follows:

Part 1: Convergence to the equilibrium point of the disease-free equilibrium and endemic equilibrium

The disease-free equilibrium, illustrated in Figure 4.2, demonstrates the population dynamics under effective control measures that eradicate disease transmission. The susceptible population converges to a steady state of 491 individuals after approximately 2,500 days, indicating the proportion of individuals who remain unvaccinated or unaffected. The vaccinated population stabilizes at 26,884 within 210 days, reflecting the significant impact of widespread vaccination in reducing susceptibility. Other compartments, including exposed, infected, quarantined, hospitalized, and recovered populations, all decline to zero after 300 days, confirming the system's capacity to achieve a disease-free state when control measures are optimally implemented.

The endemic equilibrium results in Figure 4.3 portray a scenario where the disease persists but stabilizes within the population. The numerical results of the model provide specific equilibrium values for each population compartment under

endemic conditions, illustrating the long-term dynamics of the disease. The susceptible population stabilizes at 4673, representing individuals who remain unvaccinated and vulnerable to infection. The vaccinated population, at 158, indicates limited immunity achieved through vaccination, potentially due to low coverage or waning effectiveness. The exposed population reaches 2269, reflecting individuals in the incubation phase transitioning to becoming infectious or recovering. The infected population stabilizes at 13,088, highlighting the active cases contributing to disease transmission within the community. The quarantine population, at 7048, underscores the role of isolation measures in preventing further spread. The hospitalized population, stabilizing at 3725, represents the severe cases requiring medical care, emphasizing the need for adequate healthcare resources. Finally, the recovered population, at 13,431,100, reflects the majority of individuals who have overcome the disease and gained immunity, contributing to herd immunity. These equilibrium values collectively portray the persistent nature of the disease and the importance of vaccination, quarantine, and healthcare interventions in maintaining control under endemic conditions.

Part 2: 2D and 3D phase trajectories

The 2D and 3D phase trajectories in Figures 4.4 and 4.5 illustrate the interactions and dynamics of the model's population compartments as they progress toward equilibrium.

The 2D phase trajectories in Figure 4.4 focus on the relationships between specific compartments. Subfigure (a) demonstrates the interaction between the susceptible (S_1^*) and infected (I_1^*) populations. The spiral pattern indicates oscillations in the population levels before stabilizing at the equilibrium point, where disease transmission and recovery reach a balance. Similarly, subfigure (b) highlights the relationship between the vaccinated (V_1^*) and infected (I_1^*) populations, with a similar convergence pattern reflecting the dynamic impact of vaccination on disease control.

The 3D phase trajectories in Figure 4.5 expand this analysis by incorporating additional variables, providing a more comprehensive visualization of the system's behavior. Subfigure (a) illustrates the interaction among the vaccinated (V_1^*), exposed (E_1^*), and infected (I_1^*) populations. The spiral trajectory converging toward the equilibrium point emphasizes the interdependent dynamics of vaccination, exposure, and infection rates. Subfigure (b) adds another layer by showing the relationship among

the exposed (E_1^*), susceptible (S_1^*), and vaccinated (V_1^*) populations. The trajectory highlights how the interactions among these compartments influence the system's progression toward stability.

These phase trajectories provide crucial insights into the system's stability and the effects of various factors such as vaccination and exposure rates. The combined use of 2D and 3D visualizations enables a detailed understanding of the dynamics, emphasizing the interactions that guide the system toward equilibrium. By analyzing these trajectories, policymakers and researchers can better assess the effectiveness of interventions and predict the long-term behavior of the epidemic.

Part 3: Comparison of the parameters used in the study

Figures 4.6 and 4.7 present a detailed comparison of key parameters and their influence on the system. Figure 4.6 examines the infection rates (β) ranging from 0.0000009 to 0.0000005. Higher infection rates, such as β = 0.0000009, lead to faster convergence to equilibrium, as the population moves through the infected state more rapidly. Conversely, lower infection rates, such as β = 0.0000005, result in a slower stabilization, indicating that the speed of disease transmission significantly impacts the time required to reach equilibrium. This comparison underscores the critical role of infection rates in shaping the dynamics of disease spread and control.

Figure 4.7 focuses on vaccine efficacy, comparing levels of 40%, 50%, 60%, 70%, and 80%. The analysis demonstrates that higher vaccine efficacy substantially enhances disease control. For instance, with an 80% vaccine efficacy, the decline in the infected population is much sharper compared to a 40% efficacy. This improvement reduces the time to stabilization by nearly half, emphasizing the importance of effective vaccination strategies. The results highlight that higher vaccine efficacy not only reduces infection rates but also minimizes the burden on healthcare systems and improves long-term outcomes.

4.1.3.3 Sensitivity Analysis of Model 1

The sensitivity analysis of the basic reproduction number R_0 examines how variations in model parameters impact R_0, a key indicator of the epidemic's severity and progression. Understanding this relationship is essential for identifying the most influential parameters in disease transmission and for developing effective control

measures. The analysis uses the normalized forward sensitivity index, a metric that quantifies the proportional change in R_0 relative to proportional changes in individual parameters. This approach highlights the parameters that play critical roles in shaping R_0, such as vaccination rates, contact rates, or quarantine efficacy. By identifying these influential factors, targeted interventions can be designed to effectively reduce R_0 and control the outbreak, ensuring optimal resource allocation and strategy development for epidemic management, which can be calculated as follows [94,95]:

$$\Upsilon_{\sigma}^{R_0} = \frac{\partial R_0}{\partial \sigma} \times \frac{\sigma}{R_0}. \tag{4.20}$$

Where σ is the parameter associated with the transmission of the disease, and R_0 is the basic reproduction number. The parameters used in this analysis are taken from Table 4.2, and the results of the sensitivity analysis are presented in Table 4.3.

Table 4.3 Sensitivity Indices of the Basic Reproduction Number for Model 1.

Parameters	Sensitivity
Π	+1.000000
β	+1.000000
ε	-0.017304
ρ	+0.964758
ϕ	+0.827651
ψ	-0.827274
θ	-0.692125
ω	-0.173031
γ_I	-0.034606
μ	-0.984337
τ	-0.098973

Table 4.2 presents the results of the sensitivity index analysis for the basic reproduction number R_0. The results of the sensitivity index analysis for the basic reproduction number R_0 reveal the extent to which each parameter influences disease transmission. Parameters with a positive impact on R_0 include the initial population size (Π), infection rate (β), vaccination efficacy (ρ), and incubation rate (ϕ), indicating that increases in these parameters lead to a proportional increase in R_0. Conversely,

parameters with a negative impact include the vaccination rate (ε), transition rates to quarantine or hospitalization (ψ, θ, ω), recovery rates (γ_I), natural mortality rate (μ), and mortality rate due to COVID-19 (τ), suggesting that increases in these parameters result in a reduction of R_0.

Building on these results, the most influential parameters are the initial population size (Π) and infection rate (β), both with a sensitivity index of +1. This implies that a 10% increase or decrease in either of these parameters directly translates into a 10% increase or decrease in R_0. These findings emphasize the need for stringent measures to reduce contact rates and infection opportunities. For instance, interventions such as wearing masks, maintaining social distancing, and minimizing exposure to high-risk individuals can significantly lower R_0, thereby curbing disease spread. Other critical parameters include the vaccination efficacy (ρ), with a sensitivity index of +0.964758, and the incubation rate (ϕ), with a sensitivity index of +0.827651. These values highlight the importance of highly effective vaccines and timely identification of exposed individuals to control the spread of the disease. Parameters such as the recovery rates (γ_I), and transition rates (ψ, θ, ω) have moderate to low sensitivity indices, indicating their influence is less direct but still significant in reducing R_0. For example, higher recovery rates or efficient transition to quarantine and hospitalization help contain the outbreak and lower transmission rates. Finally, the negative sensitivity indices for the vaccination rate (ε) and mortality rates (μ and τ) highlight their role in reducing R_0. A higher vaccination rate decreases the susceptible population, while mortality rates, although unfavorable from a humanitarian perspective, reduce the pool of infected individuals capable of further transmission. These findings underscore the complex interplay between parameters and their collective impact on R_0.

In conclusion, the sensitivity analysis demonstrates that targeted control measures focusing on reducing the infection rate (β), enhancing vaccination efficacy (ρ), and increasing vaccination rates (ε) are the most effective strategies for lowering R_0. Understanding the sensitivity of these parameters allows policymakers to prioritize interventions, allocate resources efficiently, and achieve optimal epidemic control, ultimately contributing to more effective and sustainable disease management strategies.

4.2 Mathematical Model Analysis of Model 2

From the mathematical model for COVID-19, the population is divided into those who have been vaccinated and those who have not. The model further considers the infection status of individuals, distinguishing between symptomatic and asymptomatic cases, as well as hospitalization. Based on these considerations, Model 2 is represented by the following set of equations:

$$\frac{dS_n}{dt} = (1-b)\sigma N_h - \eta_1 S_n - \mu S_n, \tag{4.21}$$

$$\frac{dE_n}{dt} = \eta_1 S_n - \phi E_n - (1-\phi)E_n - \mu E_n, \tag{4.22}$$

$$\frac{dI_{an}}{dt} = \phi E_n - (\omega_1 + \gamma_2 + \mu + d)I_{an}, \tag{4.23}$$

$$\frac{dI_{sn}}{dt} = (1-\phi)E_n - (\omega_2 + \mu + d)I_{sn}, \tag{4.24}$$

$$\frac{dS_v}{dt} = b\sigma N_h - \eta_2 S_v - \mu S_v, \tag{4.25}$$

$$\frac{dE_v}{dt} = \eta_2 S_v - (1-\delta)\phi E_v - (1-\delta)(1-\phi)E_v - \mu E_v, \tag{4.26}$$

$$\frac{dI_{av}}{dt} = (1-\delta)\phi E_v - (\omega_4 + \gamma_3 + \mu + d)I_{av}, \tag{4.27}$$

$$\frac{dI_{sn}}{dt} = (1-\delta)(1-\phi)E_v - (\omega_3 + \mu + d)I_{sv}, \tag{4.28}$$

$$\frac{dH_p}{dt} = \omega_1 I_{an} + \omega_2 I_{sn} + \omega_3 I_{sv} + \omega_4 I_{av} - (\gamma_1 + \mu + d)H_p, \tag{4.29}$$

$$\frac{dR}{dt} = \gamma_1 H_p + \gamma_2 I_{an} + \gamma_3 I_{av} - \mu R, \tag{4.30}$$

where $N_h = S_n + E_n + I_{an} + I_{sn} + S_v + E_v + I_{av} + I_{sv} + H_p + R.$ (4.31)

Lemma 4.2 [85,86] Initial condition $S_n(0) > 0, E_n(0) > 0, I_{an}(0) > 0, I_{sn}(0) > 0, S_v(0) > 0, E_v(0) > 0, I_{av}(0) > 0, I_{sv}(0) > 0, H_p(0) > 0,$ and $R(0) > 0$ from the Equation (4.21)-(4.30) the invariant set $\Psi = \left\{(S_n, E_n, I_{an}, I_{sn}, S_v, E_v, I_{av}, I_{sv}, H_p, R) \in R_+^{10} : N_h \le \frac{\sigma}{\mu}\right\}$, and then the closed set Ψ is positive invariant.

Proof. Given that $N_h = S_n + E_n + I_{an} + I_{sn} + S_v + E_v + I_{av} + I_{sv} + H_p + R$, we have

$$\frac{dN_h}{dt} = \frac{dS_n}{dt} + \frac{dE_n}{dt} + \frac{dI_{an}}{dt} + \frac{dI_{sn}}{dt} + \frac{dS_v}{dt} + \frac{dE_v}{dt} + \frac{dI_{av}}{dt} + \frac{dI_{sv}}{dt} + \frac{dH_p}{dt} + \frac{dR}{dt}$$

$$\frac{dN_h}{dt} = \sigma - \mu N_h - d(I_{an} + I_{sn} + I_{av} + I_{sv} + H_p)$$

$$\le \sigma - \mu N_h$$

It can be observed that $\frac{dN_h}{dt} \le \sigma - \mu N_h$, and therefore $N_h(t) \le N(0)e^{-\mu t} + \frac{\sigma}{\mu}[1 - e^{-\mu t}]$ when $t \to \infty, e^{-\mu t} \to 0$, which leads to $N_h \le \frac{\sigma}{\mu}$ with respect to the condition $N_h(0) \le \frac{\sigma}{\mu}$.

Consequently, we define Ψ as positively invariant, meaning that every solution of the system of equations (4.21) - (4.30) remains within the set Ψ. The values of Ψ derived from the system of equations (4.21) - (4.30) are considered mathematically and epidemiologically appropriate, as epidemiological parameters are assumed to be positive. Thus, the boundary of all solutions Ψ will be contained within R_{+}^{10}. □

4.2.1 Equilibrium Points and Basic Reproduction Number of Model 2

Equilibrium Points

The equilibrium points of Model 2 can be determined by setting the right-hand side of the system of equations (4.21) - (4.30) to zero, yielding:

$$(1-b)\sigma N_h - \eta_1 S_n - \mu S_n = 0 \tag{4.32}$$

$$\eta_1 S_n - \phi E_n - (1-\phi)E_n - \mu E_n = 0 \tag{4.33}$$

$$\phi E_n - (\omega_1 + \gamma_2 + \mu + d)I_{an} = 0 \tag{4.34}$$

$$(1-\phi)E_n - (\omega_2 + \mu + d)I_{sn} = 0 \tag{4.35}$$

$$b\sigma N_h - \eta_2 S_v - \mu S_v = 0 \tag{4.36}$$

$$\eta_2 S_v - (1-\delta)\phi E_v - (1-\delta)(1-\phi)E_v - \mu E_v = 0 \tag{4.37}$$

$$(1-\delta)\phi E_v - (\omega_4 + \gamma_3 + \mu + d)I_{av} = 0 \tag{4.38}$$

$$(1-\delta)(1-\phi)E_v - (\omega_3 + \mu + d)I_{sv} = 0 \tag{4.39}$$

$$\omega_1 I_{an} + \omega_2 I_{sn} + \omega_3 I_{sv} + \omega_4 I_{av} - (\gamma_1 + \mu + d)H_p = 0 \tag{4.40}$$

$$\gamma_1 H_p + \gamma_2 I_{an} + \gamma_3 I_{av} - \mu R = 0 \tag{4.41}$$

From the equilibrium analysis using Mathematica, two equilibrium points are identified as follows:

I. The first equilibrium point is the disease-free equilibrium point.

$$G_0^* = \left(S^*_n, E^*_n, I^*_{an}, I^*_{sn}, S^*_v, E^*_v, I^*_{av}, I^*_{sv}, H_p^*, R^*\right) = \left(\frac{(1-b)\sigma}{\mu}, 0, 0, 0, \frac{b\sigma}{\mu}, 0, 0, 0, 0, 0\right) \tag{4.42}$$

II. The second equilibrium point is the endemic equilibrium point.

$$G_1^* = \left(S^*_n, E^*_n, I^*_{an}, I^*_{sn}, S^*_v, E^*_v, I^*_{av}, I^*_{sv}, H_p^*, R^*\right), \tag{4.43}$$

where

$$S^*_n = \frac{(1-b)\sigma}{(\mu + \eta_1^*)},$$

$$E^*_n = \frac{(1-b)\sigma\eta_1^*}{(1+\mu)(\mu + \eta_1^*)},$$

$$I^*_{an} = \frac{(1-b)\phi\sigma\eta_1^*}{k_1},$$

$$I^*_{sn} = \frac{(1-b)(1-\phi)\sigma\eta^*_1}{k_2},$$

$$S^*_v = \frac{b\sigma}{(\mu+\eta^*_2)},$$

$$E^*_v = \frac{b\sigma\eta^*_2}{(1+\mu-\delta)(\mu+\eta^*_2)},$$

$$I^*_{av} = \frac{b(1-\delta)\phi\sigma\eta^*_2}{(1+\mu-\delta)k_3},$$

$$I^*_{sv} = \frac{b(1-\delta)(1-\phi)\sigma\eta^*_2}{(1+\mu-\delta)k_4},$$

$$H^*_p = k_5\left(\frac{(1-b)\phi\omega_1\eta^*_1}{k_1} + \frac{(1-b)(1-\phi)\omega_2\eta^*_1}{k_2} + \frac{b(1-\delta)\phi\omega_4\eta^*_2}{(1+\mu-\delta)k_3} + \frac{b(1-\delta)(1-\phi)\omega_3\eta^*_2}{(1+\mu-\delta)k_4}\right),$$

$$R^* = k_6\left(\frac{(1-b)\phi\gamma_2\eta^*_1}{k_1} + \frac{b(1-\delta)\phi\gamma_3\eta^*_2}{(1+\mu-\delta)k_3} + k_7\left(\frac{(1-b)\phi\omega_1\eta^*_1}{k_1} + \frac{(1-b)(1-\phi)\omega_2\eta^*_1}{k_2} + \frac{b(1-\delta)\phi\omega_4\eta^*_2}{(1+\mu-\delta)k_3} + \frac{b(1-\delta)(1-\phi)\omega_3\eta^*_2}{(1+\mu-\delta)k_4}\right)\right),$$

where $k_1 = (1+\mu)(d+\gamma_2+\mu+\omega_1)(\mu+\eta^*_1),\ k_2 = (1+\mu)(d+\mu+\omega_2)(\mu+\eta^*_1),$

$k_3 = (d+\gamma_3+\mu+\omega_4)(\mu+\eta^*_2),\ k_4 = (d+\mu+\omega_3)(\mu+\eta^*_2),\ k_5 = \frac{\sigma}{\gamma_1+\mu+d},\ k_6 = \frac{\sigma}{\mu},\ k_7 = \frac{\gamma_1}{\gamma_1+\mu+d}.$

when $R_0 > 1$.

The force of infection η^*_1, η^*_2, appearing in the components the of endemic equilibrium point can be determined by using the following expression

$$\eta^*_1 = \beta_{an} I^*_{an} + \beta_{sn} I^*_{sn} \quad (4.44)$$

and

$$\eta^*_2 = \beta_{av} I^*_{av} + \beta_{sv} I^*_{sv} \quad (4.45)$$

Basic Reproduction Number

The basic reproduction number R_0 represents the average number of secondary infections caused by one infected individual in a fully susceptible population. To evaluate Model 2, the next-generation matrix method is applied [64,96,97], a widely used mathematical tool in epidemiology and population dynamics for determining R_0. This method systematically derives R_0 by examining the rate of new infections produced and the rate of transitions between compartments. The derived expressions provide a comprehensive framework to assess the potential spread of the disease and guide the design of effective control measures. The expressions derived for this analysis are as follows:

$$\frac{dE_n}{dt} = \eta_1 S_n - \phi E_n - (1-\phi)E_n - \mu E_n,$$

$$\frac{dI_{an}}{dt} = \phi E_n - (\omega_1 + \gamma_2 + \mu + d)I_{an},$$

$$\frac{dI_{sn}}{dt} = (1-\phi)E_n - (\omega_2 + \mu + d)I_{sn},$$

$$\frac{dE_v}{dt} = \eta_2 S_v - (1-\delta)\phi E_v - (1-\delta)(1-\phi)E_v - \mu E_v,$$
$$\frac{dI_{av}}{dt} = (1-\delta)\phi E_v - (\omega_4 + \gamma_3 + \mu + d)I_{av},$$
$$\frac{dI_{sn}}{dt} = (1-\delta)(1-\phi)E_v - (\omega_3 + \mu + d)I_{sv}.$$

It follows that:

$$\begin{vmatrix} Gains\ \ to\ \ E_n & \eta_1 S_n \\ Gains\ \ to\ \ I_{an} & 0 \\ Gains\ \ to\ \ I_{an} & 0 \\ Gains\ \ to\ \ E_v & \eta_2 S_v \\ Gains\ \ to\ \ I_{av} & 0 \\ Gains\ \ to\ \ I_{sv} & 0 \end{vmatrix}, \quad \begin{vmatrix} Losses\ \ from\ \ E_n & \phi E_n + (1-\phi)E_n + \mu E_n \\ Losses\ \ from\ \ I_{an} & -\phi E_n + (\omega_1 + \gamma_2 + \mu + d)I_{an} \\ Losses\ \ from\ \ I_{an} & -(1-\phi)E_n + (\omega_2 + \mu + d)I_{sn} \\ Losses\ \ from\ \ E_v & (1-\delta)\phi E_v + (1-\delta)(1-\phi)E_v + \mu E_v \\ Losses\ \ from\ \ I_{av} & -(1-\delta)\phi E_v + (\omega_4 + \gamma_3 + \mu + d)I_{av} \\ Losses\ \ from\ \ I_{sv} & -(1-\delta)(1-\phi)E_v + (\omega_3 + \mu + d)I_{sv} \end{vmatrix}$$

Where F is the Jacobian matrix of the gains matrix and V is the Jacobian matrix of the losses matrix, Then we have

$$F = \begin{bmatrix} 0 & \beta_{an}S_n & \beta_{sn}S_n & 0 & 0 & 0 \\ 0 & 0 & 0 & 0 & 0 & 0 \\ 0 & 0 & 0 & 0 & 0 & 0 \\ 0 & 0 & 0 & 0 & \beta_{av}S_v & \beta_{sv}S_v \\ 0 & 0 & 0 & 0 & 0 & 0 \\ 0 & 0 & 0 & 0 & 0 & 0 \end{bmatrix},$$

$$V = \begin{bmatrix} \phi + (1-\phi) + \mu & 0 & 0 & 0 & 0 & 0 \\ -\phi & \omega_1 + \mu + d & 0 & 0 & 0 & 0 \\ -(1-\phi) & 0 & \omega_2 + \mu + d & 0 & 0 & 0 \\ 0 & 0 & 0 & (1-\delta)\phi + (1-\delta)(1-\phi) + \mu & 0 & 0 \\ 0 & 0 & 0 & -(1-\delta)\phi & \omega_4 + \gamma_3 + \mu + d & 0 \\ 0 & 0 & 0 & -(1-\delta)(1-\phi) & 0 & \omega_3 + \mu + d \end{bmatrix}.$$

Substituting the disease-free equilibrium point

$$G_0^* = \left(S^*_n, E^*_n, I^*_{an}, I^*_{sn}, S^*_v, E^*_v, I^*_{av}, I^*_{sv}, H_p^*, R^*\right) = \left(\frac{(1-b)\sigma}{\mu}, 0, 0, 0, \frac{b\sigma}{\mu}, 0, 0, 0, 0, 0\right)$$

Since $R_0 = FV^{-1}$, R_0 is determined by the eigenvalues of the matrix. The basic reproduction number R_0 is obtained by considering the largest positive eigenvalue. Therefore, we have

$$R_0 = \max\left\{R_n, R_v\right\}. \qquad (4.46)$$

When

$$R_n = \frac{(b-1)\ \sigma(d\ (\beta_{sn}\ (\phi-1) - \beta_{an}\phi) + \beta_{sn}\ (\phi-1)\ (\gamma_2 + \mu + \omega_1) - \beta_{an}\phi\ (\mu + \omega_2))}{\mu\ (1+\mu)\ (d+\gamma_2 + \mu + \omega_1)\ (d+\mu+\omega_2)},$$
$$R_v = \frac{b\sigma(\delta-1)\ (d\ (\beta_{sv}\ (\phi-1) - \beta_{av}\phi) - \beta_{av}\ \phi\ (\mu+\omega_3) + \beta_{sv}\ (\phi-1)\ (\gamma_3 + \mu + \omega_4))}{(\mu(1 - \delta + \mu)\ (\mathrm{d} + \mu + \omega_3)\ (\mathrm{d} + \gamma_3 + \mu + \omega_4)}.$$

4.2.2 Stability Analysis of Model 2

The stability analysis of the model (4.21) - (4.30) is conducted using the Lyapunov function to evaluate the stability of the two equilibrium points. The Lyapunov function is an effective tool for analyzing the stability of dynamic systems, as it provides a method to assess the system's behavior comprehensively. The application of this method is demonstrated in the following theorem.

Theorem 4.3 Let G_0^* be the disease-free equilibrium (DFE) of the model described by the system (4.21)–(4.30). Suppose that all parameters (e.g., infection rates, recovery rates) are positive, and all state variables (e.g., susceptible, exposed, infected) remain nonnegative within the positively invariant set Ψ. If $R_0 < 1$, then G_0^* is globally asymptotically stable in Ψ.

Proof. Consider the Lyapunov function as follows:

$$V(t) = V(E_n(t), I_{an}(t), I_{sn}(t), E_v(t), I_{av}(t), I_{sv}(t)) = k_1 E_n + k_2 I_{an} + k_3 I_{sn} + k_4 E_v + k_5 I_{av} + k_6 I_{sv}$$

It can be observed that $V(t) > 0$ for all $(E_n(t), I_{an}(t), I_{sn}(t), E_v(t), I_{av}(t), I_{sv}(t))^T \in \Psi$ and it follows that

$$\begin{aligned} V(E^*_n, I^*_{an}, I^*_{sn}, E^*_v, I^*_{av}, I^*_{sv}) &= k_1(0) + k_2(0) + k_3(0) + k_4(0) + k_5(0) + k_6(0) \\ &= 0, \end{aligned}$$

where k_1, k_2, k_3, k_4, k_5, and k_6 be positive constants. The derivative can be obtained as follows:

$$\frac{dV}{dt} = k_1 E'_n + k_2 I'_{an} + k_3 I'_{sn} + k_4 E'_v + k_5 I'_{av} + k_6 I'_{sv}$$

Substituting the values from the system of equations (4.21) - (4.30), we obtain

$$\begin{aligned} \frac{dV}{dt} &= k_1(\eta_1 S_n - \phi E_n - (1-\phi)E_n - \mu E_n) + k_2(\phi E_n - (\omega_1 + \gamma_2 + \mu + d)I_{an}) + k_3((1-\phi)E_n - (\omega_2 + \mu + d)I_{sn}) \\ &\quad + k_4(\eta_2 S_v - (1-\delta)\phi E_v - (1-\delta)(1-\phi)E_v - \mu E_v) + k_5((1-\delta)\phi E_v - (\omega_4 + \gamma_3 + \mu + d)I_{av}) \\ &\quad + k_6((1-\delta)(1-\phi)E_v - (\omega_3 + \mu + d)I_{sv}) \end{aligned}$$

Rearranging the equation to facilitate analysis, and substituting $S_n^* = \frac{(1-b)\sigma}{\mu}, S_v^* = \frac{b\sigma}{\mu}$ at the disease-free equilibrium, we obtain

we obtain:

$$\begin{aligned} \frac{dV}{dt} &= k_1((\beta_{an} I_{an} + \beta_{sn} I_{sn})S_n - \phi E_n - (1-\phi)E_n - \mu E_n) + k_2(\phi E_n - (\omega_1 + \gamma_2 + \mu + d)I_{an}) \\ &\quad + k_3((1-\phi)E_n - (\omega_2 + \mu + d)I_{sn}) + k_4((\beta_{av} I_{av} + \beta_{sv} I_{sv})S_v - (1-\delta)\phi E_v - (1-\delta)(1-\phi)E_v - \mu E_v) \\ &\quad + k_5((1-\delta)\phi E_v - (\omega_4 + \gamma_3 + \mu + d)I_{av}) + k_6((1-\delta)(1-\phi)E_v - (\omega_3 + \mu + d)I_{sv}) \\ &= \left(k_2\phi + k_3(1-\phi) - k_1(\phi + (1-\phi) + \mu)\right)E_n + \left(k_1\beta_{an}S_n - k_2(\omega_1 + \gamma_2 + \mu + d)\right)I_{an} + \left(k_1\beta_{sn}S_n - k_3(\omega_2 + \mu + d)\right)I_{sn} \\ &\quad + \left(k_5(1-\delta)\phi + k_6(1-\delta)(1-\phi) - k_4((1-\delta)\phi + (1-\delta)(1-\phi) + \mu)\right)E_v + \left(k_4\beta_{av}S_v - k_5(\omega_4 + \gamma_3 + \mu + d)\right)I_{av} \\ &\quad + \left(k_4\beta_{sv}S_v - k_6(\omega_3 + \mu + d)\right)I_{sv} \end{aligned}$$

$$\frac{dV}{dt} = \left(k_2\phi + k_3(1-\phi) - k_1(\phi+(1-\phi)+\mu)\right)E_n + \left(k_1\beta_{an}\frac{(1-b)\sigma}{\mu} - k_2(\omega_1+\gamma_2+\mu+d)\right)I_{an} + \left(k_1\beta_{sn}\frac{(1-b)\sigma}{\mu} - k_3(\omega_2+\mu+d)\right)I_{sn}$$
$$+\left(k_5(1-\delta)\phi + k_6(1-\delta)(1-\phi) - k_4((1-\delta)\phi+(1-\delta)(1-\phi)+\mu)\right)E_v + \left(k_4\beta_{av}\frac{b\sigma}{\mu} - k_5(\omega_4+\gamma_3+\mu+d)\right)I_{av}$$
$$+\left(k_4\beta_{sv}\frac{b\sigma}{\mu} - k_6(\omega_3+\mu+d)\right)I_{sv}$$

Let $k_1 = \frac{\mu}{(1-b)\sigma}, k_2 = \frac{\beta_{an}}{(\omega_1+\gamma_2+\mu+d)}, k_3 = \frac{\beta_{sn}}{(\omega_2+\mu+d)}, k_4 = \frac{\mu}{b\sigma}, k_5 = \frac{\beta_{av}}{(\omega_4+\gamma_3+\mu+d)}$,

$k_6 = \frac{\beta_{sv}}{(\omega_3+\mu+d)}$, then we obtain:

$$\frac{dV}{dt} = \left(\frac{\beta_{an}}{(\omega_1+\gamma_2+\mu+d)}\phi + \frac{\beta_{sn}}{(\omega_2+\mu+d)}(1-\phi) - \frac{\mu}{(1-b)\sigma}(\phi+(1-\phi)+\mu)\right)E_n$$
$$+\left(\frac{\beta_{av}}{(\omega_4+\gamma_3+\mu+d)}(1-\delta)\phi + \frac{\beta_{sv}}{(\omega_3+\mu+d)}(1-\delta)(1-\phi) - \frac{\mu}{b\sigma}((1-\delta)\phi+(1-\delta)(1-\phi)+\mu)\right)E_v$$
$$= \left(\frac{\beta_{an}\phi}{(\omega_1+\gamma_2+\mu+d)} + \frac{\beta_{sn}(1-\phi)}{(\omega_2+\mu+d)} - \frac{\mu(1+\mu)}{(1-b)\sigma}\right)E_n + \left(\frac{\beta_{av}(1-\delta)\phi}{(\omega_4+\gamma_3+\mu+d)} + \frac{\beta_{sv}(1-\delta)(1-\phi)}{(\omega_3+\mu+d)} - \frac{\mu(1-\delta+\mu)}{b\sigma}\right)E_v$$
$$= \frac{\mu(1+\mu)}{(1-b)\sigma}\left(\frac{(\beta_{an}\phi(\omega_2+\mu+d)+\beta_{sn}(1-\phi)(\omega_1+\gamma_2+\mu+d))(1-b)\sigma}{\mu(\omega_1+\gamma_2+\mu+d)(\omega_2+\mu+d)(1+\mu)} - 1\right)E_n$$
$$+\frac{\mu(1-\delta+\mu)}{b\sigma}\left(\frac{(\beta_{av}(1-\delta)\phi(\omega_3+\mu+d)+\beta_{sv}(1-\delta)(1-\phi)(\omega_4+\gamma_3+\mu+d))b\sigma}{\mu(\omega_4+\gamma_3+\mu+d)(\omega_3+\mu+d)(1-\delta+\mu)} - 1\right)E_v$$
$$= \frac{\mu(1+\mu)}{(1-b)\sigma}\left(\frac{(\beta_{an}\phi(\omega_2+\mu+d)+\beta_{sn}(1-\phi)(\omega_1+\gamma_2+\mu+d))(1-b)\sigma}{\mu(\omega_1+\gamma_2+\mu+d)(\omega_2+\mu+d)(1+\mu)} - 1\right)E_n$$
$$+\frac{\mu(1-\delta+\mu)}{b\sigma}\left(\frac{(\beta_{av}(1-\delta)\phi(\omega_3+\mu+d)+\beta_{sv}(1-\delta)(1-\phi)(\omega_4+\gamma_3+\mu+d))b\sigma}{\mu(\omega_4+\gamma_3+\mu+d)(\omega_3+\mu+d)(1-\delta+\mu)} - 1\right)E_v$$
$$\frac{dV}{dt} = \frac{\mu(1+\mu)}{(1-b)\sigma}(R_n-1)E_n + \frac{\mu(1-\delta+\mu)}{b\sigma}(R_v-1)E_v. \qquad (4.47)$$

Thus, it can be observed that equation (4.47), $\frac{dV}{dt} = 0$ if $R_n < 0$ and $R_v < 0$. Additionally, $\frac{dV}{dt} = 0$ if $E_n = 0$, and $E_v = 0$. According to LaSalle's invariance principle [65,97,98], this implies that the disease-free steady state G_0^* is globally asymptotically stable on Ψ. □

Theorem 4.4 Consider the model given by the system (4.21)–(4.30) and let G_1^* be its endemic equilibrium. Assume that all parameters are positive, that all state variables remain nonnegative within a positively invariant region Ψ, and that the model admits equilibrium G_1^* for $R_0 > 1$. Then, if $R_0 > 1$, G_1^* is globally asymptotically stable in Ψ.

We assume that

$$\begin{cases} \eta_1^* = \eta_2^* \\ \mu = (\mu + \eta_1^*) \\ \beta_{sn} = \dfrac{\omega_2 + \mu + d}{S_n^*} \\ \beta_{sv} \dfrac{\omega_3 + \mu + d}{S_v^*} \\ \beta_{an} = \dfrac{\omega_1 + \gamma_2 + \mu + d}{S_n^*} \\ \beta_{av} = \dfrac{\omega_4 + \gamma_3 + \mu + d}{S_v^*} \end{cases} \tag{4.48}$$

Proof. Consider the Lyapunov function defined as follows:

$$K(t) = \left(S_n - S_n^* - S_n^* \ln \frac{S_n}{S_n^*} \right) + E_n + I_{an} + I_{sn} + \left(S_v - S_v^* - S_v^* \ln \frac{S_v}{S_v^*} \right) + E_v + I_{av} + I_{sv} .$$

The derivative of the function K is obtained as follows

$$\begin{aligned}
\frac{dK}{dt} &= S_n' \left(1 - \frac{S_n^*}{S_n} \right) + E_n' + I_{an}' + I_{sn}' + S_n' \left(1 - \frac{S_v^*}{S_v} \right) + E_v' + I_{av}' + I_{sv}' \\
&= \left((1-b)\sigma - \eta_1 S_n - \mu S_n \right) \left(1 - \frac{S_n^*}{S_n} \right) + \left(\eta_1 S_n - \phi E_n - (1-\phi) E_n - \mu E_n \right) + \left(\phi E_n - (\omega_1 + \gamma_2 + \mu + d) I_{an} \right) \\
&\quad + \left((1-\phi) E_n - (\omega_2 + \mu + d) I_{sn} \right) + \left(b\sigma - \eta_2 S_v - \mu S_v \right) \left(1 - \frac{S_v^*}{S_v} \right) + \left(\eta_2 S_v - (1-\delta)\phi E_v - (1-\delta)(1-\phi) E_v - \mu E_v \right) \\
&\quad + \left((1-\delta)\phi E_v - (\omega_4 + \gamma_3 + \mu + d) I_{av} \right) + \left((1-\delta)(1-\phi) E_v - (\omega_3 + \mu + d) I_{sv} \right) \\
&= \left((1-b)\sigma - \left(\beta_{an} I_{an} + \beta_{sn} I_{sn} \right) S_n - \mu S_n \right) \left(1 - \frac{S_n^*}{S_n} \right) + \left(\left(\beta_{an} I_{an} + \beta_{sn} I_{sn} \right) S_n - \phi E_n - (1-\phi) E_n - \mu E_n \right) \\
&\quad + \left(\phi E_n - (\omega_1 + \gamma_2 + \mu + d) I_{an} \right) + \left((1-\phi) E_n - (\omega_2 + \mu + d) I_{sn} \right) + \left(b\sigma - \left(\beta_{av} I_{av} + \beta_{sv} I_{sv} \right) S_v - \mu S_v \right) \left(1 - \frac{S_v^*}{S_v} \right) \\
&\quad + \left(\left(\beta_{av} I_{av} + \beta_{sv} I_{sv} \right) S_v - (1-\delta)\phi E_v - (1-\delta)(1-\phi) E_v - \mu E_v \right) + \left((1-\delta)\phi E_v - (\omega_4 + \gamma_3 + \mu + d) I_{av} \right) \\
&\quad + \left((1-\delta)(1-\phi) E_v - (\omega_3 + \mu + d) I_{sv} \right) \\
&= (1-b)\sigma \left(1 - \frac{S_n^*}{S_n} \right) - \mu S_n \left(1 - \frac{S_n^*}{S_n} \right) + \left(\beta_{an} I_{an} + \beta_{sn} I_{sn} \right) S_n^* - \mu E_n - (\omega_1 + \gamma_2 + \mu + d) I_{an} - (\omega_2 + \mu + d) I_{sn} \\
&\quad + b\sigma \left(1 - \frac{S_v^*}{S_v} \right) - \mu S_v \left(1 - \frac{S_v^*}{S_v} \right) + \left(\beta_{av} I_{av} + \beta_{sv} I_{sv} \right) S_v^* - \mu E_v - (\omega_4 + \gamma_3 + \mu + d) I_{av} - (\omega_3 + \mu + d) I_{sv} \\
&= (1-b)\sigma \left(1 - \frac{S_n^*}{S_n} \right) - \mu S_n^* \left(1 - \frac{S_n}{S_n^*} \right) + I_{an} (\beta_{an} S_n^* - (\omega_1 + \gamma_2 + \mu + d)) + I_{sn} (\beta_{sn} S_n^* - (\omega_2 + \mu + d)) - \mu E_n \\
&\quad + b\sigma \left(1 - \frac{S_v^*}{S_v} \right) - \mu S_v^* \left(1 - \frac{S_v}{S_v^*} \right) + I_{av} (\beta_{av} S_v^* - (\omega_4 + \gamma_3 + \mu + d)) + I_{sv} (\beta_{sv} S_v^* - (\omega_3 + \mu + d)) - \mu E_v
\end{aligned}$$

Substituting $S_n^* = \dfrac{(1-b)\sigma}{(\mu + \eta_1^*)}, S_v^* = \dfrac{b\sigma}{(\mu + \eta_2^*)}$ at the endemic equilibrium, we obtain

$$\begin{aligned}
\frac{dK}{dt} &= (1-b)\sigma \left(1 - \frac{S_n^*}{S_n} \right) - \mu \frac{(1-b)\sigma}{(\mu + \eta_1^*)} \left(1 - \frac{S_n}{S_n^*} \right) + I_{an} (\beta_{an} S_n^* - (\omega_1 + \gamma_2 + \mu + d)) + I_{sn} (\beta_{sn} S_n^* - (\omega_2 + \mu + d)) - \mu E_n \\
&\quad + b\sigma \left(1 - \frac{S_v^*}{S_v} \right) - \mu \frac{b\sigma}{(\mu + \eta_2^*)} \left(1 - \frac{S_v}{S_v^*} \right) + I_{av} (\beta_{av} S_v^* - (\omega_4 + \gamma_3 + \mu + d)) + I_{sv} (\beta_{sv} S_v^* - (\omega_3 + \mu + d)) - \mu E_v
\end{aligned}$$

From the condition (4.48), we obtain

$$\frac{dK}{dt} = (1-b)\sigma\left(1-\frac{S_n^*}{S_n}\right) - (1-b)\sigma\left(1-\frac{S_n}{S_n^*}\right) + b\sigma\left(1-\frac{S_v^*}{S_v}\right) - b\sigma\left(1-\frac{S_v}{S_v^*}\right) - \mu E_n - \mu E_v$$

$$= (1-b)\sigma\left(2-\frac{S_n^*}{S_n}-\frac{S_n}{S_n^*}\right) + b\sigma\left(2-\frac{S_v^*}{S_v}-\frac{S_v}{S_v^*}\right) - \mu E_n - \mu E_v$$

$$= -(1-b)\sigma\left(\frac{\left(S_n^*-S_n\right)^2}{S_n S_n^*}\right) - b\sigma\left(\frac{\left(S_v^*-S_v\right)^2}{S_v S_v^*}\right) - \mu E_n - \mu E_v$$

$$\frac{dK}{dt} = -\left[(1-b)\sigma\left(\frac{\left(S_n^*-S_n\right)^2}{S_n S_n^*}\right) + b\sigma\left(\frac{\left(S_v^*-S_v\right)^2}{S_v S_v^*}\right) + \mu E_n + \mu E_v\right] \le 0 \quad (4.49)$$

From equation (4.49), it is evident that $\frac{dK}{dt} < 0$. Therefore, according to LaSalle's invariance principle, the endemic equilibrium point G_1^* is globally asymptotically stable in Ψ. □

4.2.3 Numerical Analysis Results of Model 2

The numerical analysis results of Model 2 are presented using parameters obtained through model fitting, ensuring alignment with observed data, while additional parameters were sourced from a comprehensive literature review. These parameters, listed in Tables 4.4 and 4.5, form the foundation for the analysis, allowing for a detailed evaluation of the model's behavior under various scenarios. This approach ensures a robust and accurate representation of the system, facilitating the assessment of its dynamics and potential control strategies.

Table 4.4 Parameter Values Used in the Numerical Analysis of Model 2 at the Disease-Free Equilibrium.

Parameters	The disease-free	Units	Source
b	0.5	Per person · days^{-1}	Estimated
σ	1	N/A	Estimated
β_{an}	0.00001	Per person · days^{-1}	Estimated
β_{sn}	0.000009	Per person · days^{-1}	Estimated
β_{av}	0.000008	Per person · days^{-1}	Estimated
β_{sv}	0.00001	Per person · days^{-1}	Estimated
ϕ	1/7	day^{-1}	[27,100]
δ	0.8	day^{-1}	Assumed
ω_1	0.1	day^{-1}	[17,19,27]
ω_2	0.1	day^{-1}	[17,19,27]

ω_3	0.1	day^{-1}	[17,19,27]
ω_4	0.1	day^{-1}	[17,19,27]
γ_1	1/7	day^{-1}	[27]
γ_2	1/14	day^{-1}	[10]
γ_3	1/14	day^{-1}	[27]
μ	0.0000365	day^{-1}	[43,101]
d	0.00286	day^{-1}	[97]

Table 4.5 Parameter Values Used in the Numerical Analysis of Model 2 at the Endemic Equilibrium.

Parameters	The Endemic	Units	Source
b	0.5	Per person · $days^{-1}$	Estimated
σ	1,400	N/A	Estimated
β_{an}	0.00001	Per person · $days^{-1}$	Data fitted
β_{sn}	0.000009	Per person · $days^{-1}$	Data fitted
β_{av}	0.000008	Per person · $days^{-1}$	Data fitted
β_{sv}	0.00001	Per person · $days^{-1}$	Data fitted
ϕ	1/7	day^{-1}	[27,100]
δ	0.8	day^{-1}	Assumed
ω_1	0.1	day^{-1}	[17,19,27]
ω_2	0.1	day^{-1}	[17,19,27]
ω_3	0.1	day^{-1}	[17,19,27]
ω_4	0.1	day^{-1}	[17,19,27]
γ_1	1/7	day^{-1}	[27]
γ_2	1/14	day^{-1}	[10]
γ_3	1/14	day^{-1}	[27]
μ	0.0000365	day^{-1}	[43,101]
d	0.00286	day^{-1}	[97]

4.2.3.1 Model Fitting of Model 2

The numerical results of the model (4.21) – (4.30) are compared with real epidemic data from Thailand to evaluate its accuracy. Parameter values were obtained

through model fitting to align closely with daily reported infections recorded from January 1, 2022, to March 1, 2022 [102]. The blue circles in Figure 4.8 represent the actual daily reported cases, while the solid red line illustrates the model's predictions. This comparison demonstrates the model's capability to replicate observed epidemic trends, reflecting both the rise and decline in cumulative cases during the specified period. The agreement between the data and the model validates its reliability in describing epidemic dynamics and supports its application for effective control strategies. Specifically, the coefficient of determination for Figure 4.8(a) is R^2=0.9010, while for Figure 4.8 (b), it is R^2=0.9300, indicating a strong correlation between the model predictions and the observed data, further reinforcing the model's accuracy in capturing the real-world epidemic dynamics.

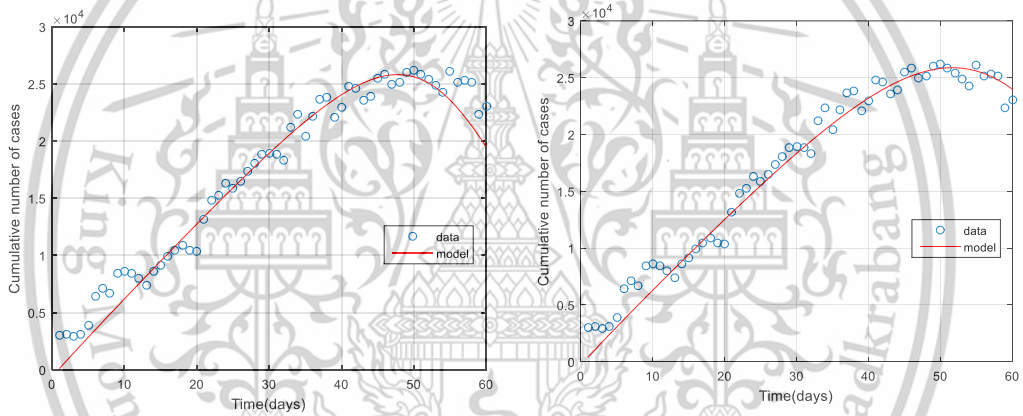

Figure 4.8 Plot of Daily Reported Cases Alongside Model (4.21) - (4.30) Solutions Over Time, Using Data from January 1, 2022, to March 1, 2022 [102].

4.2.3.2 Numerical Analysis Result of Model 2

Numerical Analysis of the Disease-Free State

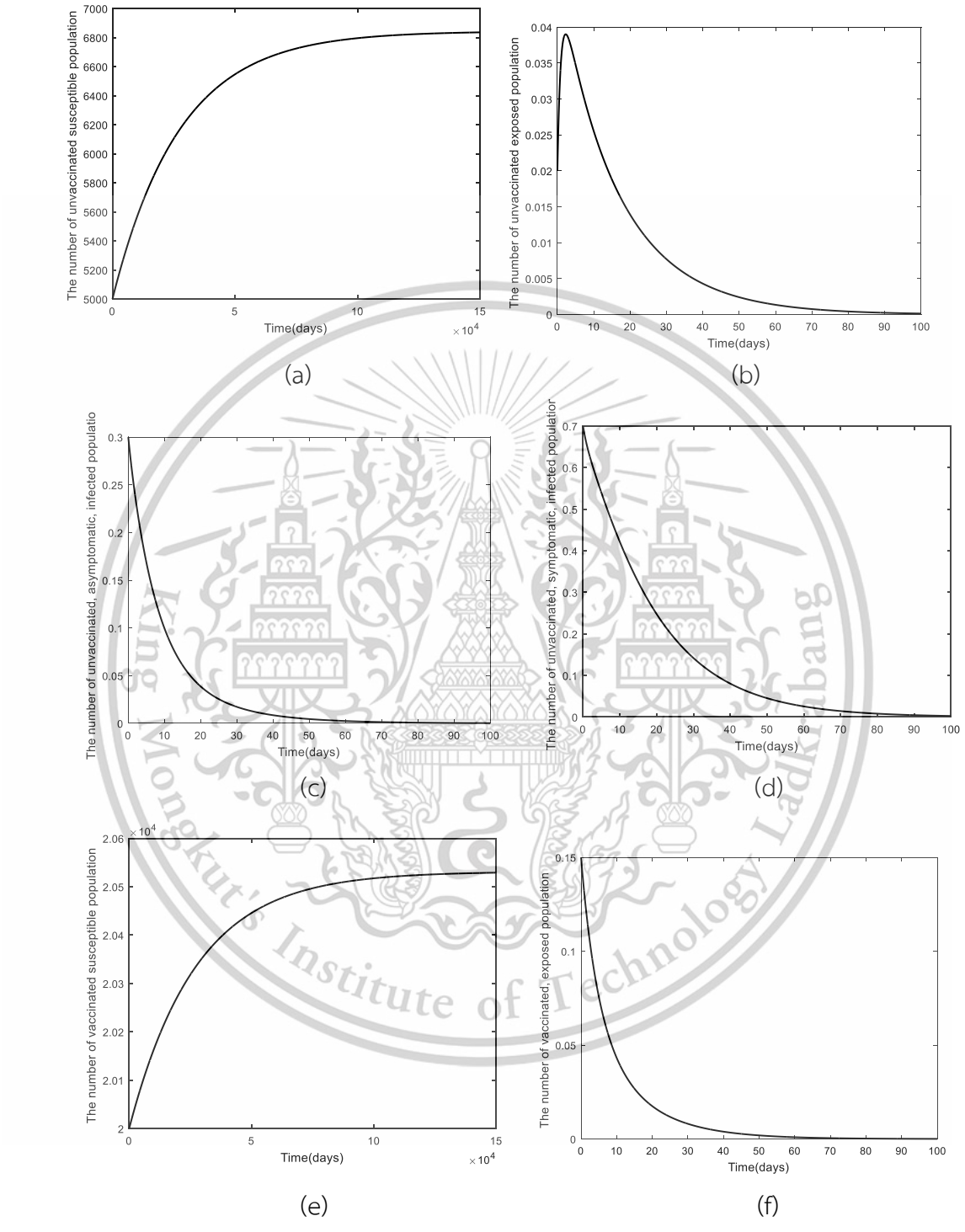

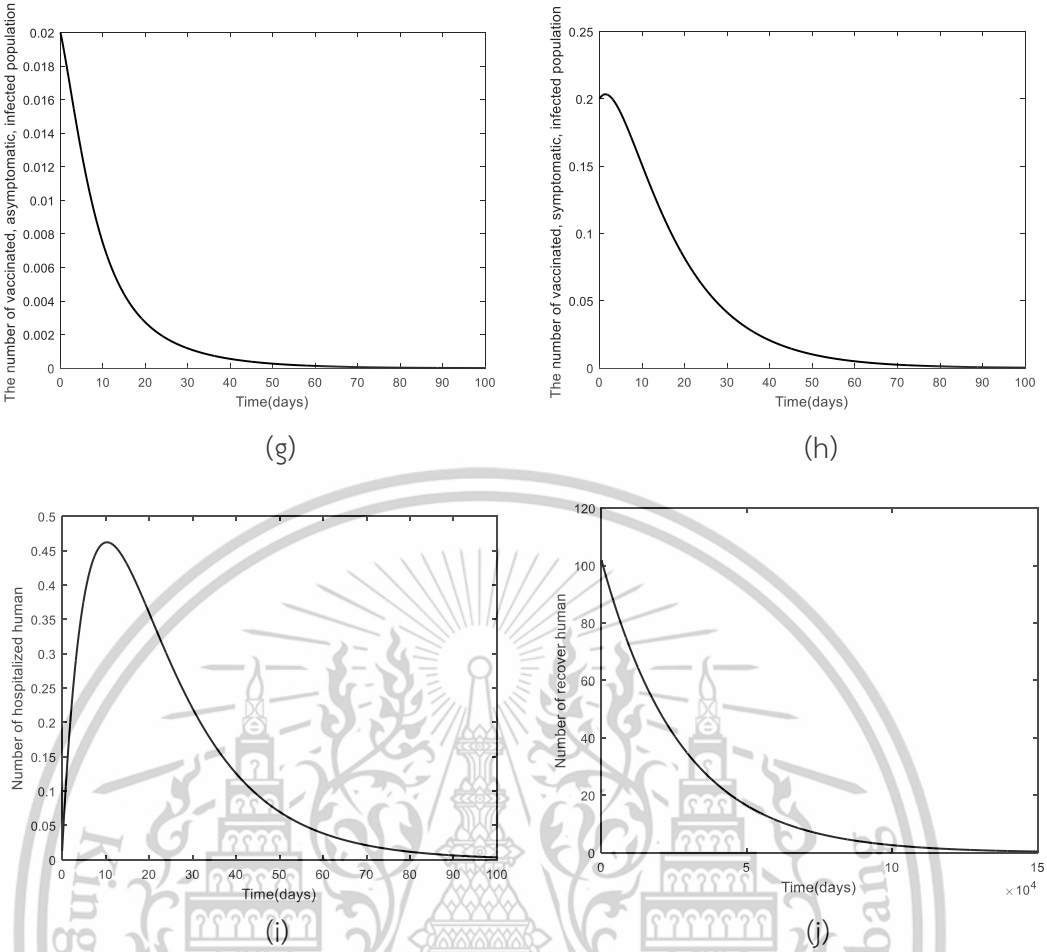

Figure 4.9 Solutions of the system of equations (4.21) - (4.30): Graph showing the relationship between time and $S_n, E_n, I_{an}, I_{sn}, S_v, E_v, I_{av}, I_{sv}, H_p, R$ when $R_0 = 0.58072$.

Numerical Analysis of the Endemic State

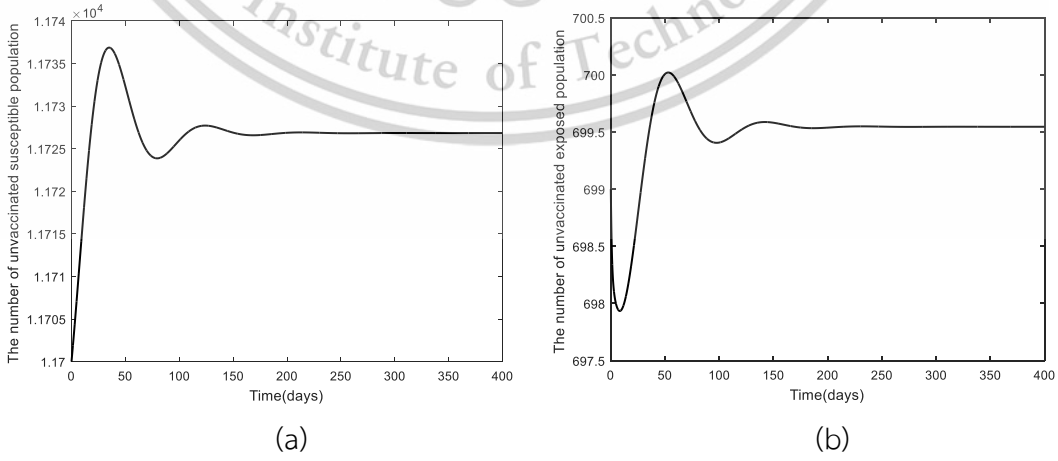

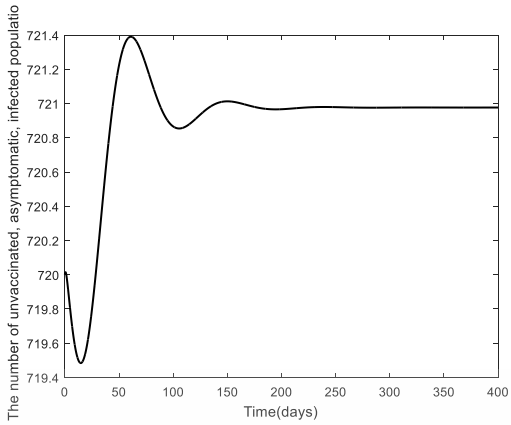

(c)

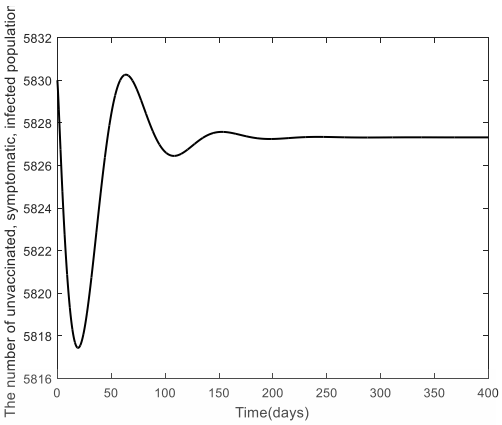

(d)

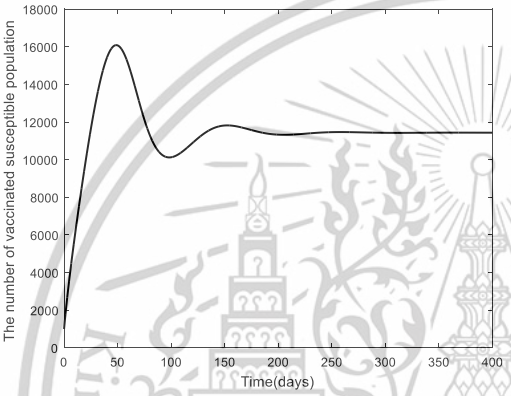

(e)

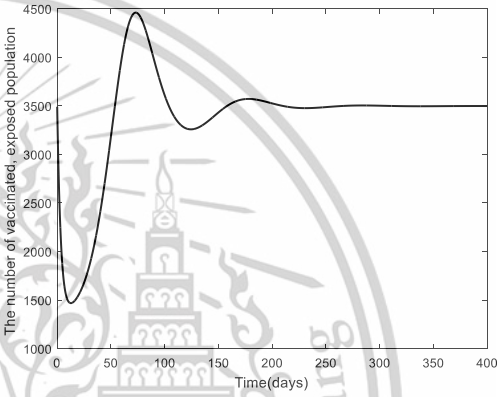

(f)

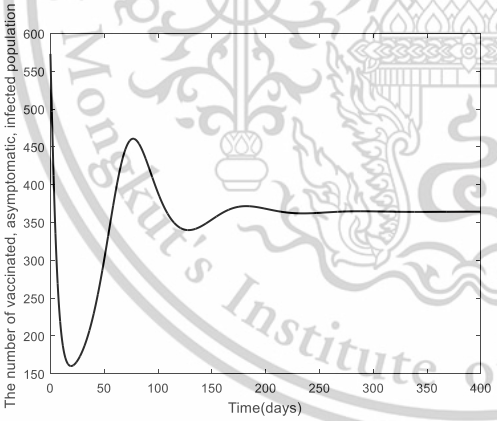

(g)

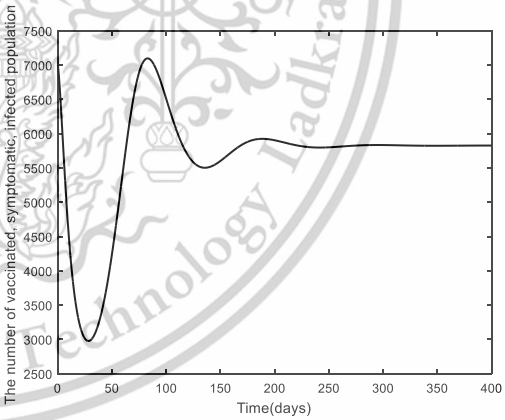

(h)

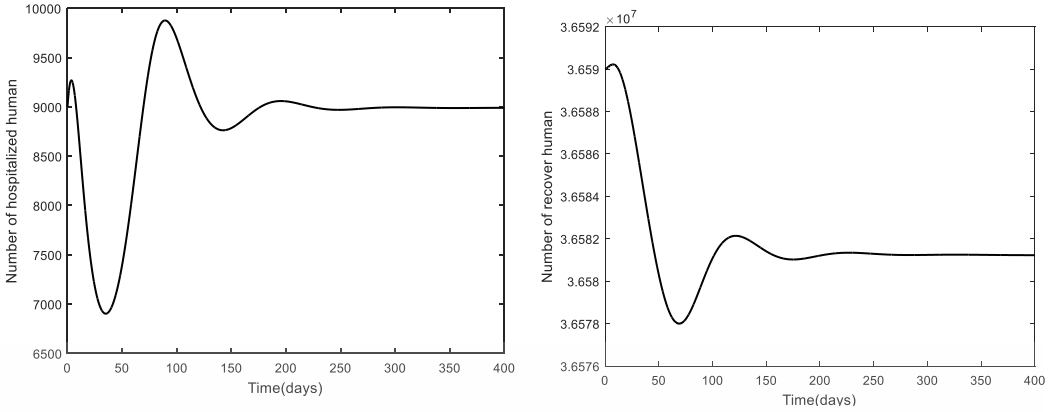

(i) (j)

Figure 4.10 Solutions of the system of equations (4.21)-(4.30): Graph showing the relationship between time and $S_n, E_n, I_{an}, I_{sn}, S_v, E_v, I_{av}, I_{sv}, H_p, R$ when $R_0 = 1.72298$.

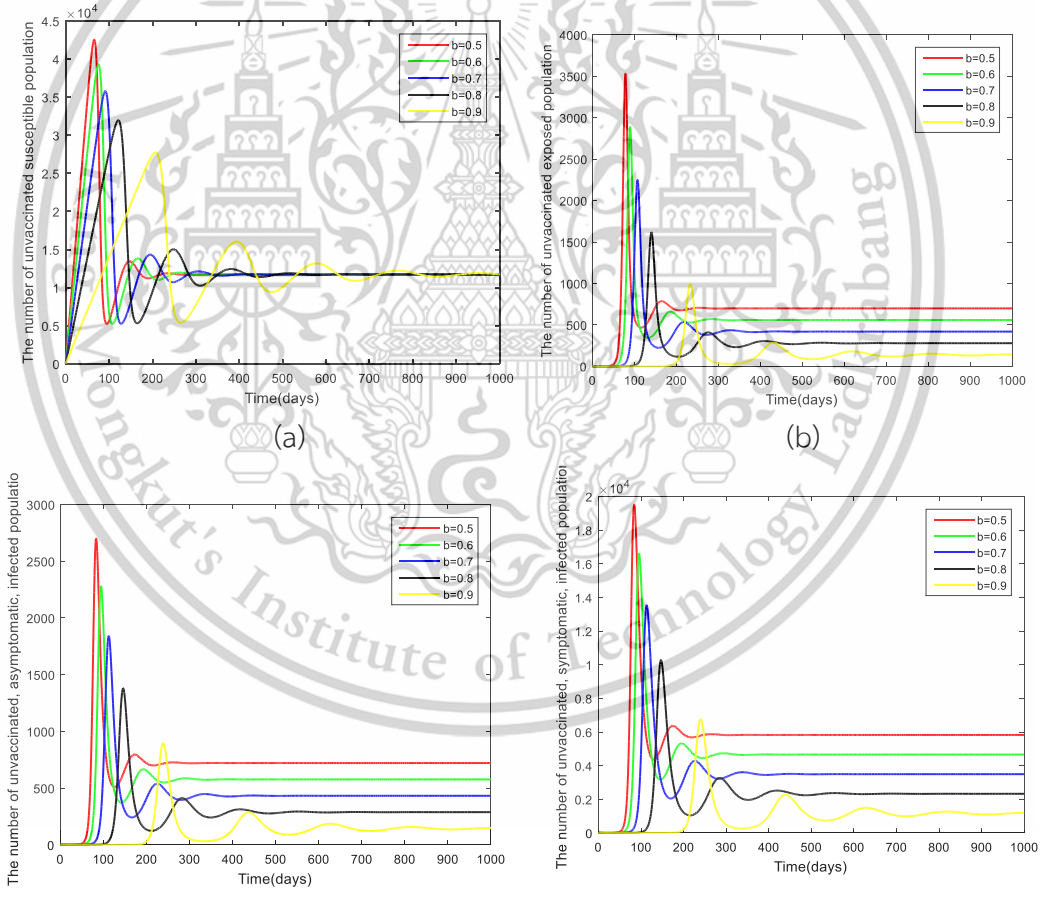

(a) (b)

(c) (d)

Figure 4.11 Solutions of the system of equations (4.21) - (4.30): Graph showing the relationship between time and the comparison of vaccination rates (b) when $R_0 > 1$.

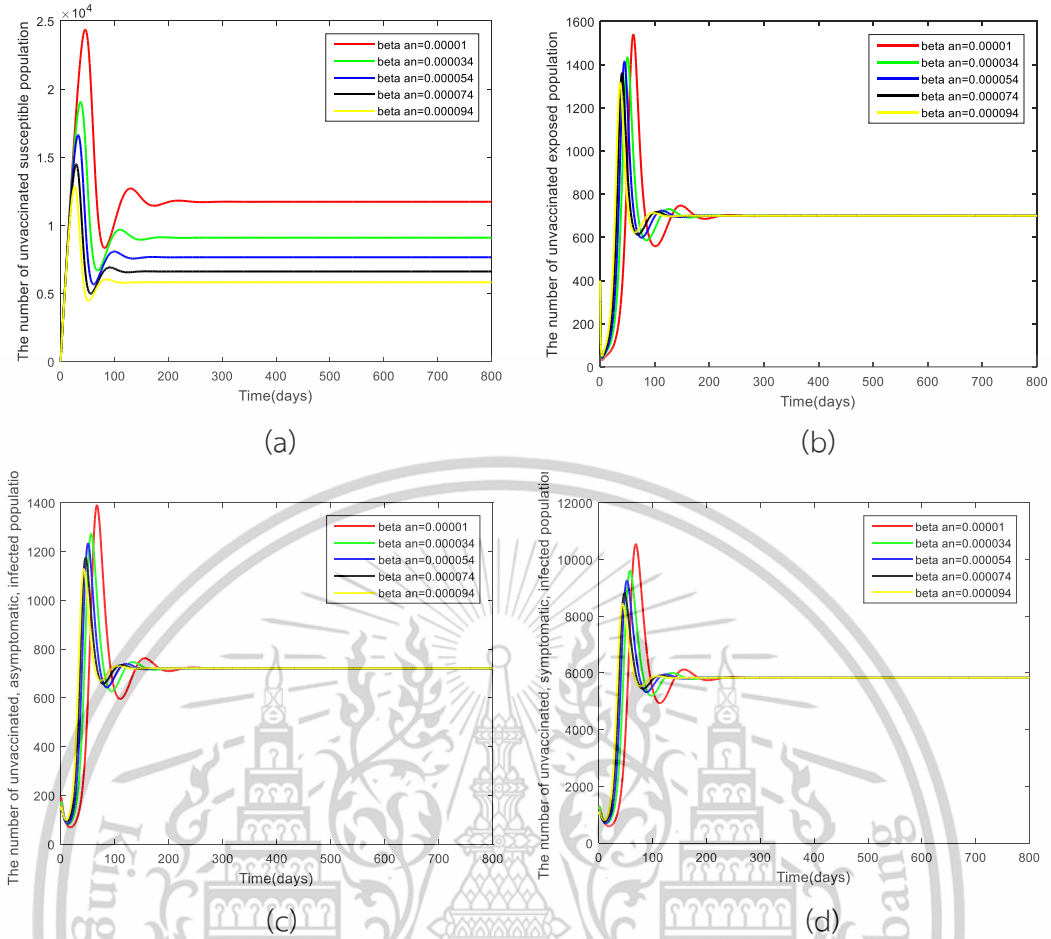

Figure 4.12 Solutions of the system of equations (4.21) - (4.30): Graph showing the relationship between time and the comparison of infection rates among unvaccinated asymptomatic individuals (β_{an}) when $R_0 > 1$.

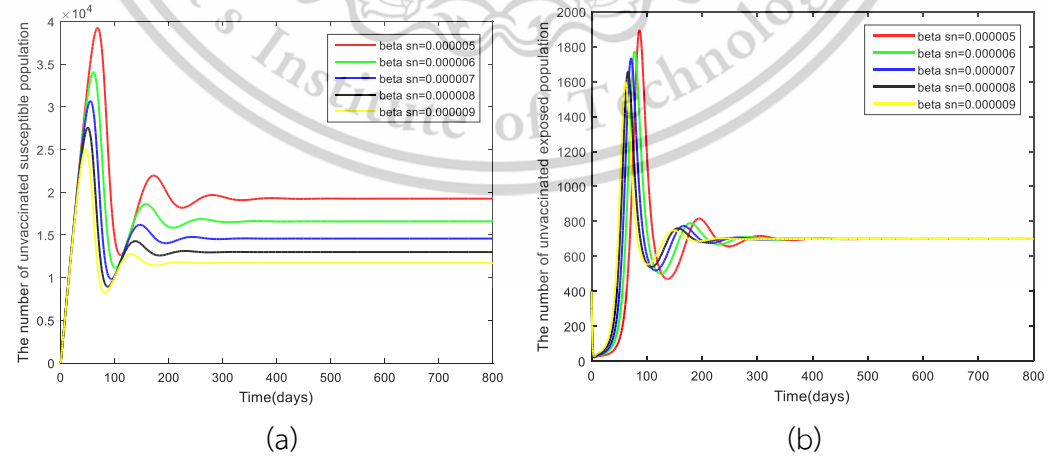

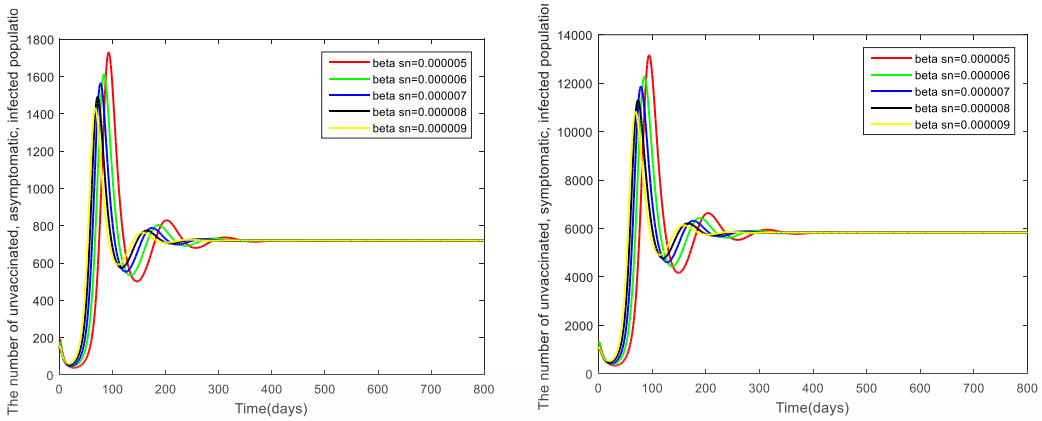

(e) (f)

Figure 4.13 Solutions of the system of equations (4.21) - (4.30): Graph showing the relationship between time and the comparison of infection rates among unvaccinated symptomatic individuals (β_{sn}) when $R_0 > 1$.

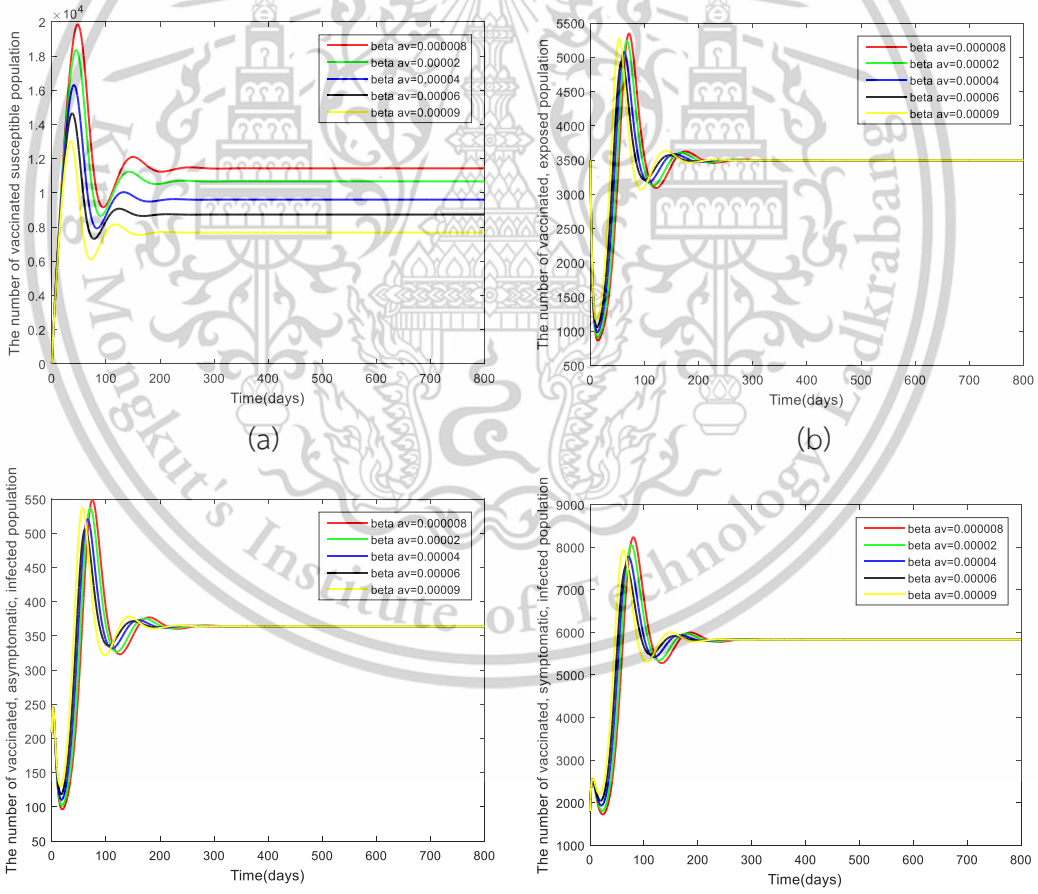

(a) (b)

(c) (d)

Figure 4.14 Solutions of the system of equations (4.21) - (4.30): Graph showing the relationship between time and the comparison of infection rates among vaccinated asymptomatic individuals (β_{av}) When $R_0 > 1$.

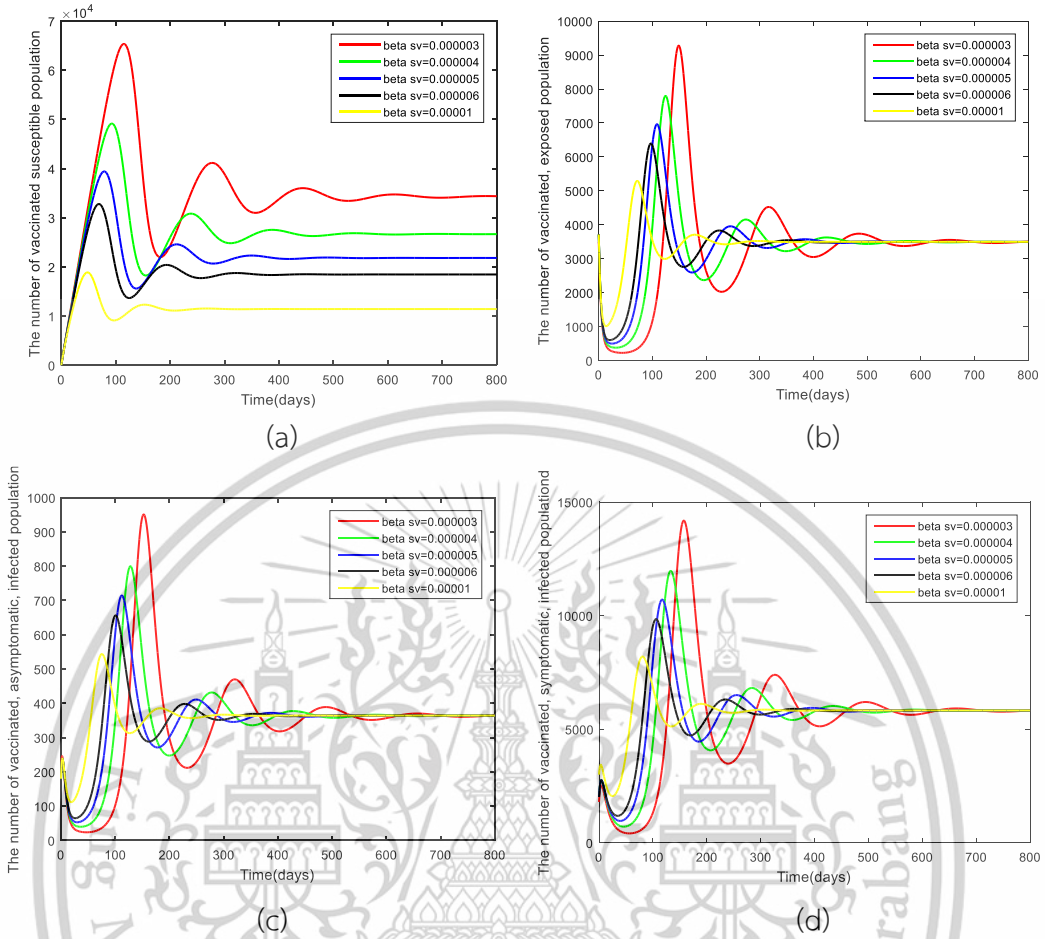

Figure 4.15 Solutions of the system of equations (4.21) - (4.30): Graph showing the relationship between time and the comparison of infection rates among vaccinated symptomatic individuals (β_{sv}) when $R_0 > 1$.

We have conducted a numerical analysis of the model (4.21) - (4.30). In Part 1, we analyzed the disease-free equilibrium and the endemic equilibrium. In Part 2, we compared the parameters that influence the spread of the disease. These analyses will be explained in detail in the following sections.

Part 1: Analysis of the Disease-Free and Endemic Equilibria

From Figure 4.9, it is evident that the number of unvaccinated individuals at risk of infection, as well as the number of vaccinated individuals at risk, gradually increases over time. Eventually, the populations converge to equilibrium points at 6,849 and 20,547, respectively. In contrast, the populations of unvaccinated individuals in the exposed state, unvaccinated asymptomatic individuals, unvaccinated symptomatic individuals, vaccinated individuals in the exposed state, vaccinated

asymptomatic individuals, vaccinated symptomatic individuals, hospitalized individuals, and those who have recovered from the disease, all gradually decrease and eventually reach zero. This behavior is consistent with the dynamics of the disease-free state. Figure 4.10 illustrates the convergence to the endemic equilibrium. As time progresses, the solutions converge to the equilibrium point $G_1^* = (11726, 699.54, 720.97, 5828, 11130, 3497, 573, 5826, 8888, 3.65966 \times 10^7)$. This demonstrates the long-term persistence of the disease within the population, characteristic of the endemic state.

Part 2: Comparison of Parameters Affecting Disease Transmission

In this section, we compare various parameters to observe their influence on the spread of the disease. Specifically, we examine the vaccination rate (b), and the infection rates among unvaccinated asymptomatic individuals (β_{an}), unvaccinated symptomatic individuals (β_{sn}), vaccinated asymptomatic individuals (β_{av}), and vaccinated symptomatic individuals (β_{sv}). From Figure 4.11, we compare the vaccination rates at $b =$ 0.5, 0.6, 0.7, 0.8 and 0.9. An increase in the vaccination rate leads to a corresponding decrease in the number of infections in each epidemic scenario. This demonstrates that vaccination is an effective strategy for controlling the epidemic and reducing the spread of the disease. Figures 4.12 and 4.13 compare the infection rates among unvaccinated asymptomatic individuals at β_{an} = 0.00001, 0.000034, 0.000054, 0.000074, 0.000094, and among unvaccinated symptomatic individuals at β_{sn} = 0.000005, 0.000006, 0.000007, 0.000008, 0.000009. The numerical analysis reveals that as the infection rate increases, the number of infections in each state decreases among the unvaccinated population, including those at risk of infection, those in the exposed state, asymptomatic individuals, and symptomatic individuals. In Figures 4.14 and 4.15, the infection rates among vaccinated asymptomatic individuals at β_{av} = 0.000008, 0.00002, 0.00004, 0.00006, 0.00009, and among vaccinated symptomatic individuals at β_{sv} = 0.000003, 0.000004, 0.000005, 0.000006, 0.00001 are analyzed. The results indicate that as the infection rate decreases in each state, the number of infections increases, leading to faster control of the disease. Therefore, implementing measures to reduce infection rates, such as social distancing and wearing masks, can be effective strategies for reducing the spread of the disease.

4.2.3.3 Sensitivity Analysis of Model 2

In this section, we analyze the sensitivity indices affecting the basic reproduction number R_0 of Model 2. This analysis is conducted to assess the influence of various parameters on the changes in R_0. The sensitivity indices can be calculated using the following formula [94,95]:

$$\Upsilon_{\kappa}^{R_0} = \frac{\partial R_0}{\partial \kappa} \times \frac{\kappa}{R_0}. \tag{4.50}$$

Where κ represents the parameter being analyzed and R_0 is the basic reproduction number. The results of this analysis are presented in Table 4.6, as shown below.

Table 4.6 Sensitivity Indices of the Basic Reproduction Number for Model 2.

Parameters	Sensitivity Indices
b	+1.000000
σ	+1.000000
β_{an}	+0.120900
β_{sn}	+0.879100
β_{av}	+0.073000
β_{sv}	+0.927000
δ	+0.000700
ϕ	-0.002600
ω_1	-0.087200
ω_2	-0.854400
ω_3	-0.900900
ω_4	-0.041900
γ_2	-0.031100
γ_3	-0.029900
μ	-1.000400
d	-0.023900

The results of the sensitivity analysis, as shown in Table 4.6, indicate that vaccine administration should be a key consideration in designing control strategies. This is because increasing or decreasing the vaccination rate significantly impacts the basic reproduction number R_0. The analysis reveals that the vaccination rate has the highest

sensitivity index, meaning it plays a crucial role in controlling the spread of the disease. The development of an optimal control model, which will be discussed in the following sections, should therefore prioritize vaccination strategies.

4.2.4 Optimal control problem of model 2

4.2.4.1 Optimal Control Model of Model 2

The design of the control strategy for Model 2 involves creating an optimal control model. In this model, the control functions are defined as u_1, representing the vaccination rate, and u_2, representing the immunity gained from vaccination. The mathematical model for controlling the spread of COVID-19, incorporating these control functions, can be formulated as follows:

$$\frac{dS_n}{dt} = (1-b)\sigma - \eta_1 S_n - \mu S_n - u_1(t)S_n, \tag{4.51}$$

$$\frac{dE_n}{dt} = \eta_1 S_n - \phi E_n - (1-\phi)E_n - \mu E_n, \tag{4.52}$$

$$\frac{dI_{an}}{dt} = \phi E_n - (\omega_1 + \gamma_2 + \mu + d)I_{an}, \tag{4.53}$$

$$\frac{dI_{sn}}{dt} = (1-\phi)E_n - (\omega_2 + \mu + d)I_{sn}, \tag{4.54}$$

$$\frac{dS_v}{dt} = b\sigma - \eta_2 S_v - \mu S_v - u_2(t)S_v, \tag{4.55}$$

$$\frac{dE_v}{dt} = \eta_2 S_v - (1-\delta)\phi E_v - (1-\delta)(1-\phi)E_v - \mu E_v, \tag{4.56}$$

$$\frac{dI_{av}}{dt} = (1-\delta)\phi E_v - (\omega_4 + \gamma_3 + \mu + d)I_{av}, \tag{4.57}$$

$$\frac{dI_{sn}}{dt} = (1-\delta)(1-\phi)E_v - (\omega_3 + \mu + d)I_{sv}, \tag{4.58}$$

$$\frac{dH_p}{dt} = \omega_1 I_{an} + \omega_2 I_{sn} + \omega_3 I_{sv} + \omega_4 I_{av} - (\gamma_1 + \mu + d)H_p, \tag{4.59}$$

$$\frac{dR}{dt} = \gamma_1 H_p + \gamma_2 I_{an} + \gamma_3 I_{av} - \mu R + u_1(t)S_n + u_2(t)S_v. \tag{4.60}$$

By applying Pontryagin's Maximum Principle [67,69], the objective function can be defined as follows

$$J\left(u_1(t), u_2(t)\right) = \int_0^T \left(A_1 I_{an}(t) + A_2 I_{sn}(t) + A_3 I_{av}(t) + A_4 I_{sv}(t) + \frac{1}{2}A_5 u_1^2(t) + \frac{1}{2}A_6 u_2^2(t) \right) dt \tag{4.61}$$

Where $A_1, A_2, A_3, A_4, A_5,$ and A_6 are weight constants (which may represent the costs associated with implementing control measures), the Lagrangian and Hamiltonian functions can be defined as follows

$$L\left(I_{an}, I_{sn}, I_{av}, I_{sv}, u_1, u_2\right) = A_1 I_{an} + A_2 I_{sn} + A_3 I_{av} + A_4 I_{sv} + \frac{1}{2}A_5 u_1^2 + \frac{1}{2}A_6 u_2^2, \tag{4.62}$$

and

$$H = L(I_{an}, I_{sn}, I_{av}, I_{sv}, u_1, u_2) + \lambda_1 \frac{dS_n}{dt} + \lambda_2 \frac{dE_n}{dt} + \lambda_3 \frac{dI_{an}}{dt} + \lambda_4 \frac{dI_{sn}}{dt} + \lambda_5 \frac{dS_v}{dt} + \lambda_6 \frac{dE_v}{dt} + \lambda_7 \frac{dI_{av}}{dt} + \lambda_8 \frac{dI_{sv}}{dt} + \lambda_9 \frac{dH}{dt} + \lambda_{10} \frac{dR}{dt}. \quad (4.63)$$

Theorem 4.5 With the optimal control $u^* = (u^*_1, u^*_2)$ and the corresponding solutions for $S_n, E_n, I_{an}, I_{sn}, S_v, E_v, I_{av}, I_{sv}, H_p$ and R for the initial problem (4.51)-(4.60) that minimize $J(u_1, u_2)$, there exist adjoint variables $\lambda_i, i = 1,2,3,...,10$ under the control that satisfy the following conditions

$$\frac{d\lambda_i}{dt} = -\frac{\partial H}{\partial \psi} \quad (4.64)$$

When $\psi = (S_n, E_n, I_{an}, I_{sn}, S_v, E_v, I_{av}, I_{sv}, H_p, R)$, together with the transversality conditions given as $\lambda_i(T) = 0$ for all $i = 1,2,3,...,10$

and

$$u^*_1 = \begin{cases} 0 & if \ \frac{\lambda_1 S_n - \lambda_{10} S_n}{A_5} \le 0 \\ \frac{\lambda_1 S_n - \lambda_{10} S_n}{A_5} & if \ \frac{\lambda_1 S_n - \lambda_{10} S_n}{A_5} < u_1^{\max} \\ u_1^{\max} & if \ \frac{\lambda_1 S_n - \lambda_{10} S_n}{A_5} \ge u_1^{\max} \end{cases} \quad (4.65)$$

$$u^*_2 = \begin{cases} 0 & if \ \frac{\lambda_5 S_v - \lambda_{10} S_v}{A_6} \le 0 \\ \frac{\lambda_5 S_v - \lambda_{10} S_v}{A_6} & if \ \frac{\lambda_5 S_v - \lambda_{10} S_v}{A_6} < u_2^{\max} \\ u_2^{\max} & if \ \frac{\lambda_5 S_v - \lambda_{10} S_v}{A_6} \ge u_2^{\max} \end{cases} \quad (4.66)$$

Proof. Consider the Hamiltonian function as follows:

$$H = L(I_{an}, I_{sn}, I_{av}, I_{sv}, u_1, u_2) + \lambda_1 \frac{dS_n}{dt} + \lambda_2 \frac{dE_n}{dt} + \lambda_3 \frac{dI_{an}}{dt} + \lambda_4 \frac{dI_{sn}}{dt} + \lambda_5 \frac{dS_v}{dt} + \lambda_6 \frac{dE_v}{dt} + \lambda_7 \frac{dI_{av}}{dt} + \lambda_8 \frac{dI_{sv}}{dt} + \lambda_9 \frac{dH}{dt} + \lambda_{10} \frac{dR}{dt}$$

Given that $L(I_{an}, I_{sn}, I_{av}, I_{sv}, u_1, u_2) = A_1 I_{an} + A_2 I_{sn} + A_3 I_{av} + A_4 I_{sv} + \frac{1}{2} A_5 u_1^2 + \frac{1}{2} A_6 u_2^2$, substituting the Lagrangian function and the system of equations (4.51) - (4.60) yields

$$
\begin{aligned}
H = {} & A_1 I_{an} + A_2 I_{sn} + A_3 I_{av} + A_4 I_{sv} + \frac{1}{2} A_5 u_1^2 + \frac{1}{2} A_6 u_2^2 \\
& + \lambda_1 \left[(1-b)\sigma - (\beta_{an} I_{an} + \beta_{sn} I_{sn}) S_n - \mu S_n - u_1(t) S_n \right] \\
& + \lambda_2 \left[(\beta_{an} I_{an} + \beta_{sn} I_{sn}) S_n - \phi E_n - (1-\phi) E_n - \mu E_n \right] \\
& + \lambda_3 \left[\phi E_n - (\omega_1 + \gamma_2 + \mu + d) I_{an} \right] \\
& + \lambda_4 \left[(1-\phi) E_n - (\omega_2 + \mu + d) I_{sn} \right] \\
& + \lambda_5 \left[b\sigma - (\beta_{av} I_{av} + \beta_{sv} I_{sv}) S_v - \mu S_v - u_2(t) S_v \right] \\
& + \lambda_6 \left[(\beta_{av} I_{av} + \beta_{sv} I_{sv}) S_v - (1-\delta)\phi E_v - (1-\delta)(1-\phi) E_v - \mu E_v \right] \\
& + \lambda_7 \left[(1-\delta)\phi E_v - (\omega_4 + \gamma_3 + \mu + d) I_{av} \right] \\
& + \lambda_8 \left[(1-\delta)(1-\phi) E_v - (\omega_3 + \mu + d) I_{sv} \right] \\
& + \lambda_9 \left[\omega_1 I_{an} + \omega_2 I_{sn} + \omega_3 I_{sv} + \omega_4 I_{av} - (\gamma_1 + \mu + d) H \right] \\
& + \lambda_{10} \left[\gamma_1 H + \gamma_2 I_{an} + \gamma_3 I_{av} - \mu R + u_1(t) S_n + u_2(t) S_v \right].
\end{aligned} \tag{4.67}
$$

Under the condition (4.64), the adjoint function is obtained as follows:

$$
\begin{aligned}
\frac{d\lambda_1}{dt} &= -\frac{\partial H}{\partial S_n} = \lambda_1(t)\,(\beta_{an} I_{an} + \beta_{sn} I_{sn} + \mu + u_1^*(t)) - \lambda_2(t)(\beta_{an} I_{an} + \beta_{sn} I_{sn}) - \lambda_{10}(t) u_1^*(t), \\
\frac{d\lambda_2}{dt} &= -\frac{\partial H}{\partial E_n} = \lambda_2(t)(1+\mu) - \lambda_3(t)\phi - \lambda_4(t)(1-\phi), \\
\frac{d\lambda_3}{dt} &= -\frac{\partial H}{\partial I_{an}} = \beta_{an} S_n (\lambda_1(t) - \lambda_2(t)) + \lambda_3(t)(d + \gamma_2 + \mu + \omega_1) - \lambda_9(t)\omega_1 - \lambda_{10}(t)\gamma_2 - A_1, \\
\frac{d\lambda_4}{dt} &= -\frac{\partial H}{\partial I_{sn}} = \beta_{sn} S_n (\lambda_1(t) - \lambda_2(t)) + \lambda_4(t)(d + \mu + \omega_2) - \lambda_9(t)\omega_2 - A_2, \\
\frac{d\lambda_5}{dt} &= -\frac{\partial H}{\partial S_v} = \lambda_5(t)\,(\beta_{av} I_{av} + \beta_{sv} I_{sv} + \mu + u_2^*(t)) - \lambda_6(t)(\beta_{av} I_{av} + \beta_{sv} I_{sv}) - \lambda_{10}(t) u_2^*(t), \\
\frac{d\lambda_6}{dt} &= -\frac{\partial H}{\partial E_v} = \lambda_6(t)(\mu + (1-\delta)\,(1-\phi) + (1-\delta)\phi) - \lambda_7(t)(1-\delta)\phi - \lambda_8(t)(1-\delta)\,(1-\phi), \\
\frac{d\lambda_7}{dt} &= -\frac{\partial H}{\partial I_{av}} = \beta_{av} S_v (\lambda_5(t) - \lambda_6(t)) + \lambda_7(t)(d + \mu + \gamma_3 + \omega_4) - \lambda_9(t)\omega_4 - \lambda_{10}(t)\gamma_3 - A_3, \\
\frac{d\lambda_8}{dt} &= -\frac{\partial H}{\partial I_{sv}} = \beta_{sv} S_v (\lambda_5(t) - \lambda_6(t)) + \lambda_8(t)(d + \mu + \omega_3) - \lambda_9(t)\omega_3 - A_4, \\
\frac{d\lambda_9}{dt} &= -\frac{\partial H}{\partial H_p} = \lambda_9(t)(d + \mu + \gamma_1) - \lambda_{10}(t)\gamma_1, \\
\frac{d\lambda_{10}}{dt} &= -\frac{\partial H}{\partial R} = \lambda_{10}(t)\mu.
\end{aligned}
$$

The characterization of the optimal control u^*_1, u^*_2 is determined by the condition

$\frac{\partial H}{\partial u_j} = 0$ for all $j = 1,2$ at $u_j = u^*_j$

Therefore, we obtain

$$
\begin{aligned}
\frac{\partial H}{\partial u_1} &= A_5 u_1 - \lambda_1 S_n + \lambda_{10} S_n \Rightarrow u^*_1 = \frac{\lambda_1 S_n - \lambda_{10} S_n}{A_5}, \\
\frac{\partial H}{\partial u_2} &= A_6 u_2 - \lambda_5 S_v + \lambda_{10} S_v \Rightarrow u^*_2 = \frac{\lambda_5 S_v - \lambda_{10} S_v}{A_6}.
\end{aligned}
$$

The optimal control function is thus obtained as follows

$$u^*_1 = \begin{cases} 0 & if \ \frac{\lambda_1 S_n - \lambda_{10} S_n}{A_5} \le 0 \\ \frac{\lambda_1 S_n - \lambda_{10} S_n}{A_5} & if \ \frac{\lambda_1 S_n - \lambda_{10} S_n}{A_5} < u_1^{\max} \\ u_1^{\max} & if \ \frac{\lambda_1 S_n - \lambda_{10} S_n}{A_5} \ge u_1^{\max} \end{cases}$$

$$u^*_2 = \begin{cases} 0 & if \ \frac{\lambda_5 S_v - \lambda_{10} S_v}{A_6} \le 0 \\ \frac{\lambda_5 S_v - \lambda_{10} S_v}{A_6} & if \ \frac{\lambda_5 S_v - \lambda_{10} S_v}{A_6} < u_2^{\max} \\ u_2^{\max} & if \ \frac{\lambda_5 S_v - \lambda_{10} S_v}{A_6} \ge u_2^{\max} \end{cases}$$

□

4.2.4.2 Numerical Analysis of the Optimal Control Problem for Model 2

Numerical Analysis of the Control Problem at the Endemic Equilibrium

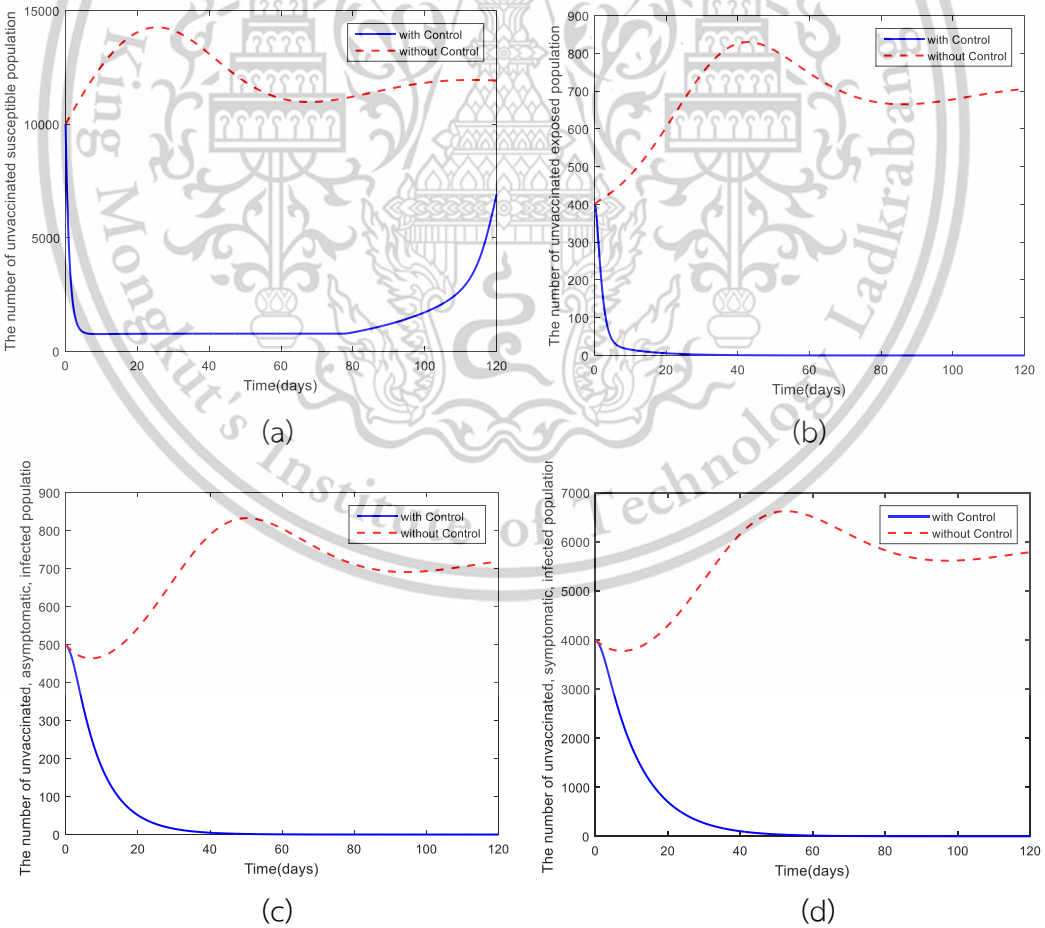

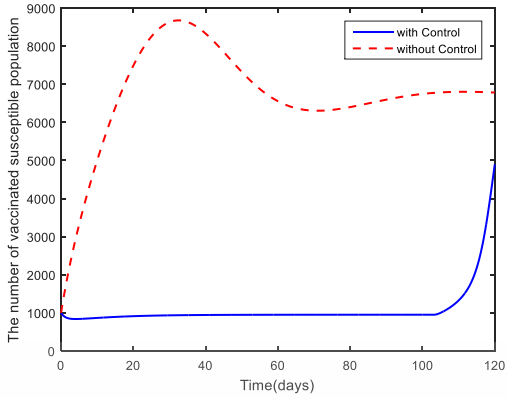

(e)

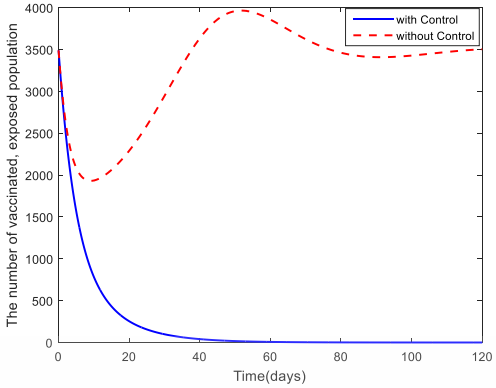

(f)

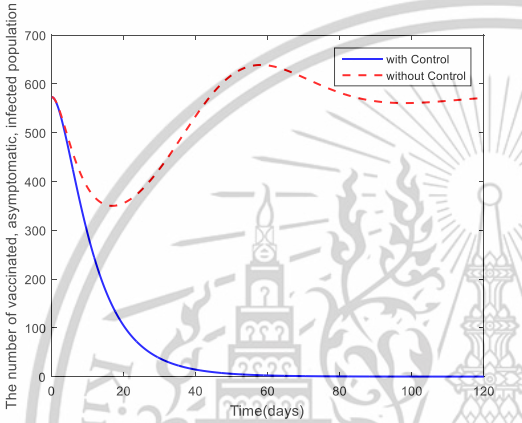

(g)

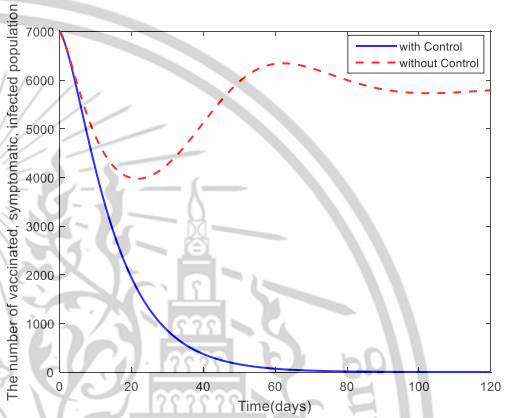

(h)

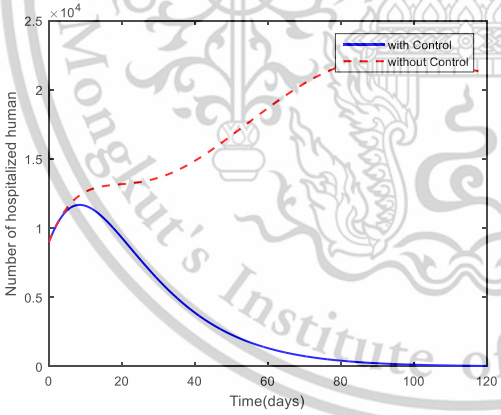

(i)

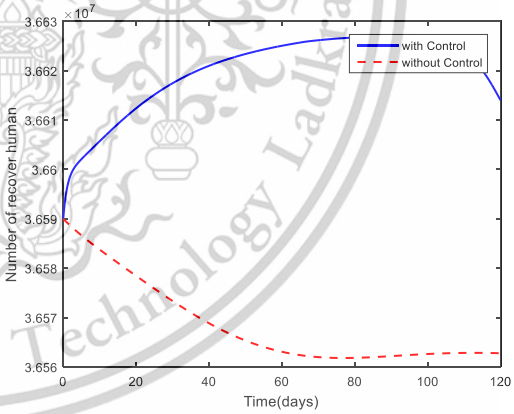

(j)

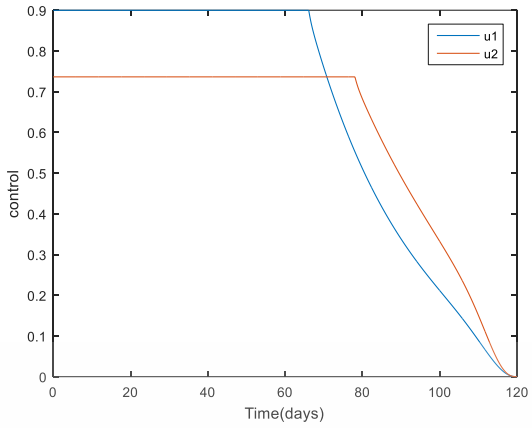

(k)

Figure 4.16 Graph showing the comparison between the model with control strategy and the model without control strategy over time when $R_0 > 1$.

Figures 4.16 illustrate the numerical results comparing the model with a control strategy to the model without a control strategy at the endemic equilibrium, respectively. The graphs clearly show that, over time, the population with a control strategy can contain the spread of the disease more quickly than the model without a control strategy. Therefore, implementing control strategies such as vaccination and immunity gained from vaccination is an effective approach to managing the spread of the disease. However, there may be additional factors influencing the epidemic's spread. Proper planning and preparedness can further enhance the effectiveness of disease control efforts.

4.3 Mathematical Model Analysis of Model 3

From the mathematical model for COVID-1 9 , Model 3 incorporates the expansion of symptomatic infections, asymptomatic infections, and quarantine measures. The resulting system of equations for Model 3 is as follows:

$$\frac{dS(t)}{dt} = \Lambda - \lambda S(t) - dS(t), \tag{4.68}$$

$$\frac{dE(t)}{dt} = \lambda S(t) - (\tau\varepsilon + \tau(1-\varepsilon) + d)E(t), \tag{4.69}$$

$$\frac{dtI_1(t)}{dt} = \tau\varepsilon E(t) - (\alpha + g + d)I_1(t), \tag{4.70}$$

$$\frac{dI_2(t)}{dt} = \tau(1-\varepsilon)E(t) - (\gamma_a + g + d)I_2(t), \tag{4.71}$$

$$\frac{dQ(t)}{dt} = \alpha I_1(t) - (\gamma_q + d)Q(t), \tag{4.72}$$

$$\frac{dR(t)}{dt} = \gamma_a I_2(t) + \gamma_q Q(t) - dR(t), \tag{4.73}$$

and $$N = S + E + I_1 + I_2 + Q + R. \tag{4.74}$$

Lemma 4.3 [85,86] Initial conditions $S(0) > 0, E(0) > 0, I_1(0) > 0, I_2(0) > 0, R(0) > 0$ and $N(0) > 0$ from mathematical model (4.68)-(4.73) the invariant set $\phi = \left\{ (S, E, I_1, I_2, Q, R) \in \mathbb{R}^6_+ : N \le \frac{\Lambda}{d} \right\}$, and then the closed set ϕ is positive invariant.

Proof. Consider the total population, which can be expressed as $N = S + E + I_1 + I_2 + Q + R$. Therefore, we have

$$\frac{dN}{dt} = \frac{dS}{dt} + \frac{dE}{dt} + \frac{dI_1}{dt} + \frac{dI_2}{dt} + \frac{dQ}{dt} + \frac{dR}{dt}$$

$$\frac{dN}{dt} = \Lambda - gI_1 - gI_2 - dN. \tag{4.75}$$

From equation (4.75), we obtain

$$\frac{dN}{dt} \le \Lambda - dN$$

By finding the derivative, we obtain

$$N(t) \le \frac{\Lambda}{d} + \left(N(0) - \frac{\Lambda}{d} \right) e^{-dt}$$

Given that $N(0)$ represents the initial value, we can further observe that $N(t) \to \frac{\Lambda}{d}$ as $t \to \infty$. Therefore, it can be concluded that $N(t)$ is bounded as $0 \le N(t) \le \frac{\Lambda}{d}$. Since all the parameters are positive, it follows that the problem-solving area is within $\mathbb{R}^6_+$. Thus, $\phi = \left\{ (S, E, I_1, I_2, Q, R) \in \mathbb{R}^6_+ : N \le \frac{\Lambda}{d} \right\}$ is a positively invariant set. □

4.3.1 Equilibrium Points and Basic Reproduction Number of Model 3

Equilibrium Points

The equilibrium points of Model 3 can be calculated by setting the system of equations (4.68) - (4.73) to zero, yielding:

$$\Lambda - \lambda^* S^* - dS^* = 0 \tag{4.76}$$

$$\lambda^* S^* - (\tau\varepsilon + \tau(1-\varepsilon) + d)E^* = 0 \tag{4.77}$$

$$\tau\varepsilon E^* - (\alpha + g + d)I_1^* = 0 \tag{4.78}$$

$$\tau(1-\varepsilon)E^* - (\gamma_a + g + d)I_2^* = 0 \tag{4.78}$$

$$\alpha I_1^* - (\gamma_q + d)Q^* = 0 \tag{4.80}$$

$$\gamma_a I_2^* + \gamma_q Q^* - dR^* = 0 \tag{4.81}$$

By evaluating equations (4.76) - (4.81), we obtain two equilibrium points as follows:

I. The first equilibrium point is the disease-free equilibrium point

$$K_0^* = (S^*{}_0, E_0^*, I_{0,1}^*, I_{0,2}^*, Q_0^*, R_0^*) = \left(\frac{\Lambda}{d}, 0, 0, 0, 0, 0\right) \tag{4.82}$$

II. The second equilibrium point is the endemic equilibrium point

$$K_1^* = (S_1^*, E_1^*, I_{1,1}^*, I_{1,2}^*, Q_1^*, R_1^*), \tag{4.83}$$

where

$$S_1^* = \frac{(\tau\varepsilon + \tau(1-\varepsilon) + d)\Lambda}{R_0 d(d+\tau)},$$

$$E_1^* = \frac{\Lambda d(R_0 - 1)}{R_0(\tau + d)},$$

$$I_{1,1}^* = \frac{\Lambda\tau\varepsilon(R_0 - 1)}{R_0(\alpha + g + d)(\tau + d)},$$

$$I_{1,2}^* = \frac{\Lambda\tau(1-\varepsilon)(R_0 - 1)}{R_0(\gamma_a + g + d)(\tau + d)},$$

$$Q_1^* = \frac{\Lambda\tau\alpha\varepsilon(R_0 - 1)}{R_0(\alpha + g + d)(\gamma_q + d)(\tau + d)},$$

$$R_1^* = \frac{\Lambda\tau(R_0 - 1)\left(\frac{\gamma_a(1-\varepsilon)}{(\gamma_a + g + d)} - \frac{\alpha\varepsilon\gamma_q}{(\alpha + g + d)(\gamma_q + d)}\right)}{R_0 d(\tau + d)}.$$

The basic reproduction number

In this section, we calculate the basic reproduction number R_0 for Model 3 using the next-generation matrix method [64,103,104]. Here, we consider the expressions for E, I_1 and I_2 as follows

$$\frac{dE(t)}{dt} = \lambda S(t) - (\tau\varepsilon + \tau(1-\varepsilon) + d)E(t),$$

$$\frac{dtI_1(t)}{dt} = \tau\varepsilon E(t) - (\alpha + g + d)I_1(t),$$

$$\frac{dI_2(t)}{dt} = \tau(1-\varepsilon)E(t) - (\gamma_a + g + d)I_2(t).$$

This yields the following

$$\begin{vmatrix} Gains\ to\ E & (\beta_s I_1(t) + \beta_a I_2(t))S(t) \\ Gains\ to\ I_1 & 0 \\ Gains\ to\ I_2 & 0 \end{vmatrix}, \begin{vmatrix} Losses\ to\ E & (\tau + \tau(1-\varepsilon) + d)E(t) \\ Losses\ to\ I_1 & -\tau\varepsilon E(t) + (\alpha + g + d)I_1(t) \\ Losses\ to\ I_2 & -\tau(1-\varepsilon)E(t) + (\gamma_a + g + d)I_2(t) \end{vmatrix}.$$

Consider the Jacobian matrix, which is obtained as follows

$$F = \begin{bmatrix} 0 & \beta_s S(t) & \beta_a S(t) \\ 0 & 0 & 0 \\ 0 & 0 & 0 \end{bmatrix}, \quad V = \begin{bmatrix} (\tau + \tau(1-\varepsilon) + d) & 0 & 0 \\ -\tau\varepsilon & \alpha + g + d & 0 \\ -\tau(1-\varepsilon) & 0 & \gamma_a + g + d \end{bmatrix}.$$

Substituting the values at the disease-free equilibrium

$K_0^* = (S^*{}_0, E_0^*, I_{0,1}^*, I_{0,2}^*, Q_0^*, R_0^*) = \left(\frac{\Lambda}{d}, 0, 0, 0, 0, 0\right)$, we obtain

$$FV^{-1}\left(K_0^*\right)=\begin{bmatrix} H_1 & H_2 & H_3 \\ 0 & 0 & 0 \\ 0 & 0 & 0 \end{bmatrix},$$

where

$$H_1=\frac{(d+g+\alpha)(1-\varepsilon)\Lambda\tau\beta_a}{d(d+g+\gamma_a)(d^2+dg+d\alpha+d\tau+g\tau+\alpha\tau)}+\frac{\Lambda\varepsilon\tau\beta_s}{d(d^2+dg+d\alpha+d\tau+g\tau+\alpha\tau)},$$

$$H_2=\frac{(d^2+dg+d\gamma_a+d\tau+g\tau+\tau\gamma_a)\Lambda\beta_s}{d(d+g+\gamma_a)(d^2+dg+d\alpha+d\tau+g\tau+\alpha\tau)},$$

$$H_3=\frac{\Lambda\beta_a}{d(d+g+\gamma_a)}.$$

Since the basic reproduction number R_0 can be calculated from $\rho(FV^{-1})$, which is determined by the eigenvalues, we obtain

$$R_0=\frac{((1-\varepsilon)\alpha\beta_a+(1-\varepsilon)(d+g)\beta_a+\beta_s\varepsilon(g+\gamma_a+d))\Lambda\tau}{d(d+g+\alpha)(d+g+\gamma_a)(d+\tau)}. \quad (4.84)$$

4.3.2 Stability Analysis of Model 3

Theorem 4.6 Consider the model given by the system (4.68)–(4.73), and let ϕ be the positively invariant region where all state variables remain nonnegative and biologically meaningful. Suppose K_0^* is the disease-free equilibrium of this system. If $R_0<1,$, then the disease-free equilibrium is globally asymptotically stable in

Proof. To obtain the results, the Lyapunov function can be considered as follows:

$$G(t)=G(E(t),I_1(t),I_2(t))=c_1E+c_2I_1+c_3I_2$$

It can be observed that $G(t)>0$ for all $(E(t),I(t))^T\in\Gamma$ and it follows that

$$G(E_0^*,I_{0,1}^*,I_{0,2}^*)=c_1(0)+c_2(0)+c_3(0)=0,$$

where a_1, and a_2 be positive constants. Consider the derivative of the function G, which is obtained as follows

$$\frac{dG}{dt}=c_1E'+c_2I_1'+c_3I_2'.$$

Substituting the values from the system of equations (4.70) - (4.75), we obtain

$$\frac{dG}{dt}=c_1\left((\beta_sI_1+\beta_aI_2)S-(\tau\varepsilon+\tau(1-\varepsilon)+d)E\right)+c_2\left(\tau\varepsilon E-(\alpha+g+d)I_1\right)+c_3\left(\tau(1-\varepsilon)E-(\gamma_a+g+d)I_2\right).$$

Modify the equation's structure and substituting $S_0^*=\frac{\Lambda}{d}$ at the disease-free equilibrium is obtained:

$$\frac{dG}{dt}=\left(c_2\tau\varepsilon+c_3\tau(1-\varepsilon)-c_1(\tau\varepsilon+\tau(1-\varepsilon)+d)\right)E+\left(c_1\beta_sS-c_2(\alpha+g+d)\right)I_1+\left(c_1\beta_aS-c_3(\gamma_a+g+d)\right)I_2$$

$$=\left(c_2\tau\varepsilon+c_3\tau(1-\varepsilon)-c_1(\tau\varepsilon+\tau(1-\varepsilon)+d)\right)E+\left(c_1\beta_s\frac{\Lambda}{d}-c_2(\alpha+g+d)\right)I_1+\left(c_1\beta_a\frac{\Lambda}{d}-c_3(\gamma_a+g+d)\right)I_2$$

Given that $c_1 = \frac{d}{\Lambda}, c_2 = \frac{\beta_s}{\alpha+g+d}$, and $c_3 = \frac{\beta_a}{\gamma_a+g+d}$, it follows that:

$$\frac{dG}{dt} = \left(\frac{\beta_s}{\alpha+g+d}\tau\varepsilon + \frac{\beta_a}{\gamma_a+g+d}\tau(1-\varepsilon) - \frac{d}{\Lambda}(\tau\varepsilon+\tau(1-\varepsilon)+d) \right) E$$

$$= \frac{d(\tau+d)}{\Lambda}\left(\frac{(\beta_s\tau\varepsilon(\gamma_a+g+d)+\beta_a\tau(1-\varepsilon)(\alpha+g+d))\Lambda}{(\alpha+g+d)(\gamma_a+g+d)d(\tau+d)} - 1 \right) E$$

$$= \frac{d(\tau+d)}{\Lambda}\left(\frac{((1-\varepsilon)\alpha\beta_a + (1-\varepsilon)(d+g)\beta_a + \beta_s\varepsilon(g+\gamma_a+d))\Lambda\tau}{d(d+g+\alpha)(d+g+\gamma_a)(d+\tau)} - 1 \right) E$$

$$\frac{dG}{dt} = \frac{d(\tau+d)}{\Lambda}(R_0 - 1)E. \tag{4.85}$$

From equation (4.86), it can be seen that $\frac{dG}{dt} < 0$ if $R_0 < 1$ and $\frac{dG}{dt} = 0$ when $E = 0$, then, according to LaSalle's Invariance Principle, the disease-free equilibrium point K_0^* is globally asymptotically stable on ϕ if $R_0 < 1$. □

Theorem 4.7 Consider the system (4.68)–(4.73) with a positively invariant region ϕ, and let K_1^* be its endemic equilibrium. Suppose that all parameters are positive, and all state variables remain nonnegative in ϕ. If $R_0 > 1$, then K_1^* is globally asymptotically stable in ϕ.

Proof. The Lyapunov function is defined as follows:

$$M(t) = (S - S_1^* - S_1^* \ln\frac{S}{S_1^*}) + (E - E_1^* - E_1^* \ln\frac{E}{E_1^*}) + (I_1 - I_{1,1}^* - I_{1,1}^* \ln\frac{I_1}{I_{1,1}^*}) + (I_2 - I_{1,2}^* - I_{1,2}^* \ln\frac{I_2}{I_{1,2}^*})$$
$$+ (Q - Q_1^* - Q_1^* \ln\frac{Q}{Q_1^*}) + (R - R_1^* - R_1^* \ln\frac{R}{R_1^*}).$$

It can be observed that $M(t) > 0$ for all $(S(t), E(t), I_1(t), I_2(t), Q(t), R(t))^T \in \Gamma$ and it follows that

$$M(S_1^*, E_1^*, I_{1,1}^*, I_{1,2}^*, Q_1^*, R_1^*) = (S_1^* - S_1^* - S_1^* \ln\frac{S_1^*}{S_1^*}) + (E_1^* - E_1^* - E_1^* \ln\frac{E_1^*}{E_1^*}) + (I_{1,1}^* - I_{1,1}^* - I_{1,1}^* \ln\frac{I_{1,1}^*}{I_{1,1}^*})$$
$$+ (I_{1,2}^* - I_{1,2}^* - I_{1,2}^* \ln\frac{I_{1,2}^*}{I_{1,2}^*}) + (Q_1^* - Q_1^* - Q_1^* \ln\frac{Q_1^*}{Q_1^*}) + (R_1^* - R_1^* - R_1^* \ln\frac{R_1^*}{R_1^*})$$
$$= 0.$$

Consider the derivative of the function M, which is given by:

$$\frac{dM}{dt} = S'\left(1-\frac{S_1^*}{S}\right)+E'\left(1-\frac{E_1^*}{E}\right)+I_1'\left(1-\frac{I_{1,1}^*}{I_1}\right)+I_2'\left(1-\frac{I_{1,2}^*}{I_2}\right)+Q'\left(1-\frac{Q_1^*}{Q}\right)+R'\left(1-\frac{R_1^*}{R}\right)$$

$$= \{\Lambda-\lambda S-dS\}\left(1-\frac{S_1^*}{S}\right)+\{\lambda S-(\tau\varepsilon+\tau(1-\varepsilon)+d)E\}\left(1-\frac{E_1^*}{E}\right)$$

$$+\{\tau\varepsilon E-(\alpha+g+d)I_1\}\left(1-\frac{I_{1,1}^*}{I_1}\right)+\{\tau(1-\varepsilon)E-(\gamma_a+g+d)I_2\}\left(1-\frac{I_{1,2}^*}{I_2}\right)$$

$$+\{\alpha I_1-(\gamma_q+d)Q\}\left(1-\frac{Q_1^*}{Q}\right)+\{\gamma_a I_2+\gamma_q Q-dR\}\left(1-\frac{R_1^*}{R}\right)$$

putting $S = S-S_1^*, E = E-E_1^*, I_1 = I_1-I_{1,1}^*, I_2 = I_2-I_{1,2}^*, Q = Q-Q_1^*$ and $R = R-R_1^*$,then

$$\frac{dM}{dt} = \left\{\Lambda-(\beta_s I_1+\beta_a I_2)\left(S-S_1^*\right)-d\left(S-S_1^*\right)\right\}\left(\frac{S-S_1^*}{S}\right)$$

$$+\left\{(\beta_s I_1+\beta_a I_2)S-(\tau\varepsilon+\tau(1-\varepsilon)+d)\left(E-E_1^*\right)\right\}\left(\frac{E-E_1^*}{E}\right)$$

$$+\left\{\tau\varepsilon E-(\alpha+g+d)\left(I_1-I_{1,1}^*\right)\right\}\left(\frac{I_1-I_{1,1}^*}{I_1}\right)+\left\{\tau(1-\varepsilon)E-(\gamma_a+g+d)\left(I_2-I_{1,2}^*\right)\right\}\left(\frac{I_2-I_{1,2}^*}{I_2}\right)$$

$$+\left\{\alpha I_1-(\gamma_q+d)\left(Q-Q_1^*\right)\right\}\left(\frac{Q-Q_1^*}{Q}\right)+\left\{\gamma_a I_2+\gamma_q Q-d\left(R-R_1^*\right)\right\}\left(\frac{R-R_1^*}{R}\right)$$

$$= \Lambda-\Lambda\left(\frac{S_1^*}{S}\right)-(\beta_s I_1+\beta_a I_2)\frac{\left(S-S_1^*\right)^2}{S}-d\frac{\left(S-S_1^*\right)^2}{S}+(\beta_s I_1+\beta_a I_2)S-(\beta_s I_1+\beta_a I_2)S\frac{E_1^*}{E}$$

$$-(\tau\varepsilon+\tau(1-\varepsilon)+d)\frac{\left(E-E_1^*\right)^2}{E}+\tau\varepsilon E-\tau\varepsilon E\left(\frac{I_{1,1}^*}{I_1}\right)-(\alpha+g+d)\frac{\left(I_1-I_{1,1}^*\right)^2}{I_1}$$

$$+\tau(1-\varepsilon)E-\tau(1-\varepsilon)E\left(\frac{I_{1,2}^*}{I_2}\right)-(\gamma_a+g+d)\frac{\left(I_1-I_{1,1}^*\right)^2}{I_1}+\alpha I_1-\alpha I_1\left(1-\frac{Q_1^*}{Q}\right)$$

$$-(\gamma_q+d)\frac{\left(Q-Q_1^*\right)^2}{Q}+\gamma_a I_2-\gamma_a I_2\left(\frac{R_1^*}{R}\right)+\gamma_q Q-\gamma_q Q\left(\frac{R_1^*}{R}\right)-d\frac{\left(R-R_1^*\right)^2}{R}.$$

Rearranging the equation for easier consideration, we obtain

$$\frac{dM}{dt} = Z_1 - Z_2,$$

when

$$Z_1 = \Lambda+(\beta_s I_1+\beta_a I_2)S+\tau\varepsilon E+\tau(1-\varepsilon)E+\alpha I_1+\gamma_a I_2+\gamma_q Q,$$

and

$$Z_2 = \Lambda\left(\frac{S_1^*}{S}\right)+(\beta_s I_1+\beta_a I_2)\frac{\left(S-S_1^*\right)^2}{S}+d\frac{\left(S-S_1^*\right)^2}{S}+(\beta_s I_1+\beta_a I_2)S\frac{E_1^*}{E}+(\tau\varepsilon+\tau(1-\varepsilon)+d)\frac{\left(E-E_1^*\right)^2}{E}$$

$$+\tau\varepsilon E\left(\frac{I_{1,1}^*}{I_1}\right)+(\alpha+g+d)\frac{\left(I_1-I_{1,1}^*\right)^2}{I_1}+\tau(1-\varepsilon)E\left(\frac{I_{1,2}^*}{I_2}\right)+(\gamma_a+g+d)\frac{\left(I_1-I_{1,2}^*\right)^2}{I_1}$$

$$+\alpha I_1\left(1-\frac{Q_1^*}{Q}\right)+(\gamma_q+d)\frac{\left(Q-Q_1^*\right)^2}{Q}+\gamma_a I_2\left(\frac{R_1^*}{R}\right)+\gamma_q Q\left(\frac{R_1^*}{R}\right)+d\frac{\left(R-R_1^*\right)^2}{R}.$$

Thus, we have $\frac{dM}{dt} < 0$ if $Z_1 < Z_2$, and if $\frac{dM}{dt} = 0$, then $S_1^* = S, E_1^* = E, I_{1,1}^* = I_1, I_{1,2}^* = I_2, Q_1^* = Q$ and $R = R_1^*$. Therefore, according to LaSalle's Invariance Principle, it can be concluded that the endemic equilibrium point K_1^* is globally asymptotically stable on ϕ if $Z_1 < Z_2$. □

4.3.3 Numerical Analysis of Model 3

In this subsection, we present the numerical analysis of Model 3. The parameters used in this analysis were obtained through model fitting, while the remaining parameters were derived from a literature review. The parameters analyzed in this study are shown in Tables 4.7 and 4.8 as follows:

Table 4.7 Parameters Used for the Numerical Analysis of Model 3 at the Disease-Free Equilibrium.

Parameters	Disease-free	Units	Source
Λ	1	person	Assume
β_s	0.0000075	Per person · days^{-1}	Estimated
β_a	0.0000009	Per person · days^{-1}	Estimated
τ	1/6	day^{-1}	[18,71]
ε	0.01	day^{-1}	Estimated
α	0.2	day^{-1}	[18]
γ_q	0.05	day^{-1}	[18]
γ_a	1/10	day^{-1}	[18]
g	0.00286	day^{-1}	[18]
d	0.000036529	day^{-1}	[18,103]

Table 4.8 Parameters Used for the Numerical Analysis of Model 3 at the Endemic Equilibrium.

Parameters	Endemic	Units	Source
Λ	700	person	Assume
β_s	0.0000075	Per person · days^{-1}	Fitting
β_a	0.0000009	Per person · days^{-1}	Fitting
τ	1/6	day^{-1}	[18,71]

ε	0.01	day^{-1}	Fitting
α	0.2	day^{-1}	[18]
γ_q	0.05	day^{-1}	[18]
γ_a	1/10	day^{-1}	[18]
g	0.00286	day^{-1}	[18]
d	0.000036529	day^{-1}	[18,103]

4.3.3.1 Model Fitting of Model 3

In this subsection, we present Model (4.68) - (4.73) numerical results, comparing them with actual epidemic data from Thailand. Model fitting was performed using the fminunc algorithm in MATLAB to obtain parameters that closely align with the real epidemic data. The data considered includes the daily number of reported cases from January 1, 2022, to March 1, 2022 [106]. The blue circles represent the daily reported cases, while the solid red line represents the model's outcomes, as illustrated in Figure 4.17. The coefficient of determination for this model fitting is R^2=0.9210, indicating a strong correlation between the model's predictions and the observed data. This result highlights the model's ability to accurately capture the epidemic dynamics and enhances its applicability in analyzing and forecasting disease transmission trends.

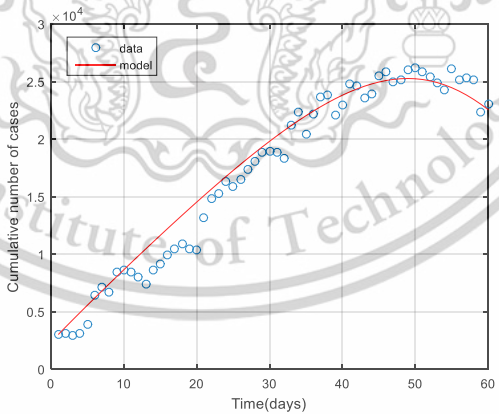

Figure 4.17 Graph showing the daily number of reported cases alongside the model solutions (4.68) - (4.73) over time, based on data from January 1, 2022, to March 1, 2022 [106].

4.3.3.2 Numerical Analysis Result of Model 3

Numerical Analysis of the Disease-Free Equilibrium

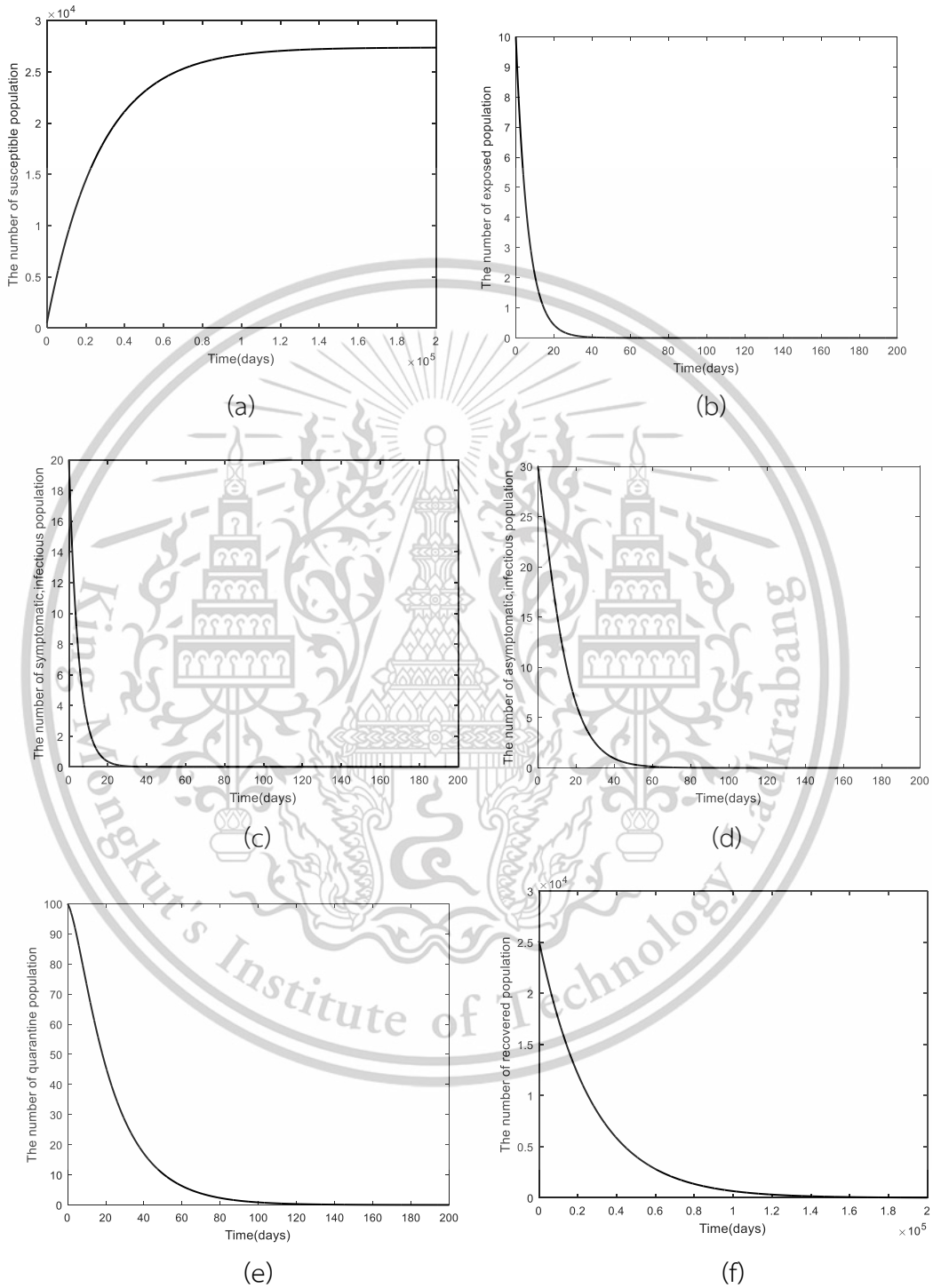

Figure 4.18 Solution of the system of equations (4.68) - (4.73): Graph showing the relationship between time and S, E, I_1, I_2, Q, R when $R_0 = 0.247311$.

Numerical Analysis of the Endemic Equilibrium Point

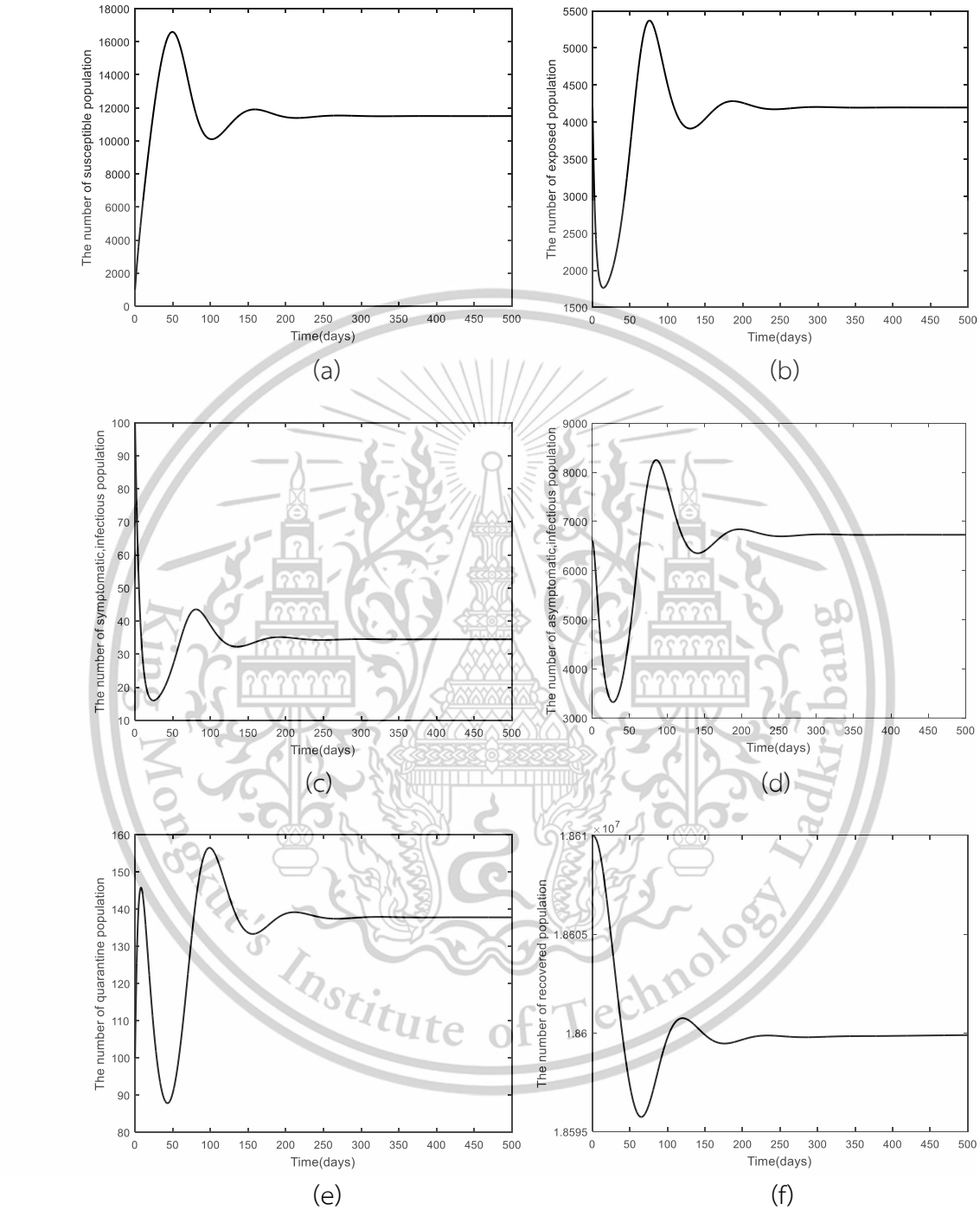

Figure 4.19 Solution of the System of Equations (4.68) - (4.73): Graph Showing the Relationship Between Time, S, E, I_1, I_2, Q and R when $R_0 = 1.73118$.

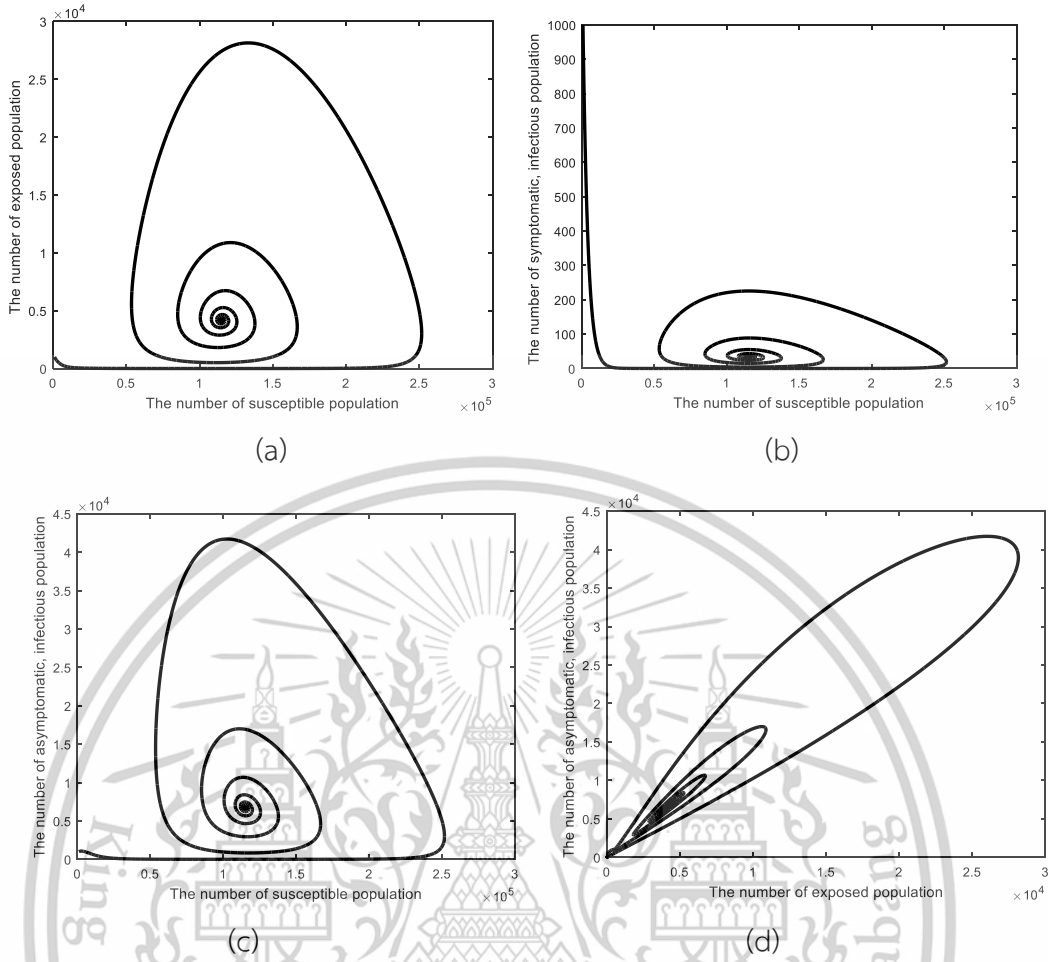

Figure 4.20 Solution of the System of Equations (4.68)-(4.73): Graph Showing the Relationship Between $(S,E),(S,I_1),(S,I_2)$ and (E,I_2) for $R_0 = 1.73118$.

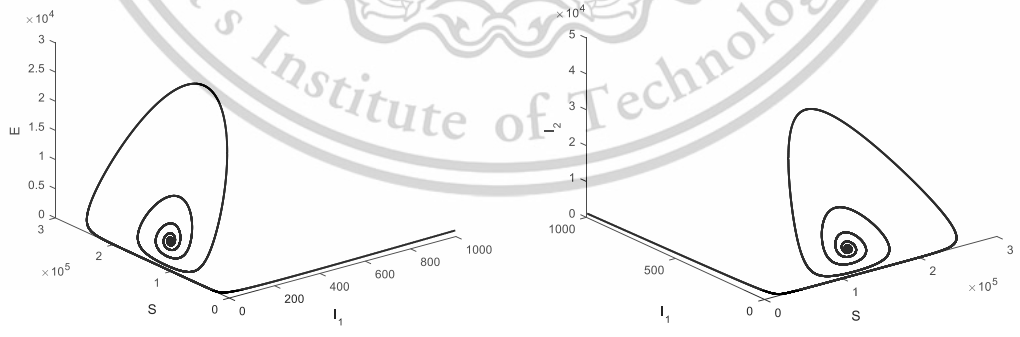

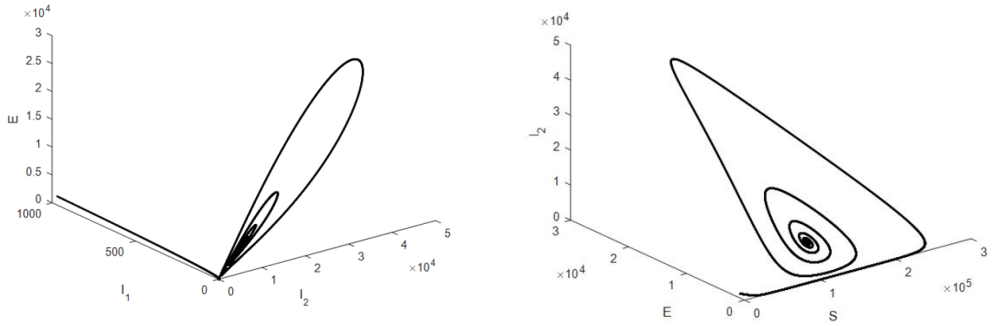

(c) (d)

Figure 4.21 Solution of the System of Equations (4.68) - (4.73): Graph Showing the Relationship Between $(I_1, S, E), (S, I_1, I_2), (I_2, I_1, E)$ and (S, E, I_2) for $R_0 = 1.73118$.

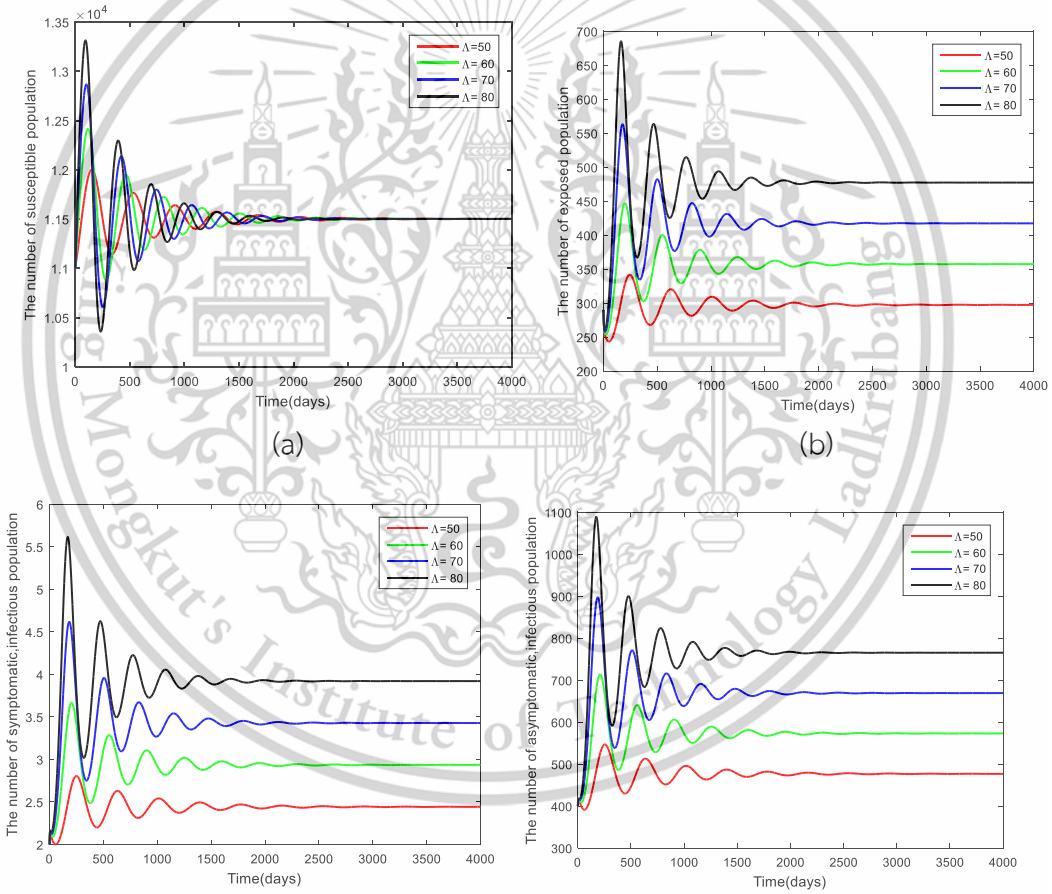

(a) (b)

(c) (d)

Figure 4.22 Solution of the System of Equations (4.68) - (4.73): Graph Comparing Initial Population (Λ) for $R_0 > 0$.

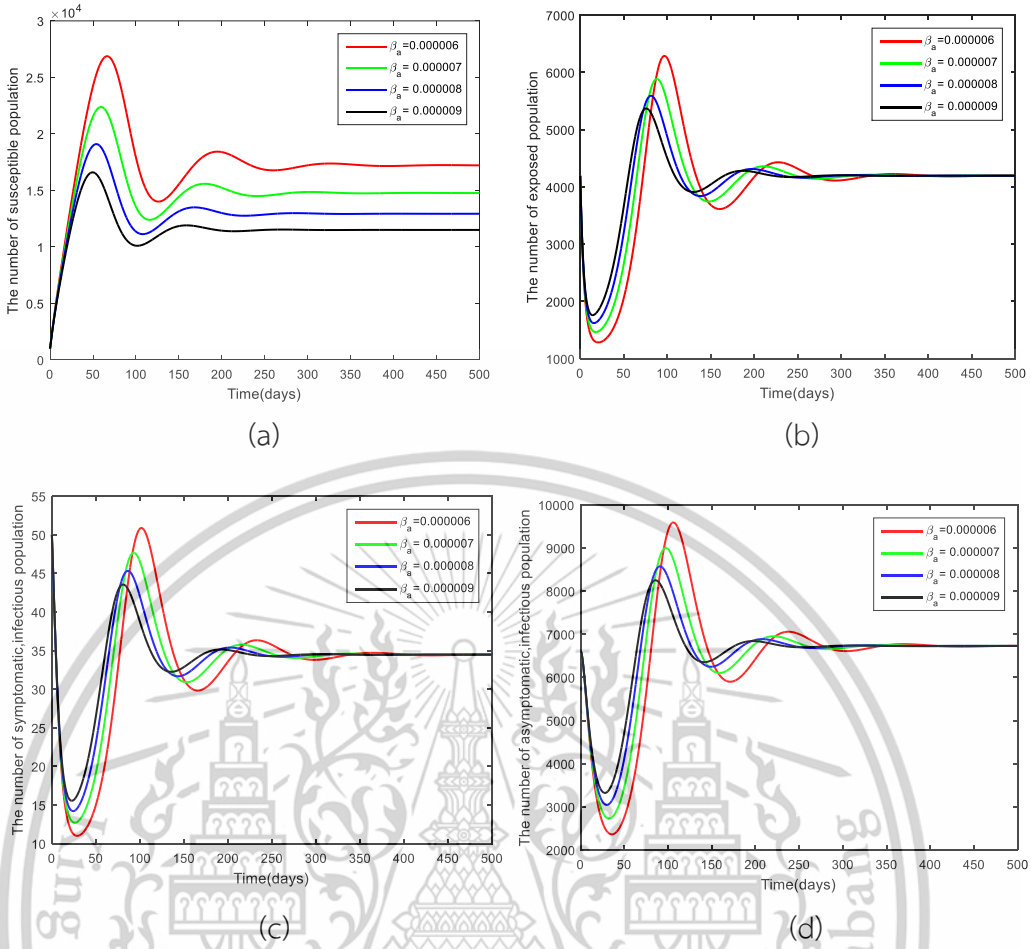

Figure 4.23 Solution of the System of Equations (4.68) - (4.73): Graph Comparing the Transmission Rate of the Asymptomatic Population (β_a) for $R_0 > 0$.

In this section, we have analyzed the numerical solutions of equations (4.68)-(4.73), dividing the analysis into two parts.

- Part 1 focuses on the numerical solutions at the disease-free equilibrium and the endemic equilibrium points.
- Part 2 compares the initial population sizes and the transmission rates of the asymptomatic infected population.

These aspects will be explained in further detail in the following sections.

Part 1: Numerical Solutions

In Part 1, we analyzed the numerical solutions of the model (4.68)-(4.73) at the disease-free equilibrium and the endemic equilibrium points. Additionally, we plotted the 2D and 3D trajectories at the endemic equilibrium point, as shown in Figure 4.18. For the disease-free equilibrium, when $R_0 = 0.247311$, the analysis reveals that the

number of susceptible individuals increases gradually and converges to a steady point at 27,397 over 1,000 days. Meanwhile, the remaining populations converge to zero (e.g., $E_0 = 0, I_{0,1} = 0, I_{0,2} = 0, Q_0 = 0, R_0 = 0$). Specifically, the population groups, including those infected but unable to transmit, symptomatic infected, asymptomatic infected, isolated, and recovered individuals, converge to equilibrium over periods of 50 days, 40 days, 70 days, 120 days, and 160,000 days, respectively. In Figure 4.19, the endemic equilibrium is analyzed for $R_0 = 1.7311$. Here, the susceptible population converges to an equilibrium point of 1,150 within 300 days. The population infected and able to transmit stabilizes at 4,196 within 350 days. The symptomatic infected group reaches equilibrium at 34 over 275 days, while the asymptomatic infected population converges to 6,729 within 350 days. The isolated population stabilizes at 137, and the recovered population converges to an equilibrium point of 18,248,000 within 350 days. Figures 4.20-4.21 present the 2D and 3D trajectories at the endemic equilibrium point with parameters $\beta_s = 0.00000075$ and $\beta_a = 0.000009$. These figures clearly illustrate the convergence path towards the equilibrium, highlighting the stability of the trajectories as they approach the endemic equilibrium.

Part 2: Comparison of Parameters Affecting the Epidemic Spread

In Part 2, we compared the initial population sizes (Λ) and the infection rates of asymptomatic infected individuals (β_a). In Figure 4.22, we analyzed the impact of varying initial population sizes with Λ = 50, 60, 70 and 80. We observed the solutions for susceptible populations, populations infected and able to transmit, symptomatic infected populations, and asymptomatic infected populations. The findings consistently indicated that a reduction in the initial population size significantly decreases the number of infected individuals in each category. Figure 4.23 presents a comparison of the infection rate among asymptomatic individuals with values of β_a = 0.000006, 0.000007, 0.000008 and 0.000009. It was observed that as the infection rate increases, the time required to control the epidemic decreases, enabling quicker containment compared to scenarios with lower infection rates. This demonstrates that higher infection rates facilitate more efficient epidemic control through faster attainment of herd immunity or other dynamic factors within the model.

4.3.3.3 Sensitivity Analysis of Model 3

We analyzed the sensitivity of parameters affecting the basic reproduction number (R_0) in Model 3. The basic reproduction number is crucial for understanding epidemic dynamics and designing strategies to control disease spread. Sensitivity analysis allows us to assess how changes in parameters influence R_0, providing insights for epidemic control planning. The sensitivity analysis can be calculated using the following formula [94,95]:

$$\Upsilon_{\psi}^{R_0} = \frac{\partial R_0}{\partial \psi} \times \frac{\psi}{R_0}, \tag{4.86}$$

where ψ represents the parameter used in the analysis, and R_0 denotes the basic reproduction number. The parameters used in this analysis are listed in Table 4.8, and the results of the sensitivity analysis are presented in Table 4.9.

Table 4.9 Sensitivity Values of the Basic Reproduction Number (R_0) for Model 3.

Parameter	Sensitivity
Λ	+1.000000
β_s	+0.000425
β_a	+0.995749
τ	+0.000219
ε	-0.005807
α	-0.004190
γ_a	-0.967719
g	-0.027737
d	+1.000570

The parameter analysis in Table 4.9 shows that parameters $\Lambda, \beta_s, \beta_a, \tau$ and d have a positive impact on the basic reproduction number, while parameters $\varepsilon, \alpha, \gamma_a$ and g have a negative impact. Examining the positive parameters reveals that the initial population size and the infection rate among asymptomatic individuals significantly influence the increase or decrease of R_0. Therefore, implementing strategies to reduce the initial population size (Λ) and the infection rate of asymptomatic individuals (β_a) can help decrease the infection rate. Control strategies to address these factors will be presented in the following section.

4.3.4 Optimal Control Problem of Model 3

4.3.4.1 Optimal Control Model of Model 3

In this section, we formulate the optimal control model for Model 3. The goal is to determine the best strategies to minimize the spread of infection by applying control measures effectively. This involves identifying control variables, such as social distancing combined with mask-wearing (u_1) and vaccination control (u_2), that can be adjusted to minimize the number of infections over time. The optimal control model is developed by incorporating these control variables into the differential equations of the original model, allowing us to evaluate the impact of different strategies on the epidemic dynamics and achieve an effective and sustainable reduction in the basic reproduction number (R_0).

$$S'(t) = \Lambda - (1-u_1(t))(\beta_s I_1(t) + \beta_a I_2(t))S(t) - dS(t) - u_2(t)S(t), \tag{4.87}$$

$$E'(t) = (1-u_1(t))(\beta_s I_1(t) + \beta_a I_2(t))S(t) - (\tau\varepsilon + \tau(1-\varepsilon) + d)E(t), \tag{4.88}$$

$$I_1'(t) = \tau\varepsilon E(t) - (\alpha + g + d)I_1(t), \tag{4.89}$$

$$I_2'(t) = \tau(1-\varepsilon)E(t) - (\gamma_a + g + d)I_2(t), \tag{4.90}$$

$$Q'(t) = \alpha I_1(t) - (\gamma_q + d)Q(t), \tag{4.91}$$

$$R'(t) = \gamma_a I_2(t) + \gamma_q Q(t) - dR(t) + u_2(t)S(t). \tag{4.92}$$

According to Pontryagin's Maximum Principle [70,107], the objective function can be defined as follows:

$$J(u_1, u_2) = \int_0^T \left(W_1 I_1(t) + W_2 I_2(t) + \frac{1}{2} W_3 u^2{}_1(t) + \frac{1}{2} W_4 u^2{}_2(t) \right) dt. \tag{4.93}$$

where $W_1, W_2, W_3,$ and W_4 are defined as constant weighting factors.

For solving the optimal control problem, the Lagrangian and Hamiltonian functions are defined as follows:

$$L(I_1, I_2, u_1, u_2) = W_1 I_1(t) + W_2 I_2(t) + \frac{1}{2} W_3 u^2{}_1(t) + \frac{1}{2} W_4 u^2{}_2(t), \tag{4.94}$$

and

$$H = L(I_1, I_2, u_1, u_2) + \lambda_1 \frac{dS}{dt} + \lambda_2 \frac{dE}{dt} + \lambda_3 \frac{dI_1}{dt} + \lambda_4 \frac{dI_2}{dt} + \lambda_5 \frac{dQ}{dt} + \lambda_6 \frac{dR}{dt}. \tag{4.95}$$

Theorem 4.8 (Pontryagin's Minimum Principle for control problem [108]) Optimal control was determined. $u^*{}_1, u^*{}_2$ and S, E, I_1, I_2, Q, R were the results of the control equation system (4.87)-(4.92) that minimize $J(u_1(t), u_2(t))$ over U. Then there exists an adjoint variable $\lambda_i; i = 1,2,3,4,5,6$ under the control equations :

$$\frac{d\lambda_1}{dt}=-\frac{\partial H}{\partial S},\frac{d\lambda_2}{dt}=-\frac{\partial H}{\partial E},\frac{d\lambda_3}{dt}=-\frac{\partial H}{\partial I_1}=,\frac{d\lambda_4}{dt}=-\frac{\partial H}{\partial I_2},\frac{d\lambda_5}{dt}=-\frac{\partial H}{\partial Q},\frac{d\lambda_6}{dt}=-\frac{\partial H}{\partial R}. \tag{4.96}$$

And transversality conditions given as $\lambda_i(T)=0$ for all $i=1,2,3,4,5,6$.

Then the characteristic values u^*_1, u^*_2 are given by;

$$u^*_1(t)=\begin{cases} 0 & if \ \dfrac{(\lambda_2-\lambda_1)((\beta_s I_1(t)+\beta_a I_2(t))S(t))}{W_3}\le 0, \\ \dfrac{(\lambda_2-\lambda_1)((\beta_s I_1(t)+\beta_a I_2(t))S(t))}{W_3} & if \ \dfrac{(\lambda_2-\lambda_1)((\beta_s I_1(t)+\beta_a I_2(t))S(t))}{W_3}< u_1^{\max}, \\ u_1^{\max} & if \ \dfrac{(\lambda_2-\lambda_1)((\beta_s I_1(t)+\beta_a I_2(t))S(t))}{W_3}\ge u_1^{\max}. \end{cases} \tag{4.97}$$

$$u^*_2(t)=\begin{cases} 0 & if \ \dfrac{(\lambda_1-\lambda_6)S(t)}{W_4}\le 0, \\ \dfrac{(\lambda_1-\lambda_6)S(t)}{W_4} & if \ \dfrac{(\lambda_1-\lambda_6)S(t)}{W_4}< u_2^{\max}, \\ u_2^{\max} & if \ \dfrac{(\lambda_1-\lambda_6)S(t)}{W_4}\ge u_2^{\max}. \end{cases} \tag{4.98}$$

Proof. Consider the Hamiltonian function as defined by equation (4.95)

$$H=L(I_1,I_2,u_1,u_2)+\lambda_1\frac{dS}{dt}+\lambda_2\frac{dE}{dt}+\lambda_3\frac{dI_1}{dt}+\lambda_4\frac{dI_2}{dt}+\lambda_5\frac{dQ}{dt}+\lambda_6\frac{dR}{dt}.$$

Substituting the Lagrangian function and the differential equations (4.87) - (4.92), we obtain:

$$\begin{aligned} H=&W_1I_1(t)+W_2I_2(t)+\frac{1}{2}W_3u^2_1(t)+\frac{1}{2}W_4u^2_2(t)\\ &+\lambda_1\left[\Lambda-(1-u_1(t))(\beta_sI_1(t)+\beta_aI_2(t))S(t)-dS(t)-u_2(t)S(t)\right]\\ &+\lambda_2\left[(1-u_1(t))(\beta_sI_1(t)+\beta_aI_2(t))S(t)-(\tau\varepsilon+\tau(1-\varepsilon)+d)E(t)\right]\\ &+\lambda_3\left[\tau\varepsilon E(t)-(\alpha+g+d)I_1(t)\right]\\ &+\lambda_4\left[\tau(1-\varepsilon)E(t)-(\gamma_a+g+d)I_2(t)\right]\\ &+\lambda_5\left[\alpha I_1(t)-(\gamma_q+d)Q(t)\right]\\ &+\lambda_6\left[\gamma_aI_2(t)+\gamma_qQ(t)-dR(t)+u_2(t)S(t)\right]. \end{aligned} \tag{4.99}$$

The adjoint system satisfies the following ordinary differential equations

$$\frac{d\lambda_1}{dt}=-\frac{\partial H}{\partial S}=\lambda_1\left((1-u^*_1(t))(\beta_sI_1(t)+\beta_aI_2(t))+d+u^*_2(t)\right)-\lambda_2\left((1-u^*_1(t))(\beta_sI_1(t)+\beta_aI_2(t))\right)-\lambda_6u^*_2(t),$$

$$\frac{d\lambda_2}{dt}=-\frac{\partial H}{\partial E}=\lambda_2(\tau\varepsilon+\tau(1-\varepsilon)+d)-\lambda_3\tau\varepsilon-\lambda_4\tau(1-\varepsilon),$$

$$\frac{d\lambda_3}{dt}=-\frac{\partial H}{\partial I_1}=\lambda_1\left((1-u^*_1(t))\beta_sS(t)\right)-\lambda_2\left((1-u^*_1(t))\beta_sS(t)\right)+\lambda_3(\alpha+g+d)-\lambda_5\alpha-W_1,$$

$$\frac{d\lambda_4}{dt}=-\frac{\partial H}{\partial I_2}=\lambda_1\left((1-u^*_1(t))\beta_aS(t)\right)-\lambda_2\left((1-u^*_1(t))\beta_aS(t)\right)+\lambda_4(\gamma_a+g+d)-\lambda_6\gamma_a-W_2,$$

$$\frac{d\lambda_5}{dt}=-\frac{\partial H}{\partial Q}=\lambda_5(\gamma_q+d)-\lambda_6\gamma_q,$$

$$\frac{d\lambda_6}{dt}=-\frac{\partial H}{\partial R}=\lambda_6d.$$

With transversality conditions $\lambda_i(T)=0$ for all $i=1,2,3,...,6$ and From the conditions of the Hamiltonian, we have: $\frac{\partial H}{\partial u_j}=0$ for all $j=1,2$ at $u_j=u^*_j$.

Therefore, we obtain:

$$\frac{\partial H}{\partial u_1}=W_3u^*_1(t)+\lambda_1\left((\beta_sI_1(t)+\beta_aI_2(t))S(t)\right)-\lambda_2\left((\beta_sI_1(t)+\beta_aI_2(t))S(t)\right)\Rightarrow$$

$$u^*_1(t)=\frac{\left(\lambda_2-\lambda_1\right)\left((\beta_sI_1(t)+\beta_aI_2(t))S(t)\right)}{W_3}$$

$$\frac{\partial H}{\partial u_2}=W_4u^*_2(t)-\lambda_1S(t)+\lambda_6S(t)\Rightarrow u^*_2(t)=\frac{(\lambda_1-\lambda_6)S(t)}{W_4}.$$

Based on the above, the optimal control equations for the model (4.87) - (4.92) are as follows:

$$u^*_1(t)=\begin{cases}0 & if\ \frac{\left(\lambda_2-\lambda_1\right)\left((\beta_sI_1(t)+\beta_aI_2(t))S(t)\right)}{W_3}\le 0,\\ \frac{\left(\lambda_2-\lambda_1\right)\left((\beta_sI_1(t)+\beta_aI_2(t))S(t)\right)}{W_3} & if\ \frac{\left(\lambda_2-\lambda_1\right)\left((\beta_sI_1(t)+\beta_aI_2(t))S(t)\right)}{W_3}<u_1^{\max},\\ u_1^{\max} & if\ \frac{\left(\lambda_2-\lambda_1\right)\left((\beta_sI_1(t)+\beta_aI_2(t))S(t)\right)}{W_3}\ge u_1^{\max}.\end{cases}$$

$$u^*_2(t)=\begin{cases}0 & if\ \frac{(\lambda_1-\lambda_6)S(t)}{W_4}\le 0,\\ \frac{(\lambda_1-\lambda_6)S(t)}{W_4} & if\ \frac{(\lambda_1-\lambda_6)S(t)}{W_4}<u_2^{\max},\\ u_2^{\max} & if\ \frac{(\lambda_1-\lambda_6)S(t)}{W_4}\ge u_2^{\max}.\end{cases}$$

□

4.3.4.2 Numerical Analysis of the Optimal Control Problem for Model 3

In this section, we present the numerical analysis of the optimal control problem for Model 3. This analysis involves implementing the optimal control strategies identified in the previous section to evaluate their effectiveness in minimizing infection spread. By solving the system of differential equations with control variables (e.g., social distancing, mask-wearing, and vaccination) included, we can observe the impact of these interventions over time.

Numerical Analysis of the Control Problem at the Endemic Equilibrium

This section presents the numerical analysis of the control problem at the endemic equilibrium point. Here, we assess the impact of optimal control strategies—such as social distancing, mask-wearing, and vaccination—on the stability of the

endemic equilibrium, where the disease persists at a constant level within the population. By implementing these control measures in the model and evaluating the resulting dynamics, we can determine the effectiveness of each strategy in reducing the infection prevalence and shifting the system towards a lower endemic state or potentially eliminating the disease. This analysis is crucial for understanding how to manage and mitigate the spread of infection sustainably when eradication is not immediately achievable.

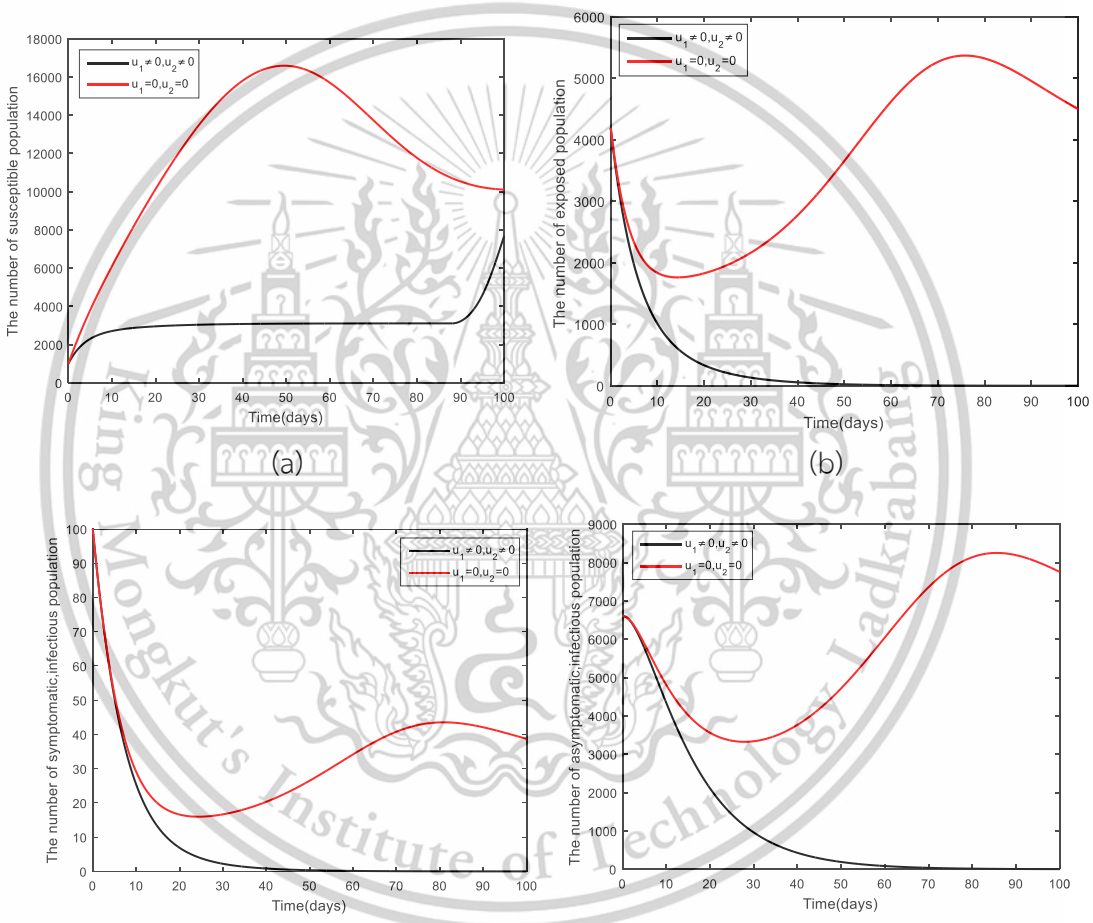

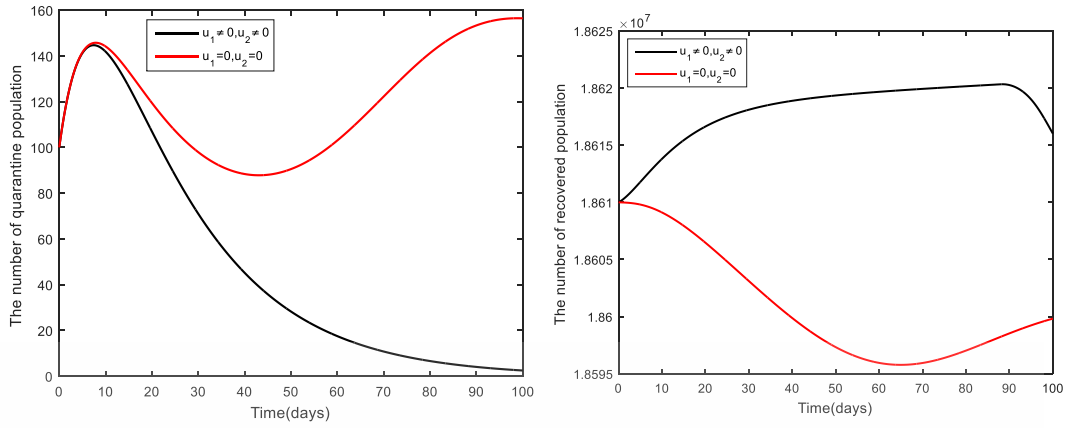

(e) (f)

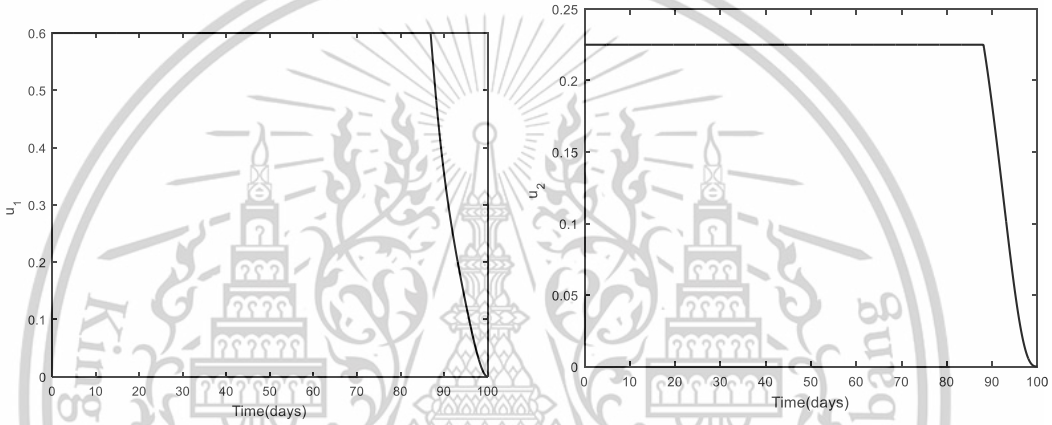

(g) (h)

Figure 4.24 Graph showing the solutions of models (4.68)-(4.73) and (4.87)-(4.93), comparing the model with control strategies to the model without control strategies ($u_1 = 0, u_2 = 0$ and $u_1 \neq 0, u_2 \neq 0$) when $R_0 > 1$.

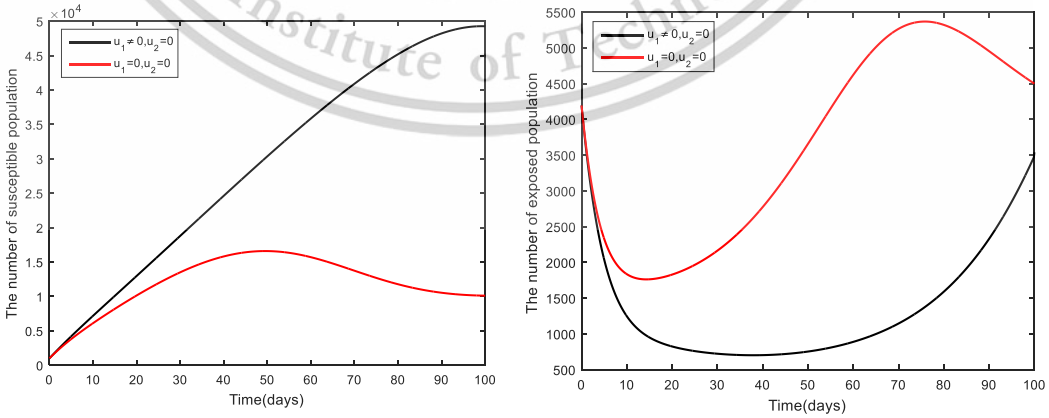

(a) (b)

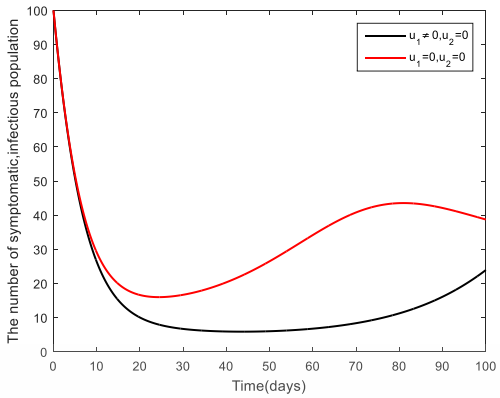

(c)

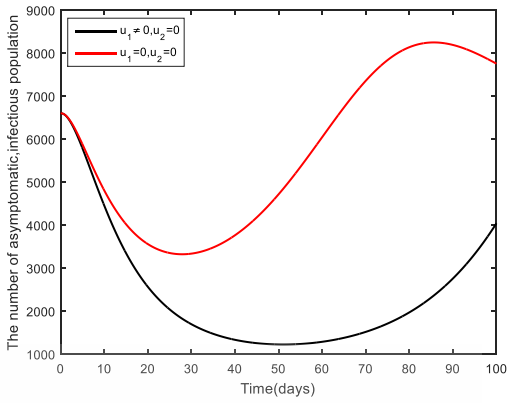

(d)

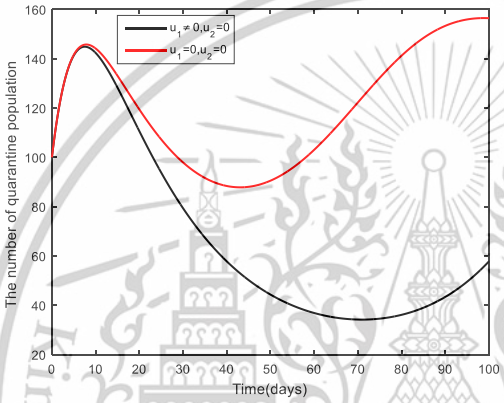

(e)

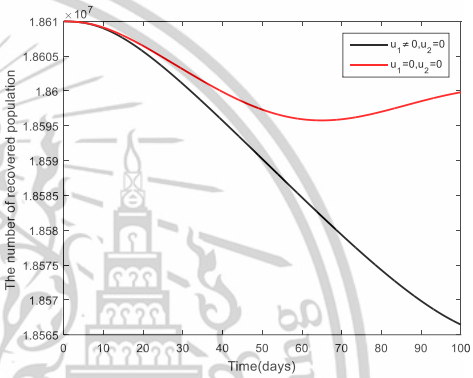

(f)

Figure 4.25 Graph showing the solutions of models (4.68)-(4.73) and (4.87)-(4.93), comparing the model using only the social distancing and mask-wearing control strategy to the model without any control strategies ($u_1 = 0, u_2 = 0$ and $u_1 \neq 0, u_2 = 0$) when $R_0 > 1$.

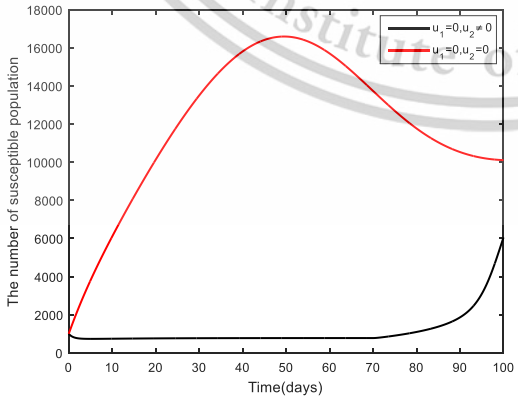

(a)

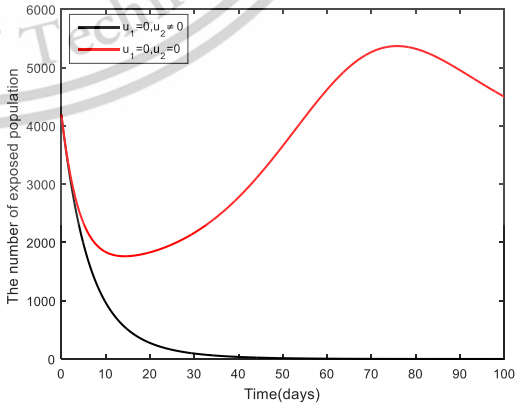

(b)

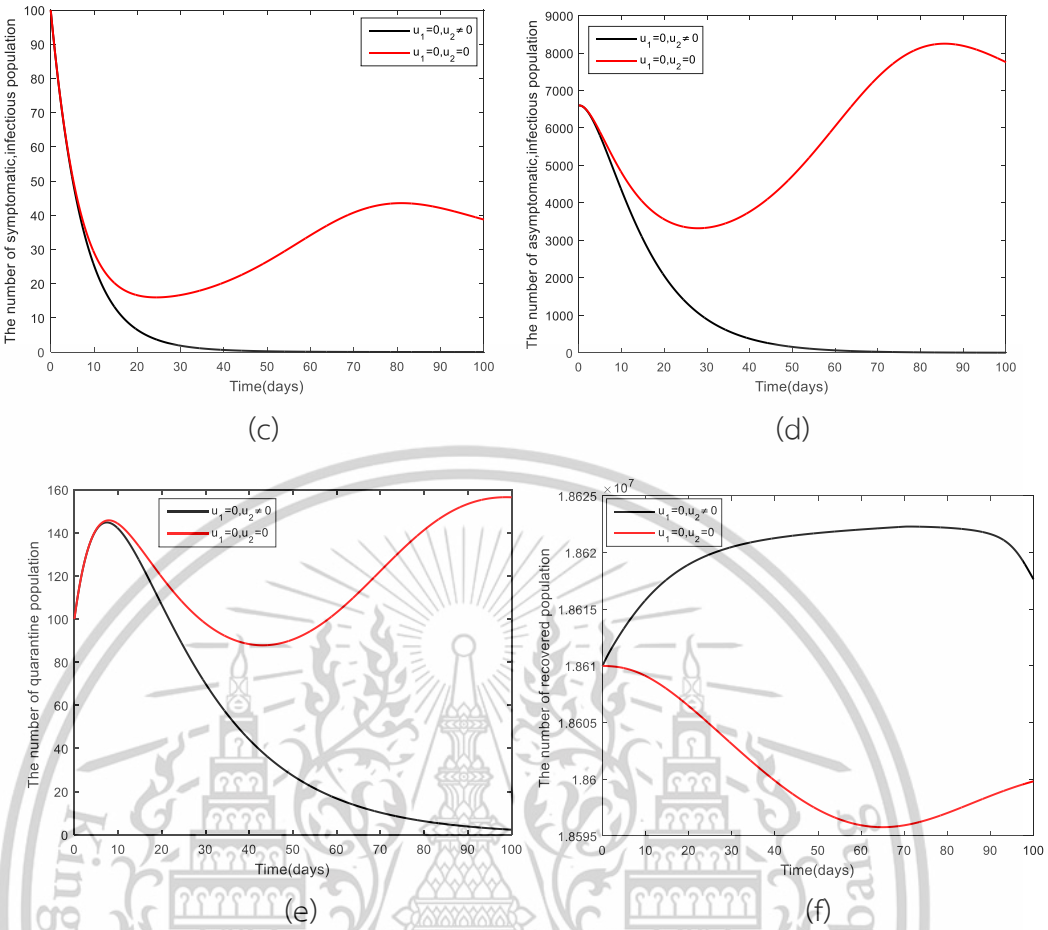

Figure 4.26 Graph showing the solutions of models (4.68)-(4.73) and (4.87)-(4.93), comparing the model using only the vaccination control strategy to the model without any control strategies ($u_1=0,u_2=0$ and $u_1=0,u_2\neq 0$) when $R_0>1$.

In this section, we perform a numerical analysis comparing the uncontrolled model (4.68) - (4.73) with the controlled model (4.87) - (4.93). For this simulation, the parameters are set as follows: $W_1=10,W_2=20,W_3=30,W_4=40$, and the simulation period is 100 days. The analysis is divided into three parts:

Part 1: Analyzing Both Strategies Together

In this part, we apply social distancing with mask-wearing $(u_1\neq 0)$ and vaccination control strategies $(u_2\neq 0)$. The analysis is conducted at endemic equilibrium points, as shown in Figures 4.24, respectively. Observing the graphs, it is clear that the model with control strategies results in a lower number of infections in each category compared to the model without control. Additionally, the time required for disease control is shorter when both strategies are implemented together than in the absence of control.

Part 2: Analyzing Social Distancing and Mask-Wearing Strategy Alone

Here, we examine only the social distancing and mask-wearing control strategy $(u_1 \neq 0)$. From Figure 4.25, it is evident that the model with this single control strategy manages to control the spread of disease more effectively than the uncontrolled model. However, when comparing the time taken for disease control, using both strategies together proves to be more effective than using only social distancing and mask-wearing.

Part 3: Analyzing Vaccination Control Strategy Alone

In this part, we implement the vaccination control strategy alone $(u_2 \neq 0)$. As shown in Figure 4.26, the vaccination-only strategy controls the disease better than the model without any control. Furthermore, the time taken for control when using only vaccination is close to that of using both strategies together. This suggests that vaccination control plays a significant role in managing potential outbreaks effectively.

Chapter 5
Conclusions and suggestions

5.1 Conclusions

The COVID-19 pandemic has presented unprecedented challenges to global public health, requiring innovative solutions to understand and mitigate its spread. This research has addressed the critical need for a comprehensive analysis of COVID-19 transmission dynamics in Thailand, particularly in the context of vaccination, isolation, and preventive strategies. With the rapidly evolving nature of the pandemic, previous studies lacked the detailed and localized models necessary for developing tailored intervention strategies, thus underscoring the necessity of this work.

This research contributes to addressing these challenges by developing a mathematical model that differentiates between vaccinated and unvaccinated populations, ensuring a more precise representation of disease transmission patterns. By incorporating localized epidemiological data, the model accurately reflects real-world conditions in Thailand, allowing for a more relevant analysis of intervention strategies. The implementation of optimal control theory further enhances the model's applicability by identifying the most effective strategies for vaccination, quarantine, and movement restrictions to minimize infection rates. The model's stability is validated through rigorous mathematical techniques, such as Lyapunov functions and the next-generation matrix method, confirming its reliability for predicting the course of the epidemic. The findings offer valuable insights for policymakers, enabling them to formulate informed decisions regarding public health measures to control the spread of COVID-19. By bridging the gap in previous research and providing a more refined analytical framework, this study serves as a critical tool for developing targeted interventions and ensuring an adaptive response to the evolving pandemic landscape.

To achieve this, three interconnected mathematical models were developed and analyzed, each addressing distinct aspects of the pandemic. Model 1 was designed to reflect the current pandemic scenario by incorporating vaccinated populations, patient quarantine, and hospitalization. It established a foundational understanding of how these measures interact to influence disease transmission. Model 2 expanded upon this by distinctly separating vaccinated and unvaccinated populations, as well as

asymptomatic and symptomatic infected groups, and further analyzing the role of hospitalization. This model introduced an optimal control strategy to refine intervention measures. Finally, Model 3 focused on symptomatic and asymptomatic cases, emphasizing isolation strategies for symptomatic individuals and designing the most suitable control strategies to mitigate the spread effectively. These models are interconnected through their progressive structure, where each model builds upon the findings and refinements of the previous one. Model 1 lays the groundwork by integrating fundamental intervention strategies. Model 2 enhances this by introducing population differentiation and optimal control strategies, allowing for more targeted interventions. Model 3 refines these strategies further by focusing on isolation measures and control optimization, providing a more precise and effective means of reducing transmission. The continuous refinement across models ensures a comprehensive approach to understanding and mitigating the spread of COVID-19. This interconnected structure allows for an evolving and adaptive framework, aligning intervention strategies with the dynamic nature of the pandemic and ensuring that public health responses remain effective and data-driven.

The computational results demonstrate the efficacy of these models in simulating the outbreak's dynamics and evaluating the effectiveness of control measures. By employing real epidemiological data, these models allow for an accurate assessment of different intervention strategies and their potential impact on reducing the spread of infection. Key findings include a significant reduction in the basic reproduction number (R_0) when optimal vaccination and isolation strategies were implemented, underscoring the critical role of these measures in controlling disease spread. Sensitivity analysis of model parameters further highlights the impact of vaccination rates and isolation effectiveness in mitigating the outbreak. The insights gained from this research offer valuable guidance for policymakers in refining public health interventions and adapting strategies in response to evolving pandemic conditions. Furthermore, the study demonstrates that incorporating dynamic intervention strategies based on real-time data significantly enhances the efficiency of disease control measures. The integration of adaptive modeling approaches ensures that response measures remain relevant and effective in varying epidemiological conditions, providing a robust foundation for future public health planning and preparedness. Despite these strengths, the models have some limitations. The study

assumes homogeneous mixing of populations, which may not fully capture the complexities of human interactions. Additionally, factors such as behavioral responses to public health measures and socio-economic influences were not explicitly modeled, potentially affecting the accuracy of predictions. These aspects highlight areas for future research to improve model applicability and robustness.

This research has yielded several impactful findings. First, it confirms the importance of combining vaccination with isolation measures to achieve sustainable control of COVID-19. Second, the study's localized approach aligns the models with Thailand's specific outbreak patterns, offering actionable recommendations for the Ministry of Public Health. Lastly, the integration of real-world data enhances the practical relevance of the findings, establishing a robust framework for managing future pandemics.

Future developments could explore additional factors such as age-dependent parameters, behavioral influences, and environmental conditions. Incorporating variants of concern and multi-disease dynamics would further improve the applicability of the models. Additionally, integrating machine learning techniques with mathematical modeling could enhance parameter estimation and predictive capabilities.

In conclusion, this work advances the understanding of COVID-19 dynamics through the innovative design of three mathematical models, each addressing the different designs for infection and control. The findings not only support immediate public health interventions but also contribute to the broader field of epidemiological modeling, ensuring preparedness for future health crises.

5.2 Suggestions

This research opens numerous possibilities for further exploration and development in the mathematical modeling of infectious diseases. Future work could include the following suggestions:

1. Incorporation of Additional Factors: Expanding the models to include age-dependent parameters, behavioral influences, and environmental conditions would improve the accuracy and applicability of the models. Factors such as age-specific transmission rates, hospitalization rates, and mortality rates could provide more detailed insights. In designing future research, it is essential to consider vulnerable

groups such as the elderly and individuals with pre-existing health conditions, as their immune responses may differ significantly from other populations. Tailored interventions for these groups can enhance the overall effectiveness of disease control strategies.

2. Addressing Variants of Concern: With the emergence of new variants, incorporating their characteristics into the models would enhance their ability to predict and manage the spread effectively. This includes understanding changes in transmissibility, severity, and vaccine efficacy.

3. Multi-Disease Dynamics: Extending the models to include co-infection scenarios or other diseases prevalent in the region would provide a broader perspective on public health management.

4. Policy and Economic Analysis: Including economic evaluations and policy-driven simulations could help decision-makers balance the trade-offs between public health measures and socio-economic impacts.

5. Real-Time Adaptation: Developing real-time adaptable models that integrate ongoing data collection could allow for immediate application in dynamic outbreak situations, enhancing their utility in managing future pandemics.

Despite vaccination being a key strategy in controlling disease spread, several barriers may limit vaccine uptake. These include age restrictions for vaccine eligibility, health risks in individuals with pre-existing conditions, and concerns over the efficacy of current vaccines. Therefore, it is crucial to consider these factors comprehensively and develop diverse control strategies to address uncertainties effectively. Implementing a multi-faceted approach will not only enhance disease control measures but also mitigate potential challenges in future outbreak scenarios. These directions would not only refine the existing models but also provide versatile tools for public health authorities to effectively manage infectious disease outbreaks and future pandemics.

References

[1] Kumar, H. Arora, P.K. Pant, M. Kumar, A. and Shahroz, A.K. 2021. "A simple mathematical model to predict and validate the spread of Covid-19 in India." *Mater. Today Proc.* 47(2021): 3859–3864.

[2] Thirthar, A.A. Abboubakar, H. Khan, A. and Abdeljawad, T. 2023. "Mathematical modeling of the COVID-19 epidemic with fear impact." *AIMS Math.* 8(3): 6447–6465.

[3] Khan, M.A. and Atangana, A. 2022. "Mathematical modeling and analysis of COVID-19: A study of new variant Omicron." *Phys. A.* 599(2022): 127452.

[4] Zhang, Z. Zeb, A. Hussain, S. and Alzahrani, E. 2020. "Dynamics of COVID-19 mathematical model with stochastic perturbation." *Adv. Differ. Equ.* 2020(2020): 451.

[5] Shen, Z.H. Chu, Y.M. Khan, M.A. Al-Hartomy, O.A. and Higazy, M. 2021. "Mathematical modeling and optimal control of the COVID-19 dynamics." Results Phys. 31(2021): 105028.

[6] Tian, J. Wu, J. Bao, Y. Weng, X. Shi, L. Liu, B. Yu, X. Qi, L. and Liu, Z. 2020. "Modeling analysis of COVID-19 based on morbidity data in Anhui, China." *Math. Biosci. Eng.* 17(4): 2842–2852.

[7] Chaharborj, S.S. Hassanzadeh, J. and Phang, P.C. 2021. "Controlling of pandemic COVID-19 using optimal control theory." *Results Phys*. 26(2021): 104311.

[8] Ghazizadeh, H. Shakour, N. Ghofchi, S. Mansoori, A. Saberi-Karimiam, M. Rashidmayvan, M. Ferns, G. Esmaily, H. and Ghayour Mobarhan, M. 2023. "Use of data mining approaches to explore the association between type 2 diabetes mellitus with SARS-CoV-2." *BMC Pulm. Med.* 23(2023): 203

[9] Sepulveda, G. Arenas, A.J. and González-Parra, G. 2023. "Mathematical Modeling of COVID-19 Dynamics under Two Vaccination Doses and Delay Effects." *Mathematics.* 11(2023): 369.

[10] Khan, A.A. Ullaha, S. and Amin, R. 2022. "Optimal control analysis of COVID-19 vaccine epidemic model: A case study." *Eur. Phys. J. Plus.* 137(2022): 156.

[11] Philip, N.A.A. Seidu, B. and Bornaa, C.S. 2022. "Mathematical Analysis of COVID-19 Transmission Dynamics Model in Ghana with Double-Dose Vaccination and Quarantine." *Comput. Math. Methods Med.* 2022(2022): 7493087.

[12] Wickramaarachchi, W.P.T.M. and Perera, S.S.N. 2021. "An SIER model to estimate optimal transmission rate and initial parameters of COVD-19 dynamic in Sri Lanka." *Alex. Eng. J.* 60(2021): 1557–1563.

[13] Daniel, D.O. 2020. "Mathematical Model for the Transmission of COVID-19 with Nonlinear Forces of Infection and the Need for Prevention Measure in Nigeria." *J. Infect. Dis. Epidemiol.* 6(2020): 158.

[14] Veera Krishna, M. and Prakas, J. 2020. "Mathematical modelling on phase based transmissibility of Coronavirus." *Infect. Dis. Model.* 5(2020): 375–385.

[15] Mishraa, A.M. Purohit, S.D. Owolabi, K.M. and Sharma, Y.D. 2020. "A nonlinear epidemiological model considering asymptotic and quarantine classes for SARS CoV-2 virus." *Chaos Solitons Fractals.* 138(2020):109953.

[16] Feng, L.X. Jing, S.L. Hu, S.K. Wang, D.F. and Huo, H.F. 2020. "Modelling the effects of media coverage and quarantine on the COVID-19 infections in the UK." *Math. Biosci. Eng.* 17(4): 3618–3636.

[17] Prathumwan, D. Trachoo, K. and Chaiya, I. 2020. "Mathematical Modeling for Prediction Dynamics of the Coronavirus Disease 2019 (COVID-19) Pandemic, Quarantine Control Measures." *Symmetry*. 12(2020): 1404.

[18] Riyapan, P. Shuaib, S.E. and Intarasit, A. 2021. "A Mathematical Model of COVID-19 Pandemic: A Case Study of Bangkok, Thailand COVID-19." *Comput. Math. Methods Med.* 2021(2021): 6664483.

[19] Win, Z.T. Eissa, M.A. and Tian, B. 2022. "Stochastic Epidemic Model for COVID-19 Transmission under Intervention Strategies in China." *Mathematics.* 10(2022): 3119.

[20] Theparod, T. Kreabkhontho, P. and Teparos, W. 2023. "Booster Dose Vaccination and Dynamics of COVID-19 Pandemic in the Fifth Wave: An Efficient and Simple Mathematical Model for Disease Progression." *Vaccines.* 11(2023): 589.

[21] Satar, H.A. and Naji, R.K. 2023. "A Mathematical Study for the Transmission of Coronavirus Disease." Mathematics. 11(2023): 2330.

[22] Zamir, M. Abdeljawad, T. Nadeem, F. and Yousef, A. 2021. "An optimal control analysis of a COVID-19 model." Alex. Eng. J. 60(2021): 2875–2884.

[23] Baba, I.A. Nasidi, B.A. Baleanu, D. and Saadi, S.H. 2021. "A mathematical model to optimize the available control measures of COVID–19." *Ecol. Complex.* 46(2021): 100930.

[24] Kifle, Z. S. and Obsu, L.L. 2022. "Mathematical modeling for COVID-19 transmission dynamics: A case study in Ethiopia." *Results Phys.* 34 (2022): 105191.

[25] Akinwande, N.I. Ashezua, T.T. Gweryina, R.I. Somma, S.A. Oguntolu, F.A. Usman, A. Abdurrahman, O.N. Kaduna, F.S. Adajime, T.P. Kuta, F.A. Abdulrahman, S. Olayiwola, R.O. Enagi, A.I. Bolarin, G.A. and Shehu, M.D. 2022. "Mathematical model of COVID-19 transmission dynamics incorporating booster vaccine program and environmental contamination." *Heliyon.* 8 (2022): e11513.

[26] Jankhonkhan, J. and Sawangtong, W. 2021. "Model Predictive Control of COVID-19 pandemic Concerning Social Isolation and Vaccination Policies in Thailand." *Axioms.* 10(2021): 274.

[27] Yang, C. and Wang, J. 2021. "Modeling the transmission of COVID-19 in the US-A case study." *Infect. Dis. Model.* 6(2021):195–211.

[28] Zhanga, Z. and Jain, S. 2020. "Mathematical model of Ebola and Covid-19 with fractional differential operators: Non-Markovian process and class for virus pathogen in the environment." *Chaos Solit. Fract.* 140(2020): 110175.

[29] Kumari, P. Singh, S. and Singh, H.P. 2022. "Dynamical Analysis of COVID-19 Model Incorporating Environmental Factors." *Iran J. Sci. Technol. Trans. Sci.* 46(2022): 1651–1666.

[30] World Health Organization. 2023. **COVID-19 - WHO World Situation Reports.** [Online]. Available: https://data.who.int/dashboards/covid19/cases?m49=001&n=c

[31] World Health Organization. 2023. **Number of COVID-19 deaths reported to WHO.** [Online]. Available: https://data.who.int/dashboards/covid19/deaths?m49= 001&n=c

[32] World Health Organization. 2023. **COVID-19 - WHO Thailand Situation Reports.** [Online]. Available: https://data.who.int/dashboards/covid19/cases?m49=764&n=c

[33] World Health Organization. 2023. **Trends in COVID-19 deaths, Thailand.** [Online]. Available: https://data.who.int/dashboards/covid19/deaths?m49=764&n=c

[34] Sun, T.-C. DarAssi, M.H. Alfwzan, W.F. Khan, M.A. Alshahrani, A.S. Alqahtani, S.S. and Muhammad, T. 2023. "Mathematical Modeling of COVID-19 with Vaccination Using Fractional Derivative: A Case Study." *Fractal Fract.* 7(2023): 234.

[35] Gumu, O.A. Selvam, A.G.M. Janagaraj, R. Selvam, G.M. and Janagaraj, R. 2022. "Dynamics of the Mathematical Model Related to COVID-19 Pandemic with Treatment." *Thai J. Math.* 20(2022): 957–970.

[36] Chhetri, B. Bhagat, V.M. Muthusamy, S. Ananth, V.S. Vamsi, D.K.K. and Sanjeevi, C.B. 2021. "Time Optimal Control Studies on COVID-19 Incorporating Adverse Events of the Antiviral Drugs." *Comput. Math. Biophys.* 9(2021): 214–241.

[37] Nabi,K.N. Kumar, P. and Erturk, V.S. 2021. "Projections and fractional dynamics of COVID-19 with optimal control strategies." *Chaos Solitons Fractals.* 145(2021): 110689.

[38] Saha, S. and Saha, A.K. 2023. "Modeling the Dynamics of COVID-19 in the Presence of Delta and Omicron Variants with Vaccination and Non-Pharmaceutical Interventions." *Heliyon.* 9(2023): e17900.

[39] Rajput, A. Tanvi, Aggarwal, R. Sharma, A. Sahdev, S.K. Kumar, M. and Jaimala. 2023. "Fractional Order on Modeling the Transmission of Devastative COVID-19Infection: Efficacy of Vaccination." *Applications and Applied Mathematics: An International Journal (AAM).* 18(1): 1-24.

[40] Department of disease control. 2024. **COVID-19 vaccine, Thailand**. [Online]. Available: https://ddc.moph.go.th/vaccine-covid19/

[41] World Health Organization. 2023. **COVID-19 vaccination, World data.** [Online]. Available: https://data.who.int/dashboards/covid19/vaccines?m49=001&n=c

[42] World Health Organization. 2023. **COVID-19 vaccination, Thailand data.** [Online]. Available: https://data.who.int/dashboards/covid19/vaccines?m49=764&n=c

[43] Lamwong, J. Tang, I. and Pongsumpun, P. 2018. "Mers model of Thai and South Korean population." *Curr. Appl. Sci. Technol.* 18(1): 45–57.

[44] Gardner, L.M. Rey, D. Heywood, A.E. Toms, R. Wood, J. Travis Waller, S. and Raina MacIntyre, C. 2014. "A scenario-based evaluation of the Middle East respiratory syndrome coronavirus and the Hajj." *Risk. Anal.* 34(8): 1391–1400.

[45] Mwalili, S. Kimathi, M. Ojiambo, V. Gathungu, D. and Mbogo, R. 2020. "SEIR model for COVID-19 dynamics incorporating the environment and social distancing." *BMC. Res. Notes.* 13(2020): 352.

[46] Mahardika, Y.D. 2021. "Dynamical Modeling of COVID-19 and Use of Optimal Control to Reduce the Infected Population and Minimize the Cost of Vaccination and Treatment." *ComTech Comput. Math. Eng. Appl.* 12(2): 65–73.

[47] Iboi, E.A. Sharomi, O. Ngonghala, C.N. and Gumel, A.B. 2020. "Mathematical modeling and analysis of COVID-19 pandemic in Nigeria." *Math. Biosci. Eng.* 17(6): 7192–7220.

[48] Hezam, I.M. Foul, A. and Alrasheedi, A. 2021. "A dynamic optimal control model for COVID-19 and cholera co-infection in Yemen." *Adv. Differ. Equ.* 2021(2021): 108.

[49] Babaei, A. Ahmadi, M. Jafari, H. and Liya, A. 2021. "A mathematical model to examine the effect of quarantine on the spread of coronavirus." *Chaos Solitons Fractals*. 142(2021): 110418.

[50] Mendoza, V.M.P. Mendoza, R. Lee, J. and Jung, E. 2023. "Managing bed capacity and timing of interventions: A COVID-19 model considering behavior and underreporting." *AIMS Math.* 8(1): 2201–2225.

[51] Ghiasi Hafezi, S. Seif, N. Bahari, H. Mohammadi, M. Ghasemabadi, A. Ferns, G.A. Farkhani, E.M. and Ghayour-mobarhan, M. 2023. "The association between macronutrient intakes and coronavirus disease 2019 (COVID-19) in an Iranian population: Applying a dynamical system model." *J. Health Popul. Nutr.* 42(2023): 114.

[52] Modnak, C. 2013. **Optimal Control Modeling and Simulation, with Application to Cholera Dynamics.** Dissertation, Mathematics & Statistics, Old Dominion University.

[53] Nainggolan, J. and Ansori, M.F. 2022. "Stability and Sensitivity Analysis of the COVID-19 Spread with Comorbid Diseases." *Symmetry*. 14(2022): 2269.

[54] Lina, Q. Zhaob, S. Gaod, D. Loue, Y. Yangf, S. Musae, S.S. Wangb, M.H. Caig, Y. Wangg, W. Yangh, L. Wangg, W. Yangh, L. and He, D. 2020. "A conceptual model for the coronavirus disease 2019 (COVID-19) outbreak in Wuhan, China with individual reaction and governmental action." *Int. J. Infect. Dis.* 93(2020): 211–216.

[55] World Health Organization. 2024. **Coronavirus disease (COVID-19)**. [Online]. Available:https://www.who.int/emergencies/diseases/novel-coronavirus2019/question-and-answers-hub/q-a-detail/coronavirus-disease-covid-19

[56] Diagne, M.L. Rwezaura, H. Tchoumi, S.Y. and Tchuenche, J.M. 2021. "A Mathematical Model of COVID-19 with Vaccination and Treatment." *Comput. Math. Methods Med.* 2021(2021): 1250129.

[57] Ndaïrou, F. Area, L. Nietoc, J.J. and Torres, D.F.M. 2020. "Mathematical modeling of COVID-19 transmission dynamics with a case study of Wuhan." *Chaos Solit. Fract.* 135(2020): 109846.

[58] Faruk, O. and Kar, S. 2021. "A Data Driven Analysis and Forecast of COVID-19 Dynamics during the Third Wave Using SIRD Model in Bangladesh." *COVID.* 1(2021): 503-517.

[59] Wang, L. Dai, Y. Wang, R. Sun, Y. Zhang, C. Yang, Z. and Sun, Y. 2022. “SEIARN: Intelligent Early Warning Model of Epidemic Spread Based on LSTMTrajectory Prediction.” *Mathematics.* 10(2022): 3046.

[60] Department of Disease Control. 2023. **Coronavirus disease (COVID-19).** [Online]. Available:https://ddc.moph.go.th/viralpneumonia/file/int_operator/int_operator01_110463.pdf

[61] Department of Disease Control. 2023. **COVID-1 9 disease situation.** [Online]. Available:http://www.thaincd.com/document/file/download/knowledge/COVID19.65.pdf

[62] Department of Disease Control. **Vaccine covid-19 of Thailand.** [online]. Available: https://ddc.moph.go.th/vaccine-covid19/

[63] Department of Disease Control. 2023. **Vaccine covid-19 of Thailand.** [online]. Available from: https://ddc.moph.go.th/vaccine-covid19/guidelines

[64] Driessche, P.V. and Watmough, J. 2002. “Reproduction numbers and sub-threshold endemic equilibria for compartmental models of disease transmission.” *Math. Biosci.* 180(2002): 29–48.

[65] LaSalle, J.P. 1976. **The Stability of Dynamical Systems; Society for Industrial and Applied Mathematics**. Philadelphia, PA, USA.

[66] MichaelY.Li. 2017. **An Introduction to Mathematical Modeling of Infectious Diseases.** Mathematical and Statistical Sciences University of Alberta Edmonton, AB Canada.

[67] Lenhart, S. and Workman, J.T. 2007. **Optimal Control Applied to Biological Models.** Chapman & Hall/CRC: London, UK.

[68] Rodrigues, HSF. 2012. **Optimal control and numerical optimization applied to epidemiological models.** Department of Mathematics, University of Aveiro.

[69] Pontryagin, L.S. Boltyanskii, V.G. Gamkrelidze, R.V. and Mishchenko, E.F. 1962. **The Mathematical Theory of Optimal Processes**. Wiley: New York, NY, USA.

[70] Kamien, M.I. and Schwartz, N.L. 1991. **Dynamic Optimization: The Calculus of Variations and Optimal Control in Economics and Management**. Elsevier: Amsterdam, The Netherlands.

[71] Carcione, J.M. Santos, J.E. Bagaini, C. and Ba, J. 2020. “A Simulation of a COVID-19 Epidemic Based on a Deterministic SEIR Model.” *Front. Public Health.* 8(2020): 230.

[72] Bhadauria, A.S. Devi, S. and Nivedita, G. 2022. “Modelling and analysis of a SEIQR model on COVID-19 pandemic with delay.” *Model. Earth Syst. Environ.* 8(2022): 3201–3214.

[73] Hussain, T. Ozair, M. Ali, F. Rehman, S. Assiri, T.A. and Mahmoud, E.E. 2021. “Sensitivity analysis and optimal control of COVID-19 dynamics based on SEIQR model.” *Results Phys.* 22(2021): 103956.

[74] Sen, D. and Sen, D. 2021. “Use of a Modified SIRD Model to Analyze COVID-19 Data.” *Ind. Eng. Chem. Res.* 60(11): 4251–4260.

[75] González-Parra, G. and Arenas, A.J. 2023. “Mathematical Modeling of SARS-CoV-2 Omicron Wave under Vaccination Effects.” *Computation.* 11(2023): 36.

[76] Youssef, H. Alghamdi, N. Ezzat, M.A. El-Bary, A.A. and Shawky, A.M. 2021. “Study on the SEIQR model and applying the epidemiological rates of COVID-19 epidemic spread in Saudi Arabia.” *Infect. Dis. Model.* 6(2021): 678–692.

[77] Li, M.-T. Sun, G.-Q. Zhang, J. Zhao, Y. Pei, X. Li, L. Wang, Y. Zhang, W.-Y. Zhang, Z.-K. and Jin, Z. 2020. “Analysis of COVID-19 transmission in Shanxi Province with discrete time imported cases.” *Math. Biosci. Eng.* 17(4): 3710–3720.

[78] Yavuz, M. Coşar, F.Ö. Günay, F. and Özdemir, F.N. 2021. “A New Mathematical Modeling of the COVID-19 Pandemic Including the Vaccination Campaign” *Open Journal of Modelling and Simulation.* 9(2021): 299-321.

[79] Khoshnaw, S.H.A. Salih, R.H. and Sulaimany, S. 2020. “Mathematical Modelling for Coronavirus Disease (COVID-19) in Predicting Future Behaviours and Sensitivity Analysis.” *Math. Model. Nat. Phenom.* 15(33): 1-13.

[80] Rajput, A. Sajid, M. Tanvi Shekhar, C. and Aggarwal, R. 2021. “Optimal control strategies on COVID-19 infection to bolster the efcacy of vaccination in India.” *Sci. Rep.* 11(2021): 20124.

[81] Omame,A. Rwezaura, H. Diagne, M.L. Inyama, S.C. and Tchuenche, J.M. 2021. “COVID-19 and dengue co-infection in Brazil: Optimal control and cost-effectiveness analysis.” *Eur. Phys. J. Plus*. 136(2021): 1090.

[82] Khan, A. Zarin, R. Hussain, G. Ahmad, N.A. Mohd, M.H. and Yusuf, A. 2021. “Stability analysis and optimal control of COVID-19 with convex incidence rate in Khyber Pakhtunkhawa (Pakistan).” *Results. Phys.* 20(2021): 103703.

[83] Adepoju, O.A. and Samson Olaniyi, S. 2021. "Stability and optimal control of a disease model with vertical transmission and saturated incidence." *Sci. Afr.* 12(2021): e00800.

[84] Lamwong, J. Pongsumpun, P. Tang, I.M. and Wongvanich, N. 2019. "The Lyapunov Analyses of MERS-Cov Transmission in Thailand." *Curr. Appl. Sci. Technol.* 19(2): 112–123.

[85] DipoAldila, D. Shahzad, M. Khoshnaw, A.H.A. Ali, M. Sultan, F. Islamilova, A. Anwar, Y.R. and Samiadji, B.M. 2022. "Optimal control problem arising from COVID-19 transmission model with rapid-test." *Results Phys.* 37(2022): 105501.

[86] Tchoumi, S.Y. Diagne, M.L. Rwezaurac, H. and Tchuenche, J.M. 2021. "Malaria and COVID-19 co-dynamics: A mathematical model and optimal control." *Appl. Math. Model.* 99(2021): 294–327.

[87] Kim, Y. Lee, S. Chu, C. Choe, S. Hong, S. and Shin, Y. 2016. "The Characteristics of Middle Eastern Respiratory Syndrome Coronavirus Transmission Dynamics in South Korea." *Osong Public Health Res Perspect.* 7(1): 49-55.

[88] Sarkar, K. Khajanchi, S. and Nieto, J. J. 2020. "Modeling and forecasting the COVID-19 pandemic in India." *Chaos Solitons Fractals.* 139(2020): 110049.

[89] Ibrahim, A. Humphries, U.W. Ngiamsunthorn, P.S. Baba, I. Qureshi, S. and Khan, A. 2023. "Modeling the dynamics of COVID-19 with real data from Thailand." *Sci Rep.* 13: 13082.

[90] Haq, I.U. Ullah, N. Ali, N. and Nisar, K.S. 2023. "A New Mathematical Model of COVID-19 with Quarantine and Vaccination." *Mathematics.* 11: 142.

[91] Yang, W. 2021. "Modeling COVID-19 Pandemic with Hierarchical Quarantine and Time Delay." *Dyn. Games. Appl.* 11(4): 892–914.

[92] Lamwong, J. Pongsumpun, P. Tang, I.-M. and N. Wongvanich. 2022. " Vaccination's Role in Combating the Omicron Variant Outbreak in Thailand: An Optimal Control Approach." *Mathematics.* 10(20): 1-29.

[93] World Health Organization. **COVID-19 - WHO Thailand Situation Reports.** [online]. Available:https://www.who.int/thailand/emergencies/novel-coronavirus-2019/situation-reports

[94] Chitnis, N. Hyman, J.M. and Cushing, J.M. 2008. "Determining important parameters in the spread of malaria through the sensitivity analysis of a mathematical model." *Bull. Math. Biol.* 70(2008): 1272–1296.

[95] Bandekara, S.R. and Ghosh, M. 2021. "Mathematical modeling of COVID-19 in India and Nepal with optimal control and sensitivity analysis." *Eur. Phys. J. Plus.* 136(2021): 1058.

[96] Islam, R. Biswas, M.H.A. and Jamali, A.R.M. 2017. "Mathematical analysis of Epidemiological Model of Influenza A (H1N1) Virus Transmission Dynamics in Bangladesh Perspective. GANIT J. Bangladesh." *Math. Soc.* 37(2017): 39–50.

[97] Abioye, A.I. Peter, O.J. Ogunseye, H.A. Oguntolu, F.A. Oshinubi, K. Ibrahim, A.A. and Khan, I. 2021. "Mathematical model of COVID-19 in Nigeria with optimal control." *Results Phys.* 28(2021): 104598.

[98] Adepoju, O.A. and Samson Olaniyi, S. 2021. "Stability and optimal control of a disease model with vertical transmission and saturated incidence." *Sci. Afri.* 12(2021): e00800.

[99] Gatyeni, S.P. Chirove, F. and Nyabadza, F. 2022. "Modelling the Potential Impact of Stigma on the Transmission Dynamics of COVID-19 in South Africa." *Mathematics.* 10(2022): 3253.

[100] Arruda, E.F. Das, S.S. Dias, C.M. and Pastore, D.H. 2021. "Modelling and optimal control of multi strain epidemics, with application to COVID-19." *PLoS ONE.* 16(9): e0257512.

[101] Husniah, H. Ruhanda, R. Supriatna, A.K. and Biswas, M.H.A. 2021. "SEIR Mathematical Model of Convalescent Plasma Transfusion to Reduce COVID-19 Disease Transmission." *Mathematics*. 9(2021): 2857.

[102] World Health Organization. 2022. **COVID-19-WHO Thailand Situation Reports**. [Online]. Available: https://www.who.int/thailand/ emergencies/novel-coronavirus-2019/situation-reports

[103] Bhuju, G. Phaijoo, G.R. and Gurung, D.B. 2020. "Fuzzy Approach Analyzing SEIR-SEI Dengue Dynamics." *Biomed. Res. Int.* 2020(2020): 11.

[104] Lamwong, J. Pongsumpun, P. Tang, I.-M. and Wongvanich, N. 2023. "Optimal Control Strategy of a Mathematical Model for the Fifth Wave of COVID-19 Outbreak (Omicron) in Thailand." *Mathematics*, 12(1), 14.

[105] Alshammari, F.S. 2020. "A Mathematical Model to Investigate the Transmission of COVID19 in the Kingdom of Saudi Arabia." *Comput. Math. Methods Med.* 2020(2020), 1–13.

[106] World Health Organization. **COVID-19—WHO Thailand Situation Reports.** [Online] Available https://www.who.int/thailand/ emergencies/novel-coronavirus-2019/situation-reports

[107] Guo, T. and Li, Y. 2022. "Modeling and optimal control of mutated COVID-19 (Delta strain) with imperfect vaccination." *Chaos Solitons Fractals*. 156(2022): 111825.

[108] Perkins, T.A. and España, G. 2020. "Optimal Control of the COVID-19 Pandemic with Non-pharmaceutical Interventions." *Bull. Math. Biol.* 82(2020): 118.

Appendix

Appendix A

Paper 1

Mathematical Model for the Dynamic of COVID-19 Spread and Impacts of Vaccination, Quarantine, and Hospitalization among the 5th Wave of COVID-19 in Thailand

Proceedings of the
28th Annual Meeting in Mathematics (AMM 2024)
Department of Mathematics Statistics and Computer,
Faculty of Science, Ubon Ratchathani University,
Thailand

Mathematical Model for the Dynamic of COVID-19 Spread and Impacts of Vaccination, Quarantine, and Hospitalization among the 5th Wave of COVID-19 in Thailand

Jiraporn Lamwong[1] and Puntani Pongsumpun[2,‡]

[1]Department of Mathematics, School of Science, King Mongkut's Institute of Technology Ladkrabang, Bangkok 10520, Thailand

[2]Department of Mathematics, School of Science, King Mongkut's Institute of Technology Ladkrabang, Bangkok 10520, Thailand

Abstract

The novel Coronavirus or COVID-19 pandemic is a massive outbreak that has affected almost every country in the world. Many methods have been sought to stop its spreading. A mathematical model is an effective instrument that helps analyze the pandemic situation. In this research, a new model of transmission in Thailand consisting of vaccination, quarantine, and hospitalization is presented, aiming at seeking factors affecting the pandemic and guidelines for reducing the spread of this disease. Equilibrium points and basic reproduction numbers were analyzed and stability was tested. Model fitting was performed to obtain parameter values suitable for the pandemic. Besides, numerical results revealed that infection rates and the efficiency of vaccines played a significant role in reducing the number of patients and controlling the pandemic situation.

Keywords: COVID-19, standard dynamical modeling, model fitting, sensitivity analysis, globally.

2020 MSC: 92-10; 93D20.

1 Introduction

Recently, the world faced the fifth wave of the spread of severe acute respiratory syndrome Coronavirus (SARS-COV-2), widely known as COVID-19 [1]. It was indicated as the most infectious wave since the pandemic was reported. It had a huge effect on those

*This research was financially supported by School of Science, King Mongkut's Institute of Technology Ladkrabang, grant number RA/TA-2565-D-001.

‡ Corresponding author. Puntani Pongsumpun
E-mail address: 65056018@kmitl.ac.th (J. Lamwong), puntani.po@kmitl.ac.th (P. Pongsumpun)

having underlying diseases since the pandemic occurred rapidly. The infection can be transmitted by small respiratory droplets, such as sneezing or coughing or exposure to secretions on surfaces [2]. Therefore, social distancing and wearing surgical masks are one of the various methods that can help prevent the spread of the disease. After getting the infection, the incubation period for the coronavirus is between 2 and 14 days [3-4]. Next, if the human body loses immunity, symptoms among infected people range from muscle pain, body aches, sore throat, dry throat, and high fever to severe symptoms that can destroy the respiratory system [3, 5].

According to the global situation report on 2 November 2023, there were 771,679,618 confirmed cases and 6,977,023 deaths. On 23 October 2023, a total of 13,534,457,273 vaccine doses were reported. As for the situation in Thailand, there were 4,758,125 confirmed cases and 34,487 deaths and on 31 August 2023, a total of 139,343,323 vaccine doses were reported [6]. Based on the current situation, prevention by vaccination is a strategy that the government is focusing on helping to control the disease spread [2,7-8]. Many companies develop their vaccines to be efficient to meet people's needs promptly. Vaccines that are accepted and widely used by the Thai government and private sector are AstraZeneca which is suitable for people aged 18 years and above with 2 doses of the vaccine, 10-12 weeks apart, CoronaVac or Sinovac COVID-19 vaccine is an inactivated vaccine suitable for people aged $18-59$ years with 2 doses, 2-4 weeks apart, Pfizer is a messenger RNA (mRNA) vaccine suitable for those aged 16 years and above with doses, 21-28 days or 3-4 weeks apart, and other vaccines [9-10]. Preventing vaccination is one of the strategies. Many other strategies will help control the situation like social distancing, wearing surgical masks, and quarantine to help reduce the spread of the virus.

Mathematical modeling plays a vital role in assessing the situation, control efficiency, and preparedness to cope with a future outbreak [11-12]. A lot of researchers are interested in developing a model to keep pace with the current situation. Yang [13] proposed an epidemic model by considering the quarantine population in the pre-incubation phase including the home isolation and hospital isolation. It was found that early isolation could help to control the spread of disease effectively. Ibrahim et al. [14] designed SVEI$_a$I$_m$R model to keep up-to-date with the situation by considering vaccination factors, asymptomatic infection, symptomatic infection, and Omicron infection to finely isolate people. The study revealed that vaccination alone was not enough to fight against the spread of COVID-19. There should be other measures to help stop the spread of co-infection. Lamwong et al. [15] designed a standard dynamic model by considering vaccinated people, asymptomatic people, symptomatic people, and hospitalized people and determining the most suitable strategy to control the spread of the disease. Strategies used for the control were vaccination measures and people who received immunity from vaccination. It was found that disease control could be implemented by setting other measures to help control the situation, such as wearing face masks and social distancing, making the disease control more effective.

In this article, importance is given to vaccination, quarantine, and hospitalization. Topics are arranged as follows: Part 2 designs and describes the dynamic of the disease in the model. Equilibrium points and basic reproduction number are found and the stability of DEF and EE is tested. Part 3 presents a numerical model by analyzing actual data of the spread in Thailand in conjunction with the model. Meanwhile, the sensitivity index is analyzed to

examine input parameters affecting basic reproduction number. The final part prepares the conclusion as shown in Part 4.

2 Materials and Methods

2.1 Model Formulation

Mathematical modeling is a method that helps analyze the spread situation, designing control measures and finding strategies to help prevent the spread of COVID-19. In this research, the model was designed by dividing people into 7 groups, i.e. susceptible group (S), vaccinated group (V), exposed group (E), infected group (I), quarantine group (Q), hospitalized group (H), and recovered group (R). The basis is from the SEIQR model and importance is given to vaccinated people, quarantine people, and hospitalized people as shown in Figure 1.

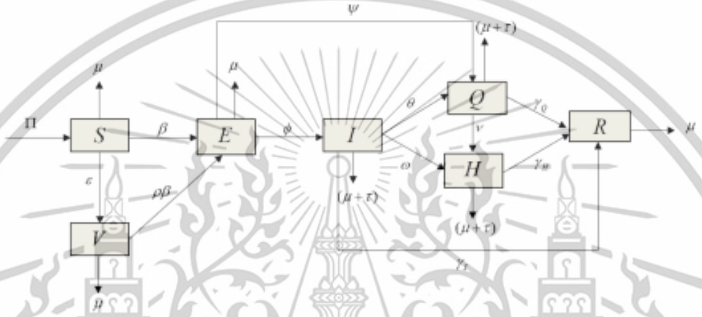

Figure 1. Diagram showing the relationship of the 5th wave of COVID-19 spread

Table 1. Definitions of variables and parameters

Variables/Parameters	Description	Units
S	The number of susceptible group	Person
V	The number of vaccinated group	Person
E	The number of exposed group	Person
I	The number of infected group	Person
Q	The number of quarantine group	Person
H	The number of hospitalized group	Person
R	The number of recovered group	Person
Π	Initial population.	day^{-1}
β	Infection rate.	Per person · $days^{-1}$
ε	Vaccination rate.	day^{-1}
ρ	Vaccination prevention efficacy.	N/A
ϕ	Incubation rate.	$days^{-1}$
ψ	Transition rate from incubation group to quarantine group.	$days^{-1}$

θ	Transition rate from infected group to quarantine group.	days^{-1}
ω	Transition rate from infected group to hospitalized group.	days^{-1}
ν	Transition rate from quarantine group to hospitalized group.	days^{-1}
γ_I	Recovery rate from infected group.	days^{-1}
γ_Q	Recovery rate from quarantine group.	days^{-1}
γ_H	Recovery rate from hospitalized group.	days^{-1}
μ	Natural mortality rate.	days^{-1}
τ	Mortality rate from COVID-19.	days^{-1}

From Figure 1, the relationship of the spread can be described as follow: The initial population Π is at risk of getting infected with COVID-19 from the group of susceptible population and the group of vaccinated population at a rate of β and $\rho\beta$ respectively. When the population is infected, the virus incubates in the body at a rate of ϕ. Some people get vaccinated to prevent the spread of disease at a rate of ε. When getting vaccinated, some individuals improve their immunity while some people have low immunity and they can get infected. Once they get infected with COVID-19, they are required to stay in quarantine at a rate of θ as their symptoms are not much severe. However, during staying in quarantine, they express severe symptoms, they need to be transferred to a hospital at a rate of ω . During the infection period, infected group, quarantine group, and hospitalized group, patients may die from the disease at a rate of τ. After they completely undergo treatments, they enter into recovered group at a rate of γ_I, γ_Q and γ_H respectively. The differential equation can be written in the following form.

$$\begin{cases} S'(t) = \Pi - \beta S(t)I(t) - (\varepsilon + \mu)S(t), \\ V'(t) = \varepsilon S(t) - \rho\beta V(t)I(t) - \mu V(t), \\ E'(t) = \beta S(t)I(t) + \rho\beta V(t)I(t) - (\phi + \psi + \mu)E(t), \\ I'(t) = \phi E(t) - (\theta + \omega + \gamma_I + \mu + \tau)I(t), \\ Q'(t) = \theta I(t) + \psi E(t) - (\nu + \gamma_Q + \mu + \tau)Q(t), \\ H'(t) = \omega I(t) + \nu Q(t) - (\gamma_H + \mu + \tau)H(t), \\ R'(t) = \gamma_I I(t) + \gamma_Q Q(t) + \gamma_H H(t) - \mu R(t). \end{cases} \tag{2.1}$$

Where $$N(t) = S(t) + V(t) + E(t) + I(t) + Q(t) + H(t) + R(t). \tag{2.2}$$

With initial conditions as follow:

$$S(0) > 0, V(0) > 0, E(0) > 0, I(0) > 0, Q(0) > 0, H(0) > 0, R(0) > 0. \tag{2.3}$$

Since the initial conditions are all positive (2.3), all time t > 0, the biologically feasible region will be considered:

$$\Omega = \left\{ (S, V, E, I, Q, H, R) \in \mathbb{R}^7_+ : N \le \frac{\Pi}{\mu} \right\}. \tag{2.4}$$

2.2 Stability Analysis

In this subpart, standard dynamical modeling is performed to analyze an equilibrium point, basic reproduction number and stability of the model, which can be seen as follows.

2.2.1 Equilibrium Point and Basic Reproduction Number

To find the equilibrium point of the system, simply set all the ordinary differential equations in the system (2.1) equal to zero as follows: $S'(t)=0, V'(t)=0, E'(t)=0, I'(t)=0, Q'(t)=0, H'(t)=0, R'(t)=0$. Two equilibrium points are obtained, i.e. disease-free equilibrium point

$$K_0^* = (S_0^*, V_0^*, E_0^*, I_0^*, Q_0^*, H_0^*, R_0^*) = \left(\frac{\Pi}{\varepsilon+\mu}, \frac{\varepsilon\Pi}{\mu(\varepsilon+\mu)}, 0,0,0,0,0 \right) \tag{2.5}$$

where $R_0 < 1$

and the endemic equilibrium point $K_1^* = (S_1^*, V_1^*, E_1^*, I_1^*, Q_1^*, H_1^*, R_1^*)$, (2.6)

where $S_1^* = \frac{\Pi}{\beta I_1^* + \varepsilon + \mu}$, $V_1^* = \frac{\varepsilon\Pi}{(\beta I_1^* + \varepsilon + \mu)(\rho\beta I_1^* + \mu)}$, $E_1^* = \frac{\Pi\beta I_1^*(\mu + (\beta I_1^* + \varepsilon)\rho)}{(\beta I_1^* + \varepsilon + \mu)(\rho\beta I_1^* + \mu)(\phi + \psi + \mu)}$,

$I_1^* = \frac{\phi E_1^*}{\theta + \omega + \gamma_I + \mu + \tau}$, $Q_1^* = \frac{\theta I_1^* + \psi E_1^*}{\nu + \gamma_Q + \mu + \tau}$, $H_1^* = \frac{\nu Q_1^* + \omega I_1^*}{\gamma_H + \mu + \tau}$, $R_1^* = \frac{\gamma_I I_1^* + \gamma_Q Q_1^* + \gamma_H H_1^*}{\mu}$,

where $R_0 > 1$.

Where R_0 is basic reproduction number. Basic reproduction number is calculated by using next-generation method. In this study $E(t), I(t), Q(t)$ and $H(t)$ expressions are taken into consideration for calculating basic reproduction number from next-generation method [16-17]. The non-linear differential equation is arranged in the following form: $\frac{dx}{dt} = F(x) - V(x)$, where $F(x)$ is the matrix of new infection and $V(x)$ is the matrix of transfer as follows:

$$F = \begin{bmatrix} \beta SI + \rho\beta VI \\ 0 \\ 0 \\ 0 \end{bmatrix}, \quad V = \begin{bmatrix} (\phi+\psi+\mu)E \\ -\phi E + (\theta+\omega+\gamma_I+\mu+\tau)I \\ -\theta I - \psi E + (\nu+\gamma_Q+\mu+\tau)Q \\ -\omega I - \nu Q + (\gamma_H+\mu+\tau)H \end{bmatrix}.$$

Thus, the Jacobian matrix can be obtained at the disease-free equilibrium point (2.5) as follow:

$$F = \begin{bmatrix} 0 & \beta S + \rho\beta V & 0 & 0 \\ 0 & 0 & 0 & 0 \\ 0 & 0 & 0 & 0 \\ 0 & 0 & 0 & 0 \end{bmatrix}, V = \begin{bmatrix} (\phi+\psi+\mu) & 0 & 0 & 0 \\ -\phi & (\theta+\omega+\gamma_I+\mu+\tau) & 0 & 0 \\ -\psi & -\theta & (\nu+\gamma_Q+\mu+\tau) & 0 \\ 0 & -\omega & -\nu & (\gamma_H+\mu+\tau) \end{bmatrix}.$$

The basic reproduction number (R_0) can be calculated from the spectral radius of $\rho(FV^{-1})$ by considering eigenvalues which can be obtained from the following:

$$R_0 = \rho(FV^{-1}) = \frac{\Pi\beta\phi(\mu+\varepsilon\rho)}{\mu(\varepsilon+\mu)(\phi+\psi+\mu)(\theta+\omega+\gamma_I+\mu+\tau)}. \tag{2.7}$$

2.2.2 Global Stability Analysis

Theorem 2.1. If $R_0 < 1$ and

$$\beta = \frac{\mu+\tau}{(S_0^* + \rho V)}, \tag{2.8}$$

then the disease-free equilibrium point K_0^* is globally asymptotically stable in its feasible region.

Proof. To reveal the result, Lyapunov function is considered as follows:

$$X(t) = (S - S_0^* - S_0^* \ln \frac{S}{S_0^*}) + E + I + Q + H + R.$$

The derivative of $X(t)$ will be:

$$\begin{aligned} X'(t) &= S'\left(1-\frac{S_0^*}{S}\right) + E' + I' + Q' + H' + R' \\ &= (\Pi - \beta SI - (\varepsilon+\mu)S)\left(1-\frac{S_0^*}{S}\right) + (\beta SI + \rho\beta VI - (\phi+\psi+\mu)E) + (\phi E - (\theta+\omega+\gamma_I+\mu+\tau)I) \\ &\quad + (\theta I + \psi E - (\nu+\gamma_Q+\mu+\tau)Q) + (\omega I + \nu Q - (\gamma_H+\mu+\tau)H) + (\gamma_I I + \gamma_Q Q + \gamma_H H - \mu R) \\ &= \Pi\left(1-\frac{S_0^*}{S}\right) - (\varepsilon+\mu)S\left(1-\frac{S_0^*}{S}\right) + \beta S_0^* I + \rho\beta VI - \mu E - (\mu+\tau)I - (\mu+\tau)Q - (\mu+\tau)H - \mu R \\ &= \Pi\left(1-\frac{S_0^*}{S}\right) + (\varepsilon+\mu)S_0^*\left(1-\frac{S}{S_0^*}\right) + \left(\beta(S_0^* + \rho V) - (\mu+\tau)\right)I - \mu E - (\mu+\tau)Q - (\mu+\tau)H - \mu R. \end{aligned}$$

From the hypothesis (2.8), the following equation is obtained.

$$X'(t) = \Pi\left(1-\frac{S_0^*}{S}\right) + (\varepsilon+\mu)S_0^*\left(1-\frac{S}{S_0^*}\right) - \mu E + (\mu+\tau)Q - (\mu+\tau)H - \mu R.$$

Replace the equilibrium point $K_0^* = (S_0^*, V_0^*, E_0^*, I_0^*, Q_0^*, H_0^*, R_0^*) = \left(\frac{\Pi}{\varepsilon+\mu}, \frac{\varepsilon\Pi}{\mu(\varepsilon+\mu)}, 0, 0, 0, 0, 0\right)$, shall be obtained.

$$\begin{aligned} X'(t) &= \Pi\left(1-\frac{S_0^*}{S}\right) + \Pi\left(1-\frac{S}{S_0^*}\right) - \mu E - (\mu+\tau)Q - (\mu+\tau)H - \mu R \\ &= \Pi\left(2 - \frac{S_0^*}{S} - \frac{S}{S_0^*}\right) - \mu E - (\mu+\tau)Q - (\mu+\tau)H - \mu R \\ X'(t) &= -\left[\Pi\left(\frac{(S_0^* - S)^2}{S_0^* S}\right) + \mu E + (\mu+\tau)Q + (\mu+\tau)H + \mu R\right] \le 0 \end{aligned} \qquad (2.9)$$

Since all parameters have positive value, $X'(t) \le 0$. $X'(t) = 0$, if $S_0^* = S$, $E = 0, Q = 0, H = 0$ and $R = 0$. Therefore, it is compliant with the LaSalle's Invariance Principle. It means that the model (2.1) is globally asymptotically stable in Ω. □

Theorem 2.2. If $R_0 > 1$, then the endemic equilibrium point K_1^* is globally asymptotically stable in its feasible region.

Proof. Lyapunov function is determined as follow [14].

$$\begin{aligned} Y(t) &= (S - S_1^* - S_1^* \ln \frac{S}{S_1^*}) + (V - V_1^* - V_1^* \ln \frac{V}{V_1^*}) + (E - E_1^* - E_1^* \ln \frac{E}{E_1^*}) + (I - I_1^* - I_1^* \ln \frac{I}{I_1^*}) \\ &\quad + (Q - Q_1^* - Q_1^* \ln \frac{Q}{Q_1^*}) + (H - H_1^* - H_1^* \ln \frac{H}{H_1^*}) + (R - R_1^* - R_1^* \ln \frac{R}{R_1^*}). \end{aligned}$$

The derivative of Lyapunov function is considered, is obtained.

$$Y'(t) = S'\left(1-\frac{S_1^*}{S}\right) + V'\left(1-\frac{V_1^*}{V}\right) + E'\left(1-\frac{E_1^*}{E}\right) + I'\left(1-\frac{I_1^*}{I}\right) + Q'\left(1-\frac{Q_1^*}{Q}\right) + H'\left(1-\frac{H_1^*}{H}\right) + R'\left(1-\frac{R_1^*}{R}\right).$$

The derivative from the system (2.1) is replaced,

$$Y'(t)=\{\Pi-\beta SI-(\varepsilon+\mu)S\}\left(1-\frac{S_1^*}{S}\right)+\{\varepsilon S-\rho\beta VI-\mu V\}\left(1-\frac{V_1^*}{V}\right)+\{\beta SI+\rho\beta VI-(\phi+\psi+\mu)E\}\left(1-\frac{E_1^*}{E}\right)$$
$$+\{\phi E-(\theta+\omega+\gamma_I+\mu+\tau)I\}\left(1-\frac{I_1^*}{I}\right)+\{\theta I+\psi E-(\nu+\gamma_Q+\mu+\tau)Q\}\left(1-\frac{Q_1^*}{Q}\right)$$
$$+\{\omega I+\nu Q-(\gamma_H+\mu+\tau)H\}\left(1-\frac{H_1^*}{H}\right)+\{\gamma_I I+\gamma_Q Q+\gamma_H H-\mu R\}\left(1-\frac{R_1^*}{R}\right).$$

Putting $S=S-S_1^*, V=V-V_1^*, E=E-E_1^*, I=I-I_1^*, Q=Q-Q_1^*, H=H-H_1^*$ and $R=R-R_1^*$ is obtained.

$$Y'(t)=\left\{\Pi-\beta I\left(S-S_1^*\right)-(\varepsilon+\mu)\left(S-S_1^*\right)\right\}\left(\frac{S-S_1^*}{S}\right)+\left\{\varepsilon S-\rho\beta I\left(V-V_1^*\right)-\mu\left(V-V_1^*\right)\right\}\left(\frac{V-V_1^*}{V}\right)$$
$$+\left\{\beta SI+\rho\beta VI-(\phi+\psi+\mu)\left(E-E_1^*\right)\right\}\left(\frac{E-E_1^*}{E}\right)+\left\{\phi E-(\theta+\omega+\gamma_I+\mu+\tau)\left(I-I_1^*\right)\right\}\left(\frac{I-I_1^*}{I}\right)$$
$$+\left\{\theta I+\psi E-(\nu+\gamma_Q+\mu+\tau)\left(Q-Q^*\right)\right\}\left(\frac{Q-Q_1^*}{Q}\right)+\left\{\omega I+\nu Q-(\gamma_H+\mu+\tau)\left(H-H_1^*\right)\right\}\left(\frac{H-H_1^*}{H}\right)$$
$$+\left\{\gamma_I I+\gamma_Q Q+\gamma_H H-\mu\left(R-R_1^*\right)\right\}\left(\frac{R-R_1^*}{R}\right)$$
$$=\Pi-\Pi\left(\frac{S_1^*}{S}\right)-\beta I\frac{\left(S-S_1^*\right)^2}{S}-(\varepsilon+\mu)\frac{\left(S-S_1^*\right)^2}{S}+\varepsilon S-\varepsilon S\left(\frac{V_1^*}{V}\right)-\rho\beta I\frac{\left(V-V_1^*\right)^2}{V}-\mu\frac{\left(V-V_1^*\right)^2}{V}$$
$$+\beta SI-\beta SI\left(\frac{E_1^*}{E}\right)+\rho\beta VI-\rho\beta VI\left(\frac{E_1^*}{E}\right)-(\phi+\psi+\mu)\frac{\left(E-E_1^*\right)^2}{E}+\phi E-\phi EI_1^*-(\theta+\omega+\gamma_I+\mu+\tau)\frac{\left(I-I_1^*\right)^2}{I}$$
$$+\theta I-\theta I\left(\frac{Q_1^*}{Q}\right)+\psi E-\psi E\left(\frac{Q_1^*}{Q}\right)-(\nu+\gamma_Q+\mu+\tau)\frac{\left(Q-Q_1^*\right)^2}{Q}+\omega I-\omega I\left(\frac{H_1^*}{H}\right)+\nu Q-\nu Q\left(\frac{H_1^*}{H}\right)$$
$$-(\gamma_H+\mu+\tau)\frac{\left(H-H_1^*\right)^2}{H}+\gamma_I I-\gamma_I I\left(\frac{R_1^*}{R}\right)+\gamma_Q Q-\gamma_Q Q\left(\frac{R_1^*}{R}\right)+\gamma_Q Q-\gamma_Q Q\left(\frac{R_1^*}{R}\right)-\mu\frac{\left(R-R_1^*\right)^2}{R}.$$

A new equation is arranged as

$$Y'(t)=A-B$$

where

$$A=\Pi+\varepsilon S+\beta SI+\rho\beta VI+\phi E+\theta I+\psi E+\omega I+\nu Q+\gamma_I I+\gamma_Q Q+\gamma_Q Q,$$
$$B=\Pi\left(\frac{S_1^*}{S}\right)+\beta I\frac{\left(S-S_1^*\right)^2}{S}+(\varepsilon+\mu)\frac{\left(S-S_1^*\right)^2}{S}+\varepsilon S\left(\frac{V_1^*}{V}\right)+\rho\beta I\frac{\left(V-V_1^*\right)^2}{V}+\mu\frac{\left(V-V_1^*\right)^2}{V}$$
$$+\beta SI\left(\frac{E_1^*}{E}\right)+\rho\beta VI\left(\frac{E_1^*}{E}\right)+(\phi+\psi+\mu)\frac{\left(E-E_1^*\right)^2}{E}+\phi E\left(\frac{I_1^*}{I}\right)+(\theta+\omega+\gamma_I+\mu+\tau)\frac{\left(I-I_1^*\right)^2}{I}$$
$$+\theta I\left(\frac{Q_1^*}{Q}\right)+\psi E\left(\frac{Q_1^*}{Q}\right)+(\nu+\gamma_Q+\mu+\tau)\frac{\left(Q-Q_1^*\right)^2}{Q}+\omega I\left(\frac{H_1^*}{H}\right)+\nu Q\left(\frac{H_1^*}{H}\right)+(\gamma_H+\mu+\tau)\frac{\left(H-H_1^*\right)^2}{H}$$
$$+\gamma_I I\left(\frac{R_1^*}{R}\right)+\gamma_Q Q\left(\frac{R_1^*}{R}\right)+\gamma_Q Q\left(\frac{R_1^*}{R}\right)+\mu\frac{\left(R-R_1^*\right)^2}{R}.$$

It can be seen that, $Y'(t)<0$, when $A<B$ for $R_0>1$ and $Y'(t)=0$ when $S=S_1^*, V=V_1^*, E=E_1^*, I=I_1^*, Q=Q_1^*, H=H_1^*$ and $R=R_1^*$. Since all parameters have positive values, it is compliant with LaSalle's invariance principle. The endemic equilibrium point K_1^* is global asymptotically stable in its feasible region, if $A<B$. □

3 Numerical Results

3.1 Model Fitting

In this part, the fitting of the parameters of the model (2.1) is performed. As some parameters are difficult to predict. We obtain parameters that are precise and suitable for the model, fmincon algorithm in MATLAB is employed to analyze parameters suitable for the actual data of the disease spread in Thailand. The parameters performed fitting are shown in Table 2. The remaining parameters are obtained from the observation of disease behavior and demographic factors connected to the disease. In this study, the data analyzed referred to the actual data of the disease spread in Thailand, in which daily infection data from 11 January 2022 to 1 May 2022 were considered (since the spread of Omicron was reported), concerning the data collection of Ministry of Public Health [18]. The black circle displays the data on daily infection in Thailand while the opaque line displays the numerical analysis of the model (2.1) with $R^2 = 0.9544$ as seen in Figure 2.

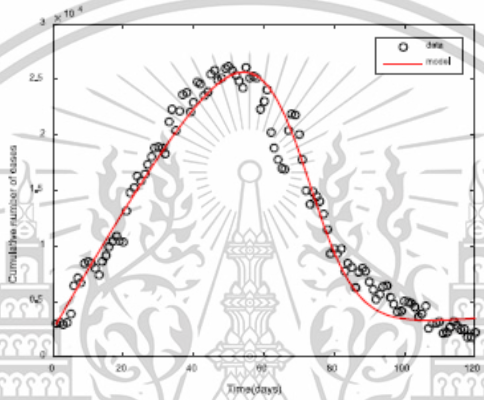

Figure 2. Fitting model with the data of daily infection in Thailand

3.2 Numerical Analysis Result

In this subpart, numerical simulation of the model (2.1) was presented by considering the stability of the endemic equilibrium point. The parameters used in this simulation are shown in Table 2. In the simulation, initial population values were determined as follow: $S(0) = 1000, V(0) = 1000, E(0) = 100, I(0) = 100, Q(0) = 1053, H(0) = 1002$ and $R(0) = 13456000$ show the stability of the endemic equilibrium point. It can be seen that the time is passed, the results were convergent to the equilibrium point at K_1^*. Figure 4 – Figure 5 show numerical results in 2D and 3D trajectories. In the simulation, $\beta = 0.00000009$ was used to display the trajectory of convergence to the equilibrium more clearly. A comparison between infection rate (β) and vaccination prevention efficacy (ρ) was made and presented in Figure 6 – Figure 7. From Figure 6, when the infection rate reduced from $\beta = 0.0000009, 0.0000008, 0.0000007, 0.0000006, 0.0000005$, it can be clearly seen that the population number increased, indicating that a high infection rate results in a faster control period than a lower infection rate. Figure 7 shows an increase in the vaccination prevention

efficacy. From $\rho = 0.4, 0.5, 0.6, 0.7, 0.8$, it can be noticeable that when the vaccine efficacy is higher, the control of disease spread is better. It is evident that vaccination strategy is a method to control the spread of COVID-19 in an efficient manner.

Table 2. Shows the parameters used in the numerical analysis

Parameters	Description	Value	Source
Π	Initial population.	560	Fitted
β	Infection rate.	0.000009	Fitted
ε	Vaccination rate.	0.4	Fitted
ρ	Vaccination prevention efficacy.	0.5	Fitted
ϕ	Incubation rate.	1/6	Fitted
ψ	Transition rate from incubation group to quarantine group.	0.08	Fitted
θ	Transition rate from infected group to quarantine group.	0.02	Fitted
ω	Transition rate from infected group to hospitalized group.	0.005	[19]
ν	Transition rate from quarantine group to hospitalized group.	0.03	Fitted
γ_I	Recovery rate from infected group.	0.001	[13]
γ_Q	Recovery rate from quarantine group.	0.03	[13]
γ_H	Recovery rate from hospitalized group.	1/14	[19]
μ	Natural mortality rate.	0.000036529	[14]
τ	Mortality rate from COVID-19.	0.00286	[15]

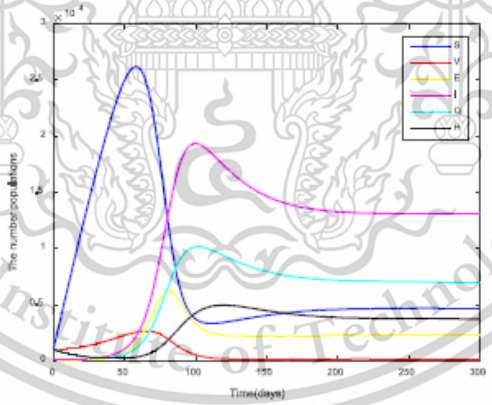

Figure 3. Graph showing the numerical results of the model (2.1) for $R_0 > 1$ and the parameters used in this simulation are shown in Table 2

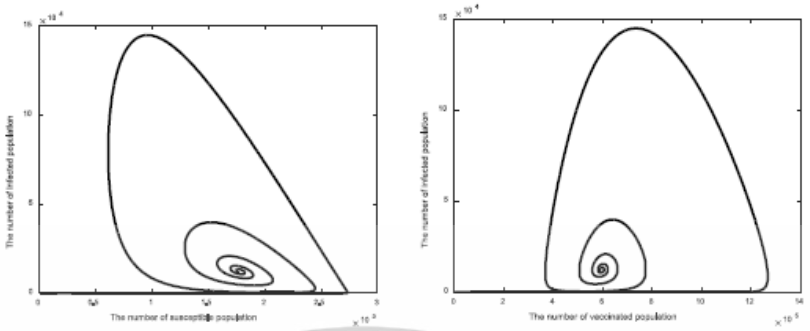

Figure 4. Graph showing 2D trajectory of the results (2.1) on the plane (S_1^*, I_1^*) and (V_1^*, I_1^*) for $R_0 > 1$ and the parameters used in this simulation are shown in Table 2

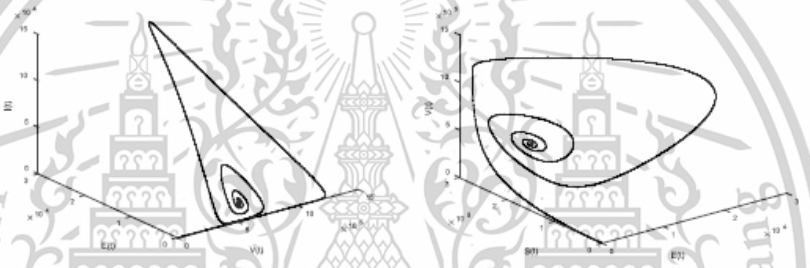

Figure 5. Graph showing 3D trajectory of the results (2.1) on the plane for $R_0 > 1$ and the parameters used in this simulation are shown in Table 2

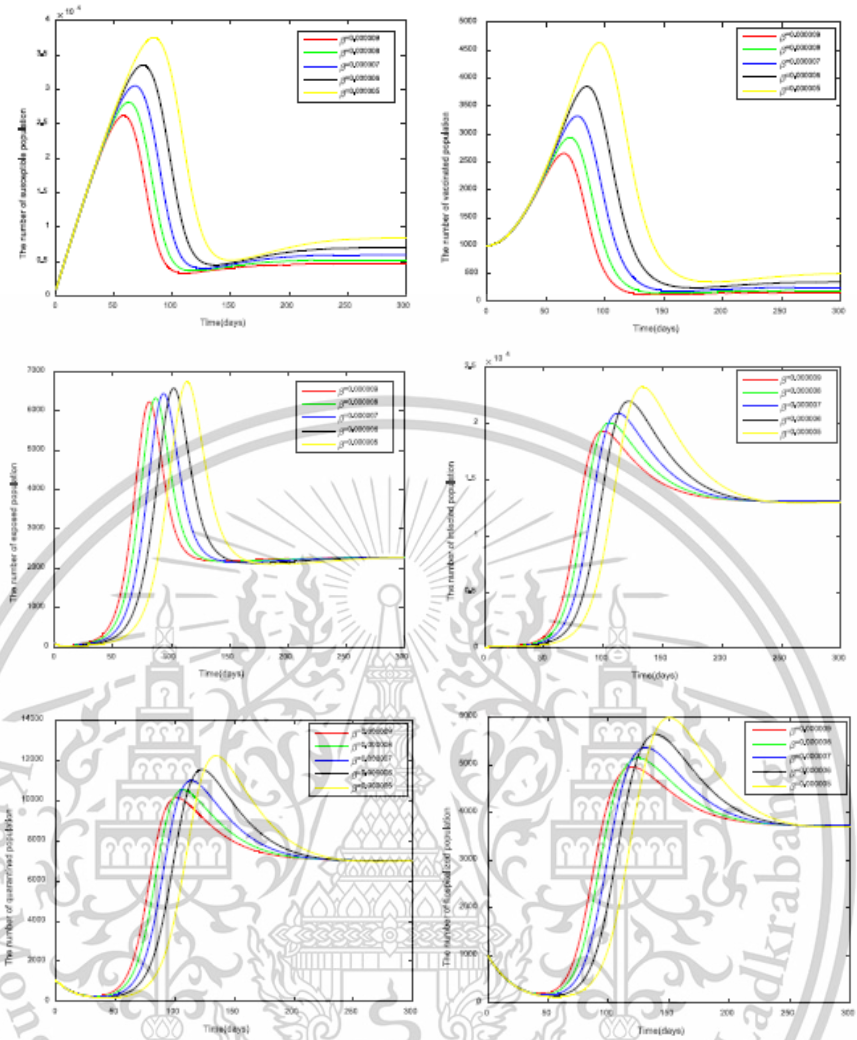

Figure 6. Graph showing the numerical results of the model (2.1) by comparing the infection rate (β) for $R_0 > 1$ and the parameters used in this simulation are shown in Table 2

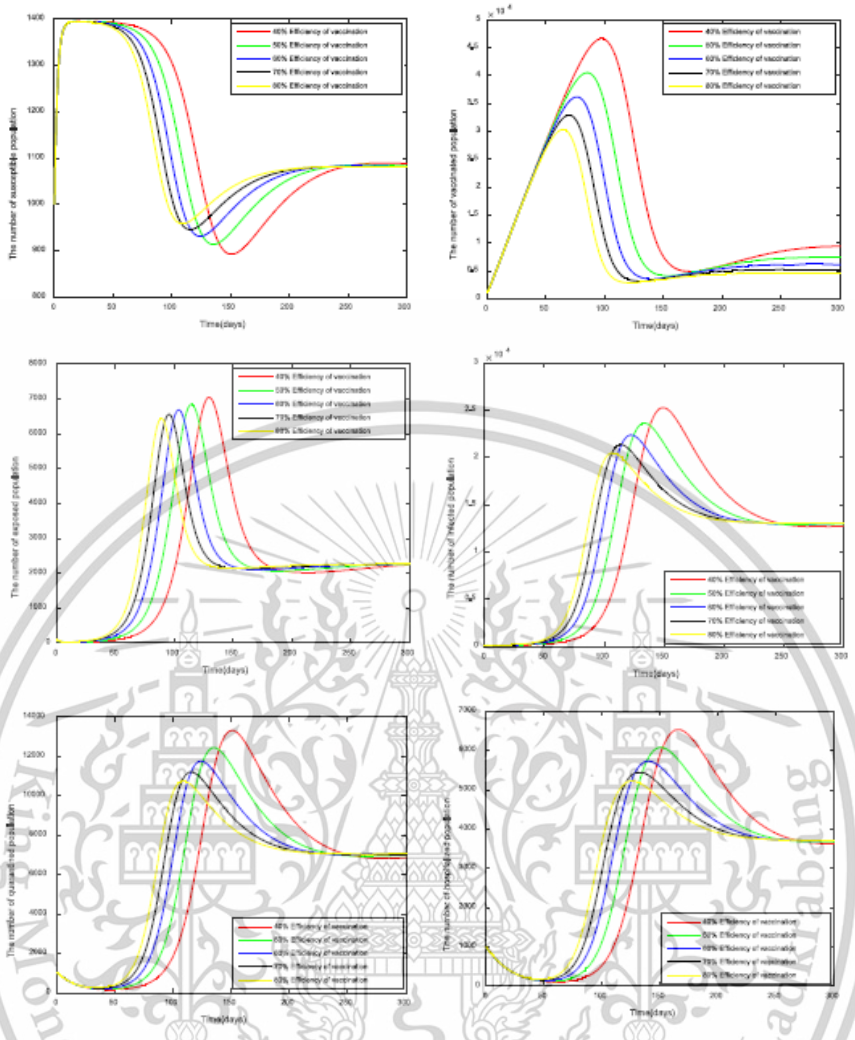

Figure 7. Graph showing the numerical results of the model (2.1) by comparing the vaccination prevention efficacy (ρ) for $R_0 > 1$ and the parameters used in this simulation are shown in Table 2

3.3 Sensitivity Analysis

In this subpart, sensitivity analysis of the basic reproduction number (R_0) was performed since the basic reproduction number indicates the status of the disease spread. Sensitivity analysis was performed to verify parameters significantly affecting the disease spread. The normalized forward sensitivity index can be calculated as follows:

$$\Upsilon_{\sigma}^{R_0} = \frac{\partial R_0}{\partial \sigma} \times \frac{\sigma}{R_0}. \quad (3.1)$$

Where σ are parameters of the disease spread and R_0 is the basic reproduction number. The parameters used in the sensitivity index are shown in Table 2 and the analysis results are shown in Table 3.

Table 3. Basic reproduction number sensitivity index

Parameters	Sensitivity
Π	1.000000
β	1.00000
ε	-0.017304
ρ	0.964758
ϕ	0.827651
ψ	-0.827274
θ	-0.692125
ω	-0.173031
γ_i	-0.034606
μ	-0.984337
τ	-0.098973

From Table 3, the sensitivity index results showed that the parameters that most likely affected the disease spread were initial population (Π) and infection rate (β), which can be described as follow: The initial population and infection rate is equal to 1, meaning that an increase or decrease of the initial population and the infection rate of 10% shall result in an increase or decrease of the basic reproduction number by 10%. Consequently, to achieve efficient disease control, it is necessary to have tight control, avoid meeting people at risk of getting infected, maintain social distancing, and wear a face mask to reduce the infection rate.

4 Conclusions

In conclusion, to describe the dynamic of COVID-19 spread, a new model for the Omicron variant in Thailand was introduced. The model gives importance to the vaccinated population, quarantine population, and hospitalized population. Equilibrium points, basic reproduction number, and model stability were analyzed. The findings from the study revealed that at the disease-free equilibrium point, the model was stable when $R_0 < 1$ and at the endemic equilibrium point, the model was stable when $R_0 > 1$. According to the numerical result analysis, we describe the dynamic of the disease spread and to ensure the results obtained are close to actual data of the spread in Thailand. Model fitting was performed to obtain parameter values suitable for the model and the disease spread in Thailand. Meanwhile, the basic reproduction number sensitivity index was analyzed. The basic reproduction number was defined in the form of R_0 and it was given by

$$R_0 = \frac{\Pi\beta\phi(\mu + \varepsilon\rho)}{\mu(\varepsilon + \mu)(\phi + \psi + \mu)(\theta + \omega + \gamma_i + \mu + \tau)}.$$

According to the basic reproductive number analysis of the parameters, the top 3 positive parameters that affected the basic reproduction number are the initial population (Π), infection rate (β) and vaccination prevention efficacy (ρ), respectively and the top 3 negative parameters that affected the basic reproduction number are natural mortality rate (μ), transition rate from incubation group to quarantine group (ψ) and transition rate from infected group to quarantine group (θ), respectively. The analysis of parameters affecting the basic reproduction number indicated that an increase in infection rate results in faster control of the disease spread and an increase in vaccination efficacy results in significant reduction of the infection. It can be noticeable that prevention of the disease by vaccination is a strategy that helps control the disease spread. However, a combination of measures can be imposed for the prevention and reduction of COVID-19 to reduce uncertainty about the spread of this disease in the future.

Acknowledgment. Jiraporn Lamwong is the recipient of the Graduate Study Fellowship of the School of Science, King Mongkut's Institute of Technology Ladkrabang, Thailand. This research was funded by the RA-TA graduate scholarship from the School of Science, King Mongkut's Institute of Technology Ladkrabang, grant number RA/TA-2565-D-001.

References

[1] J. Tian, J. Wu, Y. Bao, X. Weng, L. Shi, B. Liu, X. Yu, L. Qi and Z. Liu, *Modeling analysis of COVID-19 based on morbidity data in Anhui, China*, Math. Biosci. Eng. **17**(4) (2020), 2842–2852.

[2] T. Theparod, P. Kreabkhontho and W. Teparos, *Booster Dose Vaccination and Dynamics of COVID-19 Pandemic in the Fifth Wave: An Efficient and Simple Mathematical Model for Disease Progression*, Vaccines. **11**(3) (2023), 1-17.

[3] Z. S. Kifle and L.L Obsu, *Mathematical modeling for COVID-19 transmission dynamics: A case study in Ethiopia*, Results Phys. **34**(1) (2022), 1-13.

[4] N.I. Akinwande, T. T. Ashezua, R. I. Gweryina, S. A. Somma, F. A. Oguntolu, A. Usman, O. N. Abdurrahman, F. S. Kaduna, T.P. Adajime, F.A. Kuta, S. Abdulrahman, R. O. Olayiwola, A. I. Enagi, G. A. Bolarin and M. D. Shehu, *Mathematical model of COVID-19 transmission dynamics incorporating booster vaccine program and environmental contamination*, Heliyon. **8**(8) (2022), 1-14.

[5] P. Kumari, S. Singh and H. P. Singh, *Dynamical Analysis of COVID-19 Model Incorporating Environmental Factors*, Iran J. Sci. Technol. Trans. Sci. **46**(6) (2022), 1651–1666.

[6] World Health Organization. WHO Coronavirus (COVID-19) Dashboard [online]. Available from: https://covid19.who.int/ (December 16, 2023).

[7] S. Saha and A. K. Saha, *Modeling the Dynamics of COVID-19 in the Presence of Delta and Omicron Variants with Vaccination and Non-Pharmaceutical Interventions*, Heliyon, **9**(7) (2023), 1-26.

[8] A. Rajput, Tanvi, R. Aggarwal, A. Sharma, S. K. Sahdev, M. Kumar and Jaimala, *Fractional Order on Modeling the Transmission of Devastative COVID-19Infection:*

Efficacy of Vaccination, Applications and Applied Mathematics: An International Journal (AAM). **18**(1) (2023), 1-24.

[9] Department of Disease Control. Vaccine covid-19 of Thailand. [online]. Available from: https://ddc.moph.go.th/vaccine-covid19/ (December 3, 2023).

[10] Department of Disease Control. Vaccine covid-19 of Thailand. [online]. Available from: https://ddc.moph.go.th/vaccine-covid19/guidelines (December 3, 2023).

[11] M. Yavuz, F.Ö. Coşar, F. Günay and F.N. Özdemir, *A New Mathematical Modeling of the COVID-19 Pandemic Including the Vaccination Campaign*, Open Journal of Modelling and Simulation. **9**(3) (2021), 299-321.

[12] S. H. A. Khoshnaw, R. H. Salih and S. Sulaimany, *Mathematical Modelling for Coronavirus Disease (COVID-19) in Predicting Future Behaviours and Sensitivity Analysis*, Math. Model. Nat. Phenom. **15**(33) (2020), 1-13.

[13] W.Yang, *Modeling COVID-19 Pandemic with Hierarchical Quarantine and Time Delay*, Dyn. Games. Appl. **11**(4) (2021), 892–914.

[14] A. Ibrahim, U. W. Humphries, P. S. Ngiamsunthorn, I. Baba, S. Qureshi and A. Khan, *Modeling the dynamics of COVID-19 with real data from Thailand*, Sci Rep. **13**(1) (2023), 1-26.

[15] J. Lamwong, P. Pongsumpun, I.-M. Tang and N. Wongvanich, *Vaccination's Role in Combating the Omicron Variant Outbreak in Thailand: An Optimal Control Approach*, Mathematics. **10**(20) (2022), 1-29.

[16] Y.Kim, S. Lee, C. Chu, S. Choe, S. Hong and Y. Shin, *The Characteristics of Middle Eastern Respiratory Syndrome Coronavirus Transmission Dynamics in South Korea*, Osong Public Health Res Perspect. **7**(1) (2016), 49-55.

[17] K. Sarkar, S. Khajanchi and J. J. Nieto, *Modeling and forecasting the COVID-19 pandemic in India*,Chaos Solitons Fractals. **139** (2020), 1-16.

[18] World Health Organization. COVID-19 - WHO Thailand Situation Reports. [online] Available:https://www.who.int/thailand/emergencies/novel-coronavirus-2019/situation-reports, (December 15, 2023).

[19] I.U. Haq, N. Ullah, N. Ali and K.S. Nisar, *A New Mathematical Model of COVID-19 with Quarantine and Vaccination*, Mathematics. **42**(11) (2023), 1-21.

Appendix B

Paper 2

Vaccination's Role in Combating the Omicron Variant Outbreak in Thailand: An Optimal Control Approach

mathematics

MDPI

Article

Vaccination's Role in Combating the Omicron Variant Outbreak in Thailand: An Optimal Control Approach

Jiraporn Lamwong [1], Puntani Pongsumpun [1,*], I-Ming Tang [2] and Napasool Wongvanich [3]

[1] Department of Mathematics, School of Science, King Mongkut's Institute of Technology Ladkrabang, Bangkok 10520, Thailand
[2] Department of Physics, Faculty of Science, Mahidol University, Bangkok 10400, Thailand
[3] Department of Instrumentation and Control Engineering, School of Engineering, King Mongkut's Institute of Technology Ladkrabang, Bangkok 10520, Thailand
* Correspondence: puntani.po@kmitl.ac.th; Tel.: +66-2329-8000

Abstract: COVID-19 is the name of the new infectious disease which has reached the pandemic stage and is named after the coronavirus (COVs) which causes it. COV is a single-stranded RNA virus which in humans leads to respiratory tract symptoms which can lead to death in those with low immunities, particularly older people. In this study, a standard dynamic model for COVID-19 was proposed by comparing a simple model and the optimal control model to reduce the number of infected people and become a guideline to control the outbreak. Control strategies are the vaccination rate and vaccine-induced immunity. An analysis was performed to find an equilibrium point, the basic reproduction number (R_0), and conditions that generate stability by using Lyapunov functions to prove the stability of the solution at the equilibrium point. Pontryagin's maximum principle was used to find the optimal control condition. Moreover, sensitivity analysis of the parameters was performed to learn about the parameters that might affect the outbreak in order to be able to control the outbreak. According to the analysis, it is seen that the efficacy of vaccines (b) and the infection rate ($\beta_{\sigma 1}$, $\beta_{\sigma 1}$, $\beta_{\sigma 2}$, $\beta_{\sigma 2}$) will affect the increased (decreased) incidence of the outbreak. Numerical analyses were performed on the Omicron variant outbreak data collected from the Thailand Ministry of Health, whose analyses then indicated that the optimal control strategy could lead to planning management and policy setting to control the COVID-19 outbreak.

Keywords: COVID-19; optimal control; Lyapunov function; global stabilities; sensitivity

MSC: 37M05

check for updates

Citation: Lamwong, J.; Pongsumpun, P.; Tang, I.-M.; Wongvanich, N. Vaccination's Role in Combating the Omicron Variant Outbreak in Thailand: An Optimal Control Approach. *Mathematics* 2022, *10*, 3899. https://doi.org/10.3390/math10203899

Academic Editor: Sophia Jang

Received: 28 September 2022
Accepted: 16 October 2022
Published: 20 October 2022

Publisher's Note: MDPI stays neutral with regard to jurisdictional claims in published maps and institutional affiliations.

1. Introduction

A huge outbreak of COVID-19 infections has reached every corner of the world. It is now considered to be the largest health threat to the world since there are now millions of confirmed cases of infection. Due to the pathogens of the COVID-19 virus, a single-stranded RNA virus [1] belonging to the family of Coronaviridae, it causes respiratory sickness. The coronaviruses can be classified into at least four genera: Alphacoronavirus, Betacoronavirus, Gammacoronavirus and Deltacoronavirus. The coronaviruses that cause diseases in humans but do not cause severe respiratory symptoms or asymptomatic syndrome are members of the Alphacoronavirus genus. The coronaviruses that cause severe diseases in humans such as severe acute respiratory syndrome (SARS) and Middle East respiratory syndrome (MERS), SARS-CoV and MERS-CoV, belong to the Betacoronavirus genus. These last two viruses originated in animals but have crossed the species (animal-to-human) barrier. The new coronaviruses in 2019 are a family of viruses which cause illnesses ranging from the common cold to more severe diseases [2,3] and appeared only recently in humans. They first appeared in bats. In humans, these viruses cause respiratory illnesses.

COVID-19 is transmitted from person to person [4,5] through the air by droplets of liquid that come from the noses and mouths of infected people when they cough, sneeze, and talk, or by touching surfaces that are contaminated with the virus [6]. The length of time between infection and the appearance of the first symptoms (incubation period) is between 1 and 14 days (5–6 days on average). More than 97% of patients begin to show symptoms of illness within 14 days. General symptoms include fever, fatigue, headache, runny nose, sore throat, coughing, rapid breathing, and difficulty breathing. In severe cases, patients may begin to show complications such as pneumonia, lung inflammation, renal failure, or death [2,4,5,7,8]. Currently, there is no clear information showing how long COVID-19 can survive on surfaces. It was found that viruses would not survive after being exposed to disinfectants [8].

The spread of COVID-19 was first reported in the city of Wuhan in China when it originated that a continuously increasing number of patients having pneumonia of unknown etiology began in December 2019. It was officially reported on 3 January 2020 that the pneumonia outbreak in Wuhan was caused by a new coronavirus (novel coronavirus 2019, 2019-nCoV) [5,9–13] through person-to-person contact. On 22 January 2020, the Thailand Department of Disease Control, Ministry of Public Health elevated the emergency operations to be level 3 (avoiding traveling). The Ministry of Public Health implemented measures for temperature monitoring and screening at immigration checkpoints to monitor and detect travelers at risk of COVID-19 infection. As of 29 June 2022, Thailand has reported a cumulative total of 4,520,220 confirmed cases with 30,634 deaths [14]. Unlike many countries in the world, Thailand has a well-developed public health system with free medical health centers in every part of the country. The health centers are staffed by medical doctors and nurses who are governmental employees working to serve the people. Nothing is preventing Thailand from controlling the COVID-19 pandemic except for the lack of knowledge on the spread of the disease, the control steps tailored to the country, and the vaccines needed for preventing the spread of the virus. This study aims to provide the knowledge needed to efficiently control the spread of the disease.

Mathematical modeling is a tool for analyzing strategies needed to control the spread of COVID-19. From past to present, numerous researchers have proposed different models of the spread of COVID-19 needed to study the dynamic of the spread. In the first half of the 20th century, the SEIR model was used to understand the behavior of infectious diseases, with many researchers incorporating its use in developing the relevant mathematical models to predict transmission dynamics with a view to control [15]. These have included well known epidemics such as MERS [16], influenza [17–19], and dengue fever [20,21]. Gardner, Rey, et al. [22] introduced a basic model to study the spread of MERS-CoV in the Arabian Peninsula, Europe, North America, Southeast Asia, the Middle East, and the United States of America. The spread of MERS-CoV is not exactly the same as that of severe acute respiratory syndrome SARS-CoV. Both of these coronaviruses are transmitted by person-to-person contact. Differences in the epidemiology are used to create the mathematical model for each coronavirus. The differences in the MERS-CoV transmission were the locations of the contact and who the human contacts were. Ndaïroua et al. [11] created a mathematical model to study the spread of COVID-19 in Wuhan, China. How humans get infected was studied, and from this, the basic reproduction number was calculated, while sensitivity of the parameters affecting the spread was considered. Enahoro et al. [10] developed a mathematical model to study the dynamic of the spread and control of COVID-19 in Nigeria. The model analyzed and determined the parameters using COVID-19 information publicized by the Nigeria Center of Disease Control (NCDC) to assess the effects across the country and within communities. Numerical simulation in the mathematical model showed that COVID-19 could be efficiently controlled in Nigeria by using a moderate level of social distancing across the country. Sen [23] created a mathematical model for the spread of COVID-19 in the form of the SEIRD model (susceptible–infected–recovered–dead model) by analyzing the spread in five countries, i.e., China, Italy, France, United States of America, and India. Curve fitting analysis was conducted to compare the spread between

real information and the created model. Kumar et al. [24] developed a simple mathematical model to predict and examine the spread of COVID-19 in India. A mathematical method was proposed to predict new cases of COVID-19 or cumulative confirmed cases in real situations. Various simulation models were presented to predict the spread of COVID-19 in India and other countries. Hezam et al. [25] proposed a dynamic mathematical model to control the spread of COVID-19 and cholera in Yemen. All four control functions were used, namely, social distancing, lockdown, number of tests, and number of chlorine tablets. Riyapan et al. [26] created a mathematical model and conducted an analysis to understand the dynamic of COVID-19 spread in Bangkok. People were divided into seven groups, i.e., susceptible group, exposed group, infected group, asymptomatic group, symptomatic group (quarantined), recovered group, and dead group. According to the model analysis and numerical results, it was shown that wearing a mask regularly could reduce the spread of COVID-19.

From what was mentioned earlier, it can be seen that this research is different from the research studies mentioned above. The objective of this research is to analyze the dynamic of COVID-19 by creating a mathematical model, and consideration is made when people get vaccinated for COVID-19. Specifically, the infective individuals' trajectories with several values of vaccination efficacies are compared against one another to see the effects that the efficacies have on these trajectories. Furthermore, a numerical analysis is also conducted on the infective data collected from the Thai Ministry of Health for the Omicron variant outbreak, whereby the rates of transmission of symptomatic and asymptomatic infections are estimated. Optimal control analyses are then performed to compare its effectiveness against the uncontrolled counterparts. It is seen that the controlled trajectories outperform the uncontrolled counterparts.

2. Materials and Methods

2.1. Mathematical Model

Yang and Wang [7] proposed a COVID-19 mathematical model in the form of the SEIHRV model (susceptible–exposed–infected–hospitalized–recovered model) to study the spread of COVID-19 by comparing different infection rates based on the Hamilton County (USA) case reports. The study found that environmental factors played an important role in the spread of COVID-19. Rajputet al. [27] proposed a nonlinear mathematical model as a strategy for controlling the spread of COVID-19 by using vaccination as a means to reduce the infection. Both studies are consistent with and are similar to the research here. The World Health Organization (WHO) has reported that peoplevaccinated against COVID-19 with one of the approved COVID-19 vaccines develop illnesses of different severity, i.e., the symptoms of patients whose infectious status are due to the exposure to mRNA fragments in the vaccine could be mild or strong enough to prevent hospitalization, depending on the immune status of the patient and which vaccine was used. It should be noted that the vaccines are only approved for different age groups. In order to be able to take into account the possibility of the responses of individuals to the exposure to mRNA of COVID-19 in its natural state or the mRNA in the vaccine, a modification of the population groups in the model is made. In this research, the population is first divided into two groups, the vaccinated population and the unvaccinated population, to study differences in the responses of both groups. In addition, each population is further divided into subgroups as follows: a group labelled unvaccinated and the susceptible population, a group of unvaccinated and the exposed population, a group of unvaccinated and the asymptomatic population, a group of unvaccinated and the symptomatic population, a group of vaccinated and the susceptible population, a group of vaccinated and the exposed population, a group of vaccinated and the asymptomatic population, a group of vaccinated and the symptomatic population, a group of the hospitalized population, and a group of the recovered population. Note that the isolated infected population group is not explicitly included in the model but is rather included in the symptomatic infectious group. This is because there was already a widespread use of the antigen testing kit amongst the Thai

population, even in the rural regions, by the time of the Omicron outbreak; the symptomatic infectious population, upon testing positive for COVID-19 with the kit, automatically isolated themselves and received appropriate treatments via post mails. The developed model is then dynamically analyzed to investigate the appropriate control measures.

The transmission dynamics are encapsulated in the following diagram.

Susceptible groups for the unvaccinated population infected with COVID-19 have the rates of β_{an} and β_{sn}. The infection rate of the unvaccinated population η_1 is determined as:

$$\eta_1 = \beta_{an} I_{an} + \beta_{sn} I_{sn} \tag{1}$$

Similarly, the infection rate of the vaccinated population η_2 is determined as:

$$\eta_2 = \beta_{av} I_{av} + \beta_{sv} I_{sv} \tag{2}$$

From the diagram in Figure 1, the infection dynamics can be described as follows:

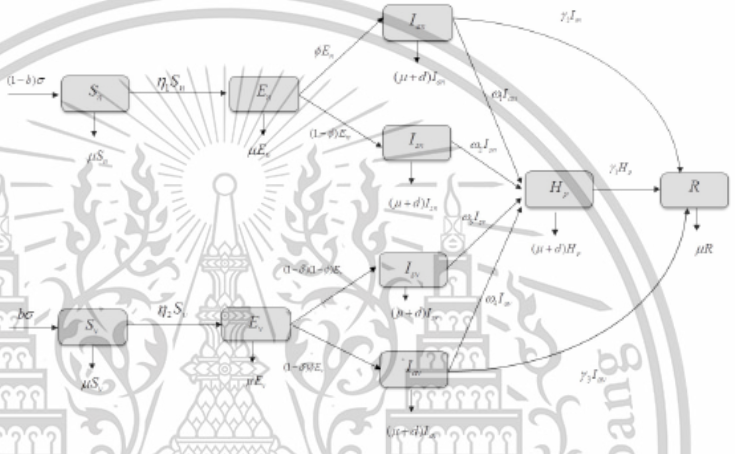

Figure 1. Diagram showing the relationship of the COVID-19 mathematical model and vaccination.

The initial number in the unvaccinated human population susceptible to COVID-19 is $(1-b)\sigma$ when $0 < b < 1$. The unvaccinated and infected human population will transmit the virus to the susceptible human population with the probabilities of β_{an} and β_{sn}, respectively. When the human population is exposed to COVID-19, the incubation period is at the rate of ϕ. If the body's immune response is absent, they become infected. Infection in humans can be symptomatic, showing symptoms, or asymptomatic, both being infectious (able to transmit the infection). After getting infected, infected persons shall be hospitalized with the rate of ω_1 and ω_2, respectively. When infected with COVID-19, some people die of the disease, with a death rate of d. However, infected people who are asymptomatic may not be hospitalized. After undergoing COVID-19 treatment, infected people will recover. The human population shall die of natural causes at a rate of μ.

The number in the vaccinated human population susceptible to COVID-19 is $b\sigma$. The vaccinated and infected human population shall transmit the virus to the susceptible human population with the probability of β_{av} and β_{sv}, respectively. When the human population is exposed to COVID-19, the incubation period is at the rate of $(1-\delta)$. If the body's immune response is absent, they become infected. Infection in humans is divided into 2 characteristics, namely, symptomatic infection and asymptomatic infection. After getting infected, infected persons shall be hospitalized with the rate of ω_3 and ω_4, respectively. When infected with COVID-19, some people die of the disease, with a death rate of d. Most

of the infected people who are asymptomatic may not be hospitalized. After undergoing COVID-19 treatment, infected people will recover. The human population shall die of natural causes at a rate of μ.

A model of COVID-19 and vaccinations can be created by describing the relationship of the mathematical model as follows:

$$\frac{dS_n}{dt} = (1-b)\sigma - \eta_1 S_n - \mu S_n \tag{3}$$

$$\frac{dE_n}{dt} = \eta_1 S_n - \phi E_n - (1-\phi)E_n - \mu E_n \tag{4}$$

$$\frac{dI_{an}}{dt} = \phi E_n - (\omega_1 + \gamma_2 + \mu + d)I_{an} \tag{5}$$

$$\frac{dI_{sn}}{dt} = (1-\phi)E_n - (\omega_2 + \mu + d)I_{sn} \tag{6}$$

$$\frac{dS_v}{dt} = b\sigma - \eta_2 S_v - \mu S_v \tag{7}$$

$$\frac{dE_v}{dt} = \eta_2 S_v - (1-\delta)\phi E_v - (1-\delta)(1-\phi)E_v - \mu E_v \tag{8}$$

$$\frac{dI_{av}}{dt} = (1-\delta)\phi E_v - (\omega_4 + \gamma_3 + \mu + d)I_{av} \tag{9}$$

$$\frac{dI_{sv}}{dt} = (1-\delta)(1-\phi)E_v - (\omega_3 + \mu + d)I_{sv} \tag{10}$$

$$\frac{dH_p}{dt} = \omega_1 I_{an} + \omega_2 I_{sv} + \omega_3 I_{sv} + \omega_4 I_{av} - (\gamma_1 + \mu + d)H_p \tag{11}$$

$$\frac{dR}{dt} = \gamma_1 H_p + \gamma_2 I_{an} + \gamma_3 I_{av} - \mu R \tag{12}$$

when

$$N_h = S_n + E_n + I_{an} + I_{sn} + S_v + E_v + I_{av} + I_{sv} + H_p + R \tag{13}$$

where the parameters of Equations (3)–(12) are defined in Table 1.

Lemma 1. (From [28,29]). *Let* $(S_n(t), E_n(t), I_{an}(t), I_{sn}(t), S_v(t), E_v(t), I_{av}(t), I_{sv}(t), H_p(t), R(t))$ *be the solution of the system (3)–(12) with positive initial conditions* $S_n(0), E_n(0), I_{an}(0), I_{sn}(0), S_v(0), E_v(0), I_{av}(0), I_{sv}(0), H_p(0), R(0)$. *Denoting also the invariant set*

$$\Omega = \left\{(S_n, E_n, I_{an}, I_{sn}, S_v, E_v, I_{av}, I_{sv}, H_p, R \in R_{10}^+ : N_h \le \frac{\sigma}{\mu}\right\}, \text{ and } \Omega \text{ is a positively invariant set for (3)–(12).}$$

Proof. Where $N_h = S_n + E_n + I_{an} + I_{sn} + S_v + E_v + I_{av} + I_{sv} + H_p + R$, the formula will be:

$$\frac{dN_h}{dt} = \frac{dS_n}{dt} + \frac{dE_n}{dt} + \frac{dI_{an}}{dt} + \frac{dI_{sn}}{dt} + \frac{dS_v}{dt} + \frac{dE_v}{dt} + \frac{dI_{av}}{dt} + \frac{dI_{sv}}{dt} + \frac{dH_p}{dt} + \frac{dR}{dt}$$

$$\frac{dN_h}{dt} = \frac{dS_n}{dt}\sigma - \mu N_h - d(I_{an} + I_{sn} + I_{av} + I_{sv} + H_p)$$

$$\le \sigma - \mu N_h$$

It can be seen that $\frac{dN_h}{dt} \le \sigma - \mu N_h \le 0$. Therefore, when $N_h(t) \le N(0)e^{-\mu t} + \frac{\sigma}{\mu}\left[1 - e^{-\mu t}\right]$, the derivative $\frac{dN_h}{dt}$ satisfies $\frac{dN_h}{dt} \le \frac{\sigma}{\mu}$. Hence, as $t \to \infty$, $e^{-\mu t} \to 0$, it then follows that all trajectories within the invariant set Ω will form a positively invariant set in R_{10}^+ for the systems (3)–(12) since all epidemiological constants are nonnegative. □

Table 1. Definitions of variables and parameters.

Variables and Parameters	Description
S_n	The number in the unvaccinated, susceptible population.
E_n	The number in the unvaccinated, exposed population.
I_{an}	The number in the unvaccinated, asymptomatic, infected population.
I_{sn}	The number in the unvaccinated, symptomatic, infected population.
S_v	The number in the vaccinated, susceptible population.
E_v	The number in the vaccinated, exposed population.
I_{av}	The number in the vaccinated, asymptomatic, infected population.
I_{sv}	The number in the vaccinated, symptomatic, infected population.
H_p	The number in the hospitalized population.
R	The number in the recovered population.
b	Efficacy of vaccination.
σ	Initial number in the population.
β_{an}	Infection rate of the unvaccinated, asymptomatic, infected population.
β_{sn}	Infection rate of the unvaccinated, symptomatic, infected population.
β_{av}	Infection rate of the vaccinated, asymptomatic, infected population.
β_{sv}	Infection rate of the vaccinated, symptomatic, infected population.
ϕ	Incubation period of the disease.
δ	Efficacy of the vaccination against COVID-19.
ω_1	Hospitalization rate of the unvaccinated, asymptomatic, infected population.
ω_2	Hospitalization rate of the unvaccinated, symptomatic, infected population.
ω_3	Hospitalization rate of the vaccinated, asymptomatic, infected population.
ω_4	Hospitalization rate of the vaccinated, symptomatic, infected population.
γ_1	Recovery rate after hospitalization.
γ_2	Recovery rate of the unvaccinated, asymptomatic, infected population.
γ_3	Recovery rate of the vaccinated, asymptomatic, infected population.
μ	Death rate from natural causes.
d	Death rate from COVID-19.
N_h	Total number in the human population.

2.2. *Stability Analysis*

2.2.1. Equilibrium Point

The dynamical systems analysis for the models of (3)–(12) can be performed, firstly, by evaluating the equilibrium of the system. This is conducted by setting Equations (3)–(12) to zero. The two such equilibrium points for this system are as follows:

The disease-free equilibrium point is:

$$G_0^* = \left(S_n^*, E_n^*, I_{an}^*, I_{sn}^*, S_v^*, E_v^*, I_{av}^*, I_{sv}^*, H_p^*, R^*\right) = \left(\frac{(1-b)\sigma}{\mu}, 0, 0, 0, \frac{b\sigma}{\mu}, 0, 0, 0, 0, 0\right) \quad (14)$$

when $R_0 < 1$, and the endemic equilibrium point is:

$$G_1^* = \left(S_n^*, E_n^*, I_{an}^*, I_{sn}^*, S_v^*, E_v^*, I_{av}^*, I_{sv}^*, H_p^*, R^*\right) \quad (15)$$

when

$$S_n^* = \frac{(1-b)\sigma}{(\mu+\eta_1^*)},$$
$$E_n^* = \frac{(1-b)\sigma\eta_1^*}{(1+\mu)(\mu+\eta_1^*)},$$
$$I_{an}^* = \frac{(1-b)\phi\sigma\eta_1^*}{k_1},$$
$$I_{sn}^* = \frac{(1-b)(1-\phi)\sigma\eta_1^*}{k_2},$$
$$S_v^* = \frac{b\sigma}{(\mu+\eta_2^*)},$$
$$E_v^* = \frac{b\sigma\eta_2^*}{(1+\mu-\delta)(\mu+\eta_2^*)},$$
$$I_{av}^* = \frac{b(1-\delta)\phi\sigma\eta_2^*}{(1+\mu-\delta)k_3},$$
$$I_{sv}^* = \frac{b(1-\delta)(1-\phi)\sigma\eta_2^*}{(1+\mu-\delta)k_4},$$

$$H_p^* = k_5\left(\frac{(1-b)\phi\omega_1\eta_1^*}{k_1} + \frac{(1-b)(1-\phi)\omega_2\eta_1^*}{k_2} + \frac{b(1-\delta)\phi\omega_4\eta_2^*}{(1+\mu-\delta)k_3} + \frac{b(1-\delta)(1-\phi)\omega_3\eta_2^*}{(1+\mu-\delta)k_4}\right)$$

$$R^* = k_6\left(\frac{\frac{(1-b)\phi\gamma_2\eta_1^*}{k_1} + \frac{b(1-\delta)\phi\gamma_3\eta_2^*}{(1+\mu-\delta)k_3} + k_7\left(\frac{(1-b)\phi\omega_1\eta_1^*}{k_1} + \frac{(1-b)(1-\phi)\omega_2\eta_1^*}{k_2} + \frac{b(1-\delta)\phi\omega_4\eta_2^*}{(1+\mu-\delta)k_3} + \frac{b(1-\delta)(1-\phi)\omega_3\eta_2^*}{(1+\mu-\delta)k_4}\right)\right)$$

where $k_1 = (1+\mu)(d+\gamma_2+\mu+\omega_1)(\mu+\eta_1^*)$, $k_2 = (1+\mu)(d+\mu+\omega_2)(\mu+\eta_1^*)$, $k_3 = (d+\gamma_3+\mu+\omega_4)(\mu+\eta_2^*)$, $k_4 = (d+\mu+\omega_3)(\mu+\eta_2^*)$, and $k_5 = \frac{\sigma}{\gamma_1+\mu+d}$, $k_6 = \frac{\sigma}{\mu}$, $k_5 = \frac{\gamma_1}{\gamma_1+\mu+d}$, when $R_0 > 1$.

The forces of infection, η_1^* and η_2^*, appearing in the components of the endemic equilibrium point can be determined by using the following expressions:

$$\eta_1^* = \beta_{an}I_{an}^* + \beta_{sn}I_{sn}^* \tag{16}$$

and

$$\eta_2^* = \beta_{av}I_{av}^* + \beta_{sv}I_{sv}^* \tag{17}$$

2.2.2. The Basic Reproduction Number

The calculation of the basic reproduction number (R_0) plays a huge and important role since it is used to measure the transmission potential of a disease. It is the average number of secondary infections which can be caused by a patient in a completely susceptible population throughout this infectious period. In this research, the basic reproduction number was calculated using the next-generation matrix method [30,31] for COVID-19 mathematical model. The states E_n, I_{an}, I_{sn}, E_v, I_{av} and I_{sv} were chosen to construct the gain and loss vectors, where the gain vector represents the possible pathways of creating new infections, and the loss vector represents the possible pathways of transferring from one group to another.

$$\begin{array}{|l|l|l|l|}
\hline
\textit{Gains to } E_n & \eta_1 S_n & \textit{Losses from } E_n & \phi E_n + (1-\phi)E_n + \mu E_n \\
\textit{Gains to } I_{an} & 0 & \textit{Losses from } I_{an} & -\phi E_n + (\omega_1+\gamma_2+\mu+d)I_{an} \\
\textit{Gains to } I_{sn} & 0 & \textit{Losses from } I_{sn} & -(1-\phi)E_n + (\omega_2+\mu+d)I_{sn} \\
\textit{Gains to } E_v & \eta_2 S_v & \textit{Losses from } E_v & (1-\delta)\phi E_v + (1-\delta)(1-\phi)E_v + \mu E_v \\
\textit{Gains to } I_{av} & 0 & \textit{Losses from } I_{av} & -(1-\delta)\phi E_v + (\omega_4+\gamma_3+\mu+d)I_{av} \\
\textit{Gains to } I_{sv} & 0 & \textit{Losses from } I_{sv} & -(1-\delta)(1-\phi)E_v + (\omega_3+\mu+d)I_{sv} \\
\hline
\end{array}$$

The required F and V matrices are the Jacobian matrices of the gain and loss vectors, respectively. Then we have

$$F = \begin{bmatrix} 0 & \beta_{an}S_n & \beta_{sn}S_n & 0 & 0 & 0 \\ 0 & 0 & 0 & 0 & 0 & 0 \\ 0 & 0 & 0 & 0 & 0 & 0 \\ 0 & 0 & 0 & 0 & \beta_{av}S_v & \beta_{sv}S_v \\ 0 & 0 & 0 & 0 & 0 & 0 \\ 0 & 0 & 0 & 0 & 0 & 0 \end{bmatrix}$$

$$V = \begin{bmatrix} \phi + (1-\phi) + \mu & 0 & 0 & 0 & 0 & 0 \\ -\phi & \omega_1 + \mu + d & 0 & 0 & 0 & 0 \\ -(1-\phi) & 0 & \omega_2 + \mu + d & 0 & 0 & 0 \\ 0 & 0 & 0 & (1-\delta)\phi + (1-\delta)(1-\phi) + \mu & 0 & 0 \\ 0 & 0 & 0 & -(1-\delta)\phi & \omega_4 + \gamma_3 + \mu + d & 0 \\ 0 & 0 & 0 & -(1-\delta)(1-\phi) & 0 & \omega_3 + \mu + d \end{bmatrix}$$

Note that we evaluate the gain and loss matrices at the disease-free equilibrium point:

$$G_0^* = \left(S_n^*, E_n^*, I_{an}^*, I_{sn}^*, S_v^*, E_v^*, I_{av}^*, I_{sv}^*, H_p^*, R^*\right) = \left(\frac{(1-b)\sigma}{\mu}, 0, 0, 0, \frac{b\sigma}{\mu}, 0, 0, 0, 0, 0\right)$$

The required basic reproduction number is computed as $R_0 = FV^{-1}$, where R_0 is the maximum positive eigenvalue of the matrix FV^{-1}. Therefore, the formula is:

$$R_0 = max\{R_n, R_v\} \tag{18}$$

when

$$R_n = \frac{(b-1)\sigma(d(\beta_{sn}(\phi-1)-\beta_{an}\phi)+\beta_{sn}(\phi-1)(\gamma_2+\mu+\omega_1)-\beta_{an}\phi(\mu+\omega_2))}{\mu(1+\mu)(d+\gamma_2+\mu+\omega_1)(d+\mu+\omega_2)}$$

$$R_v = \frac{b\sigma(\delta-1)(d(\beta_{sv}(\phi-1)-\beta_{av}\phi)-\beta_{av}\phi(\mu+\omega_3)-\beta_{sv}(\phi-1)(\gamma_3+\mu+\omega_4))}{\mu(1-\delta+\mu)(d+\mu+\omega_3)(d+\gamma_3+\mu+\omega_4)}$$

2.2.3. Global Stability Analysis

In this part, the global stability analysis of each equilibrium point of the model in the system of Equations (3)–(12) around the two steady states G_0^* and G_1^* is performed as demonstrated in the following.

Theorem 1. *The disease-free equilibrium point G_0^* of the model in the system (3)–(12) is globally asymptotically stable in Ω if $R_0 < 1$.*

We assume that

$$\begin{cases} \beta_{an} = \beta_{sn} = \frac{\mu+d}{S_n^*} \\ \beta_{av} = \beta_{sv} = \frac{\mu+d}{S_v^*} \end{cases} \tag{19}$$

Proof. Consider the continuously differentiable linear Lyapunov function defined by

$$L = (S_n - S_n^* lnS_n) + E_n + I_{an} + I_{sn} + (S_v - S_v^* lnS_v) + E_v + I_{av} + I_{sv} + H_p + R$$

To explain the use of lnS_n and lnS_v have

$$\frac{dL}{dt} = S_n'\left(1 - \frac{S_n^*}{S_n}\right) + E_n' + I_{an}' + I_{sn}' + S_v'\left(1 - \frac{S_v^*}{S_v}\right) + E_v' + I_{av}' + I_{sv}' + H_p' + R'$$

$$\begin{aligned}\frac{dL}{dt} = {} & ((1-b)\sigma - \eta_1 S_n - \mu S_n)\left(1-\frac{S_n^*}{S_n}\right) + (\eta_1 S_n - \phi E_n - (1-\phi)E_n - \mu E_n) \\ & +(\phi E_n - (\omega_1+\gamma_2+\mu+d)I_{an}) + ((1-\phi)E_n - (\omega_2+\mu+d)I_{sn}) \\ & +(b\sigma - \eta_2 S_v - \mu S_v)\left(1-\frac{S_v^*}{S_v}\right) + (\eta_2 S_v - (1-\delta)\phi E_v - (1-\delta)(1-\phi)E_v - \mu E_v) \\ & +((1-\delta)\phi E_v - (\omega_4+\gamma_3+\mu+d)I_{av}) + ((1-\delta)(1-\phi)E_v - (\omega_3+\mu+d)I_{sv}) \\ & +(\omega_1 I_{an} + \omega_2 I_{sv} + \omega_3 I_{sv} + \omega_4 I_{av} - (\gamma_1+\mu+d)H_p) \\ & +(\gamma_1 H_p + \gamma_2 I_{an} + \gamma_3 I_{av} - \mu R) \\ = {} & (1-b)\sigma\left(1-\frac{S_n^*}{S_n}\right) + \beta_{an} I_{an} S_n^* + \beta_{sn} I_{sn} S_n^* - \mu S_n + \mu S_n^* - \mu E_n - (\mu+d)I_{an} \\ & -(\mu+d)I_{sn} + b\sigma\left(1-\frac{S_v^*}{S_v}\right) + \beta_{av} I_{av} S_v^* + \beta_{sv} I_{sv} S_v^* - \mu S_v + \mu S_v^* - \mu E_v \\ & -(\mu+d)I_{av} - (\mu+d)I_{sv} - (\mu+d)H_p - \mu R \\ = {} & (1-b)\sigma\left(1-\frac{S_n^*}{S_n}\right) + \mu S_n^*\left(1-\frac{S_n}{S_n^*}\right) + (\beta_{an} S_n^* - (\mu+d))I_{an} \\ & +(\beta_{sn} S_n^* - (\mu+d))I_{sn} - \mu E_n + b\sigma\left(1-\frac{S_v^*}{S_v}\right) + \mu S_v^*\left(1-\frac{S_v}{S_v^*}\right) \\ & +(\beta_{av} S_v^* - (\mu+d))I_{av} + (\beta_{sv} S_v^* - (\mu+d))I_{sv} - \mu E_v - (\mu+d)H_p - \mu R \end{aligned}$$

Substitute Equation (19) to obtain

$$\begin{aligned}\frac{dL}{dt} = {} & (1-b)\sigma\left(1-\frac{S_n^*}{S_n}\right) + \mu S_n^*\left(1-\frac{S_n}{S_n^*}\right) - \mu E_n + b\sigma\left(1-\frac{S_v^*}{S_v}\right) + \mu S_v^*\left(1-\frac{S_v}{S_v^*}\right) - \mu E_v \\ & -(\mu+d)H_p - \mu R \end{aligned}$$

Substitute $S_n^* = \frac{(1-b)\sigma}{\mu}$ and $S_v^* = \frac{b\sigma}{\mu}$ from the disease-free equilibrium point to obtain

$$\begin{aligned}\frac{dL}{dt} = {} & (1-b)\sigma\left(1-\frac{S_n^*}{S_n}\right) + \mu\frac{(1-b)\sigma}{\mu}\left(1-\frac{S_n}{S_n^*}\right) + b\sigma\left(1-\frac{S_v^*}{S_v}\right) + \mu\frac{b\sigma}{\mu}\left(1-\frac{S_v}{S_v^*}\right) - \mu E_n \\ & -(\mu+d)H_p - \mu R \end{aligned}$$

$$\begin{aligned}\frac{dL}{dt} = {} & (1-b)\sigma\left(1-\frac{S_n^*}{S_n}\right) + (1-b)\sigma\left(1-\frac{S_n}{S_n^*}\right) + b\sigma\left(1-\frac{S_v^*}{S_v}\right) + b\sigma\left(1-\frac{S_v}{S_v^*}\right) \\ & -\mu E_n - (\mu+d)H_p - \mu R \\ = {} & (1-b)\sigma\left(2-\frac{S_n^*}{S_n}-\frac{S_n}{S_n^*}\right) + b\sigma\left(2-\frac{S_v^*}{S_v}-\frac{S_v}{S_v^*}\right) - \mu E_n - (\mu+d)H_p - \mu R \\ = {} & -(1-b)\sigma\left(\frac{(S_n^*-S_n)^2}{S_n^* S_n}\right) - b\sigma\left(\frac{(S_v^*-S_v)^2}{S_v^* S_v}\right) - \mu E_n - (\mu+d)H_p - \mu R \end{aligned}$$

$$\frac{dL}{dt} = -\left[(1-b)\sigma\left(\frac{(S_n^*-S_n)^2}{S_n^* S_n}\right) + b\sigma\left(\frac{(S_v^*-S_v)^2}{S_v^* S_v}\right) + \mu E_n + (\mu+d)H_p + \mu R\right] \leq 0 \tag{20}$$

It can be clearly seen that all conditions shown in Equation (20) are negative. Applying the LaSalle's invariance principle [4,32–34], $\frac{dL}{dt} = 0$ if $S_n^* = S_n$ and $S_v^* = S_v$, and $1-b$ is a positive number since it is known that $0 < b < 1$. Note further that, $\frac{dL}{dt} = 0$ if $E_n = 0$ $E_v = 0$, $H_p = 0$ and $R = 0$. On the other hand, the result of Theorem 1 implies that since the states E_n, E_v, H_p, and R are all positive, the resulting $\frac{dL}{dt}$ obtained in Equation (20) will be absolute negative. Consequently, LaSalle's invariant principle then implies that the disease-free steady state G_0^* is globally asymptotically stable on Ω. □

Theorem 2. *The endemic equilibrium point G_1^* of the model in the system (3)–(12) is globally asymptotically stable in Ω if $R_0 > 1$. We assume that*

$$\begin{cases} \eta_1^* = \eta_2^* \\ \mu = (\mu + \eta_1^*) \\ \beta_{sn} = \frac{\omega_2+\mu+d}{S_n^*} \\ \beta_{sv} = \frac{\omega_3+\mu+d}{S_v^*} \\ \beta_{sn} = \frac{\omega_2+\mu+d}{S_n^*} \\ \beta_{av} = \frac{\omega_4+\gamma_3+\mu+d}{S_v^*} \end{cases} \tag{21}$$

Proof. We consider the following Lyapunov function:

$$\begin{aligned} K &= (S_n - S_n^* lnS_n) + E_n + I_{an} + I_{sn} + (S_v - S_v^* lnS_v) + E_v + I_{av} + I_{sv} \\ \frac{dK}{dt} &= S_n'\left(1 - \frac{S_n^*}{S_n}\right) + E_n' + I_{an}' + I_{sn}' + S_v'\left(1 - \frac{S_v^*}{S_v}\right) + E_v' + I_{av}' + I_{sv}' \end{aligned}$$

$$\begin{aligned} \frac{dK}{dt} = {} & ((1-b)\sigma - \eta_1 S_n - \mu S_n)\left(1 - \tfrac{S_n^*}{S_n}\right) + (\eta_1 S_n - \phi E_n - (1-\phi)E_n - \mu E_n) \\ & + (\phi E_n - (\omega_1 + \gamma_2 + \mu + d)I_{an}) + ((1-\phi)E_n - (\omega_2 + \mu + d)I_{sn}) \\ & + (b\sigma - \eta_2 S_v - \mu S_v)\left(1 - \tfrac{S_v^*}{S_v}\right) + (\eta_2 S_v - (1-\delta)\phi E_v - (1-\delta)(1-\phi)E_v - \mu E_v) \\ & + ((1-\delta)\phi E_v - (\omega_4 + \gamma_3 + \mu + d)I_{av}) \\ & + ((1-\delta)(1-\phi)E_v - (\omega_3 + \mu + d)I_{sv}) \\ \frac{dK}{dt} = {} & (1-b)\sigma\left(1 - \tfrac{S_n^*}{S_n}\right) - \mu S_n\left(1 - \tfrac{S_n^*}{S_n}\right) + (\beta_{an} I_{an} + \beta_{sn} I_{sn})S_n^* - \mu E_n \\ & - (\omega_1 + \gamma_2 + \mu + d)I_{an} - (\omega_2 + \mu + d)I_{sn} + b\sigma\left(1 - \tfrac{S_v^*}{S_v}\right) - \mu S_v\left(1 - \tfrac{S_v^*}{S_v}\right) \\ & + (\beta_{av} I_{av} + \beta_{sv} I_{sv})S_v^* - \mu E_v - (\omega_4 + \gamma_3 + \mu + d)I_{av} - (\omega_3 + \mu + d)I_{sv} \\ = {} & (1-b)\sigma\left(1 - \tfrac{S_n^*}{S_n}\right) + \mu S_n^*\left(1 - \tfrac{S_n}{S_n^*}\right) + I_{an}((\beta_{an} S_n^* - (\omega_1 + \gamma_2 + \mu + d)) \\ & + I_{sn}(\beta_{sn} S_n^* - (\omega_2 + \mu + d)) - \mu E_n + b\sigma\left(1 - \tfrac{S_v^*}{S_v}\right) + \mu S_v^*\left(1 - \tfrac{S_v}{S_v^*}\right) \\ & + I_{av}(\beta_{av} S_v^* - (\omega_4 + \gamma_3 + \mu + d)) + I_{sv}(\beta_{sv} S_v^* - (\omega_3 + \mu + d)) - \mu E_v \end{aligned}$$

Substitute $S_n^* = \frac{(1-b)\sigma}{(\mu+\eta_1^*)}$ and $S_v^* = \frac{b\sigma}{(\mu+\eta_2^*)}$ from the endemic equilibrium point to obtain

$$\begin{aligned} \frac{dK}{dt} = {} & (1-b)\sigma\left(1 - \tfrac{S_n^*}{S_n}\right) + \mu\tfrac{(1-b)\sigma}{(\mu+\eta_1^*)}\left(1 - \tfrac{S_n}{S_n^*}\right) + I_{an}((\beta_{an} S_n^* - (\omega_1 + \gamma_2 + \mu + d)) \\ & + I_{sn}(\beta_{sn} S_n^* - (\omega_2 + \mu + d)) - \mu E_n + b\sigma\left(1 - \tfrac{S_v^*}{S_v}\right) + \mu\tfrac{b\sigma}{(\mu+\eta_2^*)}\left(1 - \tfrac{S_v}{S_v^*}\right) \\ & + I_{av}(\beta_{av} S_v^* - (\omega_4 + \gamma_3 + \mu + d)) + I_{sv}(\beta_{sv} S_v^* - (\omega_3 + \mu + d)) - \mu E_v \end{aligned}$$

Substitute Equation (21) to obtain

$$\begin{aligned} \frac{dK}{dt} &= (1-b)\sigma\left(1 - \tfrac{S_n^*}{S_n}\right) + (1-b)\sigma\left(1 - \tfrac{S_n}{S_n^*}\right) + b\sigma\left(1 - \tfrac{S_v^*}{S_v}\right) + b\sigma\left(1 - \tfrac{S_v}{S_v^*}\right) - \mu E_n - \mu E_v \\ &= (1-b)\sigma\left(2 - \tfrac{S_n^*}{S_n} - \tfrac{S_n}{S_n^*}\right) + b\sigma\left(2 - \tfrac{S_v^*}{S_v} - \tfrac{S_v}{S_v^*}\right) - \mu E_n - \mu E_v \\ &= -(1-b)\sigma\left(\tfrac{(S_n^* - S_n)^2}{S_n^* S_n}\right) - b\sigma\left(\tfrac{(S_v^* - S_v)^2}{S_v^* S_v}\right) - \mu E_n - \mu E_v \\ \frac{dK}{dt} &= -\left[(1-b)\sigma\left(\tfrac{(S_n^* - S_n)^2}{S_n^* S_n}\right) + b\sigma\left(\tfrac{(S_v^* - S_v)^2}{S_v^* S_v}\right) + \mu E_n + \mu E_v\right] \leq 0 \end{aligned} \tag{22}$$

From the condition of Equation (22), $\frac{dK}{dt}$ is absolute negative. Then, the endemic equilibrium point G_1^* is globally asymptotically stable in Ω. □

3. Numerical Analysis Result

3.1. Model Fitting

In this part, numerical simulation modelling of the system of Equations (3)–(12) was performed to compare information on the spread in Thailand. Data were collected from COVID-19-infected people from the Department of Disease Control, Ministry of Public Health, Thailand [14] from 1 January 2022, since the Omicron variant was confirmed, until 1 March 2022 to estimate the parameters β_{an}, β_{sn}, β_{av}, and β_{sv} using ode45 and the lsqcurvefit algorithm [12,35] in MATLA,B as shown in Figure 2. Figure 2a depicts the match between the modelled response for the unvaccinated, susceptible individuals against the COVID-19 data. Similarly, Figure 2b then compares the real data against the modelled response for the susceptible, vaccinated individuals. It can be noticed that the simulation model and real information are consistent with one another.

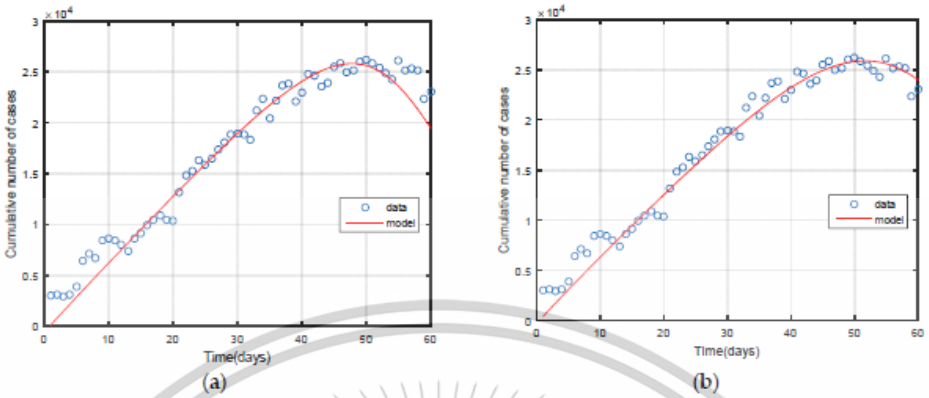

Figure 2. Data fitting of the model (3)–(12) to the actual data: (**a**) susceptible with vaccinated fitting; (**b**) susceptible with unvaccinated fitting.

3.2. Numerical Analysis Result

Numerical information on the spread of COVID-19 and getting vaccinations was analyzed using the parameters obtained from the literature review as seen in Table 2 and the data fitted for some parameters, namely, infection rate, β_{an}, β_{sn}, β_{av}, and β_{sv}. The Runge–Kutta method of order 4 in the MATLAB program was used to confirm the equilibrium point result and stability as seen in Figures 3 and 4.

Table 2. The parameters used in the numerical simulation.

Parameters	The Disease-Free	The Endemic	Reference
b	0.5	0.5	Estimated
σ	1	1400	Estimated
β_{an}	0.00001	0.00001	Data fitted
β_{sn}	0.000009	0.000009	Data fitted
β_{av}	0.000008	0.000008	Data fitted
β_{sv}	0.00001	0.00001	Data fitted
ϕ	1/7	1/7	[7,36]
δ	0.8	0.8	Assumed
ω_1	0.1	0.1	[5,7]
ω_2	0.1	0.1	[5,7]
ω_3	0.1	0.1	[5,7]
ω_4	0.1	0,1	[5,7]
γ_1	1/7	1/7	[7]
γ_2	1/14	1/14	[10]
γ_3	1/14	1/14	[7]
μ	0.0000365	0.0000365	[37,38]
d	0.00286	0.00286	[31]

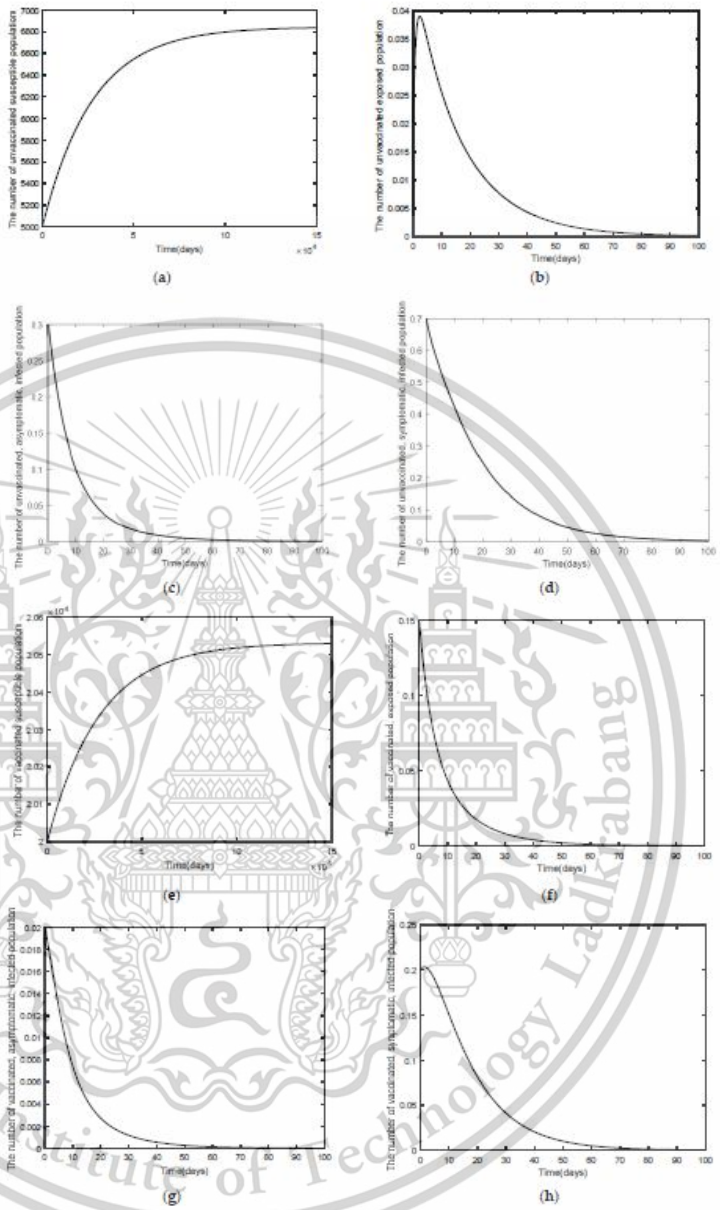

Figure 3. *Cont.*

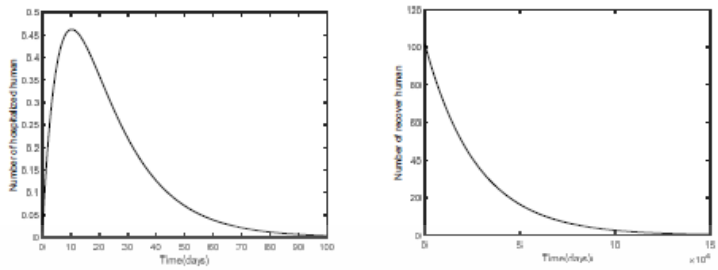

Figure 3. Graphs of the system of Equations (3)–(12) at the disease-free equilibrium point of S_n, E_n, I_{an}, I_{sn}, S_v, E_v, I_{av}, I_{sv}, H_p, and R when $R_0 < 1$: (**a**) the number in the unvaccinated, susceptible population; (**b**) the number in the unvaccinated, exposed population; (**c**) the number in the unvaccinated, asymptomatic, infected population; (**d**) the number in the unvaccinated, symptomatic, infected population; (**e**) the number in the vaccinated, susceptible population; (**f**) the number in the vaccinated, exposed population; (**g**) the number in the vaccinated, asymptomatic, infected population; (**h**) the number in the vaccinated, symptomatic, infected population; (**i**) the number in the hospitalized population; and (**j**) the number in the recovered population.

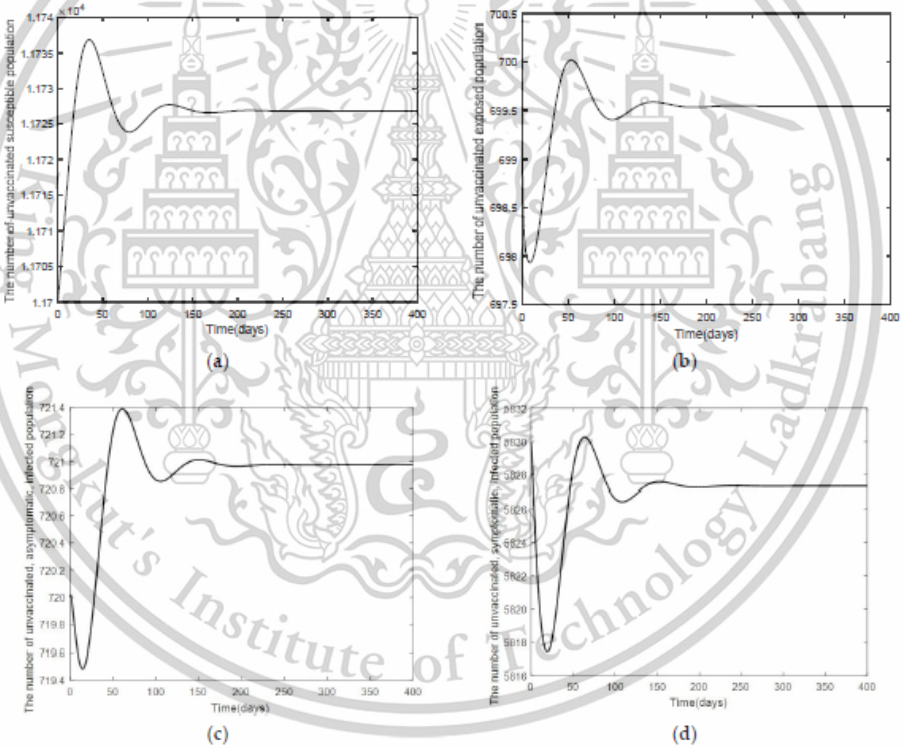

Figure 4. *Cont.*

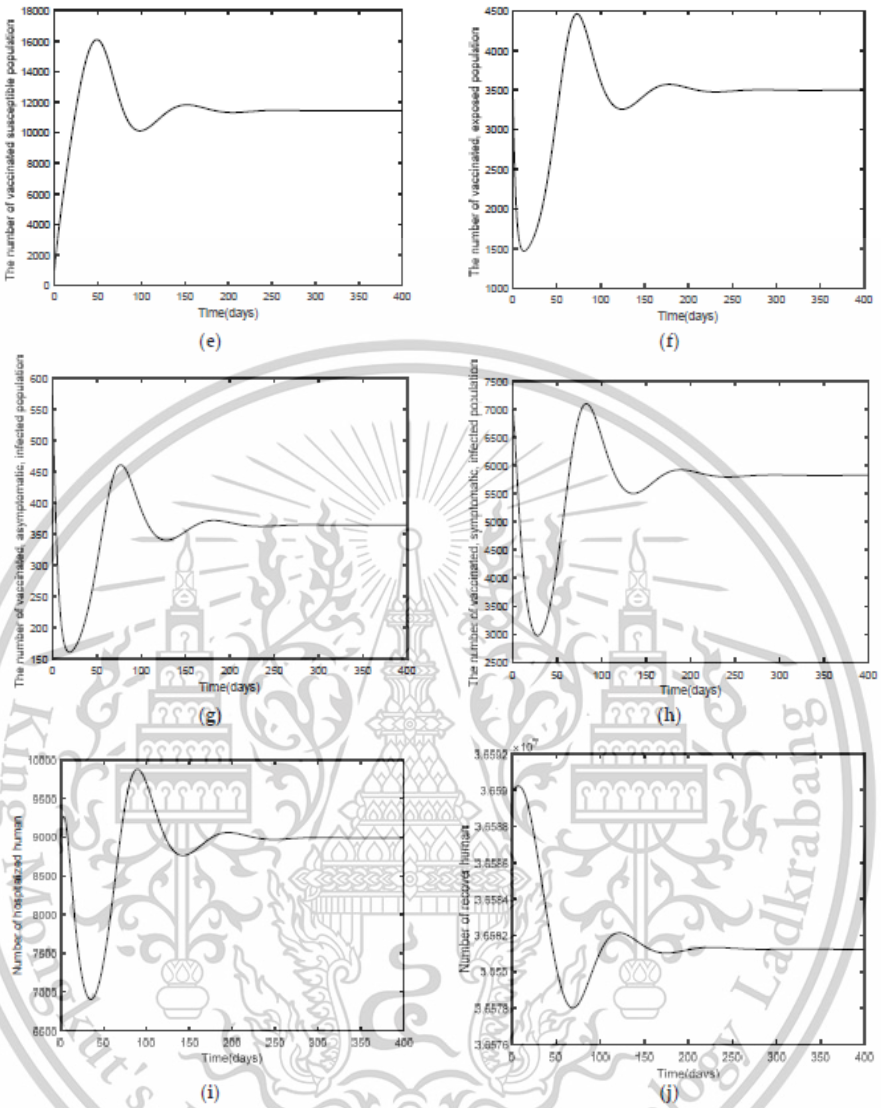

Figure 4. Graphs of the system Equations (3)–(12) at the endemic equilibrium point of S_H, E_H, I_{AH}, I_{SH}, S_V, E_V, I_{AV}, I_{SV}, H_p, and R when $R_0 > 1$: (**a**) the number in the unvaccinated, susceptible population; (**b**) the number in the unvaccinated, exposed population; (**c**) the number in the unvaccinated, asymptomatic, infected population; (**d**) the number in the unvaccinated, symptomatic, infected population; (**e**) the number in the vaccinated susceptible population; (**f**) the number in the vaccinated, exposed population; (**g**) the number in the vaccinated, asymptomatic, infected population; (**h**) the number in the vaccinated, symptomatic, infected population; (**i**) the number in the hospitalized population; and (**j**) the number in the recovered population.

Figures 3 and 4 show the convergence of the number in the unvaccinated, exposed population; the number in the unvaccinated, asymptomatic, infected population; the number in the unvaccinated, symptomatic, infected population; the number in the vaccinated, exposed population; the number in the vaccinated, asymptomatic, infected population; the number in the vaccinated, symptomatic, infected population; the number in the hospitalized population; and the number in the recovered population. It can be noticed that in Figure 3, the graph reached its maximum height and gradually declined to 0, meaning that E_n, I_{an}, I_{sn}, S_v, E_v, I_{av}, I_{sv}, H_p, and R decreased as time progressed. The number in the unvaccinated, susceptible population and the number in the vaccinated, susceptible population would converge to the equilibrium points of 6849 and 20,547, respectively. This result shows that the states S_n and S_v increase as time increases due to the disease-free steady state when $R_0 < 1$. Figure 4 shows the epidemic under the endemic equilibrium point when $R_0 > 1$. Note that in this case, the trajectories experience some overshooting at around day 100 before settling down at the equilibrium points.

The World Health Organization defines the efficacy of vaccines as an overall measure of the ability of the vaccine to reduce the chance of getting infected, the death rate, the severity of the illness, the prolonged hospitalization rate, and the ability of the vaccine to creating herd immunity. The efficacy of vaccination depends on numerous factors, such as individual basic health status, individual age when getting the vaccination, or previous exposure to the disease. All factors have effects on the efficacy of vaccines. The effects of the parameters affecting the spread of COVID-19 are shown in Figures 5–9. Figure 5 shows the comparison of the efficacy of vaccination by comparing the trajectories for the cases of $b = [0.5, 0.6, 0.7, 0.8, 0.9]$ while keeping the other parameters as given in Table 2. Looking at plots in Figure 5a–d, we see that the graphs overlap. When these graphs are magnified, we see that the number of unvaccinated states, S_n, E_n, I_{an}, and I_{sn}, decrease when the efficacy of the vaccines is increased. Another factor affecting the spread of COVID-19 is the infection rate as seen in Figures 6–9. To investigate these cases, we look at the following cases:

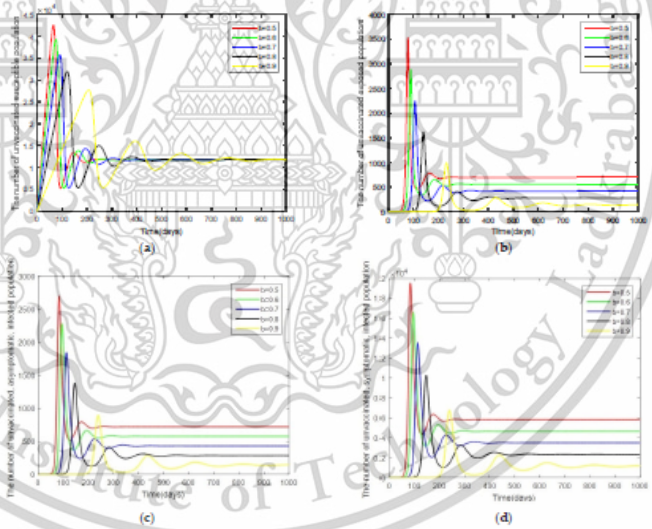

Figure 5. Graphs of the system of Equations (3)–(12) showing the comparison results of efficacy of vaccination (b) when $R_0 > 1$: (**a**) the number in the unvaccinated, susceptible population; (**b**) the number in the unvaccinated, exposed population; (**c**) the number in the unvaccinated, asymptomatic, infected population; and (**d**) the number in the unvaccinated, symptomatic, infected population.

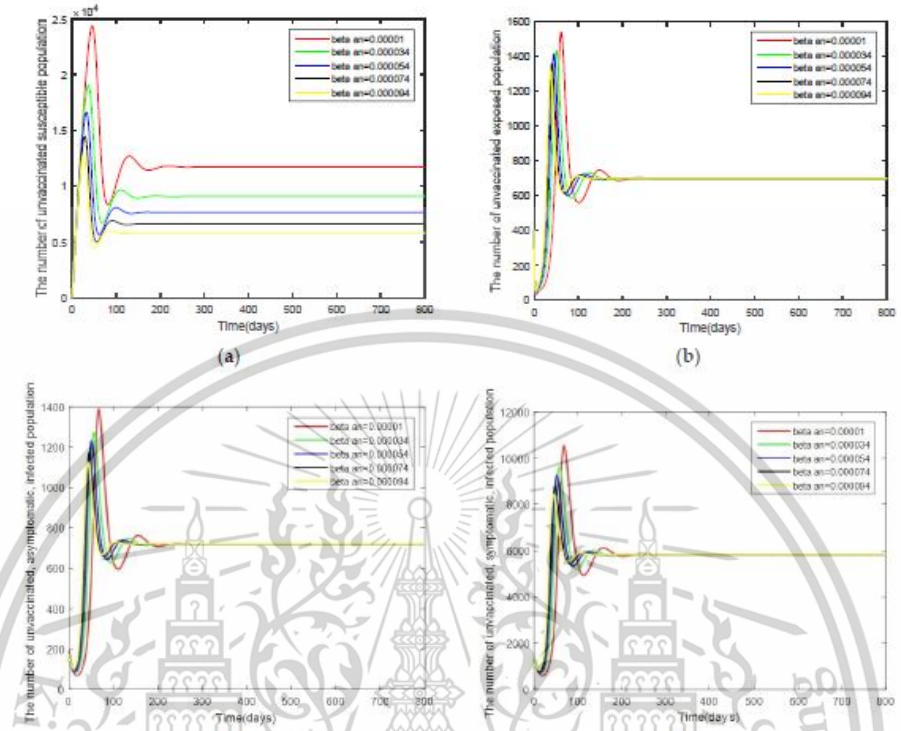

Figure 6. Graphs of the system of Equations (3)–(12) showing the comparison results of the infection rate of the asymptomatic, unvaccinated, infected population (β_{an}) when $R_0 > 1$; (**a**) the number in the unvaccinated, susceptible population; (**b**) the number in the unvaccinated, exposed population; (**c**) the number in the unvaccinated, asymptomatic, infected population; and (**d**) the number in the unvaccinated, symptomatic, infected population.

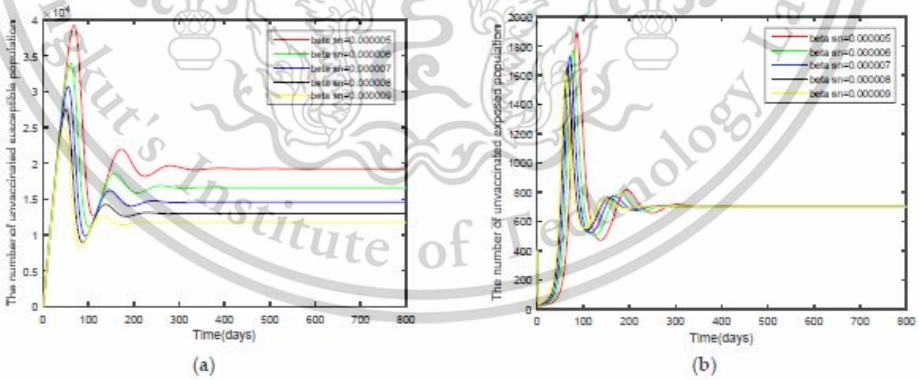

Figure 7. *Cont.*

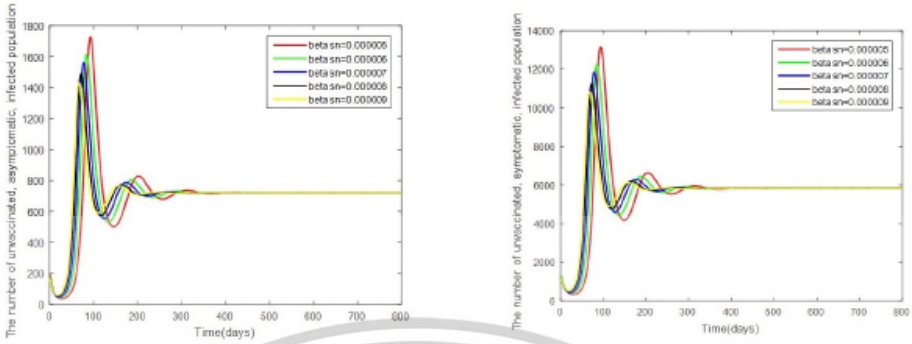

(c) (d)

Figure 7. Graphs of the system of Equations (3)–(12) showing the comparison results of the infection rate of the symptomatic, unvaccinated, infected population (β_{SU}) when $R_0 > 1$: (**a**) the number in the unvaccinated, susceptible population; (**b**) the number in the unvaccinated, exposed population; (**c**) the number in the unvaccinated, asymptomatic, infected population; and (**d**) the number in the unvaccinated, symptomatic, infected population.

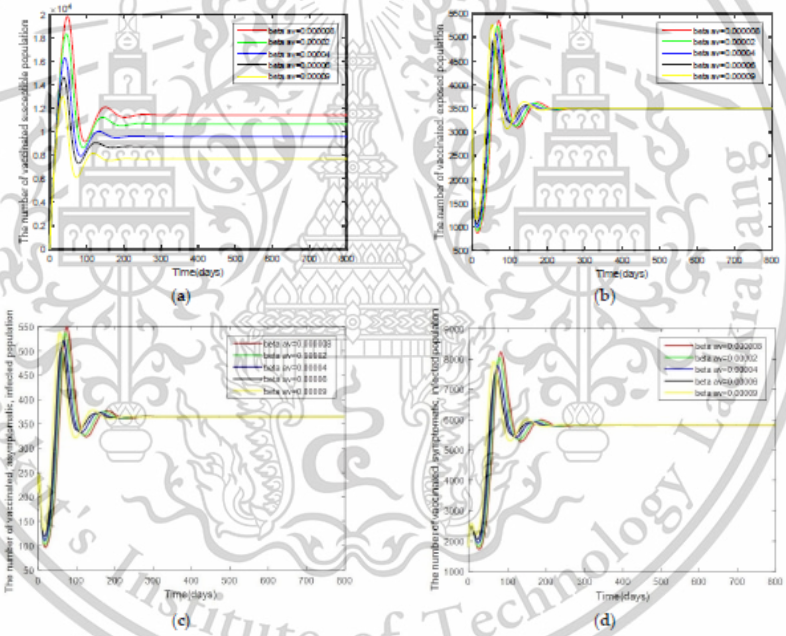

(a) (b) (c) (d)

Figure 8. Graphs of the system of Equations (3)–(12) showing the comparison results of the infection rate of the asymptomatic, vaccinated, infected population (β_{SV}) when $R_0 > 1$: (**a**) the number in the vaccinated, susceptible population; (**b**) the number in the vaccinated, exposed population; (**c**) the number in the vaccinated, asymptomatic, infected population; and (**d**) the number in the vaccinated, symptomatic, infected population.

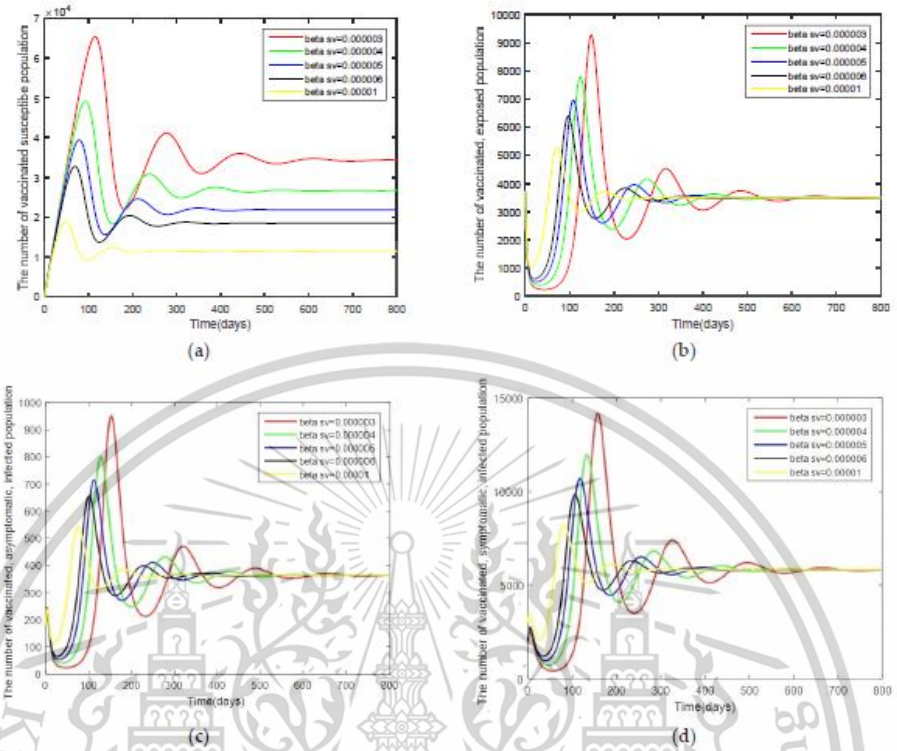

Figure 9. Graphs of the system of Equations (3)–(12) showing the comparison results of the infection rate of the symptomatic, vaccinated, infected population (β_{sv}) when $R_0 > 1$: (**a**) the number in the vaccinated, susceptible population; (**b**) the number in the vaccinated, exposed population; (**c**) the number in the vaccinated, asymptomatic, infected population; and (**d**) the number in the vaccinated, symptomatic, infected population.

Case 1: Changes in β_{av}. Here, the system is simulated with β_{av} = [0.00001, 0.000034, 0.000054, 0.000074, 0.000094] while keeping the other parameters as given by Table 2.
Case 2: Changes in β_{sv}. In this case, the system is resimulated with β_{sv} = [0.000005, 0.000006, 0.000007, 0.000008, 0.000009] while keeping the other parameters as given by Table 2.
Case 3: Changes in β_{av}. In this case, the system is resimulated with β_{av} = [0.000008, 0.00002, 0.00004, 0.00006, 0.00009] while keeping the other parameters as given by Table 2.
Case 4: Changes in β_{sv}. In this case, the system is resimulated with β_{sv} = [0.000003, 0.000004, 0.000005, 0.000006, 0.00001] while keeping the other parameters as given by Table 2.

For the susceptible people (both vaccinated and unvaccinated), it is seen from Figures 5–9 that a low infection rate causes a slow convergence to an equilibrium point, meaning that disease control will be slower. As for the group of the exposed population, both unvaccinated and vaccinated, exhibiting both symptomatic and asymptomatic symptoms, an infection rate increment causes a quicker convergence to the equilibrium point, contributing to a more rapid onset of disease control. It can be seen that the comparison of the efficacy of vaccination and the infection rate is a better means to control the spread of the dis-

ease. To minimize the spread of the disease immediately, everyone needs to strictly follow preventive measures, wear a mask, wash hands thoroughly, and keep social distancing.

3.3. Sensitivity Analysis of Parameters

A sensitivity analysis of the basic reproduction number reveals the parameter values that can affect the numerical simulation model results. In addition, it will indicate the importance of each parameter that affects the basic reproduction number, whose number indicates the spread of the disease. Therefore, a sensitivity analysis of the COVID-19 simulation model from (3)–(12) can provide in-depth information about changes in the spread and can help public health agencies to determine strategies for preventing the spread of COVID-19.

Definition 1. (Chitnis, Hyman, and Cushing [39]). *The normalized forward-sensitivity index of a variable, R_0, that depends differentiably on a parameter, κ, is defined as:*

$$Y_{\kappa}^{R_0} = \frac{\partial R_0}{\partial \kappa} \times \frac{\kappa}{R_0} \tag{23}$$

Information in Table 2 is used to show the parameter values for the numerical simulation model. The calculation results of the sensitivity of the basic reproduction number of each parameter are shown in Table 3.

Table 3. Sensitivity values of the basic reproduction numbers.

Parameters	Sensitivity Indices
b	+1.0000
σ	+1.0000
β_{an}	+0.1209
β_{sn}	+0.8791
β_{av}	+0.0730
β_{sv}	+0.9270
δ	+0.0007
ϕ	−0.0026
ω_1	−0.0872
ω_2	−0.8544
ω_3	−0.9009
ω_4	−0.0419
γ_1	−0.0311
γ_2	−0.0299
γ_3	−1.0004
μ	−0.0269

Numerical results from the sensitivity analysis of the basic reproduction number are given in Table 3. If the sensitivity index of the basic reproduction number is positive, it means that an increase (or decrease) in each parameter leads to an increase (or decrease) in the basic reproduction number. Conversely, if the sensitivity index of the basic reproduction number is negative, it means that an increase (or decrease) in each parameter leads to a decrease (or increase) in the basic reproduction number. Consequently, according to the sensitivity analysis of the models (3)–(12), parameters affecting the sensitivity to become positive are b, σ, β_{an}, β_{sn}, β_{av}, β_{sv}, and δ, while parameters affecting the sensitivity to become negative are ϕ, ω_1, ω_2, ω_3, ω_4, γ_2, γ_3, μ, and d.

To sum up, the research results indicate that the most effective control strategy is controlling the rate of vaccinated people (b) and the initial number of people (σ) since the sensitivity index of the parameters is equal to 1. It means that an increase (or decrease) in the rate of vaccinated people, the population birth rate, and the number in the population by 10% enables the basic reproduction number to increase by 10%. The sensitivity analysis

mentioned above causes a reduction in the spread of COVID-19 among people in an efficient manner.

4. Optimal Control Problem

Having analyzed the mathematical model predicting the spread of the COVID-19 in Thailand, an optimal control strategy is now sought in order to help reduce the number of infected people and control and prevent the spread of the disease. In this article, a strategy for controlling COVID-19 in Thailand was proposed by considering the control functions, u_1 and u_2, where u_1 is the rate of vaccination and u_2 is the susceptible group that is changed to the recovered group (due to immunity from the vaccination). According to the optimal control problem, the mathematical model for controlling COVID-19 can be created as follows:

$$\frac{dS_n}{dt} = (1-b)\sigma - \eta_1 S_n - \mu S_n - u_1(t)S_n \tag{24}$$

$$\frac{dE_n}{dt} = \eta_1 S_n - \phi E_n - (1-\phi)E_n - \mu E_n \tag{25}$$

$$\frac{dI_{an}}{dt} = \phi E_n - (\omega_1 + \gamma_2 + \mu + d)I_{an} \tag{26}$$

$$\frac{dI_{sn}}{dt} = (1-\phi)E_n - (\omega_2 + \mu + d)I_{sn} \tag{27}$$

$$\frac{dS_v}{dt} = b\sigma - \eta_2 S_v - \mu S_v - u_2(t)S_v \tag{28}$$

$$\frac{dE_v}{dt} = \eta_2 S_v - (1-\delta)\phi E_v - (1-\delta)(1-\phi)E_v - \mu E_v \tag{29}$$

$$\frac{dI_{av}}{dt} = (1-\delta)\phi E_v - (\omega_4 + \gamma_3 + \mu + d)I_{av} \tag{30}$$

$$\frac{dI_{sv}}{dt} = (1-\delta)(1-\phi)E_v - (\omega_3 + \mu + d)I_{sv} \tag{31}$$

$$\frac{dH_p}{dt} = \omega_1 I_{an} + \omega_2 I_{sv} + \omega_3 I_{sv} + \omega_4 I_{av} - (\gamma_1 + \mu + d)H_p \tag{32}$$

$$\frac{dR}{dt} = \gamma_1 H_p + \gamma_2 I_{an} + \gamma_3 I_{av} - \mu R + u_1(t)S_n + u_2(t)S_v \tag{33}$$

We now seek the optimal control strategy for the system of Equations (24)–(33) using Pontryagin's maximum principle [40,41] to reduce the number of infected people, in other words, the optimal values u_1 and u_2. In light of this, the optimal control problem is determined in terms of the following objective functions:

$$J(u_1(t), u_2(t)) = \int_0^T \left(A_1 I_{an}(t) + A_2 I_{sn}(t) + A_3 I_{av}(t) + A_4 I_{sv}(t) + \frac{1}{2}A_5 {u_1}^2(t) + \frac{1}{2}A_6 {u_2}^2(t) \right) \tag{34}$$

The objective function of the system of Equation (34) depends on hypotheses considering the number of $I_{an}(t)$, $I_{sn}(t)$, $I_{av}(t)$, and $I_{sv}(t)$. Please kindly note that A_1, A_2, A_3, A_4, A_5, and A_6 are the weight constants. The most suitable problem solving guideline of this model is determined by using Lagrangian and Hamiltonian approaches to solve the optimal control problem as follows:

$$L(I_{an}, I_{sn}, I_{av}, I_{sv}, u_1, u_2) = A_1 I_{an}(t) + A_2 I_{sn}(t) + A_3 I_{av}(t) + A_4 I_{sv}(t) + \frac{1}{2}A_5 {u_1}^2(t) + \frac{1}{2}A_6 {u_2}^2(t) \tag{35}$$

Theorem 3. *With a suitable control* $u^* = (u_1^*, u_2^*)$ *and a problem-solving guideline consistent with* S_n, E_n, I_{an}, I_{sn}, S_v, E_v, I_{av}, I_{sv}, H_p, *and* R *for the initial problem (24)–(33) that the minimizes*

$J(u_1, u_2)$, there exists an adjoint variable λ_i, $i = 1, 2, 3, \ldots, 10$ under the control that satisfies the following:

$$\frac{d\lambda_i}{dt} = -\frac{\partial H}{\partial \psi} \tag{36}$$

When $\psi = (S_n, E_n, I_{an}, I_{sn}, S_v, E_v, I_{av}, I_{sv}, H_p, R)$, together with the transversality conditions given as $\lambda_i(T) = 0$ for all $i = 1, 2, 3, \ldots, 10$, and

$$u_1^* = \begin{cases} 0 & if \ \frac{\lambda_1 S_n - \lambda_{10} S_n}{A_5} \leq 0 \\ \frac{\lambda_1 S_n - \lambda_{10} S_n}{A_5} & if \ \frac{\lambda_1 S_n - \lambda_{10} S_n}{A_5} < u_1^{max} \\ u_1^{max} & if \ \frac{\lambda_1 S_n - \lambda_{10} S_n}{A_5} \geq u_1^{max} \end{cases} \tag{37}$$

$$u_2^* = \begin{cases} 0 & if \ \frac{\lambda_5 S_v - \lambda_{10} S_v}{A_6} \leq 0 \\ \frac{\lambda_5 S_v - \lambda_{10} S_v}{A_6} & if \ \frac{\lambda_5 S_v - \lambda_{10} S_v}{A_6} < u_2^{max} \\ u_2^{max} & if \ \frac{\lambda_5 S_v - \lambda_{10} S_v}{A_6} \geq u_2^{max} \end{cases} \tag{38}$$

Proof. The Hamiltonian function can be defined as

$$\begin{aligned} H \quad &= L(I_{an}, I_{sn}, I_{av}, I_{sv}, u_1, u_2) + \lambda_1 \frac{dS_n}{dt} + \lambda_2 \frac{dE_n}{dt} + \lambda_3 \frac{dI_{an}}{dt} + \lambda_4 \frac{dI_{sn}}{dt} + \lambda_5 \frac{dS_v}{dt} + \lambda_6 \frac{dE_v}{dt} \\ &+ \lambda_7 \frac{dI_{av}}{dt} + \lambda_8 \frac{dI_{sv}}{dt} + \lambda_9 \frac{dH_p}{dt} + \lambda_{10} \frac{dR}{dt} \end{aligned}$$

when

$$\begin{aligned} L(I_{an}, I_{sn}, I_{av}, I_{sv}, u_1, u_2) \quad &= A_1 I_{an}(t) + A_2 I_{sn}(t) + A_3 I_{av}(t) + A_4 I_{sv}(t) + \tfrac{1}{2} A_5 {u_1}^2(t) \\ &+ \tfrac{1}{2} A_6 {u_2}^2(t) \end{aligned}$$

is the Lagrangian of the control problem, then we have

$$\begin{aligned} H = \quad & A_1 I_{an}(t) + A_2 I_{sn}(t) + A_3 I_{av}(t) + A_4 I_{sv}(t) + \tfrac{1}{2} A_5 {u_1}^2(t) + \tfrac{1}{2} A_6 {u_2}^2(t) \\ & + \lambda_1 [(1-b)\sigma - \eta_1 S_n - \mu S_n - u_1(t) S_n] \\ & + \lambda_2 [\eta_1 S_n - \phi E_n - (1-\phi) E_n - \mu E_n] \\ & + \lambda_3 [\phi E_n - (\omega_1 + \gamma_2 + \mu + d) I_{an}] \\ & + \lambda_4 [(1-\phi) E_n - (\omega_2 + \mu + d) I_{sn}] \\ & + \lambda_5 [b\sigma - \eta_2 S_v - \mu S_v - u_2(t) S_v] \\ & + \lambda_6 [\eta_2 S_v - (1-\delta)\phi E_v - (1-\delta)(1-\phi) E_v - \mu E_v] \\ & + \lambda_7 [(1-\delta)\phi E_v - (\omega_4 + \gamma_3 + \mu + d) I_{av}] \\ & + \lambda_8 [(1-\delta)(1-\phi) E_v - (\omega_3 + \mu + d) I_{sv}] \\ & + \lambda_9 [\omega_1 I_{an} + \omega_2 I_{sv} + \omega_3 I_{sv} + \omega_4 I_{av} - (\gamma_1 + \mu + d) H_p] \\ & + \lambda_{10} [\gamma_1 H_p + \gamma_2 I_{an} + \gamma_3 I_{av} - \mu R + u_1(t) S_n + u_2(t) S_v] \end{aligned} \tag{39}$$

To obtain the optimal control, adjoint function becomes

$$\begin{aligned} \frac{d\lambda_1}{dt} &= -\frac{\partial H}{\partial S_n} = \lambda_1(t)(\beta_{an} I_{an} + \beta_{sn} I_{sn} + \mu + u_1^*(t)) - \lambda_2(t)(\beta_{an} I_{an} + \beta_{sn} I_{sn}) - \lambda_{10}(t) u_1^*(t) \\ \frac{d\lambda_2}{dt} &= -\frac{\partial H}{\partial E_n} = \lambda_2(t)(1+\mu) - \lambda_3(t)\phi - \lambda_4(t)(1-\phi) \\ \frac{d\lambda_3}{dt} &= -\frac{\partial H}{\partial I_{an}} = \beta_{an} S_n(\lambda_1(t) - \lambda_2(t)) + \lambda_3(t)(d + \gamma_2 + \mu + \omega_1) - \lambda_9(t)\omega_1 - \lambda_{10}(t)\gamma_2 - A_1 \\ \frac{d\lambda_4}{dt} &= -\frac{\partial H}{\partial I_{sn}} = \beta_{sn} S_n(\lambda_1(t) - \lambda_2(t)) + \lambda_4(t)(d + \mu + \omega_2) - \lambda_9(t)\omega_2 - A_2 \\ \frac{d\lambda_5}{dt} &= -\frac{\partial H}{\partial S_v} = \lambda_5(t)(\beta_{av} I_{av} + \beta_{sv} I_{sv} + \mu + u_2^*(t)) - \lambda_6(t)(\beta_{av} I_{av} + \beta_{sv} I_{sv}) - \lambda_{10}(t) u_2^*(t) \\ \frac{d\lambda_6}{dt} &= -\frac{\partial H}{\partial E_v} = \lambda_6(t)(\mu + (1-\delta)(1-\phi) + (1-\delta)\phi) - \lambda_7(t)(1-\delta)\phi - \lambda_8(t)(1-\delta)(1-\phi) \\ \frac{d\lambda_7}{dt} &= -\frac{\partial H}{\partial I_{av}} = \beta_{av} S_v(\lambda_5(t) - \lambda_6(t)) + \lambda_7(t)(d + \gamma_3 + \mu + \omega_4) - \lambda_9(t)\omega_4 - \lambda_{10}(t)\gamma_3 - A_3 \\ \frac{d\lambda_8}{dt} &= -\frac{\partial H}{\partial I_{sv}} = \beta_{sv} S_v(\lambda_5(t) - \lambda_6(t)) + \lambda_8(t)(d + \mu + \omega_3) - \lambda_9(t)\omega_3 - A_4 \\ \frac{d\lambda_9}{dt} &= -\frac{\partial H}{\partial H_p} = \lambda_9(t)(d + \mu + \gamma_1) - \lambda_{10}(t)\gamma_1 \\ \frac{d\lambda_9}{dt} &= -\frac{\partial H}{\partial R} = \lambda_{10}(t)\mu \end{aligned}$$

The characterization of the suitable controls, u_1^* and u_2^*, depends on $\frac{\partial H}{\partial u_j} = 0$ for all $j = 1, 2$ at $u_j = u_j^*$ at $j = 1, 2$.

Therefore,

$$\frac{\partial H}{\partial u_1} = A_5 u_1 - \lambda_1 S_n + \lambda_{10} S_n \Rightarrow u_1^* = \frac{\lambda_1 S_n - \lambda_{10} S_n}{A_5}$$
$$\frac{\partial H}{\partial u_2} = A_6 u_2 - \lambda_5 S_v + \lambda_{10} S_v \Rightarrow u_2^* = \frac{\lambda_5 S_v - \lambda_{10} S_v}{A_6}$$

Thus, the optimal control function for COVID-19 can be defined as follows:

$$u_1^* = \begin{cases} 0 & if \ \frac{\lambda_1 S_n - \lambda_{10} S_n}{A_5} \leq 0 \\ \frac{\lambda_1 S_n - \lambda_{10} S_n}{A_5} & if \ \frac{\lambda_1 S_n - \lambda_{10} S_n}{A_5} < u_1^{max} \\ u_1^{max} & if \ \frac{\lambda_1 S_n - \lambda_{10} S_n}{A_5} \geq u_1^{max} \end{cases}$$

$$u_2^* = \begin{cases} 0 & if \ \frac{\lambda_5 S_v - \lambda_{10} S_v}{A_6} \leq 0 \\ \frac{\lambda_5 S_v - \lambda_{10} S_v}{A_6} & if \ \frac{\lambda_5 S_v - \lambda_{10} S_v}{A_6} < u_2^{max} \\ u_2^{max} & if \ \frac{\lambda_5 S_v - \lambda_{10} S_v}{A_6} \geq u_2^{max} \end{cases}$$

□

Figures 10 and 11 show the numerical analysis of the optimal control policy. The equations were solved using the fourth order Runge–Kutta forward–backward sweep method [33]. For all simulation models, time T was determined to be 120 days. Controlled weight values were $A_1 = 1000$, $A_2 = 900$, $A_3 = 700$, $A_4 = 500$, $A_5 = 300$, and $A_6 = 100$. It can be clearly seen that the cases with control converged to an equilibrium point more quickly than the cases without the optimal control. As a consequence, it can be concluded that a good preventive policy through vaccination to develop immunity to the body is a suitable method to reduce the prevalence of the spread of the disease.

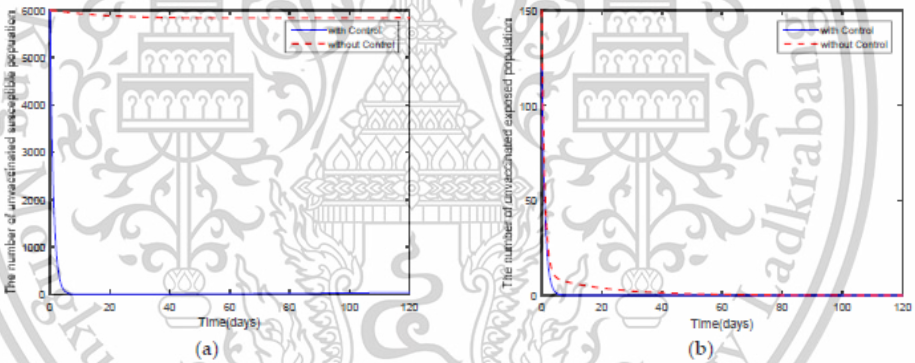

Figure 10. *Cont.*

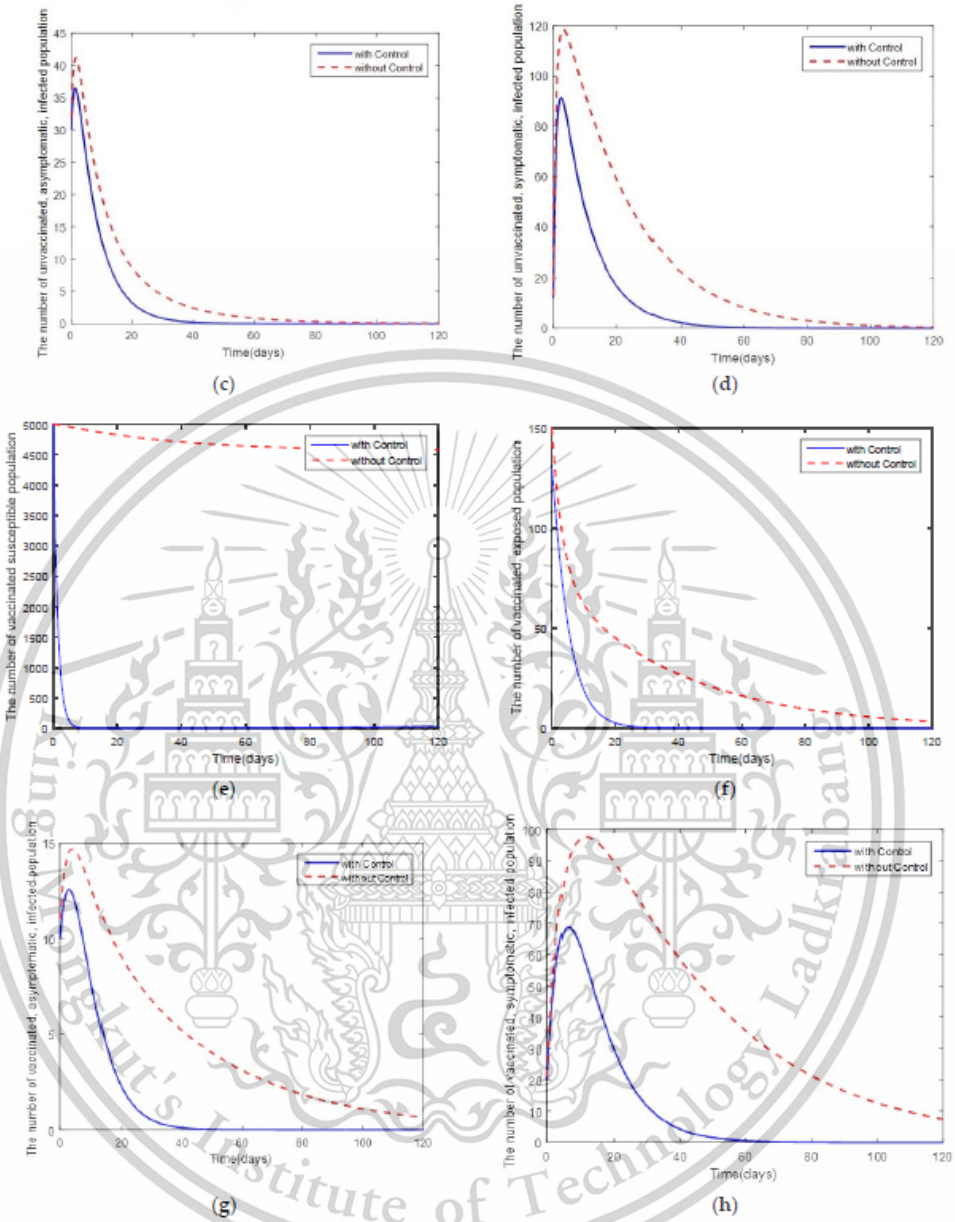

Figure 10. *Cont.*

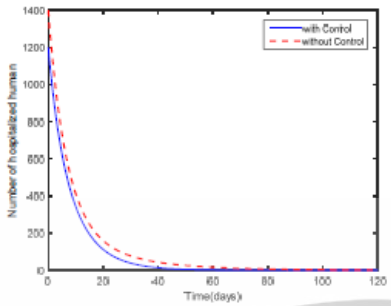

(i)

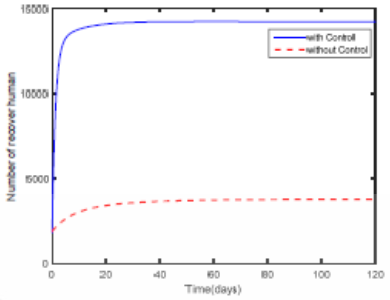

(j)

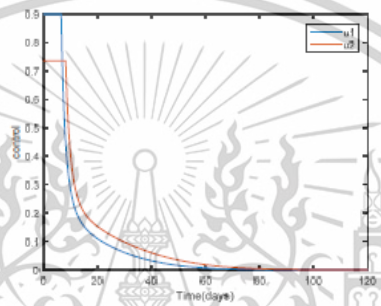

(k)

Figure 10. Comparison between the cases with control and the cases without control for the disease-free: (**a**) the number in the unvaccinated, susceptible population; (**b**) the number in the unvaccinated, exposed population; (**c**) the number in the unvaccinated, asymptomatic, infected population; (**d**) the number in the unvaccinated, symptomatic, infected population; (**e**) the number in the vaccinated, susceptible population; (**f**) the number in the vaccinated, exposed population; (**g**) the number in the vaccinated, asymptomatic, infected population; (**h**) the number in the vaccinated, symptomatic, infected population; (**i**) the number in the hospitalized population; (**j**) the number in the recovered population; and (**k**) control efforts $u_1(t)$ and $u_2(t)$.

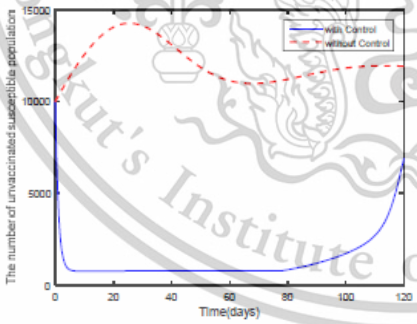

(a)

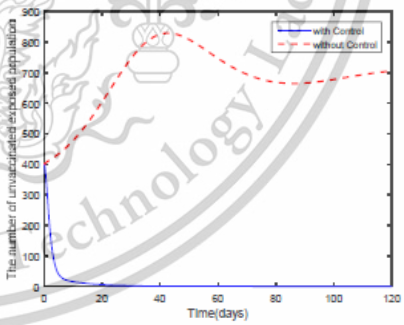

(b)

Figure 11. *Cont.*

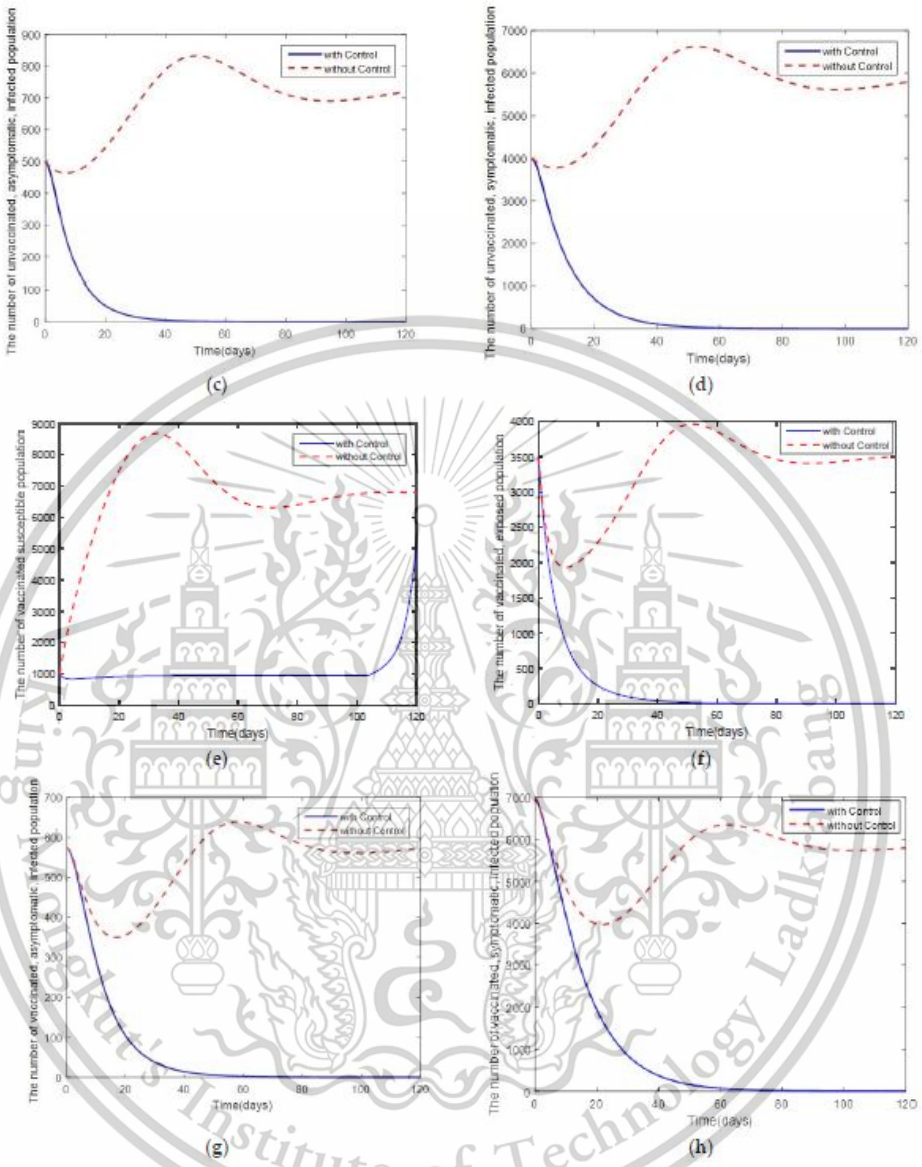

Figure 11. *Cont.*

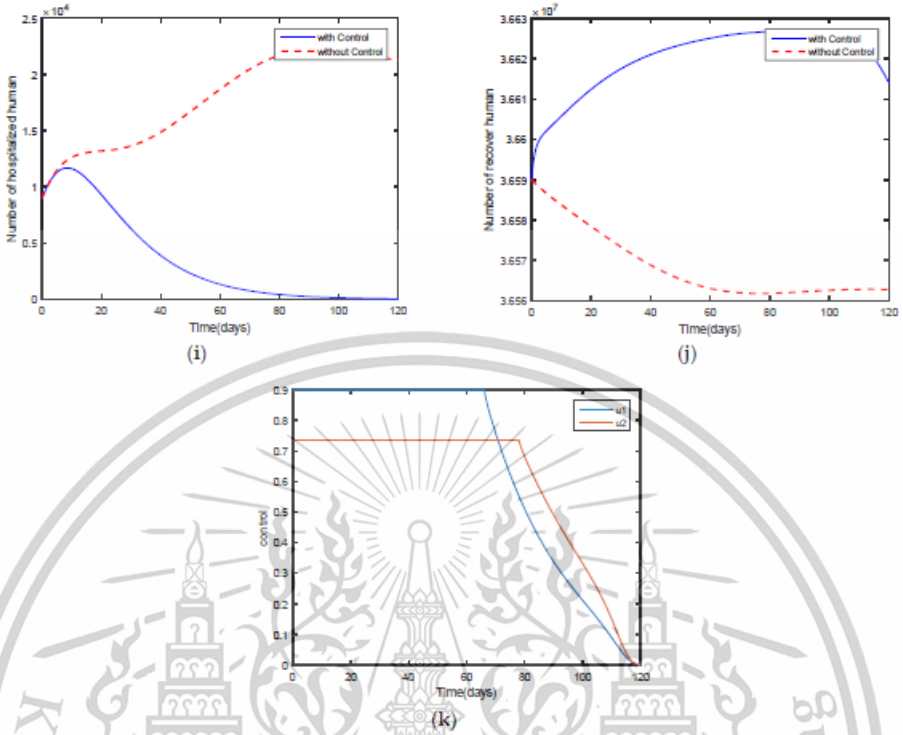

Figure 11. Comparison between the cases with control and the cases without control for the endemic: (**a**) the number in the unvaccinated, susceptible population; (**b**) the number in the unvaccinated, exposed population; (**c**) the number in the unvaccinated, asymptomatic, infected population; (**d**) the number in the unvaccinated, symptomatic, infected population; (**e**) the number in the vaccinated, susceptible population; (**f**) the number in the vaccinated, exposed population; (**g**) the number in the vaccinated, asymptomatic, infected population; (**h**) the number in the vaccinated, symptomatic, infected population; (**i**) the number in the hospitalized population; (**j**) the number in the recovered population; and (**k**) control efforts $u_1(t)$ and $u_2(t)$.

5. Discussion and Conclusions

This study shows the details of a mathematical model to control COVID-19, a pandemic currently infecting the world. It is based on the mathematical description of what is happening around the world. The current study is based on parameters which are appropriate in Thailand, one of the countries experiencing the infection. The mathematical model is created by considering two groups of people: the unvaccinated people and the vaccinated people. Standard dynamic modeling is used to study, analyze, and find the equilibrium points and establish stability. From this study, two equilibrium points were obtained, namely the disease-free equilibrium point (G_0^*) and the endemic equilibrium point (G_1^*), according to parameter conditions. The Lyapunov function was used to determine the stability of each equilibrium point. From the simulation model, the basic reproduction number (R_0) was obtained by considering the basic reproduction number of the disease-free steady states and the endemic steady states. It can be seen that the disease-free steady states are stable when ($R_0 < 1$) and the endemic steady states are stable when ($R_0 > 1$). According to *the* sensitivity analysis of the parameters, the efficacy

of vaccination (b) and the infection rates (β_{an}, β_{sn}, β_{av}, and β_{sv}) are the most sensitive parameters that contribute to an increase in the spread of COVID-19. It is noticeable that the infection rate is highly important. Therefore, to design a usable optimal control strategy for containing the spread of the Omicron variant in Thailand, a curve fitting algorithm was performed on the real-world Omicron data to analyze and seek the most suitable value of the infection rate to ensure it is similar to the current situation. The results in Figure 2 confirmed that this is so.

To examine and confirm the analysis results for the effects of the spread, parameter values were chosen to be the values given in Table 2, incorporating the fitted parameters. According to Figure 5, considering of the efficacy of the vaccines, it was found that if the efficacy of the vaccines increases, spread control is achieved more quickly. Considering the infection rate showed that when the rate of spread increased, the basic reproduction number increased, since the basic reproduction number is the average number of secondary infections which can be caused by a patient in a completely susceptible population throughout his infectious period. If the infection rate is high, the epidemic shall spread at a slower rate when the infection rate is low. Therefore, if the basic reproduction number is high, the epidemic would spread at a fast rate and converge to an equilibrium point more quickly when the basic reproduction is low. From what was mentioned above, it can be seen that Figures 6–9 follow the above-mentioned conditions. Nonetheless, there are a lot of factors affecting the spread. The spread can be minimized by planning and formulating policies. In this regard, the optimal control strategy is used by considering the rate of vaccination and immunity achieved from vaccination to reduce the spread of COVID-19. It can be concluded that the spread of COVID-19 can be controlled and minimized by vaccination and self-care practices following preventive measures, as seen in Figures 10 and 11. Note that the main limitation of our model is that we did not use the multiple-patch model, where the Omicron outbreak in the rural regions is different from the one in the city because of the population density and socioeconomics. Nevertheless, the model used in this paper is simple enough to capture the main dynamics of the system and allows for the conjuration of suitable optimal control to combat the spread.

In conclusion, the use of the control strategy for disease prevention is a guideline to help prevent and control the spread of the disease. There are many strategies for disease control, such as social distancing, wearing masks, or following preventive measures introduced by the government. Future research should determine other strategies to help control and prevent COVID-19, accordingly.

Author Contributions: Conceptualization, J.L., P.P. and N.W.; methodology, J.L.; software, N.W.; validation, J.L., P.P., L-M.T. and N.W.; writing—original draft preparation, J.L.; writing—review and editing, J.L., P.P., L-M.T. and N.W.; supervision, P.P., L-M.T. and N.W.; project administration, P.P.; funding acquisition, P.P. All authors have read and agreed to the published version of the manuscript.

Funding: This work is supported by the School of Science, King Mongkut's Institute of Technology Ladkrabang, Grant Number (2564-02-05-008).

Data Availability Statement: Data are available from the corresponding author upon reasonable request.

Acknowledgments: Jiraporn Lamwong is the recipient of the Graduate Study Fellowship of the School of Science, King Mongkut's Institute of Technology Ladkrabang, Thailand. This research was funded by the RA-TA graduate scholarship from the School of Science, King Mongkut's Institute of Technology Ladkrabang, grant number RA/TA-2565-D-001.

Conflicts of Interest: The authors declare no conflict of interest.

References

1. Chaharborj, S.S.; Hassanzadeh, J.; Phang, P.C. Controlling of pandemic COVID-19 using optimal control theory. *Results Phys.* **2021**, *26*, 104311. [CrossRef]
2. Jankhonkhan, J.; Sawangtong, W. Model Predictive Control of COVID-19 pandemic Concerning Social Isolation and Vaccination Policies in Thailand. *Axioms* **2021**, *10*, 274. [CrossRef]

3. Lina, Q.; Zhaob, S.; Gaod, D.; Loue, Y.; Yangf, S.; Musae, S.S.; Wangb, M.H.; Caig, Y.; Wangg, W.; Yangh, L.; et al. A conceptual model for the coronavirus disease 2019 (COVID-19) outbreak in Wuhan, China with individual reaction and governmental action. *Int. J. Infect. Dis.* **2020**, *93*, 211–216. [CrossRef]
4. Feng, L.X.; Jing, S.L.; Hu, S.K.; Wang, D.F.; Huo, H.F. Modelling the effects of media coverage and quarantine on the COVID-19 infections in the UK. *Math. Biosci. Eng.* **2020**, *17*, 3618–3636. [CrossRef]
5. Prathumwan, D.; Trachoo, K.; Chaiya, I. Mathematical Modeling for Prediction Dynamics of the Coronavirus Disease 2019 (COVID-19) Pandemic, Quarantine Control Measures. *Symmetry* **2020**, *12*, 1404. [CrossRef]
6. Win, Z.T.; Eissa, M.A.; Tian, B. Stochastic Epidemic Model for COVID-19 Transmission under Intervention Strategies in China. *Mathematics* **2022**, *10*, 3119. [CrossRef]
7. Yang, C.; Wang, J. Modeling the transmission of COVID-19 in the US-A case study. *Infect. Dis. Model.* **2021**, *6*, 195–211. [CrossRef]
8. Zhanga, Z.; Jain, S. Mathematical model of Ebola and Covid-19 with fractional differential operators: Non-Markovian process and class for virus pathogen in the environment. *Chaos Solit. Fract.* **2020**, *140*, 110175. [CrossRef]
9. Diagne, M.L.; Rwezaura, H.; Tchoumi, S.Y.; Tchuenche, J.M. A Mathematical Model of COVID-19 with Vaccination and Treatment. *Comput. Math. Methods Med.* **2021**, *2021*, 1250129. [CrossRef]
10. Iboi, E.A.; Sharomi, O.; Ngonghala, C.N.; Gumel, A.B. Mathematical modeling and analysis of COVID-19 pandemic in Nigeria. *Math. Biosci. Eng.* **2020**, *17*, 7192–7220. [CrossRef]
11. Ndaïrou, F.; Area, I.; Nieto, J.J.; Torres, D.F.M. Mathematical modeling of COVID-19 transmission dynamics with a case study of Wuhan. *Chaos Solit. Fract.* **2020**, *135*, 109846. [CrossRef] [PubMed]
12. Faruk, O.; Kar, S. A Data Driven Analysis and Forecast of COVID-19 Dynamics during the Third Wave Using SIRD Model in Bangladesh. *COVID* **2021**, *1*, 43. [CrossRef]
13. Wang, L.; Dai, Y.; Wang, R.; Sun, Y.; Zhang, C.; Yang, Z.; Sun, Y. SEIARN: Intelligent Early Warning Model of Epidemic Spread Based on LSTM Trajectory Prediction. *Mathematics* **2022**, *10*, 3046. [CrossRef]
14. World Health Organization. COVID-19—WHO Thailand Situation Reports. Available online: https://www.who.int/thailand/emergencies/novel-coronavirus-2019/situation-reports (accessed on 29 June 2022).
15. Kermack, W.O.; McKndrick, A.G.; Walker, G.T. A contribution to the mathematical theory of epidemics. *R. Soc. Lond. Ser. A Contain. Pap. Math. Phys. Charact.* **1927**, *115*, 700–721.
16. Lamwong, J.; Pongsumpun, P.; Tang, I.M.; Wongvanich, N. The Lyapunov Analyses of MERS-Cov Transmission in Thailand. *Curr. Appl. Sci. Technol.* **2019**, *19*, 112–123.
17. Etbaigha, F.; Willms, A.R.; Poljak, Z. An SEIR model of influenza A virus infection and reinfection within a farrow-to-finish swine farm. *PLoS ONE* **2018**, *13*, e0202493. [CrossRef]
18. Islam, R.; Biswas, M.H.A.; Jamali, A.R.M. Mathematical analysis of Epidemiological Model of Influenza A (H1N1) Virus Transmission Dynamics in Bangladesh Perspective. *GANIT J. Bangladesh. Math. Soc.* **2017**, *37*, 39–50. [CrossRef]
19. Rezapour, S.; Mohammadi, H. A study on the AH1N1/09 influenza transmission model with the fractional Caputo–Fabrizio derivative. *Adv. Diff. Equ.* **2020**, *2020*, 488. [CrossRef]
20. Chanprasopchai, P.; Pongsumpun, P.; Tang, I.M. Effect of Rainfall for the Dynamical Transmission Model of the Dengue Disease in Thailand. *Comput. Math. Methods Med.* **2017**, *2017*, 17. [CrossRef]
21. Bhuju, G.; Phaijoo, G.R.; Gurung, D.B. Fuzzy Approach Analyzing SEIR-SEI Dengue Dynamics. *Biomed. Res. Int.* **2020**, *2020*, 11. [CrossRef]
22. Gardner, L.M.; Rey, D.; Heywood, A.E.; Toms, R.; Wood, J.; Travis Waller, S.; Raina MacIntyre, C. A scenario-based evaluation of the Middle East respiratory syndrome coronavirus and the Hajj. *Risk. Anal.* **2014**, *34*, 1391–1400. [CrossRef] [PubMed]
23. Sen, D.; Sen, D. Use of a Modified SIRD Model to Analyze COVID-19 Data. *Ind. Eng. Chem. Res.* **2021**, *60*, 4251–4260. [CrossRef]
24. Kumar, H.; Arora, P.K.; Pant, M.; Kumar, A.; Shahroz, A.K. A simple mathematical model to predict and validate the spread of Covid-19 in India. *Mater. Today Proc.* **2021**, *47*, 3859–3864. [CrossRef] [PubMed]
25. Hezam, I.M.; Foul, A.; Alrasheedi, A. A dynamic optimal control model for COVID-19 and cholera co-infection in Yemen. *Adv. Differ. Equ.* **2021**, *2021*, 108. [CrossRef]
26. Riyapan, P.; Shuaib, S.E.; Intarasit, A. A Mathematical Model of COVID-19 Pandemic: A Case Study of Bangkok, Thailand COVID-19. *Comput. Math. Methods Med.* **2021**, *2021*, 6664483. [CrossRef]
27. Rajput, A.; Sajid, M.; Tanvi; Shekhar, C.; Aggarwal, R. Optimal control strategies on COVID-19 infection to bolster the efcacy of vaccination in India. *Sci. Rep.* **2021**, *11*, 20124. [CrossRef]
28. Dipo Aldila, D.; Shahzad, M.; Khoshnaw, A.H.A.; Ali, M.; Sultan, F.; Islamilova, A.; Anwar, Y.R.; Samiadji, B.M. Optimal control problem arising from COVID-19 transmission model with rapid-test. *Results Phys.* **2020**, *37*, 105501. [CrossRef]
29. Tchoumi, S.Y.; Diagne, M.L.; Rwezaurac, H.; Tchuenche, J.M. Malaria and COVID-19 co-dynamics: A mathematical model and optimal control. *Appl. Math. Model.* **2021**, *99*, 294–327. [CrossRef]
30. Driessche, P.V.; Watmough, J. Reproduction numbers and sub-threshold endemic equilibria for compartmental models of disease transmission. *Math. Biosci.* **2020**, *180*, 29–48. [CrossRef]
31. Abioye, A.I.; Peter, O.J.; Ogunseye, H.A.; Oguntolu, F.A.; Oshinubi, K.; Ibrahim, A.A.; Khan, I. Mathematical model of COVID-19 in Nigeria with optimal control. *Results Phys.* **2020**, *28*, 104598. [CrossRef]
32. La Salle, J.P. *The Stability of Dynamical Systems*; Society for Industrial and Applied Mathematics: Philadelphia, PA, USA, 1976.

33. Adepoju, O.A.; Samson Olaniyi, S. Stability and optimal control of a disease model with vertical transmission and saturated incidence. *Sci. Afri.* **2021**, *12*, e00800. [CrossRef]
34. Gatyeni, S.P.; Chirove, F.; Nyabadza, F. Modelling the Potential Impact of Stigma on the Transmission Dynamics of COVID-19 in South Africa. *Mathematics* **2022**, *10*, 3253. [CrossRef]
35. Lahodny, G. *Curve Fitting and Parameter Estimation*; Springer: Berlin/Heidelberg, Germany, 2015; pp. 1–18.
36. Arruda, E.F.; Das, S.S.; Dias, C.M.; Pastore, D.H. Modelling and optimal control of multi strain epidemics, with application to COVID-19. *PLoS ONE* **2021**, *16*, e0257512. [CrossRef] [PubMed]
37. Lamwong, J.; Tang, I.; Pongsumpun, P. Mers model of Thai and South Korean population. *Curr. Appl. Sci. Technol.* **2018**, *18*, 45–57.
38. Husniah, H.; Ruhanda, R.; Supriatna, A.K.; Biswas, M.H.A. SEIR Mathematical Model of Convalescent Plasma Transfusion to Reduce COVID-19 Disease Transmission. *Mathematics* **2021**, *9*, 2857. [CrossRef]
39. Chitnis, N.; Hyman, J.M.; Cushing, J.M. Determining important parameters in the spread of malaria through the sensitivity analysis of a mathematical model. *Bull. Math. Biol.* **2008**, *70*, 1272–1296. [CrossRef]
40. Lenhart, S.; Workman, J.T. *Optimal Control Applied to Biological Models*; Chapman & Hall/CRC: London, UK, 2007.
41. Pontryagin, L.S.; Boltyanskii, V.G.; Gamkrelidze, R.V.; Mishchenko, E.F. *The Mathematical Theory of Optimal Processes*; Wiley: New York, NY, USA, 1962.

Appendix C

Paper 3

Optimal Control Strategy of a Mathematical Model for the Fifth Wave of COVID-19 Outbreak (Omicron) in Thailand

mathematics

MDPI

Article

Optimal Control Strategy of a Mathematical Model for the Fifth Wave of COVID-19 Outbreak (Omicron) in Thailand

Jiraporn Lamwong [1], Napasool Wongvanich [2], I-Ming Tang [3] and Puntani Pongsumpun [1,*]

[1] Department of Mathematics, School of Science, King Mongkut's Institute of Technology Ladkrabang, Bangkok 10520, Thailand
[2] Department of Instrumentation and Control Engineering, School of Engineering, King Mongkut's Institute of Technology Ladkrabang, Bangkok 10520, Thailand
[3] Department of Physics, Faculty of Science, Mahidol University, Bangkok 10400, Thailand
* Correspondence: puntani.po@kmitl.ac.th; Tel.: +66-2329-8000

Abstract: The world has been fighting against the COVID-19 Coronavirus which seems to be constantly mutating. The present wave of COVID-19 illness is caused by the Omicron variant of the coronavirus. The vaccines against the five variants (α, β, γ, δ, and ω) have been quickly developed using mRNA technology. The efficacy of the vaccine developed for one of the strains is not the same as the efficacy of the vaccine developed for the other strains. In this study, a mathematical model of the spread of COVID-19 was made by considering asymptomatic population, symptomatic population, two infected populations and quarantined population. An analysis of basic reproduction numbers was made using the next-generation matrix method. Global asymptotic stability analysis was made using the Lyapunov theory to measure stability, showing an equilibrium point's stability, and examining the model with the fact of COVID-19 spread in Thailand. Moreover, an analysis of the sensitivity values of the basic reproduction numbers was made to verify the parameters affecting the spread. It was found that the most common parameter affecting the spread was the initial number in the population. Optimal control problems and social distancing strategies in conjunction with mask-wearing and vaccination control strategies were determined to find strategies to give better control of the spread of disease. Lagrangian and Hamiltonian functions were employed to determine the objective function. Pontryagin's maximum principle was employed to verify the existence of the optimal control. According to the study, the use of social distancing in conjunction with mask-wearing and vaccination control strategies was able to achieve optimal control rather than controlling just one or another.

Keywords: COVID-19; optimal control; model fitting; global stability; dynamics model

MSC: 37M05

check for updates

Citation: Lamwong, J.; Wongvanich, N.; Tang, I.-M.; Pongsumpun, P. Optimal Control Strategy of a Mathematical Model for the Fifth Wave of COVID-19 Outbreak (Omicron) in Thailand. *Mathematics* 2024, *12*, 14. https://doi.org/10.3390/math12010014

Academic Editor: Jin Wang

Received: 13 November 2023
Revised: 12 December 2023
Accepted: 15 December 2023
Published: 20 December 2023

1. Introduction

COVID-19 was first reported in December 2019 [1–6], and people all over the world have faced the challenges of the COVID-19 public health crisis. Their way of life and their economy [7] were affected since the governments needed to issue many lockdown measures to reduce the spread. Shops, department stores, and many places were closed down. Meanwhile, the use of social distancing for participating in social activities was employed to reduce the disease spread. Coronavirus disease 2019 or COVID-19 is a contagious disease caused by the virus severe acute respiratory syndrome Coronavirus 2 or SARS-CoV-2 [8–16], affecting the human respiratory system. COVID-19 virus can spread via droplets via from coughing, sneezing, and exposure to body secretions. The most common symptoms found among people infected with COVID-19 are cough, sore throat, runny nose or nasal congestion, loss of smell and taste, and breath difficulty, some people have severe pneumonia which sometimes can lead to death. The incubation period of COVID-19 is 2–14 days after

getting the virus [11,12,17–19]. COVID-19 virus is one of the most widely mutating viruses. The World Health Organization (WHO) identified all five Coronavirus variants, i.e., Alpha, Beta, Gamma, Delta, and more recently Omicron [19,20]. The Omicron COVID-19 variant was first found in South Africa towards the end of November 2021 [21–23] and Thailand detected its first case of Omicron at the beginning of January 2022. The Omicron variant has more than 50 mutations, compared to SARS-CoV-2 [22,23], and spreads significantly faster. Therefore, its spread has to be closely monitored.

The World Health Organization (WHO) reported the worldwide spread of COVID-19. As of 31 May 2023 the total number of confirmed COVID-19 cases globally was 767.36 million and the total number of COVID-19 deaths globally was 6.93 million. As for cumulative confirmed COVID-19 cases by world region, Europe had 276.46 million, Western Pacific had 203.87 million, Americans had 192.94 million, Eastern Mediterranean had 23.37 million, and Africa had 9.53 million. The top three countries with the highest number of confirmed COVID-19 cases were the United States of America (103.43 million cases), China (99.28 million cases), and India (44.99 million cases). The top three countries with the greatest number of COVID-19 deaths were the United States of America (1.12 million deaths), Brazil (702,000 deaths) and India (531,000 deaths) [24]. In Thailand, from 3 Jan 2020 to 31 May 2023, there were 4.73 million confirmed COVID-19 cases and 34,000 COVID-19 deaths [25]. Though the number of COVID-19 patients significantly decreased, the importance given to how to reduce the number of patients is necessary to reduce the spread of the disease. Social distancing, quarantine, and vaccination are effective measures that help control the outbreak and reduce the spread of the disease [10,26–29]. According to WHO's report on 29 May 2023, 1.33 billion doses of COVID-19 vaccines were given to people, and people in Thailand were given 139.17 million doses of COVID-19 vaccines. Vaccination is a measure that helps control the outbreak effectively.

In order to manage the COVID-19 pandemic, a mathematical model is employed to analyze situations and formulate policies to reduce the disease spread. Numerous researchers proposed different models of the spread of COVID-19 to investigate dynamics of COVID-19 spread. Lamwong et al. [30] proposed a SEIQR mathematical model for MERS-CoV by considering two groups of the population, namely, a group of the Thai population and a group of tourists from South Korea traveling to Thailand to see the effects of infections introduced by tourists. Sardar et al. [31] created a mathematical model for MERS-CoV infection based on the spread of two variants by monitoring social behavior to investigate and predict an outbreak during 2012–2016. Mwalili et al. [32] created a COVID-19 model based on the SEIR model by considering pathogens in the environment and social distancing. It was found that non-adherence to social distancing may contribute to an outbreak while quarantine for infectious individuals can help stop the spread. Yohanes et al. [33] proposed a SEIR model to describe the spread of COVID-19. An optimal measure was used to reduce the number of infectious patients, to reduce expenses spent on vaccines, and to reduce medical expenditures as much as possible. It was found that getting vaccinated for COVID-19 could decrease the number of risk groups and infectious people, showing that vaccination can control the spread of COVID-19. Omame et al. [34] made a mathematical model for the co-interaction of COVID-19 and dengue transmission dynamics in Brazil. There were five strategies used to control dengue and COVID-19 infection, namely, the prevention strategy for dengue infection, the control strategy for COVID-19 situation, the control strategy for co-infection for both dengue and COVID-19, the control strategy for dengue treatments, and the control strategy for COVID-19 treatments. It could be concluded that the prevention strategy for dengue infection could prevent COVID-19 infection among 870,000 new cases while controls against dengue and controls against COVID-19 could only considerably reduce the infection. Nainggolan and Ansori [35] studied a model of the spread of COVID-19 in Indonesia. Importance was given to quarantine for infectious persons. Parameters were examined and it was found that parameters affecting the spread were the recruitment rate, the transmission rate, and mortality rate of disease. Akuk et al. [11] proposed a mathematical

model in the form of the SV_1V_2EQITR model. Importance was given to quarantine for infectious individuals and getting vaccinated with two doses. Stability of the model was analyzed and sensitivity of parameters affecting the spread was considered. Satar and Naji [17] proposed a mathematical model replicating the spread of the coronavirus disease by considering asymptomatic infected people. The SEIJR model (S = susceptible, E = Exposed, I = symptomatic, J = asymptomatic, and R = Recovered) was used to meet the data. Sensitivity of parameters were defined by the factors that regulate illness breakout, from the above mentioned. In this paper, we develop the model by considering additional the quarantined population to suit the epidemic situation in Thailand.

According to the literature review of articles relevant to the spread of COVID-19, a mathematical model of COVID-19 in Thailand was made. Optimal control strategies that will help control the spread of the disease were determined. From the above mentioned, the model is suitable for the epidemic situation in Thailand. Therefore, we created a model by considering the symptoms, infected population, asymptomatic, infected population, and paying attention to the population group that is in quarantine. In Section 2, the analysis of theoretical results and the analysis of disease stability were presented. In Section 3, numerical results were presented, using model fitting to estimate the results of the model to meet the actual data of the spread of the disease in Thailand. Meanwhile, the sensitivity of parameters was analyzed to examine parameters affecting the spread. In Sections 4 and 5, optimal control strategies were presented as well as a numerical model of control strategies. A model without the determination of control strategies and a model with the determination of control strategies were compared. The research conclusion and recommendation were presented in Section 6.

2. Materials and Methods

2.1. Mathematical Model

A mathematical model is a technique to help analyze the spread of a disease and see the consequences of any actions which could be taken to prevent the spread. It is a guideline to help the government formulate policies to reduce the number of patients. The model used in the study was based on the SEIR model (Wickramaarachchi and Perera [13], Mahardika [33], Carcione et al. [36]) and the SEIQR model (Bhadauria et al. [37], Youssef et al. [38], Hussain et al. [39], Khan et al. [40], Li et al. [41], Abioye et al. [42]). As the government had a quarantine measure among infectious individuals so as to separate them from those without COVID-19, we will be concerned with the additional steps which might be taken. Therefore, the model was developed to meet the current situation. A mathematical model for COVID-19 was studied by separating people into six sub-classes, namely, susceptible classes, exposed classes, symptomatic classes, asymptomatic classes, quarantined classes, and recovered classes, where S represents the susceptible population, E represents the exposed population, I_1 represents the symptomatic, infected population with the ω variant, I_2 represents the asymptomatic, infected population with the other variant, Q represents the quarantined population, R represents the recovered population, and N represents the number of total populations.

The differential equation of the spread of COVID-19 can be written as follows:

$$\left.\begin{aligned} S'(t) &= \Lambda - \lambda S(t) - dS(t), \\ E'(t) &= \lambda S(t) - (\tau\varepsilon + \tau(1-\varepsilon) + d)E(t), \\ I'_1(t) &= \tau\varepsilon E(t) - (\alpha + g + d)I_1(t), \\ I'_2(t) &= \tau(1-\varepsilon)E(t) - (\gamma_a + g + d)I_2(t), \\ Q'(t) &= \alpha I_1(t) - (\gamma_q + d)Q(t), \\ R'(t) &= \gamma_a I_2(t) + \gamma_q Q(t) - dR(t), \end{aligned}\right\} \tag{1}$$

and

$$N = S + E + I_1 + I_2 + Q + R \tag{2}$$

where the variables and parameters of Equations (1) and (2) are defined in Tables 1 and 2.

It was determined that susceptible people were able to become infected with COVID-19 since they received the disease from people in the symptomatic group (I_1) and people in the asymptomatic group (I_2). The intensity of the infection is

$$\lambda(t) = \beta_s I_1(t) + \beta_a I_2(t). \tag{3}$$

From Figure 1, the population inflow and population outflow in the mathematical model can be described as follows: susceptible group (S) had one way of the population inflow, i.e., initial number in the population by Λ while the population outflow was the flow of people to the exposed group based on the rate λS and the outflow of people who died of natural causes based on the rate d. The exposed group had one way of the population inflow, namely, the flow of people from the susceptible group based on the rate λS while three ways of the population outflow were the flow of people to the symptomatic group and to the asymptomatic group based on the rate $\tau\varepsilon$ and the rate, $\tau(1-\varepsilon)$ respectively. The outflow of population who died of natural causes was based on the rate d. In the symptomatic group (I_1), there was population inflow from the exposed group to the symptomatic group based on the rate $\tau\varepsilon$. The population outflow was the flow of people to the quarantined group based on the rate α since the government had a measure ordering infected people to stay in quarantine to separate infected people from people who were not infected with the disease. Two ways of the population outflows were the outflow of people who died of natural causes and people who died of COVID-19 based on the rate d and g, respectively. The asymptomatic group (I_2) had one way of the population inflow, i.e., the flow of people from the exposed group based on the rate $\tau(1-\varepsilon)$. There were three ways of the population outflow, namely, the flow of people to the recovered group based on the rate γ_a, deaths caused by natural causes based on the rate d, and deaths caused by COVID-19 based on the rate g. In the quarantined group (Q), there was population inflow, namely, the flow of people from the symptomatic group to the quarantined group based on the rate α. There were two ways of population outflow, namely, the flow of people to the recovered group based on the rate γ_q and deaths caused by natural causes based on the rate d. The last one was the recovered group (R). There were two ways of population inflow, namely, the quarantined group and the asymptomatic group based on the rate γ_q and the rate, γ_a respectively. There was one way of population outflow, namely, deaths caused by natural causes based on the rate d. According to the above description, a differential equation of the spread of COVID-19 can be written as follows:

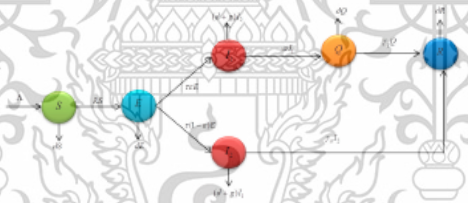

Figure 1. Shows the relationship between population inflow and population outflow in the mathematical model of COVID-19.

Table 1. Variables.

Variables	Description
S	Susceptible population.
E	Exposed population.
I_1	Symptomatic, infected population with the ω variant.
I_2	Asymptomatic, infected population with the other variant.
Q	Quarantined population.
R	Recovered population.
N	Number of total populations.

Table 2. Parameters.

Parameters	Description
Λ	The recruitment number of population.
β_s	The infection rate of symptomatic population with the ω variant.
β_a	The infection rate of asymptomatic population with the other variant.
τ	Incubation period.
ε	The rate of exposed moving to symptomatic.
α	Quarantine rate of the symptomatic, infected population.
γ_q	Rate at which quarantine to be recovered.
γ_a	Rate at which asymptomatic, infected population to be recovered.
g	Mortality rate of COVID-19.
d	Mortality rate of natural causes.

Lemma 1. *Initial condition:* $S(0) > 0$, $E(0) > 0$, $I_1(0) > 0$, $I_2(0) > 0$, $R(0) > 0$ *and* $N(0) > 0$ *from the Equation (1) the invariant set* $\phi = \left\{(S, E, I_1, I_2, Q, R) \in \mathbb{R}^6_+ : N \leq \frac{\Lambda}{d}\right\}$, *and then the closed set* ϕ *is positive invariant.*

Proof. Groups of population are considered when $N = S + E + I_1 + I_2 + Q + R$, it can be seen that

$$\frac{dN}{dt} = \frac{dS}{dt} + \frac{dE}{dt} + \frac{dI_1}{dt} + \frac{dI_2}{dt} + \frac{dQ}{dt} + \frac{dR}{dt}$$

$$\frac{dN}{dt} = \Lambda - gI_1 - gI_2 - dN. \tag{4}$$

From Equation (4), it is supposed that there is no mortality rate of the disease (g); therefore,

$$\frac{dN}{dt} \leq \Lambda - dN$$

integrating the above equation, it can be given as follows:

$$N(t) \leq \frac{\Lambda}{d} + \left(N(0) - \frac{\Lambda}{d}\right)e^{-dt}$$

where $N(0)$ initial value, and $N(t) = N(0)$ at $t = 0$. In addition, it can be noticed that $N(t) \to \frac{\Lambda}{d}$ as $t \to \infty$. Thus, it can be concluded that $N(t)$ is bounded as $0 \leq N(t) \leq \frac{\Lambda}{d}$ Epidemiological parameters are positive. It can be concluded that the problem solving area is in $\mathbb{R}^6_+$. Therefore $\phi = \left\{(S, E, I_1, I_2, Q, R) \in \mathbb{R}^6_+ : N \leq \frac{\Lambda}{d}\right\}$ is a positive invariant set. □

2.2. Stability Analysis

2.2.1. Equilibrium Point and Basic Reproduction Number

An equilibrium point is considered in this part. An equilibrium point is important to long-term epidemic behavior since it identifies a state where the output of the system remains constant, even in the presence of varying inputs and are the states when there are no changes in the number, i.e., $dX(t) = 0$. Derivatives of the equation system (1) on the right side are determined to be zero. From the model, two equilibrium points are obtained, namely:

$$\Lambda - \lambda^* S^* - dS^* = 0 \tag{5}$$

$$\lambda^* S^* - (\tau\varepsilon + \tau(1-\varepsilon) + d)E^* = 0 \tag{6}$$

$$\tau\varepsilon E^* - (\alpha + g + d)I_1^* = 0 \tag{7}$$

$$\tau(1-\varepsilon)E^* - (\gamma_a + g + d)I_2^* = 0 \tag{8}$$

$$\alpha I_1^* - (\gamma_q + d)Q^* = 0 \tag{9}$$

$$\gamma_a I_2^* + \gamma_q Q^* - dR^* = 0 \tag{10}$$

From Equation (7), we have

$$I_1^* = \frac{\tau\varepsilon E^*}{(\alpha + g + d)}$$

$$I_1^* = T_0 E^*$$

where

$$T_0 = \frac{\tau\varepsilon}{(\alpha + g + d)}.$$

From Equation (8), we have

$$I_2^* = \frac{\tau(1-\varepsilon)E^*}{(\gamma_a + g + d)}$$

$$I_2^* = T_1 E^*$$

where

$$T_1 = \frac{\tau(1-\varepsilon)}{(\gamma_a + g + d)}.$$

From Equation (9), we have

$$Q^* = \frac{\alpha I_1{}^*}{(\gamma_q + d)} = \frac{\alpha T_0 E^*}{(\gamma_q + d)}$$

$$Q^* = T_2 E^*$$

where

$$T_2 = \frac{\alpha T_0}{(\gamma_q + d)}.$$

From Equation (10), we have

$$R^* = \frac{\gamma_a I_2{}^* + \gamma_q Q^*}{d} = \frac{\gamma_a (T_1 E^*) + \gamma_q (T_2 E^*)}{d}$$

$$R^* = T_3 E^*$$

where

$$T_3 = \frac{\gamma_a T_1 + \gamma_q T_2}{d}.$$

From Equation (3), we have

$$\lambda^* = \beta_s I_1^* + \beta_a I_2^*$$

$$\lambda^* = \beta_s (T_0 E^*) + \beta_a (T_1 E^*)$$

$$\lambda^* = T_4 E^*$$

where

$$T_4 = \beta_s T_0 + \beta_a T_1 = \frac{R_0 d(d+\tau)}{\Lambda}.$$

From Equation (6), we have

$$\lambda^* S^* - (\tau\varepsilon + \tau(1-\varepsilon) + d)E^* = 0$$

$$(T_4 E^*) S^* - (\tau\varepsilon + \tau(1-\varepsilon) + d)E^* = 0$$

$$(T_4 S^* - (\tau\varepsilon + \tau(1-\varepsilon) + d))E^* = 0.$$

Therefore, $E^* = 0$ or

$$S^* = \frac{(\tau\varepsilon + \tau(1-\varepsilon) + d)}{T_4}$$

$$S^* = \frac{(\tau\varepsilon + \tau(1-\varepsilon) + d)\Lambda}{R_0 d(d+\tau)}$$

where

$$T_4 = \frac{R_0 d(d+\tau)}{\Lambda}.$$

Thus, when $E^* = 0$ we obtain the disease-free equilibrium points K_0^*, given by

$$K_0^* = (S^*, E^*, I_1^*, I_2^*, Q^*, R^*) = \left(\frac{\Lambda}{d}, 0, 0, 0, 0, 0\right).$$

Substituting $S^* = \frac{(\tau\varepsilon+\tau(1-\varepsilon)+d)\Lambda}{R_0 d(d+\tau)}$ and $\lambda^* = T_4 E^*$ in Equation (5), we have

$$E^* = \frac{\Lambda d(R_0 - 1)}{R_0(\tau + d)}$$

The remaining expressions for the endemic equilibrium points are

$$I_1^* = \frac{\Lambda\tau\varepsilon(R_0-1)}{R_0(\alpha+g+d)(\tau+d)},$$

$$I_2^* = \frac{\Lambda\tau(1-\varepsilon)(R_0-1)}{R_0(\gamma_a+g+d)(\tau+d)},$$

$$Q^* = \frac{\Lambda\tau\alpha\varepsilon(R_0-1)}{R_0(\alpha+g+d)(\gamma_q+d)(\tau+d)},$$

$$R^* = \frac{\Lambda\tau(R_0-1)\left(\frac{\gamma_a(1-\varepsilon)}{(\gamma_a+g+d)} - \frac{\alpha\varepsilon\gamma_q}{(\alpha+g+d)(\gamma_q+d)}\right)}{R_0 d(\tau+d)}.$$

Therefore, disease-free equilibrium point is:

$$K_0^* = \left(\frac{\Lambda}{d}, 0, 0, 0, 0, 0\right) \tag{11}$$

with $R_0 < 1$ and endemic equilibrium point is

$$K_1^* = (S^*, E^*, I_1^*, I_2^*, Q^*, R^*) \tag{12}$$

where

$$S^* = \frac{(\tau\varepsilon + \tau(1-\varepsilon) + d)\Lambda}{R_0 d(d+\tau)}, E^* = \frac{\Lambda d(R_0-1)}{R_0(\tau+d)}, I_1^* = \frac{\Lambda\tau\varepsilon(R_0-1)}{R_0(\alpha+g+d)(\tau+d)},$$

$$I_2^* = \frac{\Lambda\tau(1-\varepsilon)(R_0-1)}{R_0(\gamma_a+g+d)(\tau+d)}, Q^* = \frac{\Lambda\tau\alpha\varepsilon(R_0-1)}{R_0(\alpha+g+d)(\gamma_q+d)(\tau+d)},$$

$$R^* = \frac{\Lambda\tau(R_0-1)\left(\frac{\gamma_a(1-\varepsilon)}{(\gamma_a+g+d)} - \frac{\alpha\varepsilon\gamma_q}{(\alpha+g+d)(\gamma_q+d)}\right)}{R_0 d(\tau+d)},$$

with $R_0 > 1$.

The R_0 value is the basic reproduction number of the equation system (1), which can be noticed from expression E, I_1 and I_2.

$$\begin{aligned} E'(t) &= (\beta_s I_1(t) + \beta_a I_2(t))S(t) - (\tau + \tau(1-\varepsilon) + d)E(t), \\ I_1'(t) &= \tau\varepsilon E(t) - (\alpha + g + d)I_1(t), \\ I_2'(t) &= \tau(1-\varepsilon)E(t) - (\gamma_a + g + d)I_2(t). \end{aligned}$$

The next-generation matrix method [43,44] is used to derive the basic reproduction number (R_0) which can be obtained from the most outstanding characteristic determinant consistent with the spectral radius of the matrix $\rho(FV^{-1})$, when ρ is spectral radius, F is the Jacobian matrix of the gains matrix, and V is the Jacobian matrix of the losses matrix. Then we have

$$\begin{vmatrix} \text{Gains to } E & (\beta_s I_1(t) + \beta_a I_2(t))S(t) \\ \text{Gains to } I_1 & 0 \\ \text{Gains to } I_2 & 0 \end{vmatrix}, \quad \begin{vmatrix} \text{Losses to } E & (\tau + \tau(1-\varepsilon) + d)E(t) \\ \text{Losses to } I_1 & -\tau\varepsilon E(t) + (\alpha + g + d)I_1(t) \\ \text{Losses to } I_2 & -\tau(1-\varepsilon)E(t) + (\gamma_a + g + d)I_2(t) \end{vmatrix}.$$

It can be seen that

$$F = \begin{bmatrix} 0 & \beta_s S(t) & \beta_a S(t) \\ 0 & 0 & 0 \\ 0 & 0 & 0 \end{bmatrix}, \quad V = \begin{bmatrix} (\tau + \tau(1-\varepsilon) + d) & 0 & 0 \\ -\tau\varepsilon & \alpha + g + d & 0 \\ -\tau(1-\varepsilon) & 0 & \gamma_a + g + d \end{bmatrix}.$$

The disease-free equilibrium point

$$K_0^* = (S^*, E^*, I_1^*, I_2^*, Q^*, R^*) = \left(\frac{\Lambda}{d}, 0, 0, 0, 0, 0\right)$$

we have

$$FV^{-1}(K_0^*) = \begin{bmatrix} H_1 & H_2 & H_3 \\ 0 & 0 & 0 \\ 0 & 0 & 0 \end{bmatrix}$$

where

$$\begin{aligned} H_1 &= \frac{(d+g+\alpha)(1-\varepsilon)\Lambda\tau\beta_a}{d(d+g+\gamma_a)(d^2+dg+d\alpha+d\tau+g\tau+\alpha\tau)} + \frac{\Lambda\varepsilon\tau\beta_s}{d(d^2+dg+d\alpha+d\tau+g\tau+\alpha\tau)}, \\ H_2 &= \frac{(d^2+dg+d\gamma_a+d\tau+g\tau+\tau\gamma_a)\Lambda\beta_s}{d(d+g+\gamma_a)(d^2+dg+d\alpha+d\tau+g\tau+\alpha\tau)}, \\ H_3 &= \frac{\Lambda\beta_a}{d(d+g+\gamma_a)}. \end{aligned}$$

Therefore, the basic reproduction number (R_0) can be derived from the most outstanding radius of $\rho(FV^{-1})$ considered from the largest positive eigenvalue. Thus, the formula is given as:

$$R_0 = \frac{((1-\varepsilon)\alpha\beta_a + (1-\varepsilon)(d+g)\beta_a + \beta_s\varepsilon(g+\gamma_a+d))\Lambda\tau}{d(d+g+\alpha)(d+g+\gamma_a)(d+\tau)}. \tag{13}$$

The basic reproduction number (R_0) represents the average number of secondary infections produced by an infected individual in a susceptible host population [45]. In an epidemiological model, if $R_0 > 1$, the disease will spread and may cause an epidemic, when $R_0 < 1$, an epidemic can be controlled. When R_0 is larger, an epidemic is difficult to be controlled.

2.2.2. Global Stability of Equilibrium Points

In this part, the global stability of the COVID-19 model in the equation system (1) was analyzed. The Lyapunov function was used to verify stability, and two theorems were obtained as shown below.

Theorem 1. *If $R_0 < 1$, it indicates that the disease-free equilibrium point of the model (1) is globally asymptotically stable in the region ϕ.*

We assume that

$$\beta_s = \beta_a = \frac{g+d}{S^*}. \tag{14}$$

Proof. According to the results shown above, the Lyapunov function was determined as follows:

$$G = (S - S^* - S^* \ln \frac{S}{S^*}) + E + I_1 + I_2 + Q + R$$

The time differentiation of G is given by

$$\frac{dG}{dt} = S'\left(1 - \frac{S^*}{S}\right) + E' + I_1' + I_2' + Q' + R'$$

using system (1), we have

$$\begin{aligned}\frac{dG}{dt} &= (\Lambda - (\beta_s I_1 + \beta_a I)S - dS)\left(1 - \frac{S^*}{S}\right) + ((\beta_s I_1 + \beta_a I_2)S - (\tau\varepsilon + \tau(1-\varepsilon) + d)E) \\ &\quad + (\tau\varepsilon E - (\alpha + g + d)I_1) + (\tau(1-\varepsilon)E - (\gamma_a + g + d)I_2) + (\alpha I_1 - (\gamma_q + d)Q) + (\gamma_a I_2 + \gamma_q Q - dR) \\ &= \Lambda\left(1 - \frac{S^*}{S}\right) + dS^*\left(1 - \frac{S}{S^*}\right) + (\beta_s S^* - (g+d))I_1 + (\beta_a S^* - (g+d))I_2 - dE - dQ - dR\end{aligned}$$

substitution of the Equation (11)

$$\frac{dG}{dt} = \Lambda\left(1 - \frac{S^*}{S}\right) + dS^*\left(1 - \frac{S}{S^*}\right) - dE - dQ - dR$$

based on the disease-free equilibrium point $S^* = \frac{\Lambda}{d}$ is obtained

$$\begin{aligned}\frac{dG}{dt} &= \Lambda\left(1 - \frac{S^*}{S}\right) + \Lambda\left(1 - \frac{S}{S^*}\right) - dE - dQ - dR \\ &= \Lambda\left(2 - \frac{S^*}{S} - \frac{S}{S^*}\right) - dE - dQ - dR\end{aligned}$$

$$\frac{dG}{dt} = -\left[\Lambda\left(\frac{(S^* - S)^2}{S^* S}\right) + dE + dQ + dR\right] \leq 0. \tag{15}$$

Therefore, it can be seen that when $S^* = S$, $E = 0$, $Q = 0$ and $R = 0$, then $\frac{dG}{dt} = 0$ Since E, Q and R are positive. According to the Equation (15), the resul $\frac{dG}{dt}$ is definitely negative. According to LaSalle's Invariance Principle, it can be concluded that the disease-free equilibrium point K_0^* of the equation system (1) is globally asymptotically stable on ϕ if $R_0 < 1$. □

Theorem 2. *If $R_0 > 1$, it indicates that the endemic equilibrium point of the model (1) is globally asymptotically stable in the region ϕ.*

Proof. The Lyapunov function is determined as:

$$\begin{aligned}M &= (S - S^* - S^* \ln \tfrac{S}{S^*}) + (E - E^* - E^* \ln \tfrac{E}{E^*}) + (I_1 - I_1^* - I_1^* \ln \tfrac{I_1}{I_1^*}) + (I_2 - I_2^* - I_2^* \ln \tfrac{I_2}{I_2^*}) \\ &\quad + (Q - Q^* - Q^* \ln \tfrac{Q}{Q^*}) + (R - R^* - R^* \ln \tfrac{R}{R^*}).\end{aligned}$$

The time differentiation of M is given by

$$\frac{dM}{dt} = S'\left(1-\frac{S^*}{S}\right) + E'\left(1-\frac{E^*}{E}\right) + I_1'\left(1-\frac{I_1^*}{I_1}\right) + I_2'\left(1-\frac{I_2^*}{I_2}\right) + Q'\left(1-\frac{Q^*}{Q}\right) + R'\left(1-\frac{R^*}{R}\right)$$
$$= \{\Lambda - \lambda S - dS\}\left(1-\tfrac{S^*}{S}\right) + \{\lambda S - (\tau\varepsilon + \tau(1-\varepsilon) + d)E\}\left(1-\tfrac{E^*}{E}\right)$$
$$+\{\tau\varepsilon E - (\alpha+g+d)I_1\}\left(1-\tfrac{I_1^*}{I_1}\right) + \{\tau(1-\varepsilon)E - (\gamma_a+g+d)I_2\}\left(1-\tfrac{I_2^*}{I_2}\right)$$
$$+\{\alpha I_1 - (\gamma_q+d)Q\}\left(1-\tfrac{Q^*}{Q}\right) + \{\gamma_a I_2 + \gamma_q Q - dR\}\left(1-\tfrac{R^*}{R}\right)$$

putting $S = S - S^*, E = E - E^*, I_1 = I_1 - I_1^*, I_2 = I_2 - I_2^*, Q = Q - Q^*$ and $R = R - R^*$, then

$$\tfrac{dM}{dt} = \{\Lambda - (\beta_s I_1 + \beta_a I_2)(S-S^*) - d(S-S^*)\}\left(\tfrac{S-S^*}{S}\right)$$
$$+\{(\beta_s I_1 + \beta_a I_2)S - (\tau\varepsilon + \tau(1-\varepsilon) + d)(E-E^*)\}\left(\tfrac{E-E^*}{E}\right)$$
$$+\{\tau\varepsilon E - (\alpha+g+d)(I_1 - I_1^*)\}\left(\tfrac{I_1-I_1^*}{I_1}\right) + \{\tau(1-\varepsilon)E - (\gamma_a+g+d)(I_2-I_2^*)\}\left(\tfrac{I_2-I_2^*}{I_2}\right)$$
$$+\{\alpha I_1 - (\gamma_q+d)(Q-Q^*)\}\left(\tfrac{Q-Q^*}{Q}\right) + \{\gamma_a I_2 + \gamma_q Q - d(R-R^*)\}\left(\tfrac{R-R^*}{R}\right)$$

$$= \Lambda - \Lambda\left(\tfrac{S^*}{S}\right) - (\beta_s I_1 + \beta_a I_2)\tfrac{(S-S^*)^2}{S} - d\tfrac{(S-S^*)^2}{S} + (\beta_s I_1 + \beta_a I_2)S - (\beta_s I_1 + \beta_a I_2)S\tfrac{E^*}{E}$$
$$-(\tau\varepsilon + \tau(1-\varepsilon) + d)\tfrac{(E-E^*)^2}{E} + \tau\varepsilon E - \tau\varepsilon E\left(\tfrac{I_1^*}{I_1}\right) - (\alpha+g+d)\tfrac{(I_1-I_1^*)^2}{I_1}$$
$$+\tau(1-\varepsilon)E - \tau(1-\varepsilon)E\left(\tfrac{I_2^*}{I_2}\right) - (\gamma_a+g+d)\tfrac{(I_1-I_1^*)^2}{I_1} + \alpha I_1 - \alpha I_1\left(1-\tfrac{Q^*}{Q}\right)$$
$$-(\gamma_q+d)\tfrac{(Q-Q^*)^2}{Q} + \gamma_a I_2 - \gamma_a I_2\left(\tfrac{R^*}{R}\right) + \gamma_q Q - \gamma_q Q\left(\tfrac{R^*}{R}\right) - d\tfrac{(R-R^*)^2}{R}.$$

An equation that is rearranged and determined is obtained.

$$\frac{dM}{dt} = Z_1 - Z_2$$

when

$$Z_1 = \Lambda + (\beta_s I_1 + \beta_a I_2)S + \tau\varepsilon E + \tau(1-\varepsilon)E + \alpha I_1 + \gamma_a I_2 + \gamma_q Q$$

and

$$Z_2 = \Lambda\left(\tfrac{S^*}{S}\right) + (\beta_s I_1 + \beta_a I_2)\tfrac{(S-S^*)^2}{S} + d\tfrac{(S-S^*)^2}{S} + (\beta_s I_1 + \beta_a I_2)S\tfrac{E^*}{E} + (\tau\varepsilon + \tau(1-\varepsilon) + d)\tfrac{(E-E^*)^2}{E}$$
$$+\tau\varepsilon E\left(\tfrac{I_1^*}{I_1}\right) + (\alpha+g+d)\tfrac{(I_1-I_1^*)^2}{I_1} + \tau(1-\varepsilon)E\left(\tfrac{I_2^*}{I_2}\right) + (\gamma_a+g+d)\tfrac{(I_1-I_1^*)^2}{I_1}$$
$$+\alpha I_1\left(1-\tfrac{Q^*}{Q}\right) + (\gamma_q+d)\tfrac{(Q-Q^*)^2}{Q} + \gamma_a I_2\left(\tfrac{R^*}{R}\right) + \gamma_q Q\left(\tfrac{R^*}{R}\right) + d\tfrac{(R-R^*)^2}{R}$$

Since all parameters in the model (1) are positive, therefore when $S^* = S, E = 0, Q = 0$ and $R = 0$ and $\frac{dM}{dt} = 0$ sultand then the re $\frac{dM}{dt}$ is definitely negative when $Z_1 < Z_2$. According to LaSalle's Invariance Principle, it can be concluded that the equilibrium point of the endemic steady state K_1^* of the equation system (1) is globally asymptotically stable on ϕ if $R_0 > 1$. □

3. Numerical Analysis Result

3.1. Model Fitting

In this part, some parameters in the model (1) were adjusted. Parameter adjustment is essential as it helps numerical simulation close to the actual data of the epidemic. Meanwhile, it helps analyze some parameters that cannot be identified. The infection rate of the symptomatic population with the ω variant (β_s), the infection rate of the asymptomatic population with the other variant (β_a) and the rate of exposed moving to symptomatic (ε) were adjusted as seen in Table 3. The model adjusted was implemented using fmincon Algorithm in MATLAB to ensure the model was suitable for the actual epidemic data. Results obtained from the parameter adjustment are seen in Figure 2. The blue circle indicates the number of people infected with COVID-19 each day from the data collected by the

Department of Disease Control, Ministry of Public Health. The data were collected from 1 January to 1 March 2022 since the Omicron variant was confirmed. It was considered the fifth wave of COVID-19 infection [46]. The red solid line indicates results from the model (1) (susceptible group).

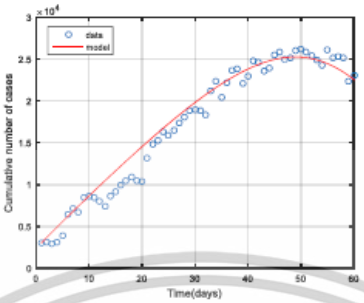

Figure 2. Data in the model and data report in case the infection was confirmed from 1 January to 1 March 2022 [46].

3.2. *Numerical Simulations*

In this part, numerical analysis of the COVID-19 model (1) is performed to verify the appropriateness of the model, i.e., it yields conclusions consistent with earlier works. The Runge—Kutta order four method in MATLAB was used to generate the numerical results. The analysis in this part was divided into three parts. Part 1 is the analysis of parameter values to be suitable for the actual epidemic data. Part 2 is the analysis of model stability (1), and part 3 is the comparison of parameter values used in this study.

3.2.1. Part 1: The Analysis of Parameter Values Suitable for the Actual Epidemic Data

According to COVID-19 epidemic data reported as of 1 January to 1 March 2022 by the time the Omicron variant was confirmed in Thailand (with reference to the report on the Omicron variant detected in this when the epidemic was found the most). As for model (1), parameter values were adjusted to be suitable for the actual epidemic data. Parameters adjusted were the infection rate of the symptomatic population with the ω variant (β_s), the infection rate of the asymptomatic population with the other variant (β_a), and the rate of exposed moving to symptomatic (ε). Parameter values adjusted to be suitable for the model were shown in Table 3 and Figure 2, showing appropriateness of parameters to be suitable for the actual epidemic data.

3.2.2. Part 2: Stability Analysis of the Model (1)

This part shows the numerical values of disease-free steady state, the endemic steady state, and global linear stability (globally asymptotically stable). Figure 3 shows the numerical results of a disease-free steady state. It can be seen that as time passed by, the number of susceptible 1000 days passed. The number of the exposed population (E), the number of symptomatic, infected population (I_1), the number of symptomatic, infected population (I_2), the number of quarantined population (Q), and the number of recovered population (R), as time passed by, would converge to zero (such as $E = 0$, $I_1 = 0$, $I_2 = 0$, $Q = 0$, $R = 0$) as there was no epidemic of the disease. Figure 4 shows endemic steady state of the disease. As time passed by, the number of people would converge to the equilibrium point at $K_1^* = (S^*, E^*, I_1^*, I_2^*, Q^*, R^*) = (11{,}501, 4196, 34, 6729, 137, 18{,}248{,}000)$ when 300 days passed. In order to see more convergence, the infection rates were adjusted to be $\beta_s = 0.00000075$ and $\beta_a = 0.000009$. The convergence was shown in the form of 2D, 3D phase portrait trajectories of model (1) as seen in Figures 5 and 6. It can be seen that the convergence was clearer in both phases. Stability analysis was essential for designing an

epidemiological model. If the model is stable, other controllers shall be designed (will be shown in Topic 4). If the model is not stable, it will not be used in real life and should be improved to ensure various conditions will have stability before being used.

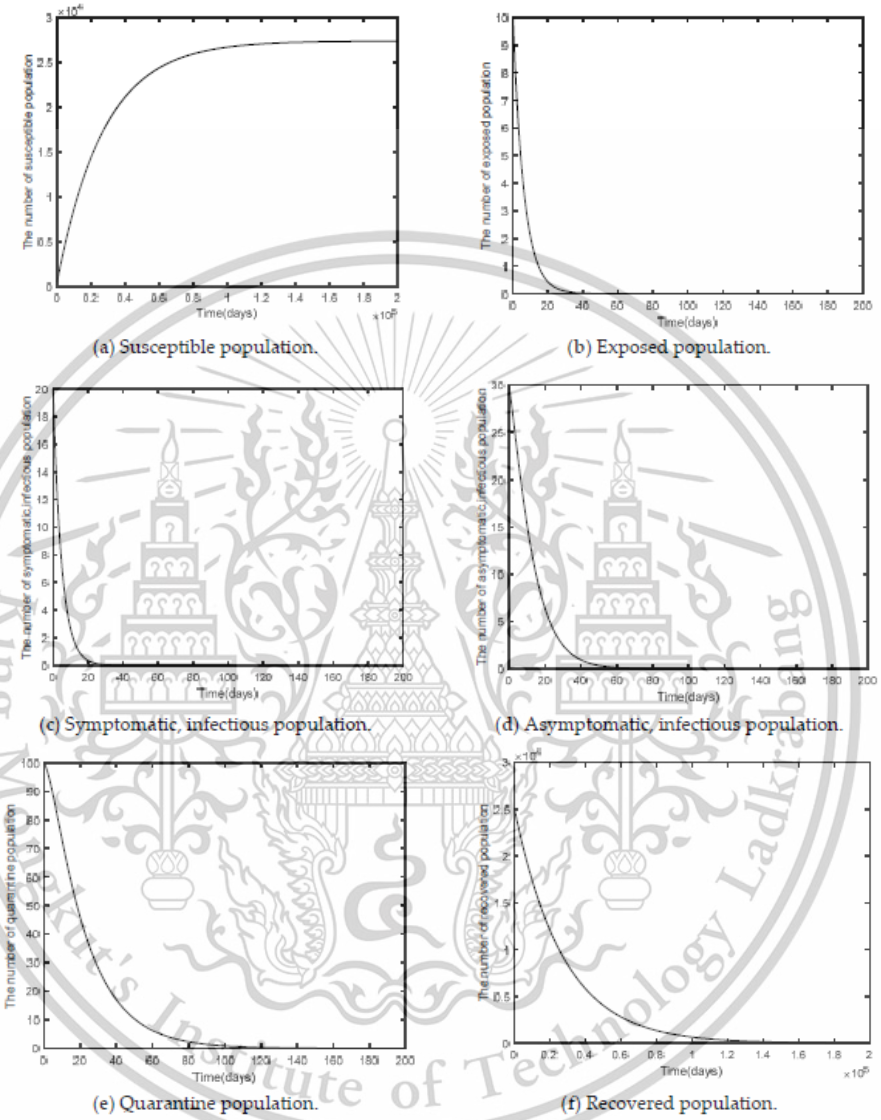

(a) Susceptible population. (b) Exposed population.

(c) Symptomatic, infectious population. (d) Asymptomatic, infectious population.

(e) Quarantine population. (f) Recovered population.

Figure 3. Time series of the system Equation (1) of the disease-free steady state K_0^* when $R_0 = 0.247311$.

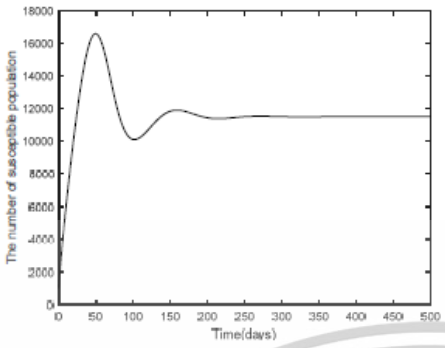

(a) Susceptible population.

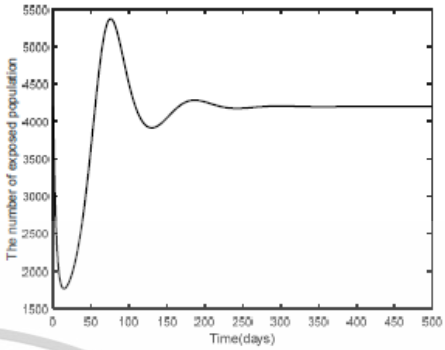

(b) Exposed population.

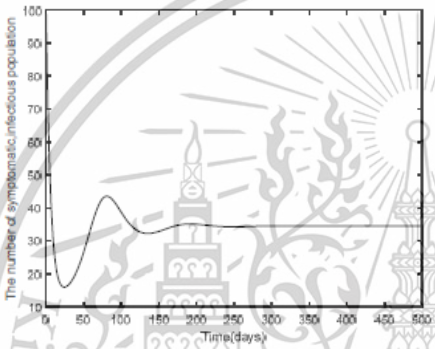

(c) Symptomatic, infectious population.

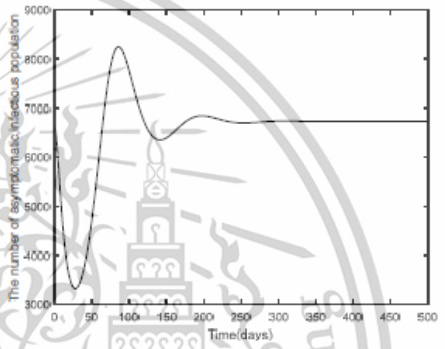

(d) Asymptomatic, infectious population.

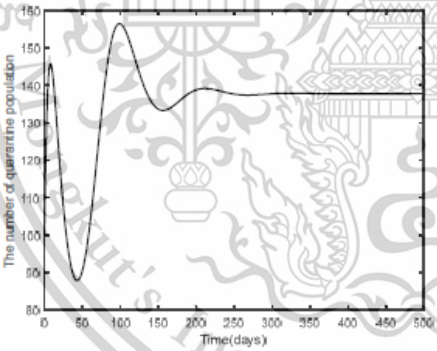

(e) Quarantine population.

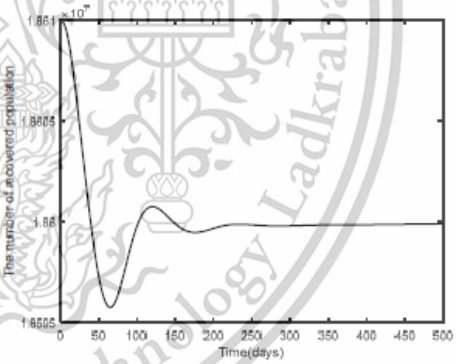

(f) Recovered population.

Figure 4. Time series of the system Equation (1) of the endemic steady state when $K_1^* R_0 = 1.73118$.

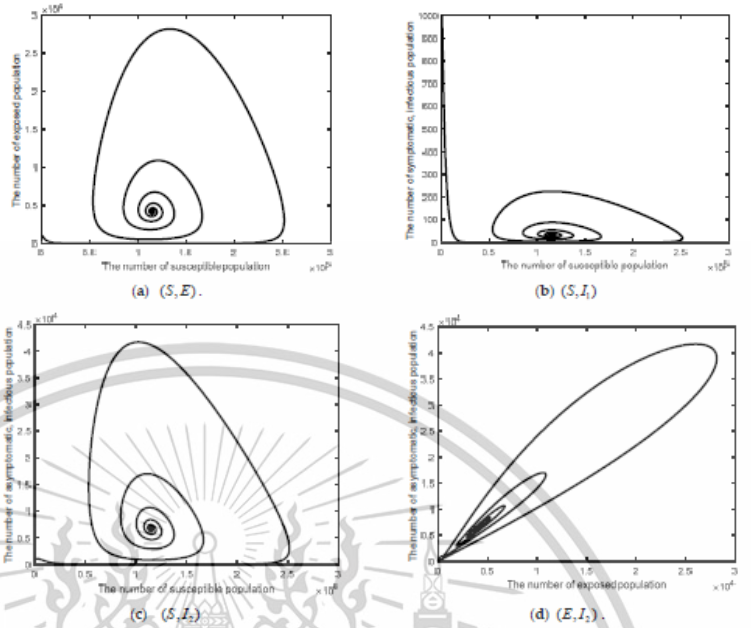

(a) (S, E). (b) (S, I_1)

(c) (S, I_2) (d) (E, I_2).

Figure 5. Time series of the system Equation (1) projected onto the 2D of the endemic steady state K_1^* when $R_0 > 1$.

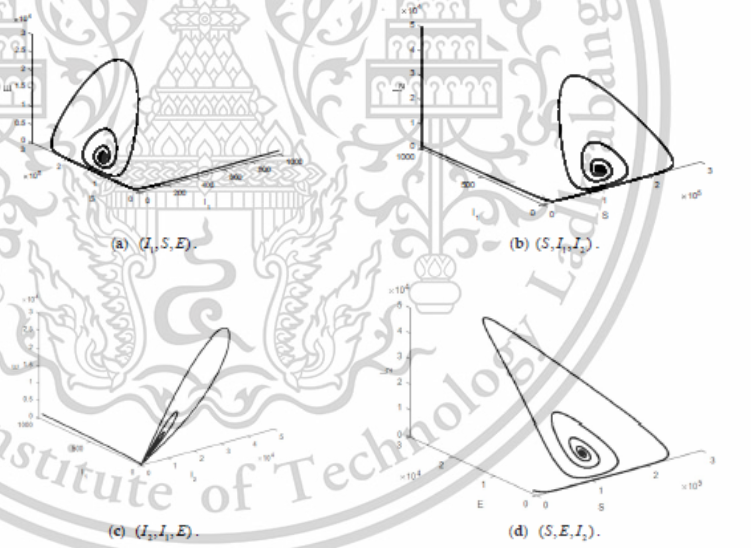

(a) (I_1, S, E). (b) (S, I_1, I_2).

(c) (I_2, I_1, E). (d) (S, E, I_2).

Figure 6. Time series of the system Equation (1) projected onto the 3D of the endemic steady state K_1^* when $R_0 > 1$.

3.2.3. Part 3: Comparison of Parameters

The parameters used in the comparison were the initial number of people (Λ) and the infection rate of the asymptomatic population with the other variant (β_a) since both parameters had an impact on a high increase in the basic reproduction number (R_0), as analyzed in Table 4. The parameters adjusted were $\Lambda = 50, 60, 70, 80$ and $\beta_a = 0.000006$, $0.000007, 0.000008$ and 0.000009. From Figures 7 and 8, it can be seen that increased parameter values contributed to the controllable spread of the disease rather than decreased parameter values.

Table 3. The parameter values of model.

Parameters	Disease-Free	Endemic	Reference
Λ	1	700	Assume
β_s	0.0000075	0.0000075	Fitting
β_a	0.0000009	0.0000009	Fitting
τ	1/6	1/6	[36,47]
e	0.01	0.01	Fitting
α	0.2	0.2	[47]
γ_q	0.05	0.05	[47]
γ_a	1/10	1/10	[47]
g	0.00286	0.00286	[47]
d	0.000036529	0.000036529	[47,48]

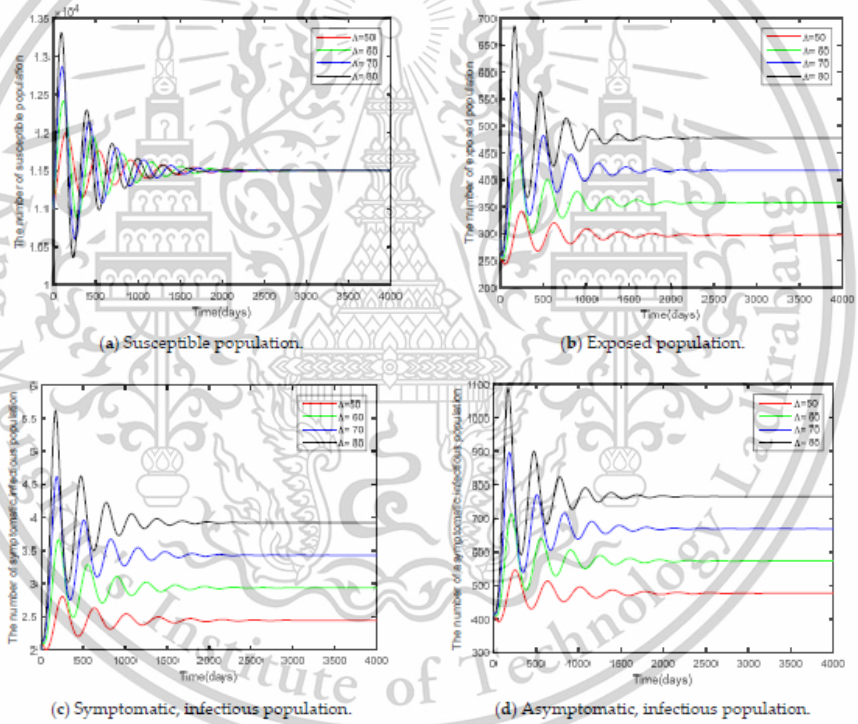

(a) Susceptible population. (b) Exposed population.

(c) Symptomatic, infectious population. (d) Asymptomatic, infectious population.

Figure 7. Time series of the system Equation (1) showing the comparison results of initial population (Λ).

Table 4. Sensitivity values of R_0.

Parameter	Sensitivity
Λ	1
β_s	0.000425
β_a	0.995749
τ	0.000219
ε	−0.005807
α	−0.004190
γ_a	−0.967719
g	−0.027737
d	1.000570

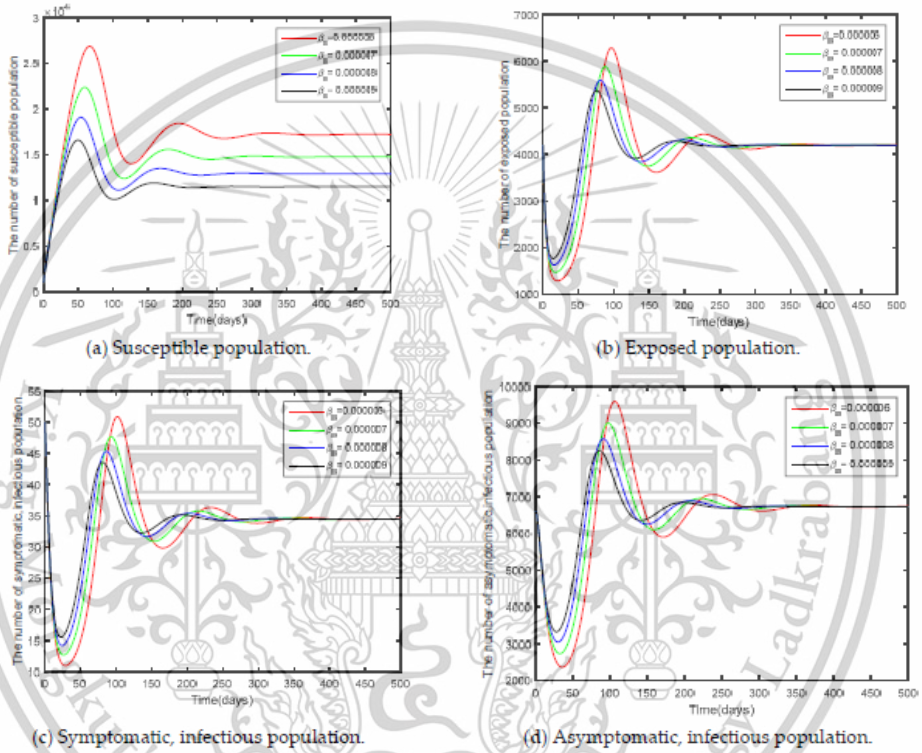

(a) Susceptible population. (b) Exposed population.

(c) Symptomatic, infectious population. (d) Asymptomatic, infectious population.

Figure 8. Time series of the system Equation (1) showing the comparison results of the transmission rate of asymptomatic population (β_a).

3.3. *Sensitivity Analysis of Parameters*

In this part, sensitivity analysis for the epidemiological model is presented, aiming to learn about factors associated with the basic reproduction number the affecting numerical simulation of the model. Moreover, the sensitivity analysis will reveal the importance of each parameter affecting the epidemic. Such data would be important to designing an experimental model and help design and determine strategies for controlling the epidemic. The sensitivity index R_0 associated with the parameters is the ratio of the relative change

in variables R_0 to the relative change in the parameters when variables are the function finding derivatives of parameter. The sensitivity index can be determined by the following derivatives:

Definition 1. [10,49] *The sensitivity index of R_0, which depends differentially on a parameter ψ, is defined by:*

$$\Upsilon_{\psi}^{R_0} = \frac{\partial R_0}{\partial \psi} \times \frac{\psi}{R_0}. \tag{16}$$

Expression for R_0 in Equation (13) used the data in Table 3 showing the basic value of the parameters used in the numerical simulation. Sensitivity analysis results of the basic reproduction number of each parameter are listed in Table 4.

According to the analysis results in Table 4, it can be seen that the most sensitive parameter was the initial number of the population (Λ), followed by β_a, β_s, τ, respectively. A positive index apparently indicated an increase (or decrease) in parameter values affected an increase (or decrease) in the basic reproduction numbers (R_0). On the contrary, indices that were negative, $\varepsilon, \alpha, \gamma_a, g, d$, led to a decrease (or increase) in the basic reproduction numbers (R_0). The research results indicated that the most effective control strategy was controlling the initial number of the population (Λ).

4. Optimal Control Problem

Lamwong et al. [45] studied the efficiency of vaccines for COVID-19 in Thailand. It was found that a 10% increase of vaccination rates would cause a 10% increase of the basic reproduction number. It can be concluded that an increase in vaccine efficacy would cause a decreased number of infected people. However, vaccination is just one measure for controlling the spread of the disease. There may be other measures that may lessen the need for everyone to be vaccinated. These are other control steps that can be taken. In this research, optimal control strategies were presented. Control strategies introduced were $u_1(t)$ and $u_2(t)$:$u_1(t)$ social distancing and mask wearing strategies. $u_2(t)$ vaccination control strategy to be the most suitable guideline is used with the dynamic of COVID-19 spread. Optimal control is determined as follows:

$$\left.\begin{aligned}
S'(t) &= \Lambda - (1-u_1(t))(\beta_s I_1(t) + \beta_a I_2(t))S(t) - dS(t) - u_2(t)S(t),\\
E'(t) &= (1-u_1(t))(\beta_s I_1(t) + \beta_a I_2(t))S(t) - (\tau\varepsilon + \tau(1-\varepsilon) + d)E(t),\\
I_1'(t) &= \tau\varepsilon E(t) - (\alpha + g + d)I_1(t),\\
I_2'(t) &= \tau(1-\varepsilon)E(t) - (\gamma_a + g + d)I_2(t),\\
Q'(t) &= \alpha I_1(t) - (\gamma_q + d)Q(t),\\
R'(t) &= \gamma_a I_2(t) + \gamma_q Q(t) - dR(t) + u_2(t)S(t).
\end{aligned}\right\} \tag{17}$$

Pontryagin's maximum principle [50,51] was used to reduce the number of COVID-19 infected people and to enable the expenditure on the control at the minimum. Therefore, the objective function was defined as follows:

$$J(u_1, u_2) = \int_0^T \left(W_1 I_1(t) + W_2 I_2(t) + \frac{1}{2} W_3 u^2{}_1(t) + \frac{1}{2} W_4 u^2{}_2(t) \right) dt \tag{18}$$

Parameter W_1, W_2 represents weight constant value of infected people, $W_3 u_1(t)$ represents the expenditure spent on social distancing campaign and mask wearing campaign, $W_4 u_2(t)$ represents the expenditure spent on vaccination at t time, and T represents the last time. Nonlinear cost function was used. Squared objective function was used for cost control measurement to achieve optimal control $u^*{}_1, u^*{}_2$,

$$J(u^*{}_1, u^*{}_2) = \min_U \{J(u_1, u_2)\}. \tag{19}$$

When $U = \{(u_1, u_2) : [0, T] \to [0, 1]\}$. Lagrangian and Hamiltonian were used for optimal problem solution.

$$L(I_1, I_2, u_1, u_2) = W_1 I_1(t) + W_2 I_2(t) + \frac{1}{2} W_3 u^2{}_1(t) + \frac{1}{2} W_4 u^2{}_2(t) \tag{20}$$

and

$$H = L(I_1, I_2, u_1, u_2) + \lambda_1 \frac{dS}{dt} + \lambda_2 \frac{dE}{dt} + \lambda_3 \frac{dI_1}{dt} + \lambda_4 \frac{dI_2}{dt} + \lambda_5 \frac{dQ}{dt} + \lambda_6 \frac{dR}{dt}. \tag{21}$$

Theorem 3. *(Pontryagin's Minimum Principle for control problem [44]) Optimal control was determined.* $u^*{}_1, u^*{}_2$ *and* S, E, I_1, I_2, Q, R *were the results of control equation system (17) that minimize* $J(u_1(t), u_2(t))$ *over* U. *Then there exist an adjoint variable* $\lambda_i; i = 1, 2, 3, 4, 5, 6$ *under the control equations:*

$$\frac{d\lambda_1}{dt} = -\frac{\partial H}{\partial S}, \frac{d\lambda_2}{dt} = -\frac{\partial H}{\partial E}, \frac{d\lambda_3}{dt} = -\frac{\partial H}{\partial I_1} =, \frac{d\lambda_4}{dt} = -\frac{\partial H}{\partial I_2}, \frac{d\lambda_5}{dt} = -\frac{\partial H}{\partial Q}, \frac{d\lambda_6}{dt} = -\frac{\partial H}{\partial R}. \tag{22}$$

And transversality conditions given as $\lambda_i(T) = 0$ *for all* $i = 1, 2, 3, 4, 5, 6$.

Then the characteristic values $u^*{}_1, u^*{}_2$ *are given by*

$$u^*{}_1(t) = \begin{cases} 0 & if \ \frac{(\lambda_2 - \lambda_1)((\beta_s I_1(t) + \beta_a I_2(t))S(t))}{W_3} \le 0, \\ \frac{(\lambda_2 - \lambda_1)((\beta_s I_1(t) + \beta_a I_2(t))S(t))}{W_3} & if \ \frac{(\lambda_2 - \lambda_1)((\beta_s I_1(t) + \beta_a I_2(t))S(t))}{W_3} < u_1^{\max}, \\ u_1^{\max} & if \ \frac{(\lambda_2 - \lambda_1)((\beta_s I_1(t) + \beta_a I_2(t))S(t))}{W_3} \ge u_1^{\max}. \end{cases} \tag{23}$$

$$u^*{}_2(t) = \begin{cases} 0 & if \ \frac{(\lambda_1 - \lambda_6)S(t)}{W_4} \le 0, \\ \frac{(\lambda_1 - \lambda_6)S(t)}{W_4} & if \ \frac{(\lambda_1 - \lambda_6)S(t)}{W_4} < u_2^{\max}, \\ u_2^{\max} & if \ \frac{(\lambda_1 - \lambda_6)S(t)}{W_4} \ge u_2^{\max}. \end{cases} \tag{24}$$

Proof. Hamiltonian function was determined in the equation system (21).

$$H = L(I_1, I_2, u_1, u_2) + \lambda_1 \frac{dS}{dt} + \lambda_2 \frac{dE}{dt} + \lambda_3 \frac{dI_1}{dt} + \lambda_4 \frac{dI_2}{dt} + \lambda_5 \frac{dQ}{dt} + \lambda_6 \frac{dR}{dt}.$$

where $L(I_1, I_2, u_1, u_2)$ is Lagrangian given in (20), therefore we have

$$\begin{aligned} H = {} & W_1 I_1(t) + W_2 I_2(t) + \tfrac{1}{2} W_3 u^2{}_1(t) + \tfrac{1}{2} W_4 u^2{}_2(t) \\ & + \lambda_1 [\Lambda - (1 - u_1(t))(\beta_s I_1(t) + \beta_a I_2(t))S(t) - dS(t) - u_2(t)S(t)] \\ & + \lambda_2 [(1 - u_1(t))(\beta_s I_1(t) + \beta_a I_2(t))S(t) - (\tau\varepsilon + \tau(1 - \varepsilon) + d)E(t)] \\ & + \lambda_3 [\tau\varepsilon E(t) - (\alpha + g + d)I_1(t)] \\ & + \lambda_4 [\tau(1 - \varepsilon)E(t) - (\gamma_a + g + d)I_2(t)] \\ & + \lambda_5 [\alpha I_1(t) - (\gamma_q + d)Q(t)] \\ & + \lambda_6 [\gamma_a I_2(t) + \gamma_q Q(t) - dR(t) + u_2(t)S(t)]. \end{aligned}$$

The adjoint system satisfying the following ordinary differential equations

$$\frac{d\lambda_1}{dt} = -\frac{\partial H}{\partial S} = \lambda_1((1 - u^*{}_1(t))(\beta_s I_1(t) + \beta_a I_2(t)) + d + u^*{}_2(t)) - \lambda_2((1 - u^*{}_1(t))(\beta_s I_1(t) + \beta_a I_2(t))) - \lambda_6 u^*{}_2(t),$$

$$\frac{d\lambda_2}{dt} = -\frac{\partial H}{\partial E} = \lambda_2(\tau\varepsilon + \tau(1 - \varepsilon) + d) - \lambda_3\tau\varepsilon - \lambda_4\tau(1 - \varepsilon),$$

$$\frac{d\lambda_3}{dt} = -\frac{\partial H}{\partial I_1} = \lambda_1((1 - u^*{}_1(t))\beta_s S(t)) - \lambda_2((1 - u^*{}_1(t))\beta_s S(t)) + \lambda_3(\alpha + g + d) - \lambda_5\alpha - W_1,$$

$$\frac{d\lambda_4}{dt} = -\frac{\partial H}{\partial I_2} = \lambda_1((1 - u^*{}_1(t))\beta_a S(t)) - \lambda_2((1 - u^*{}_1(t))\beta_a S(t)) + \lambda_4(\gamma_a + g + d) - \lambda_6\gamma_a - W_2,$$

$$\frac{d\lambda_5}{dt} = -\frac{\partial H}{\partial Q} = \lambda_5(\gamma_q + d) - \lambda_6\gamma_q,$$

$$\frac{d\lambda_6}{dt} = -\frac{\partial H}{\partial R} = \lambda_6 d.$$

With transversality conditions $\lambda_i(T) = 0$ for all $i = 1, 2, 3, \ldots, 6$ and the optimum condition for the Hamiltonian is given as $\frac{\partial H}{\partial u_j} = 0$ for all $j = 1, 2$ at $u_j = u^*j$.

Therefore,

$$\frac{\partial H}{\partial u_1} = W_3 u^*{}_1(t) + \lambda_1((\beta_s I_1(t) + \beta_a I_2(t))S(t)) - \lambda_2((\beta_s I_1(t) + \beta_a I_2(t))S(t)) \Rightarrow u^*{}_1(t) = \frac{(\lambda_2 - \lambda_1)((\beta_s I_1(t) + \beta_a I_2(t))S(t))}{W_3}$$

$$\frac{\partial H}{\partial u_2} = W_4 u^*{}_2(t) - \lambda_1 S(t) + \lambda_6 S(t) \Rightarrow u^*{}_2(t) = \frac{(\lambda_1 - \lambda_6)S(t)}{W_4}.$$

Based on the above-mentioned equation, the optimal control equation was obtained as follow:

$$u^*{}_1(t) = \begin{cases} 0 & if \ \frac{(\lambda_2 - \lambda_1)((\beta_s I_1(t) + \beta_a I_2(t))S(t))}{W_3} \leq 0, \\ \frac{(\lambda_2 - \lambda_1)((\beta_s I_1(t) + \beta_a I_2(t))S(t))}{W_3} & if \ \frac{(\lambda_2 - \lambda_1)((\beta_s I_1(t) + \beta_a I_2(t))S(t))}{W_3} < u_1^{\max}, \\ u_1^{\max} & if \ \frac{(\lambda_2 - \lambda_1)((\beta_s I_1(t) + \beta_a I_2(t))S(t))}{W_3} \geq u_1^{\max}. \end{cases}$$

$$u^*{}_2(t) = \begin{cases} 0 & if \ \frac{(\lambda_1 - \lambda_6)S(t)}{W_4} \leq 0, \\ \frac{(\lambda_1 - \lambda_6)S(t)}{W_4} & if \ \frac{(\lambda_1 - \lambda_6)S(t)}{W_4} < u_2^{\max}, \\ u_2^{\max} & if \ \frac{(\lambda_1 - \lambda_6)S(t)}{W_4} \geq u_2^{\max}. \end{cases}$$

□

5. Numerical Results for Optimal Control Problem

As for numerical simulation, numerical analysis of non-control model (1) and control model (19) was made. The red line indicates the non-control model, and the black line indicates the control model. The fourth order Runge—Kutta forward-backward sweep method [52] was used to generate the results. The parameters used are identified in Table 3. We have considered the initial conditions and weight constant values were determined as $S(0) = 500$, $E(0) = 10$, $I_1(0) = 4$, $I_2(0) = 3$, $Q(0) = 5$, $R(0) = 25,000$ $W_2 = 20$, $W_3 = 30$, $W_4 = 40$ and the period of the numerical simulation was determined as 100 days to ensure the goal of the control can be achieved. The highest value of the control was $u_1 = 0.6$, $u_2 = 0.225$. The study was divided into three cases. Case 1 is social distancing measure in conjunction with mask wearing and vaccination measure, Case 2 is social distancing measures in conjunction with mask wearing measure, and Case 3 is vaccination measures, which are described as follow:

Case 1: $u_1 \neq 0$ and $u_2 \neq 0$.

It was supposed that u_1 (social distancing in conjunction with mask-wearing) and u_2 were controlled (vaccination control measure) as shown in Figures 9 and 10. Figure 9 shows the results of the epidemic in the disease-free steady state and Figure 10 shows the results of the epidemic in the endemic steady state. From Figures 9 and 10, it is clearly seen that social distancing measure in conjunction with mask wearing and vaccination measure were able to control the disease in a more efficient manner, compared to when no measures were available.

Case 2: $u_1 \neq 0$ and $u_2 = 0$.

Social distancing measures were used together with mask wearing as seen in Figure 11. It can be noticed that the control measures took longer time for controlling the epidemic, compared to what happened in Case 1.

Case 3: $u_1 = 0$ and $u_2 \neq 0$.

Only vaccination measures were used as seen in Figure 12. From Figure 12b–d, it can be seen that vaccination measures were able to control the epidemic. According to Figure 12b,c, the number of exposed people and the number of symptomatic people shall decrease and the disease can be controlled for 60 days, showing that only vaccination measures can control the epidemic similarly, compared to Case 1.

It can be said that various control measures are highly important to help control the epidemic in an efficient manner efficiently control the epidemic. Vaccination measures are considered essential for controlling the epidemic.

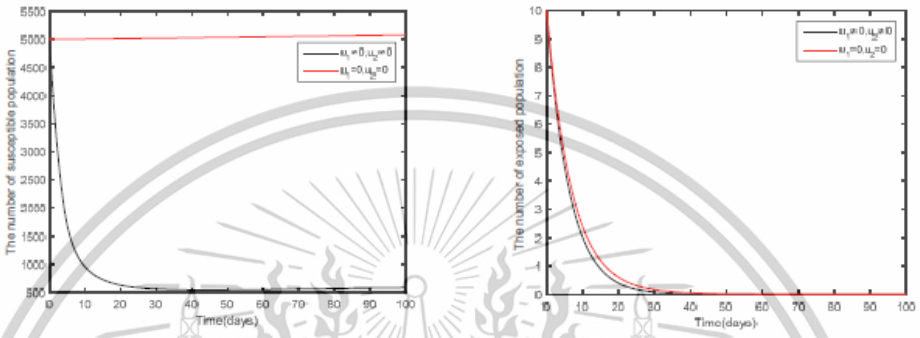

(a) Susceptible population.

(b) Exposed population.

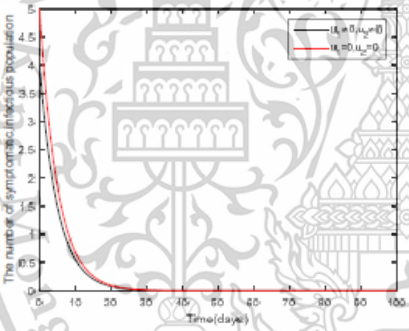

(c) Symptomatic, infectious population.

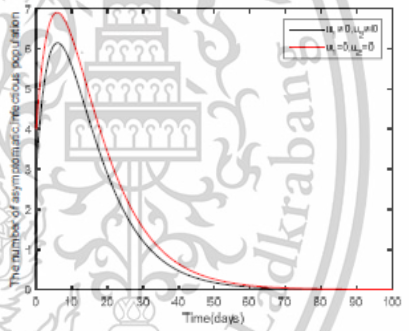

(d) Asymptomatic, infectious population.

Figure 9. *Cont.*

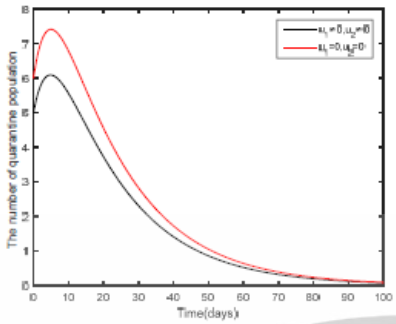

(e) Quarantine population.

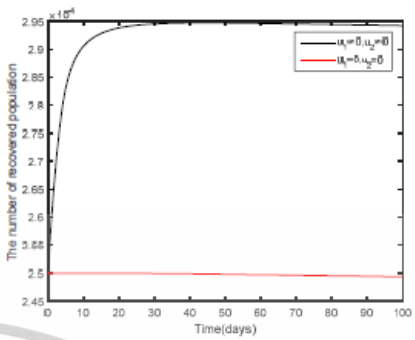

(f) Recovered population.

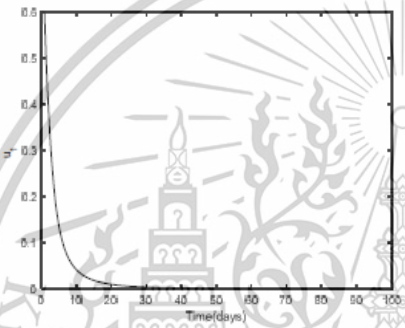

(g) Control efforts $u_1(t)$.

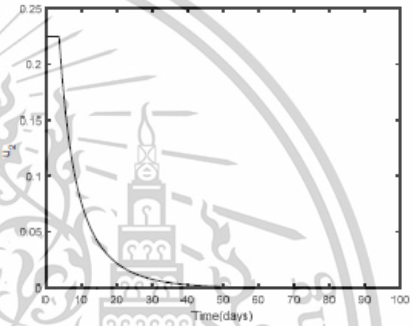

(h) Control efforts $u_2(t)$.

Figure 9. Comparison between the cases $u_1 = 0, u_2 = 0$ and $u_1 \neq 0, u_2 \neq 0$ for the disease-free steady state.

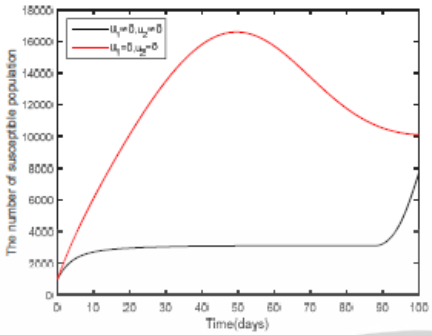

(a) Susceptible population.

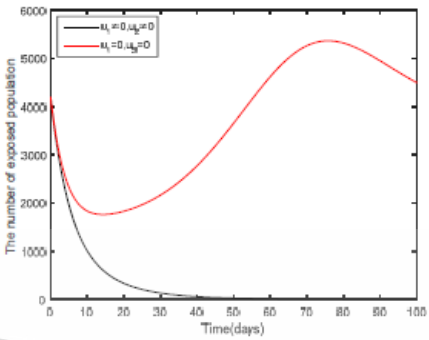

(b) Exposed population.

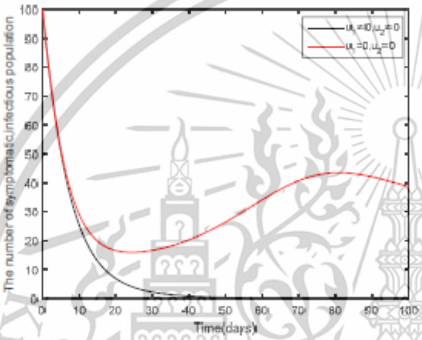

(c) Symptomatic, infectious population.

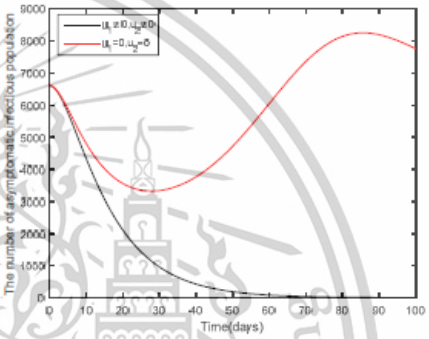

(d) Asymptomatic, infectious population.

Figure 10. *Cont.*

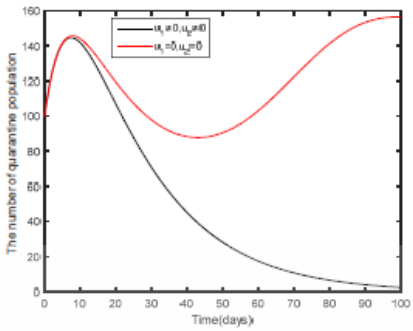

(e) Quarantine population.

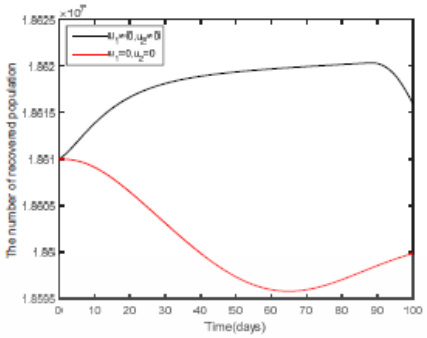

(f) Recovered population.

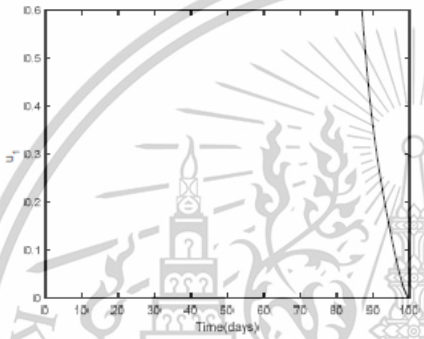

(g) Control efforts $u_1(t)$.

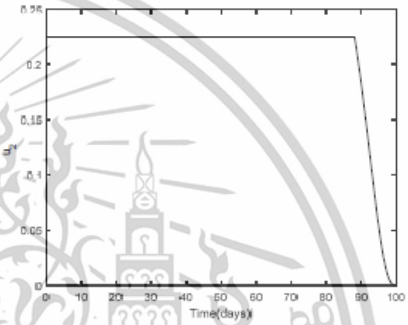

(h) Control efforts $u_2(t)$.

Figure 10. Comparison between the cases $u_1 = 0, u_2 = 0$ and $u_1 \neq 0, u_2 \neq 0$ for the endemic steady state.

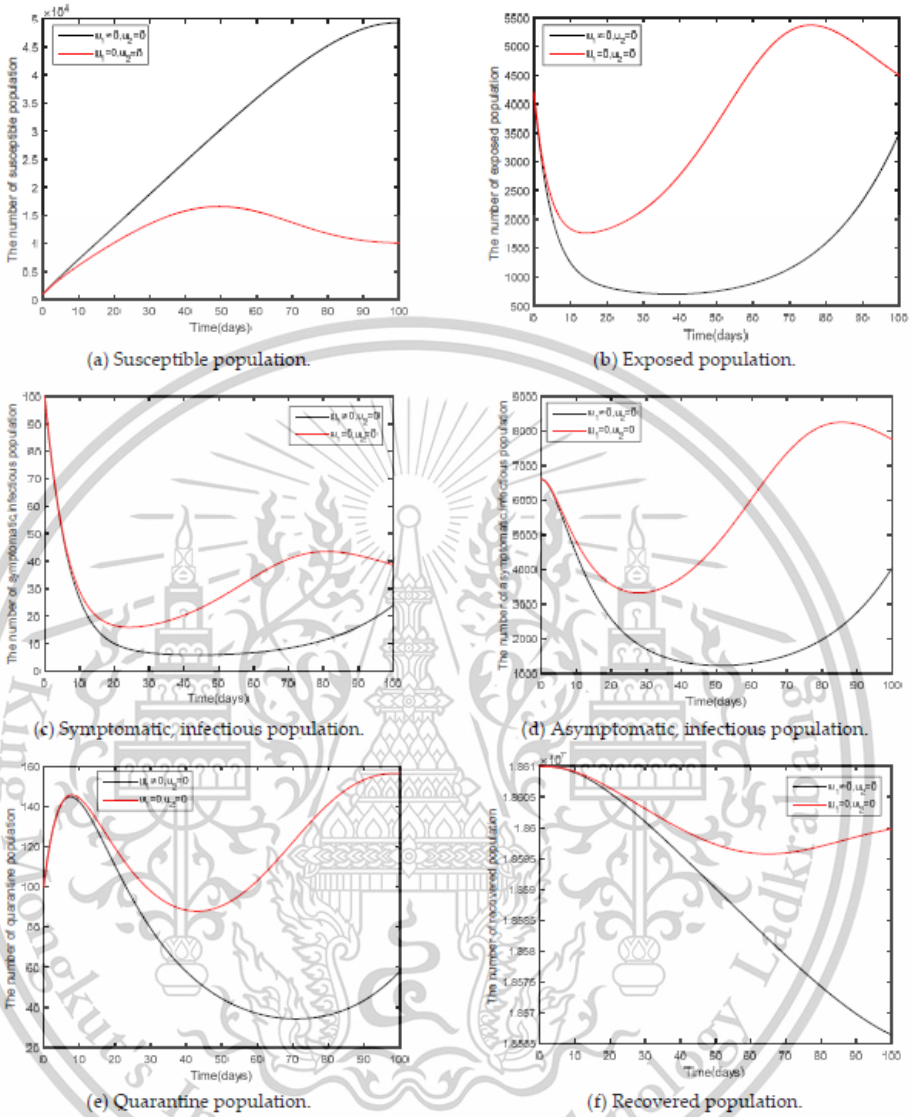

(a) Susceptible population. (b) Exposed population.

(c) Symptomatic, infectious population. (d) Asymptomatic, infectious population.

(e) Quarantine population. (f) Recovered population.

Figure 11. Comparison between the cases $u_1 = 0, u_2 = 0$ and $u_1 \neq 0, u_2 = 0$ for the endemic steady state.

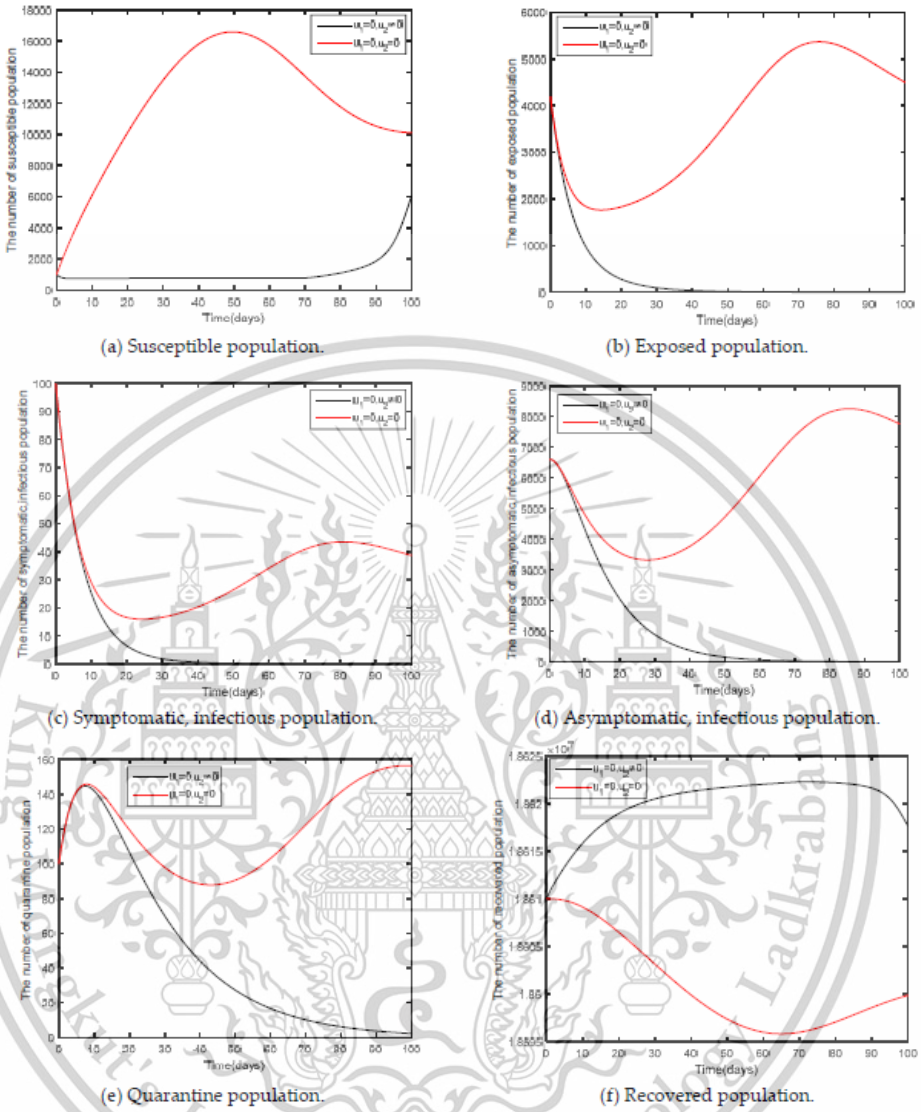

(a) Susceptible population. (b) Exposed population.

(c) Symptomatic, infectious population. (d) Asymptomatic, infectious population.

(e) Quarantine population. (f) Recovered population.

Figure 12. Comparison between the cases $u_1 = 0, u_2 = 0$ and $u_1 = 0, u_2 \neq 0$ for the endemic steady state.

6. Discussion and Conclusions

This article presents a model related to the dynamic of COVID-19 spread in Thailand. According to epidemiology, a mathematical model is a tool that has been used to help

analyze the spread of the fifth version of COVID-19 (Omicron). The vaccine against the α, β, γ, or δ variant of the COVID-19 coronavirus may not have the same efficacy against the ω variant. It appears the rate of infection by this variant of the coronavirus is much higher than that of the other variants and so before a new vaccine directed towards the ω variant can be developed, the other techniques to control the spread must be used. A new model must be used, one in which there are two variants are present, i.e., there are two types of infections, one caused by an α, β, γ, and δ variant of the COVID-19 coronavirus and another caused by the ω variant. A recent study by Lamwong et al. [45] studied the efficiency of vaccines for COVID-19 in Thailand. It was found that a 10% increase of vaccination rates would cause a 10% increase of the basic reproduction number. It can be concluded that an increase in vaccine efficacy would cause a decreased number of infected people. However, vaccination is just one measure for controlling the spread of the disease. There may be other measures that may lessen the need for everyone to be vaccinated. These are other control steps that can be taken. In this study, the SEI_1I_2QR model, developed from the $SEIQR$ model was presented. The presentation is divided into two parts. Part 1 is the non-control model. Both theoretical models and numerical analysis were available. Part 2 is the control model, developed from model (1) based on optimal control strategies to reduce the infection to the minimum. The analysis can be examined as follows:

1. Analysis of equilibrium point and the basic reproduction number of model (1). Disease-free equilibrium point (K_0^*), equilibrium point of endemic steady state (K_1^*) and the basic reproduction number (R_0) were calculated using the next-generation matrix method.
2. Stability analysis of model (1). The Lyapunov function was used to measure stability. It was found that in there was stability in the equilibrium point under the disease-free steady state when $R_0 < 1$, and under the endemic steady state there was stability in the equilibrium point when $R_0 > 1$.
3. fmincon Algorithm in MATLAB was used to be a technique for adjusting parameter values to ensure the model was suitable for the actual data of COVID-19 spread in Thailand and to estimate any spread than may come after. The parameters adjusted to be suitable for the model are the infection rate of symptomatic population (β_s), the infection rate of asymptomatic population (β_a), and the rate of exposed moving to symptomatic (ε), making the data analysis more precise.
4. Based on the model (1), numerical data analysis was presented to verify and support theoretical conditions. The comparison of parameters found that an increase in recruitment number of people (Λ) and the infection rate of asymptomatic population with the other variant (β_a) had an effect on a faster control of the epidemic.
5. Parameter sensitivity analysis showed the relationship between parameter values and the basic reproduction number (R_0), indicating the importance of each parameter value affecting the epidemic. The analysis results of the model (1) are shown in Table 4. From Table 4, it can be described that positive parameter sensitivity and increased parameters affect an increase in the basic reproduction numbers, leading to an increasing epidemic. Similarly, negative parameter sensitivity and increased parameters shall affect a decrease in the basic reproduction numbers. Based on the analysis, it was found that the most sensitive parameter was the initial number of the population (Λ).
6. In this study, there were two control strategies, namely, social distancing strategy (u_1 in conjunction with mask wearing strategy) and u_2 (vaccination control strategy). Pontryagin's maximum principle was used to analyze the needs of conditions. The analysis was divided into three cases. Case 1 is social distancing strategy in conjunction with mask wearing strategy and vaccination control strategy, Case 2 is social distancing strategy together with mask wearing, and Case 3 is vaccination control strategy.

According to the analysis, the optimal control with the shortest duration of disease control is Case 1, social distancing strategy in conjunction with mask-wearing strategy and vaccination control strategy.

The determination of various strategies is a guideline that helps control the epidemic. There are many methods that help control the epidemic. Fractional derivatives are a tool that helps assess different outcomes and determine an optimum in a better way. It is a topic to be studied in the next chapter.

Author Contributions: Conceptualization, J.L., P.P., and N.W.; methodology, J.L.; software, N.W.; validation, J.L., P.P., I.-M.T., and N.W.; writing—original draft preparation, J.L.; writing—review and editing, J.L., P.P., I.-M.T., and N.W.; supervision, P.P., I.-M.T., and N.W.; project administration, P.P.; funding acquisition, P.P. All authors have read and agreed to the published version of the manuscript.

Funding: This work is supported by the School of Science, King Mongkut's Institute of Technology Ladkrabang, Grant Number (2567-02-05-007).

Data Availability Statement: Data are available from the corresponding author upon reasonable request.

Acknowledgments: Jiraporn Lamwong is the recipient of the Graduate Study Fellowship of the School of Science, King Mongkut's Institute of Technology Ladkrabang, Thailand. This research was funded by the RA-TA graduate scholarship from the School of Science, King Mongkut's Institute of Technology Ladkrabang, grant number RA/TA-2565-D-001.

Conflicts of Interest: The authors declare that no conflicts of interest exist in the publication of this paper.

References

1. Thirthar, A.A.; Abboubakar, H.; Khan, A.; Abdeljawad, T. Mathematical modeling of the COVID-19 epidemic with fear impact. *AIMS Math.* **2023**, *8*, 6447–6465. [CrossRef]
2. Khan, M.A.; Atangana, A. Mathematical modeling and analysis of COVID-19: A study of new variant Omicron. *Phys. A* **2022**, *599*, 127452. [CrossRef]
3. Zhang, Z.; Zeb, A.; Hussain, S.; Alzahrani, E. Dynamics of COVID-19 mathematical model with stochastic perturbation. *Adv. Differ. Equ.* **2020**, *2020*, 451. [CrossRef]
4. Babaei, A.; Ahmadi, M.; Jafari, H.; Liya, A. A mathematical model to examine the effect of quarantine on the spread of coronavirus. *Chaos Solitons Fractals* **2021**, *142*, 110418. [CrossRef] [PubMed]
5. Mendoza, V.M.P.; Mendoza, R.; Lee, J.; Jung, E. Managing bed capacity and timing of interventions: A COVID-19 model considering behavior and underreporting. *AIMS Math.* **2023**, *8*, 2201–2225. [CrossRef]
6. Ghiasi Hafezi, S.; Seif, N.; Bahari, H.; Mohammadi, M.; Ghasemabadi, A.; Ferns, G.A.; Farkhani, E.M.; Ghayour-mobarhan, M. The association between macronutrient intakes and coronavirus disease 2019 (COVID-19) in an Iranian population: Applying a dynamical system model. *J. Health Popul. Nutr.* **2023**, *42*, 114. [CrossRef] [PubMed]
7. Shen, Z.H.; Chu, Y.M.; Khan, M.A.; Al-Hartomy, O.A.; Higazy, M. Mathematical modeling and optimal control of the COVID-19 dynamics. *Results Phys.* **2021**, *31*, 105028. [CrossRef]
8. Ghazizadeh, H.; Shakour, N.; Ghofchi, S.; Mansoori, A.; Saberi-Karimiam, M.; Rashidmayvan, M.; Ferns, G.; Esmaily, H.; Ghayour-Mobarhan, M. Use of data mining approaches to explore the association between type 2 diabetes mellitus with SARS-CoV-2. *BMC Pulm. Med.* **2023**, *23*, 203. [CrossRef]
9. Sepulveda, G.; Arenas, A.J.; González-Parra, G. Mathematical Modeling of COVID-19 Dynamics under Two Vaccination Doses and Delay Effects. *Mathematics* **2023**, *11*, 369. [CrossRef]
10. Khan, A.A.; Ullaha, S.; Amin, R. Optimal control analysis of COVID-19 vaccine epidemic model: A case study. *Eur. Phys. J. Plus* **2022**, *137*, 156. [CrossRef]
11. Philip, N.A.A.; Seidu, B.; Bornaa, C.S. Mathematical Analysis of COVID-19 Transmission Dynamics Model in Ghana with Double-Dose Vaccination and Quarantine. *Comput. Math. Methods Med.* **2022**, *2022*, 7493087.
12. Jankhonkhan, J.; Sawangtong, W. Model Predictive Control of COVID-19 pandemic With Social Isolation and Vaccination Policies in Thailand. *Axioms* **2021**, *10*, 274. [CrossRef]
13. Wickramaarachchi, W.P.T.M.; Perera, S.S.N. An SIER model to estimate optimal transmission rate and initial parameters of COVD-19 dynamic in Sri Lanka. *Alex. Eng. J.* **2021**, *60*, 1557–1563. [CrossRef]
14. Daniel, D.O. Mathematical Model for the Transmission of COVID-19 with Nonlinear Forces of Infection and the Need for Prevention Measure in Nigeria. *J. Infect. Dis. Epidemiol.* **2020**, *6*, 158.
15. Veera Krishna, M.; Prakas, J. Mathematical modelling on phase based transmissibility of Coronavirus. *Infect. Dis. Model.* **2020**, *5*, 375–385. [CrossRef] [PubMed]

16. Mishraa, A.M.; Purohit, S.D.; Owolabi, K.M.; Sharma, Y.D. A nonlinear epidemiological model considering asymptotic and quarantine classes for SARS CoV-2 virus. *Chaos Solitons Fractals* **2020**, *138*, 109953. [CrossRef]
17. Satar, H.A.; Naji, R.K. A Mathematical Study for the Transmission of Coronavirus Disease. *Mathematics* **2023**, *11*, 2330. [CrossRef]
18. Zamir, M.; Abdeljawad, T.; Nadeem, F.; Yousef, A. An optimal control analysis of a COVID-19 model. *Alex. Eng. J.* **2021**, *60*, 2875–2884. [CrossRef]
19. Baba, I.A.; Nasidi, B.A.; Baleanu, D.; Saadi, S.H. A mathematical model to optimize the available control measures of COVID–19. *Ecol. Complex.* **2021**, *46*, 100930. [CrossRef]
20. World Health Organization. SARS-CoV-2 Variant Tracking. Available online: https://www.who.int/fr/activities/tracking-SARS-CoV-2-variants (accessed on 31 May 2022).
21. Minka, S.; Minka, F. A tabulated summary of the evidence on humoral and cellular responses to the SARS-CoV-2 Omicron VOC, as well as vaccine efficacy against this variant. *Immunol. Lett.* **2022**, *243*, 38–43. [CrossRef]
22. González-Parra, G.; Arenas, A.J. Mathematical Modeling of SARS-CoV-2 Omicron Wave under Vaccination Effects. *Computation* **2023**, *11*, 36. [CrossRef]
23. Martin, D.P.; Lytras, S.; Lucaci, A.G.; Maier, W.; Gruning, B.; Shank, S.D.; Weaver, S.; MacLean, O.A.; Orton, R.J.; Lemey, P.; et al. Selection Analysis Identifies Significant Mutational Changes in Omicron That Are Likely to Influence Both Antibody Neutralization and Spike Function (Part 1 of 2). *Virological. Org.* 2021, 5, pp. 1–2. Available online: https://virological.org/t/selection-analysis-identifies-significant-mutational-changes-in-omicron-that-are-likely-to-influence-both-antibody-neutralization-and-spike-function-part-1-of-2/771 (accessed on 10 June 2023).
24. World Health Organization. WHO Coronavirus (COVID-19) Dashboard. 2023. Available online: https://covid19.who.int/ (accessed on 31 May 2022).
25. World Health Organization. WHO Coronavirus (COVID-19) Dashboard. 2023. Available online: https://covid19.who.int/region/searo/country/th (accessed on 31 May 2022).
26. Sun, T.-C.; DarAssi, M.H.; Alfwzan, W.F.; Khan, M.A.; Alshahrani, A.S.; Alqahtani, S.S.; Muhammad, T. Mathematical Modeling of COVID-19 with Vaccination Using Fractional Derivative: A Case Study. *Fractal Fract.* **2023**, *7*, 234. [CrossRef]
27. Gumu, O.A.; Selvam, A.G.M.; Janagaraj, R.; Selvam, G.M.; Janagaraj, R. Dynamics of the Mathematical Model Related to COVID-19 Pandemic with Treatment. *Thai J. Math.* **2022**, *20*, 957–970.
28. Chhetri, B.; Bhagat, V.M.; Muthusamy, S.; Ananth, V.S.; Vamsi, D.K.K.; Sanjeevi, C.B. Time Optimal Control Studies on COVID-19 Incorporating Adverse Events of the Antiviral Drugs. *Comput. Math. Biophys.* **2021**, *9*, 214–241. [CrossRef]
29. Nabi, K.N.; Kumar, P.; Erturk, V.S. Projections and fractional dynamics of COVID-19 with optimal control strategies. *Chaos Solitons Fractals* **2021**, *145*, 110689. [CrossRef] [PubMed]
30. Lamwong, J.; Tang, I.-M.; Pongsumpun, P. Mers Model of Thai and South Korean Population. *Curr. Appl. Sci. Technol.* **2018**, *18*, 45–57.
31. Sardar, T.; Ghosh, I.; Rodo, X.; Chattopadhyay, J. A realistic two-strain model for MERS-CoV infection uncovers the high risk for epidemic propagation. *PLoS Negl. Trop. Dis.* **2020**, *14*, e0008065. [CrossRef]
32. Mwalili, S.; Kimathi, M.; Ojiambo, V.; Gathungu, D.; Mbogo, R. SEIR model for COVID-19 dynamics incorporating the environment and social distancing. *BMC. Res. Notes* **2020**, *13*, 352. [CrossRef]
33. Mahardika, Y.D. Dynamical Modeling of COVID-19 and Use of Optimal Control to Reduce the Infected Population and Minimize the Cost of Vaccination and Treatment. *ComTech Comput. Math. Eng. Appl.* **2021**, *12*, 65–73. [CrossRef]
34. Omame, A.; Rwezaura, H.; Diagne, M.L.; Inyama, S.C.; Tchuenche, J.M. COVID-19 and dengue co-infection in Brazil: Optimal control and cost-effectiveness analysis. *Eur. Phys. J. Plus* **2021**, *136*, 1090. [CrossRef]
35. Nainggolan, J.; Ansori, M.F. Stability and Sensitivity Analysis of the COVID-19 Spread with Comorbid Diseases. *Symmetry* **2022**, *14*, 2269. [CrossRef]
36. Carcione, J.M.; Santos, J.E.; Bagaini, C.; Ba, J. A Simulation of a COVID-19 Epidemic Based on a Deterministic SEIR Model. *Front. Public Health* **2020**, *8*, 230. [CrossRef] [PubMed]
37. Bhadauria, A.S.; Devi, S.; Nivedita, G. Modelling and analysis of a SEIQR model on COVID-19 pandemic with delay. *Model. Earth Syst. Environ.* **2022**, *8*, 3201–3214. [CrossRef] [PubMed]
38. Youssef, H.; Alghamdi, N.; Ezzat, M.A.; El-Bary, A.A.; Shawky, A.M. Study on the SEIQR model and applying the epidemiological rates of COVID-19 epidemic spread in Saudi Arabia. *Infect. Dis. Model.* **2021**, *6*, 678–692. [CrossRef] [PubMed]
39. Hussain, T.; Ozair, M.; Ali, F.; Rehman, S.; Assiri, T.A.; Mahmoud, E.E. Sensitivity analysis and optimal control of COVID-19 dynamics based on SEIQR model. *Results Phys.* **2021**, *22*, 103956. [CrossRef] [PubMed]
40. Khan, A.; Zarin, R.; Hussain, G.; Ahmad, N.A.; Mohd, M.H.; Yusuf, A. Stability analysis and optimal control of COVID-19 with convex incidence rate in Khyber Pakhtunkhawa (Pakistan). *Results. Phys.* **2021**, *20*, 103703. [CrossRef] [PubMed]
41. Li, M.-T.; Sun, G.-Q.; Zhang, J.; Zhao, Y.; Pei, X.; Li, L.; Wang, Y.; Zhang, W.-Y.; Zhang, Z.-K.; Jin, Z. Analysis of COVID-19 transmission in Shanxi Province with discrete time imported cases. *Math. Biosci. Eng.* **2020**, *17*, 3710–3720. [CrossRef]
42. Abioye, A.I.; Peter, O.J.; Ogunseye, H.A.; Oguntolu, F.A.; Oshinubi, K.; Ibrahim, A.A.; Khan, I. Mathematical model of COVID-19 in Nigeria with optimal control. *Results Phys.* **2021**, *28*, 104598. [CrossRef]
43. van den Driessche, P.; Watmough, J. Reproduction numbers and sub-threshold endemic equilibria for compartmental models of disease transmission. *Math. Biosci.* **2002**, *180*, 29–48. [CrossRef]

44. Perkins, T.A.; España, G. Optimal Control of the COVID-19 Pandemic with Non-pharmaceutical Interventions. *Bull. Math. Biol.* **2020**, *82*, 118. [CrossRef]
45. Lamwong, J.; Pongsumpun, P.; Tang, I.-M.; Wongvanich, N. Vaccination's Role in Combating the Omicron Variant Outbreak in Thailand: An Optimal Control Approach. *Mathematics* **2022**, *10*, 3899. [CrossRef]
46. World Health Organization. COVID-19—WHO Thailand Situation Reports. Available online: https://www.who.int/thailand/emergencies/novel-coronavirus-2019/situation-reports (accessed on 25 January 2023).
47. Riyapan, P.; Shuaib, S.E.; Intarasit, A. A Mathematical Model of COVID-19 Pandemic: A Case Study of Bangkok, Thailand. *Comput. Math. Methods Med.* **2021**, *2021*, 6664483. [CrossRef] [PubMed]
48. Alshammari, F.S. A Mathematical Model to Investigate the Transmission of COVID19 in the Kingdom of Saudi Arabia. *Comput. Math. Methods Med.* **2020**, *2020*, 1–13. [CrossRef] [PubMed]
49. Bandekara, S.R.; Ghosh, M. Mathematical modeling of COVID-19 in India and Nepal with optimal control and sensitivity analysis. *Eur. Phys. J. Plus* **2021**, *136*, 1058. [CrossRef] [PubMed]
50. Kamien, M.I.; Schwartz, N.L. *Dynamic Optimization: The Calculus of Variations and Optimal Control in Economics and Management*; Elsevier: Amsterdam, The Netherlands, 1991.
51. Guo, T.; Li, Y. Modeling and optimal control of mutated COVID-19 (Delta strain) with imperfect vaccination. *Chaos Solitons Fractals* **2022**, *156*, 111825.
52. Adepoju, O.A.; Samson Olaniyi, S. Stability and optimal control of a disease model with vertical transmission and saturated incidence. *Sci. Afr.* **2021**, *12*, e00800. [CrossRef]

Author biography

Name	Miss Jiraporn Lamwong
Date of Birth	2 February 1990
Address	Moo 8, Non Thon Subdistrict, Mueang Khon Kaen District, Khon Kaen Province, 40000, Thailand
Education	(2013) Bachelor of Science in Applied Mathematics GPA 2.65, King Mongkut's Institute of Technology (KMITL) (2015) Master of Science in Applied Mathematics GPA 3.48, King Mongkut's Institute of Technology Ladkrabang (KMITL) (2025) Doctor of Philosophy in Applied Mathematics GPA 4.00, King Mongkut's Institute of Technology Ladkrabang (KMITL)
Scholarship	RA-TA graduate scholarship from the School of Science, King Mongkut's Institute of Technology Ladkrabang (KMITL). Grant number RA/TA-2565-D-001
Academic Publication(s)	1. Lamwong, J. and Pongsumpun, P. 2020. "Mathematical Model for the Dynamic of COVID-19 Spread and Impacts of Vaccination, Quarantine, and Hospitalization among the 5th Wave of COVID-19 in Thailand." 308-322. **In 2024, the 24th Annual Meeting in Mathematics (AMM 2024).** May 29–31, 2024, Ubon Ratchathani University, Thailand. 2. Lamwong, J. Pongsumpun, P. Tang, I.-M. and N. Wongvanich. 2022. "Vaccination's Role in Combating the Omicron Variant Outbreak in Thailand: An Optimal Control Approach." *Mathematics.* 10(20): 3899. 3. Lamwong, J., Wongvanich, N., Tang, I.-M., and Pongsumpun, P. 2024. "Optimal Control Strategy of a Mathematical Model for the Fifth Wave of COVID- 19 Outbreak (Omicron) in Thailand. " *Mathematics*. 12(1): 14.